

University of Alberta

Intra-follicular growth factors and preovulatory follicle
development in the sow

by

François Paradis

A thesis submitted to the Faculty of Graduate Studies and Research
in partial fulfillment of the requirements for the degree of

Doctor of Philosophy

in

Animal Science

Department of Agricultural, Food and Nutritional Sciences

©François Paradis

Fall 2009

Edmonton, Alberta

Permission is hereby granted to the University of Alberta Libraries to reproduce single copies of this thesis and to lend or sell such copies for private, scholarly or scientific research purposes only. Where the thesis is converted to, or otherwise made available in digital form, the University of Alberta will advise potential users of the thesis of these terms.

The author reserves all other publication and other rights in association with the copyright in the thesis and, except as herein before provided, neither the thesis nor any substantial portion thereof may be printed or otherwise reproduced in any material form whatsoever without the author's prior written permission.

Examining Committee

George R. Foxcroft, Department of Agricultural, Food and Nutritional Sciences

Walter T. Dixon, Department of Agricultural, Food and Nutritional Sciences

Michael K. Dyck, Department of Agricultural, Food and Nutritional Sciences

Denise G. Hemmings, Department of Obstetrics and Gynecology

Matthew C. Lucy, Department of Animal Science, University of Missouri

Dedicated to my loving family,

Susan, Tomas and Sara

for their continuous support, understanding and encouragement

ABSTRACT

Pig follicle development is a complex but poorly understood process involving both gonadotrophins and local ovarian factors. A series of studies sought to investigate these intrafollicular cell-to-cell interactions. Microarray analysis combined with gene ontology revealed that the oocyte, granulosa and theca cells each expressed more than 650 potential secreted factors and receptors, including members of the TGF- β , IGF1, EGF and FGF families. Using a well-defined *in vivo* experimental paradigm that generates follicles and oocytes of different quality, the temporal expression of several growth factors in the oocyte, granulosa and theca cells collected from sows during the recruitment and mid-selection phases, as well as the final selection of the preovulatory follicle population before and after the LH surge was studied. *IGF1* expression patterns indicated its potential for modulating granulosa and theca cell function during the selection stages, and an involvement in creating differences in follicular quality between the first and second preovulatory wave post-weaning. Transient up-regulation of *AREG* and *EREG* mRNA around the LH surge, suggested their involvement in ovulation. Results of a second study investigating TGF- β superfamily expression, suggested a role for GDF9 in follicle selection through the up-regulation of *TGFBRI* expression, while BMP15 could be involved in ovulation through the up-regulation of *BMPRIIB*. Expression of angiogenesis-related genes during follicle development was also investigated. During mid-selection, ANGPT2 may allow VEGFA and similar factors to stimulate vascular

development or destabilize the vasculature and cause follicular atresia, while ANGPT1 may be required in the preovulatory follicle population. Associations among the transcription factor *HIF1A*, *VEGFA* and *ANGPT1*, suggested interactions between the ligands in regulation of angiogenesis. Finally, the effects of the pig oocyte on cumulus cell function was assessed by co-culturing cumulus cell complexes with or without denuded oocytes isolated from large oestrogenic follicles. Presence of oocytes decreased *FSHR* and increased *HSD3B* expression, potentially stimulating progesterone while attenuating oestradiol production. In conclusion, oocytes were shown to control cumulus cell function in a way that reflects their specific environment and further evidence was obtained for a complex network of growth factors and receptors in the follicle and their involvement in regulation of pig follicle development.

ACKNOWLEDGMENTS

I would like to thank my supervisor, Dr. George Foxcroft for his invaluable support and guidance throughout my PhD. His continuous enthusiasm for research, his knowledge of science and his integrity will have a strong influence on my future endeavors. I would also like to thank my co-supervisors Walter Dixon and Michael Dyck for their encouragement and always helpful advice to improve the quality of my research.

I am also grateful to the present and past members of our research group for all their help and support throughout those years. Particularly, I would like to thank Jennifer Patterson for coordinating all of my animal work, Rose O'Donoghue and Pamela Wizzard for their help with the animal work, Joan Turchinsky for her invaluable technical support and Shirley Shostak for performing the RIAs. Also, to Katherine Degenstein, Harry Moore, Susanna Town, Ana-Lucia Ruiz-Sanchez, and especially to Michael Vinsky and Alex Pasternak, thank you for your help but also for the great discussion and laughter shared over the years.

I must also thank members of the Swine Research and Technology Centre, including Jay Willis, Janes and Dianna Goller for the care and attention they gave to my research animals. I must also acknowledge the Department of Agriculture, Food and Nutritional Science for facilitating my graduate studies, particularly Jody Forslund, Lynn Elmes and Urmila Basu. My appreciation also goes to the Natural Sciences and Engineering Research Council of Canada and Alberta Ingenuity Fund for the funding support.

Finally, I want to thank my spouse Susan Novak, not only for her continuous love and support but also for the great scientific discussion and her help with several aspects of my research. I would also like to thank my family for their support specifically my mom and dad, for their encouragement and interest in my research.

TABLE OF CONTENTS

CHAPTER 1

GENERAL INTRODUCTION	1
REFERENCES	7

CHAPTER 2

LITERATURE REVIEW	11
INTRODUCTION	11
DYNAMICS OF FOLLICULAR GROWTH	12
Stages of follicle development	13
Defined phases of follicular development.....	16
<i>Emergence or initial recruitment and preantral growth</i>	17
<i>Recruitment, selection and dominance</i>	19
EXTRAOVARIAN CONTROL OF FOLLICLE DEVELOPMENT	23
Hypothalamus and pituitary gland	23
<i>Hypothalamus</i>	23
<i>Pituitary gland</i>	24
Mechanism of action of the gonadotrophins and their regulation.....	26
<i>Receptor localization and signal transduction</i>	26
<i>Steroidogenesis</i>	27
<i>Modulation of gonadotrophin secretion</i>	29
INTRAFOLLICULAR FACTORS CONTROLLING FOLLICLE DEVELOPMENT AND OOCYTE GROWTH	32
Transzonal projections and gap junctions	32
<i>Role of TZP and gap junctions</i>	34
<i>Oocyte growth</i>	35
<i>Meiotic arrest</i>	36
Intrafollicular growth factors.....	39
Antral follicle development.....	40
<i>TGF-β superfamily</i>	40
<i>IGF system</i>	50
<i>Angiogenic factors</i>	53
Perioovulatory period.....	64
<i>TGF-β superfamily</i>	64
<i>EGF, EGF-like peptide and receptors</i>	66
<i>Angiogenic factors</i>	70
CONCLUSION	71
REFERENCES	73

CHAPTER 3

GLOBAL TRANSCRIPT PROFILING IN CONJUNCTION WITH GENE ONTOLOGY ANNOTATION REVEALS THE SECRETOME OF THE PORCINE OOCYTE, GRANULOSA AND THECA CELLS DURING ANTRAL FOLLICLE DEVELOPMENT	101
INTRODUCTION.....	101
MATERIALS AND METHODS	103

RESULTS.....	112
DISCUSSION.....	120
REFERENCES.....	137

CHAPTER 4

TEMPORAL REGULATION OF BMP2, BMP6, BMP15, GDF-9, BMPR1A, BMPR1B, BMPR2 AND TGFBR1 MRNA EXPRESSION IN THE OOCYTE, GRANULOSA AND THECA CELLS OF DEVELOPING PEOVULATORY FOLLICLES IN THE PIG	142
INTRODUCTION.....	142
MATERIALS AND METHODS.....	144
RESULTS.....	154
DISCUSSION.....	159
REFERENCES.....	176

CHAPTER 5

TEMPORAL EXPRESSION OF ANGIOGENIC FACTORS IN GRANULOSA AND THECA CELLS OF DEVELOPING PORCINE PEOVULATORY FOLLICLES AND THE POTENTIAL INVOLVEMENT OF ANGIOGENIN IN THE LUTEINIZING FOLLICLE	182
INTRODUCTION.....	182
MATERIALS AND METHODS.....	184
RESULTS.....	192
DISCUSSION.....	197
REFERENCES.....	214

CHAPTER 6

PORCINE PEOVULATORY GV OOCYTES SECRETE SOLUBLE FACTORS THAT MODULATE CUMULUS CELL PROTEIN EXPRESSION AND POTENTIALLY AFFECT THEIR STEROIDOGENIC ABILITY IN VITRO	219
INTRODUCTION.....	219
MATERIALS AND METHODS.....	221
RESULTS.....	231
DISCUSSION.....	233
REFERENCES.....	251

CHAPTER 7

GENERAL DISCUSSION AND CONCLUSIONS	256
REFERENCES.....	266

APPENDIX I: Supplementary Table 3.3	269
--	-----

APPENDIX II: Supplementary Table 3.4	295
---	-----

LIST OF TABLES

Table 3.1 Details of primers and probes used for Real-Time PCR.....	129
Table 3.2 Comparison of transcript localization for members of the insulin-like growth factor and epidermal growth factor family as determined by microarray and real-time PCR analysis.....	131
Table 4.1 Details of primers and probes used for Real-Time PCR.....	166
Table 4.2 Overall characteristics of the sows and follicles for each cycle irrespective of the phase of follicular development.....	167
Table 4.3 Characteristics of the sows and follicles from each stage of follicle development, irrespective of the cycle.....	168
Table 4.4 Summary of the statistical analysis of oocyte, granulosa cell and theca cell mRNA abundance (Δ Ct) at specific stages of follicular development.	169
Table 5.1 Details of primers and probes used for Real-Time PCR.....	206
Table 5.2 List of angiogenic factors expressed in the granulosa (GC) and theca (TC) cells of porcine antral follicles identified using the Affymetrix GeneChip Porcine Genome Array in combination with gene ontology annotation.....	207
Table 5.3 Steroidogenic activity of the follicles isolated during the final selection phase before and after the preovulatory LH surge from sows during the first or second preovulatory wave of follicular development after weaning.....	211
Table 6.1 Details of primers and probes used for Real-Time PCR.....	242
Table 6.2 Characteristics of the sows and preovulatory follicles (POF) from which oocytes were isolated.....	244
Table 6.3 Identity of the proteins identified by LC-MSMS that were differentially expressed between oocyctomized cumulus cells (OOX) incubated alone or with denuded oocytes (DO) isolated from large oestrogenic sow follicles prior to the LH surge.....	245

LIST OF FIGURES

- Figure 2.1** Follicle and oocyte growth and acquisition of meiotic competence in the pig. Adapted from Hunter, 2000. 13
- Figure 2.2** Images of the different stages of follicular development observed in the goat ovary. A) Primordial B) Primary C) Secondary and D) Tertiary or Antral follicles. Adapted from Silva *et al.*, 2005. These pictures have been taken of goat follicles but are very similar to porcine follicles..... 14
- Figure 2.3** Time scale for pig follicular growth. Adapted from Hunter, 2000 but based on Morbeck *et al.*, 1992 and Dailey *et al.*, 1976..... 15
- Figure 2.4** Schematic representation of the concept of cellular and hormonal interactions during pig follicular development. LDL = low density lipoprotein, cAMP = cyclic AMP, CYP11A1 = P450 side-chain cleavage, HSD3B = 3 β -hydroxysteroid dehydrogenase, CYP17A1 = 17 α -hydroxylase, CYP19A1 = P450 aromatase and ■ = receptor. Adapted from Ainsworth *et al.*, 1990..... 29
- Figure 2.5** Schematic representation of the differential regulation of LH and FSH by ovarian peptides and steroids. + and – indicate stimulatory or inhibitory effects. Adapted from Foxcroft *et al.*, 1994..... 30
- Figure 2.6** Schematic representation of the transzonal projections (TZP) with the proposed distribution of connexins (Cx) 37, 43 in the gap junctions of mouse cumulus-oocyte complexes. Adapted from Kidder and Mhawi, 2002. 33
- Figure 2.7** Schematic summary of the localization and functions of key local growth factors in the antral follicle..... 63
- Figure 2.8** Schematic representation of the model proposed for LH-mediated cumulus expansion and oocyte meiotic resumption through stimulation of the EGF-like ligand. Adapted from Conti *et al.*, 2006..... 69
- Figure 3.1** Quantification by real-time RT-PCR of *IGF1R*, *IGFBP6*, *PAPP-A* and *ADAM17* mRNA abundance in pig oocytes during recruitment (R; n=6), mid-selection (MS; n=6), final selection (FS; n=8) and final selection post-LH surge (FS/LH; n=8). Relative mRNA abundance is expressed as $\text{lsmeans} \pm \text{SEM}$ 132
- Figure 3.2** Quantification by real-time PCR of A) *IGF1*, *IGF1R*, *IGFBP2*, *IGFBP4*, *IGFBP5* and *IGFBP6* and B) *PAPP-A* mRNA abundance in pig granulosa cells during recruitment (R; n=6), mid-selection (MS; n=6) final selection (FS; n=3) and final selection post-LH (FS/LH; n=3). Data are expressed as relative mRNA abundance \pm SEM. Different letters within genes represent significant differences among phases (^{abc}P<0.05). *represents significant differences within phase between cycles (P<0.05). 133

Figure 3.3 Quantification by real-time PCR of A) IGF1R, IGFBP2, IGFBP4, IGFBP5, IGFBP6 and PAPP-A and B) IGF1 mRNA abundance in pig theca cells during recruitment (R; n=6), mid-selection (MS; n=6) final selection (FS; n=3) and final selection post-LH (FS/LH; n=3). Data are expressed as relative mRNA abundance \pm SEM. Different letters within gene represent significant differences among phases (^{abc}P<0.05). * represents significant differences between 1st and 2nd cycle (P<0.05). 134

Figure 3.4 A) Quantification by real-time PCR of EGFR, AREG, EREG, BTC and ADAM17 mRNA abundance in pig granulosa cell during recruitment (R; n=6), mid-selection (MS; n=6) final selection (FS; n=3) and final selection post-LH (FS/LH; n=3). B) AREG and EREG mRNA abundance in individual sows throughout follicular development. Different letters within gene represent significant differences among phases (P<0.05). 135

Figure 3.5 Quantification by real-time PCR of EGFR, AREG, EREG, BTC and ADAM17 mRNA abundance in pig theca cell during recruitment (R; n=6), mid-selection (MS; n=6) final selection (FS; n=3) and final selection post-LH (FS/LH; n=3). Different letters within gene represent significant differences among phases (P<0.05). 136

Figure 4.1 Comparison of *BMP2*, *BMP6*, *BMP15*, *GDF9*, *BMPRIA*, *BMPR1B*, *BMPR2* and *TGFBR1* mRNA abundance in pig oocytes (A), granulosa cells (B) and theca cells (C) for each phase of preovulatory follicle development (recruitment (R), mid-selection (MS), final selection (FS) and final selection post-LH surge (FS/LH)), irrespective of cycle. Relative mRNA abundance is expressed as $\bar{x} \pm$ SEM. Different letters between genes within phases represent significant differences ($P \leq 0.05$). 170

Figure 4.2 Quantification via real-time RT-PCR of *BMP2*, *BMP6*, *BMP15*, *GDF9*, *BMPRIA*, *BMPR1B*, *BMPR2* and *TGFBR1* mRNA abundance in pig oocytes (A), granulosa cells (B) and theca cells (C) between 1st and 2nd cycle, irrespective of the phase of the cycle. The Δ Ct values are expressed as $\bar{x} \pm$ SEM. 171

Figure 4.3 Quantification via real-time RT-PCR of A) *BMP2*, *BMP6*, *BMP15* and *GDF9* and B) *BMPRIA*, *BMPR1B*, *BMPR2* and *TGFBR1* mRNA abundance in pig oocytes during follicle recruitment (n=6), mid-selection (n=6), final selection (n=8) and final selection post-LH surge (n=8). Data are expressed as a relative mRNA abundance \pm SEM for each phase, irrespective of cycle. Different letters within gene represent significant differences among phases ($P \leq 0.05^{a,b,c}$; $P \leq 0.01^{x,y,z}$). 172

Figure 4.4 Quantification via real-time RT-PCR of A) *BMP2*, *BMP6*, *BMP15* and *GDF9* and B) *BMPRIA*, *BMPR1B*, *BMPR2* and *TGFBR1* mRNA abundance in

pig granulosa cells during follicle recruitment (n=6), mid-selection (n=6), final selection (n=3) and final selection post-LH surge (n=3). Data are expressed as a relative mRNA abundance \pm SEM for each phase, irrespective of cycle. Different letters within gene represent significant difference among phases ($P \leq 0.05^{a,b,c}$; $P \leq 0.01^{x,y,z}$)..... 173

Figure 4.5 Quantification via real-time RT-PCR of A) *BMP2*, *BMP6*, *BMP15* and *GDF9* and B) *BMPR1A*, *BMPR1B*, *BMPR2* and *TGFBRI* mRNA abundance in pig theca cells during follicle recruitment (n=6), mid-selection (n=6), final selection (n=3) and final selection post-LH surge (n=3). Data are expressed as a relative mRNA abundance \pm SEM for each phase, irrespective of cycle. Different letters within gene represent significant difference among phases ($P \leq 0.05^{a,b,c}$; $P \leq 0.01^{x,y,z}$)..... 174

Figure 4.6 Western blot analysis for the presence of BMP15 in follicular fluid (A) and BMPR1B in follicle hemisections (B) during follicle recruitment (BMP15 n=3, BMPR1B n=6), mid-selection (BMP15 n=6, BMPR1B n=6), final selection (BMP15 n= 8, BMPR1B n=3) and final selection post-LH surge (BMP15 n=6, BMPR1B n=3). Relative protein abundance is expressed as $\bar{x} \pm$ SEM. Different letters represent significant differences among phases ($P \leq 0.05$). 175

Figure 5.1 Quantification by real-time PCR of A) *VEGFA*, *ANGPT1*, *ANGPT2*, *ANG* and *HIF1A* and B) *KDR*, *FLT1* and *TEK* mRNA abundance in pig granulosa cells during recruitment (n=6), mid-selection (n=6) final selection (n=3) and final selection post-LH (n=3). Data are expressed as relative mRNA abundance \pm SEM. Different letters within gene represent significant differences among phases ($P \leq 0.05$)..... 212

Figure 5.2 Quantification by real-time PCR of A) *VEGFA*, *ANGPT1*, *ANGPT2* and *HIF1A*, B) *ANG* and C) *KDR*, *FLT1* and *TEK* mRNA abundance in pig theca cell during recruitment (n=6), mid-selection (n=6) final selection (n=3) and final selection post-LH (n=3). Data are expressed as relative mRNA abundance \pm SEM. Different letters within gene represent significant differences among phases ($P \leq 0.05$). * Significant difference within phase between cycle ($P \leq 0.05$). 213

Figure 6.1 Morphological appearance of the oocyctomized cumulus cells (OOX) after 22h of culture with and without denuded oocytes isolated from large oestrogenic sow follicles prior to the LH surge. 246

Figure 6.2 Representative 2-dimensional gel of proteins from a pool of 48 OOX incubated without oocytes. Protein spot numbers identify proteins differentially expressed between treatments (A). The proteins found to be up- and down-regulated in OOX culture alone are shown in B and C, respectively. 247

Figure 6.3 Quantification via real-time RT-PCR of the mRNA of genes involved in A) Apoptosis, B) Proliferation and C) Metabolism in pig oocyctectomized cumulus cells after 22h of culture with (n=6) and without (n=6) denuded oocytes isolated from large oestrogenic sow follicles prior to the LH surge. Data are expressed as relative mRNA abundance \pm SEM. 248

Figure 6.4 Quantification via real-time RT-PCR of A) the mRNA of genes involved in Steroidogenesis and B) YWHAH mRNA in pig oocyctectomized cumulus cells after 22h of culture with (n=6) and without (n=6) denuded oocytes isolated from large oestrogenic sow follicles prior to the LH surge. Data are expressed as relative mRNA abundance \pm SEM. The asterisks indicates differences within gene between treatment ($P \leq 0.05$ ** and $P \leq 0.1$ *). C) Correlation analysis between FSHR and YWHAH mRNA abundance (Δ Ct). .. 249

Figure 6.5 Quantification via real-time RT-PCR of A) *FSHR* mRNA B) *HSD3B* mRNA abundance in pig granulosa cells during follicle recruitment (R; n=6), mid-selection (MS; n=6), final selection (FS; n=3) and final selection post-LH surge (FS/LH; n=3). Data are expressed as relative mRNA abundance \pm SEM for each phase, irrespective of cycle. Different letters within gene represent significant difference among phases ($P \leq 0.05^{a,b,c}$)..... 250

Figure 7.1 Schematic representation of the temporal regulation of growth factors and receptors mRNA in the oocyte (Oo), granulosa (GC) and theca (TC) cells during the recruitment, mid-selection and final selection phase that are potentially involved in each specific phase of follicular development. 261

Figure 7.2 Schematic representation of the effect of the porcine preovulatory oocyte and several growth factors and receptors in large preovulatory follicles in the period immediately preceding and following the LH surge..... 263

LIST OF ABBREVIATIONS

ABI	Applied Biosystems
ACTH	Adrenocorticotrophic hormone
ACVR	Activin A receptor
ADAM17	A distintegrin and metalloproteinase domain 17
ALK	Activin receptor-type
ANG	Angiogenin
ANGPT	Angiopoietin
APOE	Apolipoprotein E
AREG	Amphiregulin
BAX	BCL2-associated protein
BCA	Bicinchoninic acid
BCL2	B-cell CLL/lymphoma 2
BMP	Bone morphogenic protein
BMPR	Bone morphogenic protein receptor
BTC	Betacellulin
cAMP	Cyclic adenosine monophosphate
dbcAMP	Dibutyryl-cyclic adenosine monophosphate
CCND2	Cell proliferation marker cyclin D2
CD34	Hematopoietic progenitor cell antigen CD34
cDNA	Complimentary deoxyribonucleic acid
CEEF	Cumulus expansion enabling factors
CGC	Cumulus granulosa cells
COC	Cumulus-oocyte complex
CRB1	Crumbs protein homologue precursor 1
Ct	Cycle threshold
CV	Coefficient of variation
Cx	Connexin
CYP17A1	Cytochrome P450 17 α -hydroxylase
CYP19A1	Cytochrome P450 aromatase
CYP11A1	Cytochrome P450 side chain cleavage
D	Day
DO	Denuded oocyte
E2	Oestradiol
eCG	Equine chorionic gonadotrophin
ECL	Enhanced chemiluminescence
EGF	Epidermal growth factor
EGFR	Epidermal growth factor receptor
EREG	Epiregulin
ESR1	Estrogen receptor 1
ESR2	Estrogen receptor 2
FF	Follicle fluid
FGF	Fibroblast growth factor
FGFR	Fibroblast growth factor receptor
FLT1	Fms-related tyrosine kinase

FS Final selection
 FS/LH Final selection/ post-LH stage
 FSH Follicle-stimulating hormone
 FSHR Follicle-stimulating hormone receptor
 g gram
 G6PD Glucose 6-phosphate dehydrogenase
 GC Granulosa Cells
 GCOS Affymetrix GeneChip Operating Software
 GDF Growth differentiation factor
 GHRH Growth hormone releasing hormone
 GnRH Gonadotrophin releasing hormone
 GO Gene ontology
 GOI Genes of interest
 GV Germinal vesicle
 GVBD Germinal vesicle breakdown
 hCG Human chorionic gonadotrophin
 HAS Hyaluronan synthase
 HEK HEK 293 cells
 HEPES 4-(2-hydroxyethyl)-1-piperazineethanesulfonic acid
 HIF1A Hypoxia-inducible factor 1A
 HRP Horseradish peroxidase
 HSD3B 3 β -hydroxysteroid dehydrogenase
 HST Hypophyseal stalk-transected
 Ig Immunoglobulin
 IGF1 Insulin-like growth factor 1
 IGF1R Insulin-like growth factor 1 receptor
 IGFBP Insulin-like growth factor binding protein
 INH Inhibin
 IRS1 Insulin receptor substrate 1
 KCIP1 Protein kinase C inhibitor
 KDR Kinase insert domain receptor
 kg Kilogram
 LC-MSMS Liquid chromatography- tandem mass spectrometry
 LDHA Lactate dehydrogenase A
 LH Lutenizing hormone
 LHCGR Lutenizing hormone receptor
 LSD Least significant difference
 MAPK Mitogen activated protein kinase
 MGC Mural granulosa cells
 MI Metaphase I
 MII Metaphase II
 ml Millilitre
 MPF Maturation promoting factor
 mRNA Messenger ribonucleic acid
 MS Mid-selection
 NADPH Nicotinic adenosine dehydrogenase phosphate

NCBI	National Center for Biotechnology Information
ng	Nanogram
NSERC	Natural Sciences and Engineering Research Council
OMI	Oocyte meiotic inhibitor
OOX	Oocyctectomized cumulus cell
P4	Progesterone
PAGE	Polyacrylamide gel
PAPP A	Pregnancy-associated plasma protein
PBS	Phosphate-buffered saline
PCR	Polymerase chain reaction
PDE	Phosphodiesterase
PDGF	Platelet-derived growth factor
PFKP	Phosphofructokinase
pFSH	Porcine follicle stimulating hormone
Pg	Picogram
PGAM1	Phosphoglycerate mutase
PKA	Protein Kinase A
PKC	Protein Kinase C
PKI	Protein kinase A inhibitor
pLH	Porcine lutenizing hormone
PMSF	Phenylmethanesulphonylfluoride
POMC	Proiomelanocortin
PPIA	Cyclophilin
PPP	Pentose phosphosate pathway
PRL	Prolactin
PVA	Polyvinyl alcohol
Q-PCR	Quantitative polymerase chain reaction (Real-time PCR)
R	Recruitment
RIA	Radioimmunoassay
RNA	Ribonucleic Acid
RT	Reverse transcription
RT-PCR	Reverse transcription-polymerase chain reaction
SAS	Statistical Analysis System
SDS	Sodium dodecyl sulfate
SEM	Standard error of the mean
STAR	Steroidogenic acute regulatory protein
TBS	Tris-buffered saline
TBS-T	Tris-buffered saline-Tween
TC	Theca cells
TCEP	tris(2-carboxyethyl)phosphine
TEK	TEK tyrosine kinase
TGFBR	Transforming growth factor β receptor
TGF	Transforming growth factor
THRA	Thyroid hormone receptor α
TL	Tyrode's lactate
TNF α	Tumor necrosis factor α

TPT1	Translationally controlled tumor protein
TSH	Thyroid stimulating hormone
TZP	Transzonal projection
U	Units
ug	Microgram
ul	Microlitre
V	Volts
v/v	volume/volume
VEGF	Vascular endothelial growth factor
Vhr	Volt-hours
w/v	weight/volume
YWHAH	14-3-3 η
ZP	Zona pellucida

CHAPTER 1

GENERAL INTRODUCTION

Nutritional manipulations and metabolic status have been shown to influence the reproductive functions of various mammalian species. This is also true in the pig and is likely to have an important impact on gilt and sow fertility in production systems since nutritional deficits have been shown to occur spontaneously in production (Prunier and Quesnel, 2000a). Nutritional manipulations are known to affect various aspects of sow reproduction. First, it was reported that primiparous sows either fed ad libitum or restricted to 50% of that amount during a 28 day lactation had very different follicle populations present on their ovaries at weaning (Quesnel *et al.*, 1998). The sows that were restricted showed a higher proportion of smaller follicles (< 1mm) and a lower proportion of follicles between 1- 2.9 mm at weaning. In a similar scenario, primiparous sows restricted to 50% of their feed intake from farrowing to day 21 of lactation and then fed ad libitum during the last week of lactation had more large follicles at slaughter (4.5 day after weaning) than the sows fed to appetite for the first 3 weeks of lactation and then restricted during the last week of lactation, suggesting that the timing of the restriction is also important (Zak *et al.*, 1997a). Other studies have also shown a relationship between the extent of protein catabolism in primiparous lactating sows and follicle size (Clowes *et al.*, 2003a, Clowes *et al.*, 2003b, Yang *et al.*, 2000).

Interestingly, smaller follicle size at weaning have been reported to increase the weaning-to-estrus interval (Bracken *et al.*, 2006), suggesting that under-nutrition could have a similar effect. A number of studies have demonstrated that feed restriction during lactation in primiparous sows delayed the return to estrus or reduced the number of sows returning to estrus within 10 days (Mao *et al.*, 1999, van den Brand *et al.*, 2000, Zak *et al.*, 1997b, Zak *et al.*, 1998). Moreover, nutritional manipulations have also been shown to modify

ovulation rate. In cyclic gilts, feed restriction starting during the luteal phase and maintained throughout the follicular phase was shown to reduce ovulation rate (Ashworth, 1991, Beltranena *et al.*, 1991, Cox *et al.*, 1987, Flowers *et al.*, 1989). Similarly, Zak *et al.* (1997b) showed that under-nutrition in sows during the last week of lactation decreased ovulation rate while King and Williams (1984) have shown a similar effect of feed restriction after weaning. Finally, a clear negative effect of nutritional restriction was also observed on embryo survival in both gilts (Almeida *et al.*, 2000) and sows (Zak *et al.*, 1997b). In these experiments, a reduction of 15 and 23%, respectively, in the number of embryos surviving to day 30 of gestation was observed. Such losses would have dramatic consequences on sow reproductive efficiency since they represent 1.5 to 2.5 fewer piglets per litter from an average litter size of 10. In a more recent series of experiments with lactating sows, Vinsky *et al.* (2006) reported that the reduction in embryo survival observed in restricted sows was linked to the specific loss of female embryos. However, in this latest experiment, weaning-to-estrus interval and ovulation rate was not affected by feed restriction.

Studies from our laboratory have clearly established that the detrimental consequences of feed restriction during the last week of lactation on sow reproductive efficiency are mediated, at least partially, through differences in follicle and oocyte quality. Using in vitro culture techniques, Zak *et al.* (1997a) demonstrated that the oocytes recovered from nutritionally restricted primiparous sows in the late follicular phase (approximately 5 days after weaning) showed a lower ability to reach metaphase II (MII). Similarly, the follicular fluid aspirated from the follicles of restricted sows was less capable of supporting the maturation of generic prepubertal gilt oocytes, as shown by a lower proportion of metaphase II and a higher proportion of metaphase I (MI) oocytes after 46 h of culture. Later studies also established a relationship between the extent of protein catabolism and follicle and oocyte quality (Clowes *et al.*, 2003a, Clowes *et al.*, 2003b, Yang *et al.* 2000). In their studies, Clowes *et al.* (2003a,b) showed that primiparous sows with greater body protein lost during lactation had fewer large follicles and lower follicular fluid oestradiol (E2) at weaning. This difference in follicle

maturity was also reflected in the diminished ability of the follicular fluid aspirated from such follicles, to support oocyte nuclear maturation of prepubertal gilt oocytes. In their study, Yang *et al.* (2000) came to the similar conclusion that lower dietary lysine intake in primiparous sows changed the ratio of medium and large follicles present among the largest 15 follicles on the ovary and that the follicular fluid obtained from those follicles was less capable of supporting oocyte nuclear maturation of generic pools of oocyte in vitro. Again, the largest follicles isolated from the sows fed low lysine had lower oestradiol concentrations. Furthermore, delay of breeding until the second oestrus post-weaning is beneficial to sow fertility and resulted in an increase of approximately 2 piglets per litter (Clowes *et al.*, 1994). This likely allows the sows to rebound from the increased catabolism associated with lactation. Recently, it was shown that the increased litter size observed in the sows bred at the second oestrus post-weaning is a reflection of the increased embryo survival observed in those sows and is likely mediated by changes in follicle maturity as observed by differences in follicle size at breeding (Foxcroft *et al.*, 2007).

Modulation of gonadotrophin secretion has been associated with the effect of sow nutrition on ovarian follicle development. Lutenizing hormone (LH) pulsatility increases gradually as lactation progresses and more dramatically at weaning, allowing for the normal development of the preovulatory follicle population (Foxcroft *et al.*, 1987, Kemp *et al.*, 1995). However, several studies have shown that underfeeding lactating sows suppressed LH secretion (mean concentration and/or pulse frequency) (Quesnel *et al.*, 1998, van den Brand *et al.*, 2000, Zak *et al.*, 1997b, Zak *et al.*, 1998), which is likely to have consequences for the ability of the follicle to grow and mature properly. In addition, LH pulsatility in weaned sows is rapidly restored after the end of the restriction (Quesnel *et al.*, 1998). On the other hand, follicle stimulating hormone (FSH) secretion does not appear to be affected by restriction in most cases (reviewed by Prunier and Quesnel, 2000b). Moreover, the effects of nutrition mediated by changes in gonadotrophin secretion, other metabolic factors, including insulin and insulin-like growth factors (IGF) could act at the ovarian level to modulate follicle

and oocyte quality. Several studies have reported that circulating levels of insulin (Mullan and Close, 1991, Zak *et al.*, 1997b) and insulin-like growth factor 1 (IGF1) (Mao *et al.*, 1999, Quesnel *et al.*, 2005, Tokach *et al.*, 1993, Zak *et al.*, 1997b) are low in restricted lactating sows, indicating that these sows are under intense catabolic conditions. In vitro studies have demonstrated that insulin and IGF1 affect granulosa cell functions, particularly proliferation and steroidogenesis (reviewed by Prunier and Quesnel, 2000a, b), strongly implying the potential for insulin and IGF1 to modulate follicle quality. However, the relationship between circulating and local IGF1 is not clear, as several studies find little change in follicular fluid IGF1 between sows of various catabolic states (Clowes *et al.*, 2003, Yang *et al.*, 2000). Again, in a study using cyclic gilts subjected to feed restriction or refeeding, circulating levels of IGF1 were lower in restricted animals while no changes in follicular fluid were observed, suggesting a disconnect between plasma and follicular fluid IGF1 (Charlton *et al.*, 1993). Although progress has been made in understanding the physiological events responsible for nutritionally-mediated effects on sow reproductive efficiency, the direct effects of under-nutrition on the follicular environment are still unclear.

In the swine industry, the number of live pigs born per sow per year is a major component of productivity and ultimately to the profit for the producers. The number of pigs born per sow per year is dependant on two main variables, the number of litters produced by the sow and the number of piglets per litter. The latter variable is affected by multiple parameters such as ovulation and fertilization rate, which are believed to be minor determining factors, and prenatal mortality that can contribute up to 40% of embryos lost (Pope, 1994). As discussed earlier, nutritional manipulations have been shown to affect sow fertility and these effects are believed to occur, at least partially, through modification of follicle and oocyte quality. Understanding the mechanisms necessary for normal follicle and oocyte growth, as well as the those leading to differences in embryo survival resulting from divergence in follicle and oocyte quality, is therefore of tremendous practical and economical significance.

The purpose of the literature review presented in Chapter 2 of this thesis is to provide a comprehensive background to the complex molecular and cellular events and interactions necessary for the coordination of antral follicle development. This chapter is therefore divided into three main sections, in which the dynamics of follicle growth, the involvement of the gonadotrophins during follicle development and the involvement of key intrafollicular growth factors in the regulation of folliculogenesis are addressed.

The objectives of the series of studies described in the subsequent experimental chapters sought to further clarify the intrafollicular mechanisms responsible for normal preovulatory follicle development in the pig, more specifically in regard to the process of recruitment, selection and establishment of the preovulatory follicle population. Moreover, a well-established experimental paradigm known to affect sow fertility was deliberately used to investigate the role of these intrafollicular factors in creating the differences in follicle and oocyte quality observed in the sows during the 1st and 2nd post-weaning oestrus. Importantly, the sequential recovery of follicles during the known preovulatory phase of follicle development, and follicular status was validated on the basis of size and follicular fluid oestradiol concentration. Therefore, the biological relevance of the current data reported, in relation to the *in vivo* process of folliculogenesis in the sows, will be much greater than data reported from other studies with ovarian tissues obtained from prepubertal gilts subjected to exogenous gonadotrophin stimulation or other manipulations.

The objective of initial study described in Chapter 3 was to identify growth factors and receptors produced by the pig oocyte, granulosa and theca cells. It also describes the temporal changes in mRNA abundance for several members of the insulin-like growth factor (IGF) and epidermal growth factor (EGF) families during follicle recruitment, mid-selection and final selection before and after the LH surge, and proposes roles for these growth factors in the developing preovulatory follicle.

The transforming growth factor β (TGF- β) superfamily has been shown in several species to affect follicle and oocyte development, as well as ovulation rate in the sheep (Juengel and McNatty, 2005, Gilchrist *et al.*, 2008). The objectives of the second study (Chapter 4) were to address the hypothesis that members of this family of growth factors are expressed in the porcine ovarian follicle and are likely to affect the process of follicle recruitment, mid-selection and final selection. Moreover, the potential for these growth factors to affect follicle and oocyte quality was investigated.

The development of appropriate blood vasculature during the development of antral follicles was shown to be important for their growth and normal function (Fraser, 2006, Shimizu *et al.*, 2003, Tamanini and De Ambrogi, 2004). The third study (Chapter 5) was therefore designed to identify angiogenic factors expressed in the granulosa and theca cells of developing porcine antral follicles, to establish the temporal regulation of several key angiogenic factors during recruitment, mid-selection and final selection before and after the LH-surge, and to evaluate if any of these factors could affect follicle quality.

The oocyte, originally thought to be passive during follicle growth, is now known to secrete soluble factors (Juengel and McNatty, 2005, Gilchrist *et al.*, 2008) that are important for orchestrating follicle development (Eppig *et al.*, 2002, Matzuk *et al.*, 2002). The last study (Chapter 6) was therefore designed to assess the role of porcine preovulatory germinal vesicle (GV) oocytes in controlling cumulus cell functions. More specifically, the effect of the oocyte on cumulus cell protein and gene expression was investigated.

Finally, Chapter 7 of this thesis presents a general discussion of the overall impact of this research on our understanding of the local interactions necessary to coordinate porcine follicle growth. It also presents a perspective of the future studies that could further improve our understanding of folliculogenesis.

REFERENCES

- Almeida FR, Kirkwood RN, Aherne FX & Foxcroft GR** 2000 Consequences of different patterns of feed intake during the estrous cycle in gilts on subsequent fertility. *J Anim Sci* **78** 1556-1563.
- Ashworth CJ** 1991 Effect of pre-mating nutritional status and post-mating progesterone supplementation on embryo survival and conceptus growth in gilts. *Anim Reprod Sci* **26** 311-321.
- Beltranena E, Aherne FX, Foxcroft GR & Kirkwood RN** 1991 Effects of pre- and postpubertal feeding on production traits at first and second estrus in gilts. *J Anim Sci* **69** 886-893.
- Bracken CJ, Radcliff RP, McCormack BL, Keisler DH & Lucy MC** 2006 Decreased follicular size during late lactation caused by treatment with charcoal-treated follicular fluid delays onset of estrus and ovulation after weaning in sows. *J Anim Sci* **84** 2110-2117.
- Charlton ST, Cosgrove JR, Glimm DR & Foxcroft GR** 1993 Ovarian and hepatic insulin-like growth factor-I gene expression and associated metabolic responses in prepubertal gilts subjected to feed restriction and refeeding. *J Endocrinol* **139** 143-152.
- Clowes EJ, Aherne FX & Foxcroft GR** 1994 Effect of delayed breeding on the endocrinology and fecundity of sows. *J Anim Sci* **72** 283-291.
- Clowes EJ, Aherne FX, Schaefer AL, Foxcroft GR & Baracos VE** 2003a Parturition body size and body protein loss during lactation influence performance during lactation and ovarian function at weaning in first-parity sows. *J Anim Sci* **81** 1517-1528.
- Clowes EJ, Aherne FX, Foxcroft GR & Baracos VE** 2003b Selective protein loss in lactating sows is associated with reduced litter growth and ovarian function. *J Anim Sci* **81** 753-764.
- Cox NM, Stuart MJ, Althen TG, Bennett WA & Miller HW** 1987 Enhancement of ovulation rate in gilts by increasing dietary energy and administering insulin during follicular growth. *J Anim Sci* **64** 507-516.
- Eppig JJ, Wigglesworth K & Pendola FL** 2002 The mammalian oocyte orchestrates the rate of ovarian follicular development. *Proc Natl Acad Sci U S A* **99** 2890-2894.
- Flowers B, Martin MJ, Cantley TC & Day BN** 1989 Endocrine changes associated with a dietary-induced increase in ovulation rate (flushing) in gilts. *J Anim Sci* **67** 771-778.

Foxcroft GR, Shaw HJ, Hunter MG, Booth PJ & Lancaster RT 1987 Relationships between luteinizing hormone, follicle-stimulating hormone and prolactin secretion and ovarian follicular development in the weaned sow. *Biol Reprod* **36** 175-191.

Foxcroft GR 1997 Mechanisms mediating nutritional effects on embryonic survival in pigs. *J Reprod Fertil Suppl* **52** 47-61.

Foxcroft GR, Vinsky MD, Paradis F, Tse WY, Town SC, Putman CT, Dyck MK & Dixon WT 2007 Macroenvironment effects on oocytes and embryos in swine. *Theriogenology* **68 Suppl 1** S30-39.

Fraser HM 2006 Regulation of the ovarian follicular vasculature. *Reprod Biol Endocrinol* **4** 18.

Gilchrist RB, Lane M & Thompson JG 2008 Oocyte-secreted factors: regulators of cumulus cell function and oocyte quality. *Hum Reprod Update* **14** 159-177.

Juengel JL & McNatty KP 2005 The role of proteins of the transforming growth factor-beta superfamily in the intraovarian regulation of follicular development. *Hum Reprod Update* **11** 143-160.

Kemp B, Soede NM, Helmond FA & Bosch MW 1995 Effects of energy source in the diet on reproductive hormones and insulin during lactation and subsequent estrus in multiparous sows. *J Anim Sci* **73** 3022-3029.

King RH & Williams IH 1984 The effect of nutrition on the reproductive performance of first-litter sows: 1. Feeding level during lactation, and between weaning and mating. *Anim Prod* **38** 241-247.

Tokach MD, Pettigrew JE, Frey RS, Hathaway MR & Dial GD 1993 Relationship of IGF-1 and B-hydroxy butyrate to LH secretion and return to estrus interval in primiparous lactating sows. *Presented at the IV International conference on pig reproduction* (Abstract).

Mao J, Zak LJ, Cosgrove JR, Shostak S & Foxcroft GR 1999 Reproductive, metabolic, and endocrine responses to feed restriction and GnRH treatment in primiparous, lactating sows. *J Anim Sci* **77** 724-735.

Matzuk MM, Burns KH, Viveiros MM & Eppig JJ 2002 Intercellular communication in the mammalian ovary: oocytes carry the conversation. *Science* **296** 2178-2180.

Mullan RH & Close WH 1991 Metabolic and endocrine changes during the reproductive cycle of the sow. In *Manipulation of Pig Production III*, p. 32, Eds ES Batterham. Attwood, Australia: Australian Pig Science Association.

Pope WF 1994 Embryonic mortality in swine. In *Embryonic mortality in domestic species*, pp 53-77, edn. Eds MT Zavy & RD Geiser. CRC Press.

Prunier A & Quesnel H 2000a Influence of the nutritional status on ovarian development in female pigs. *Anim Reprod Sci* **60-61** 185-197.

Prunier A & Quesnel H 2000b Nutritional influences on the hormonal control of reproduction in female pigs. *Livest Prod Sci* **63** 1-16.

Quesnel H, Pasquier A, Mounier AM & Prunier A 1998 Influence of feed restriction during lactation on gonadotropic hormones and ovarian development in primiparous sows. *J Anim Sci* **76** 856-863.

Quesnel H, Mejia-Guadarrama CA, Dourmad JY, Farmer C & Prunier A 2005 Dietary protein restriction during lactation in primiparous sows with different live weights at farrowing: I. Consequences on sow metabolic status and litter growth. *Reprod Nutr Dev* **45** 39-56.

Shimizu T, Kawahara M, Abe Y, Yokoo M, Sasada H & Sato E 2003 Follicular microvasculature and angiogenic factors in the ovaries of domestic animals. *J Reprod Dev* **49** 181-192.

Tamanini C & De Ambrogi M 2004 Angiogenesis in developing follicle and corpus luteum. *Reprod Domest Anim* **39** 206-216.

van den Brand H, Dieleman SJ, Soede NM & Kemp B 2000 Dietary energy source at two feeding levels during lactation of primiparous sows: I. Effects on glucose, insulin, and luteinizing hormone and on follicle development, weaning-to-estrus interval, and ovulation rate. *J Anim Sci* **78** 396-404.

Vinsky MD, Novak S, Dixon WT, Dyck MK & Foxcroft GR 2006 Nutritional restriction in lactating primiparous sows selectively affects female embryo survival and overall litter development. *Reprod Fertil Dev* **18** 347-355.

Yang H, Foxcroft GR, Pettigrew JE, Johnston LJ, Shurson GC, Costa AN & Zak LJ 2000 Impact of dietary lysine intake during lactation on follicular development and oocyte maturation after weaning in primiparous sows. *J Anim Sci* **78** 993-1000.

Zak LJ, Xu X, Hardin RT & Foxcroft GR 1997a Impact of different patterns of feed intake during lactation in the primiparous sow on follicular development and oocyte maturation. *J Reprod Fertil* **110** 99-106.

Zak LJ, Cosgrove JR, Aherne FX & Foxcroft GR 1997b Pattern of feed intake and associated metabolic and endocrine changes differentially affect postweaning fertility in primiparous lactating sows. *J Anim Sci* **75** 208-216.

Zak LJ, Williams IH, Foxcroft GR, Pluske JR, Cegielski AC, Clowes EJ & Aherne FX 1998 Feeding lactating primiparous sows to establish three divergent metabolic states: I. Associated endocrine changes and postweaning reproductive performance. *J Anim Sci* **76** 1145-1153

CHAPTER 2

LITERATURE REVIEW

INTRODUCTION

In mammals, the ability of the female to reproduce is highly dependent on the production of functional oocytes that are competent to be fertilized and to develop into viable embryos. The acquisition of oocyte developmental competence occurs over a long period of time within the ovary and is dependent on the nurturing environment of the follicle. Therefore, to maximize female fertility it is essential to understand the physiological and molecular mechanisms responsible for coordinating follicle and oocyte growth.

At birth, the ovary contains a lifetime supply of oocytes stored in quiescent primordial follicles that, once recruited to grow, will either proceed to ovulation or, in more than 99% of the cases, will become atretic (Hunter *et al.*, 2000). Follicle(s) destined to ovulate will proceed through the preantral and antral phases of follicle growth during which time the porcine primordial follicle will increase in size from approximately 20-30 μm to around 10 mm at the preovulatory stage (Hunter *et al.*, 2000). The oocyte also grows considerably, starting at 20-30 μm in the primordial follicle to reach 120 μm in the preovulatory follicle. The increase in follicle size is accompanied by substantial cell proliferation. Moreover, antrum formation leads to the differentiation of the granulosa cell population into the mural granulosa cells that remain in close contact with the follicle wall, and the cumulus granulosa cells that closely surround the oocyte. These two granulosa cell populations differ greatly in their ability to proliferate and in their steroidogenic activities. While the mural granulosa cells are actively proliferative and highly steroidogenic, the cumulus cells are in close contact with the oocyte, providing it with metabolites and other important factors necessary for the acquisition of meiotic and developmental

competence. The theca cell layer formed during the late preantral stage is also important for the steroidogenic activity in the follicle.

The series of morphological and biochemical changes required for the follicle to grow and reach ovulation are extremely dynamic and their coordination requires the participation of extragonadal hormones, most importantly the gonadotrophins, and also local growth factors to modulate ovarian cell functions. This review will summarize our current understanding of the dynamics of porcine ovarian follicle growth. It will also address the endocrine regulation of antral follicle development, focusing primarily on the role of the gonadotrophins. Finally, the importance of several key local growth factors in the regulation of follicle cell function will also be reviewed. In the context of this thesis, emphasis will be given to data on antral follicle development in the pig whenever possible, but studies in other species will be reviewed when porcine data are not available.

DYNAMICS OF FOLLICULAR GROWTH

The pool of oocytes present in the adult mammalian ovary originates from the differentiation of the primordial germ cells that colonized the ovary during prenatal development. Around the time of birth, the ovary of every species possesses a defined number of resting primordial follicles each containing a primary oocyte that will remain quiescent until they are recruited to grow. Then, starting at puberty and continuing throughout the reproductive life of the female, pools of primordial follicles will be recruited to grow. Interestingly, most of these follicles (>99%) will undergo atresia and only a very few will eventually ovulate and be fertilized. In order to better appreciate how the endocrine signals and the local growth factors act to coordinate follicular development, it is essential to understand the morphological characteristics of the different stages of follicular development that follicles pass through prior to ovulation.

Stages of follicle development

Follicular development is a long and well-coordinated series of events characterized by follicular and oocyte growth, as well as cell proliferation and differentiation (Figure 2.1). At birth or shortly after, the mammalian ovary contains a lifetime supply of primordial follicles that will be recruited in waves from the resting pools to grow and possibly ovulate. In the pig, an estimated 500,000 primordial follicles are present at birth and decrease slightly to approximately 400,000 around puberty (Black and Erickson, 1968, Gosden and Telfer, 1987, Greenwald and Moor, 1989). These primordial follicles average 22.1 μm in diameter (Greenwald and Moor, 1989) and represent the fundamental units of the ovary. They are characterized as having a single layer of flattened granulosa cells (4-8 cells in cattle) often referred to as pre-granulosa cells (Figure 2.2A) (Fair, 2003). When the necessary signals are sent to these follicles (see later section on emergence or initial recruitment), they enter a period of growth that can be divided into preantral and antral growth phases. Alternatively, according to their growth rate, the preantral and antral growth phases are also referred to as the slow and rapid growth phase, respectively (Morbeck *et al.*, 1992).

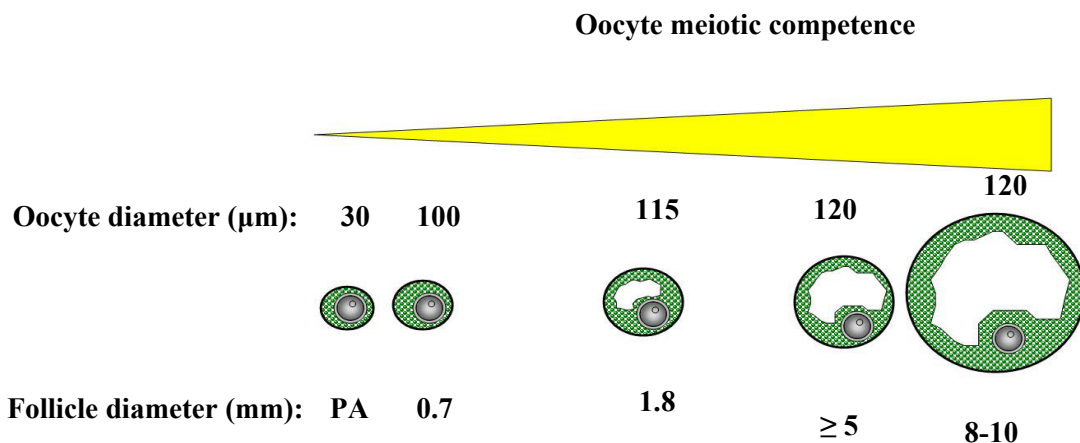


Figure 2.1 Follicle and oocyte growth and acquisition of meiotic competence in the pig. Adapted from Hunter, 2000.

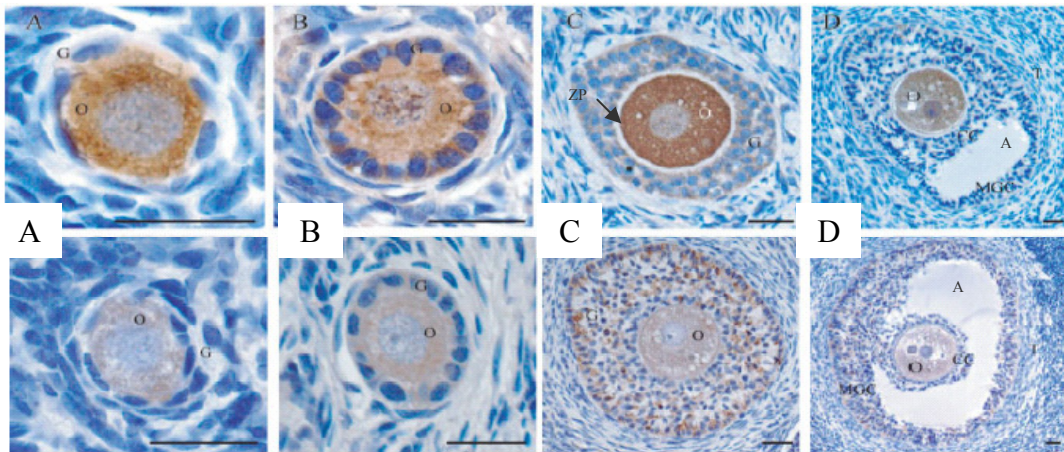


Figure 2.2 Images of the different stages of follicular development observed in the goat ovary. A) Primordial B) Primary C) Secondary and D) Tertiary or Antral follicles. Adapted from Silva *et al.*, 2005. These pictures have been taken of goat follicles but are very similar to porcine follicles. O = oocyte, GC = granulosa cell, CC = cumulus cell, MGC = mural granulosa cells, ZP = zona pellucida, A = antrum.

During preantral growth, the follicle will first go through the primary stage of development during which the surrounding layer of granulosa cells start proliferating and become cuboidal (Figure 2.2B). Then they will progress to the secondary stage that can be recognized by the presence of two or more layers of granulosa cells. Also during this period, at least in the cow, the zona pellucida can first be observed (Figure 2.2C) (Fair, 2003). Moreover, according to van den Hurk (2005), the theca cell layer also develops during the secondary stage of development. The follicle will keep growing to reach the tertiary or antral stage that is characterized by the presence of multilayered granulosa cells, and also by the formation of the antrum (Figure 2.2D). At this stage, two distinct populations of granulosa cells start to differentiate. The granulosa cells attached to the follicle wall become the mural granulosa cells (MGC). These cells are primarily responsible for the endocrine activity of the follicle, including steroidogenesis. In contrast, the granulosa cells closely surrounding the oocyte become the cumulus

granulosa cells (CGC) and their primary function is to provide the oocyte with the metabolites and other stimuli necessary for oocyte growth and for the acquisition of meiotic competence. Finally, the follicles destined to ovulate will grow until they reach the preovulatory size characteristic of each species (around 8-10 mm in the pig) (Hunter, 2000).

Based on the specific mitotic index of granulosa cells isolated from various follicle categories, Morbeck *et al.* (1992) were able to determine the growth rate for each category of porcine follicle. They established that smaller follicles grew more slowly than larger follicles. From this, they were also able to determine the time needed for porcine follicular development from the initiation of primordial follicle growth to the preovulatory stage. As shown in Figure 2.3, a primordial follicle is estimated to require approximately 84 days before reaching the antral stage. Another 14 days is then necessary for an early antral follicle to develop to a 3 mm follicle. Finally, based on an estimated growth rate of 1 mm/day for follicles larger than 3 mm (Dailey *et al.*, 1976), it was estimated that a 3 mm follicle requires 5 days to reach preovulatory status. Therefore, it was estimated that roughly 100 days are needed for a porcine primordial follicle to ovulate. Interestingly, it also takes approximately 90 days for a bovine primordial follicle to reach the preovulatory stage (Fair, 2003). However, ovine and human follicular development is much longer, requiring 175 and 200 days, respectively to reach the preovulatory stage (Cahill and Mauleon, 1980, Gougeon *et al.*, 1996).

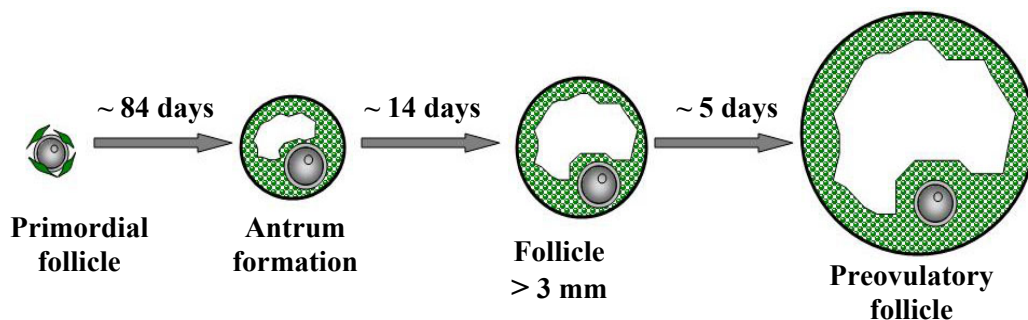


Figure 2.3 Time scale for pig follicular growth. Adapted from Hunter, 2000 but based on Morbeck *et al.*, 1992 and Dailey *et al.*, 1976.

In addition to follicular growth, oocytes also grow considerably throughout follicular development, starting at less than 30 μm in primordial follicles and reaching an average of 120 μm in the Graafian or preovulatory follicle (Figure 2.1) (Hunter, 2000). According to Morbeck *et al.* (1992), oocyte growth is almost linear until the follicle reaches 300 μm in diameter after which the size of the oocyte remains relatively constant until ovulation. These results are also in agreement with the study of Motlik and Fulka (1986) that reported that follicles of 0.3-0.7 mm contain oocytes that average 100 μm in diameter. However, according to these data, when the follicles reach 1.8 mm in diameter the oocytes are already almost at ovulatory size (115 μm). Another important event that occurs during oocyte growth is the acquisition of meiotic and developmental competence, associated with the ability of the oocyte to undergo meiotic maturation, fertilization and development. As illustrated on Figure 2.1, oocytes from smaller follicles (< 0.7 mm) are meiotically incompetent, while most of the oocytes from larger follicles (≥ 5 mm) are considered to be competent (Hunter, 2000). Interestingly, the ability to complete the metaphase I to metaphase II transition also coincides with the end of nucleolar transcriptional activity (McGaughey *et al.*, 1979), suggesting that critical factors need to be accumulated toward the end of the oocyte growth phase.

Finally, greater than 99% of follicles/oocytes will undergo atresia at one point or another during folliculogenesis. In the pig, the incidence of atresia increases with follicle size and is lowest among primordial ($\leq 6\%$) and preantral ($\leq 17\%$) follicles and highest among the antral follicle population (averaging 55% in pre- and postpubertal gilts). Detailed reviews on apoptosis and atresia in the porcine follicle have been presented by Guthrie and Garrett (2001), Manabe *et al.* (2004) and Manabe *et al.* (2008).

Defined phases of follicular development

As mentioned in the previous section, follicular growth can also be divided into the preantral or slow growth phase and the antral or rapid growth

phase. However, it can also be divided according to the gonadotrophin requirement of the follicles. In this way, the development of follicles can be grouped into gonadotrophin-independent and gonadotrophin-dependent phases. It is generally accepted that the initial recruitment of primordial follicles, as well as preantral follicle growth, is gonadotrophin-independent and relies mostly on local ovarian factors (Foxcroft *et al.*, 1994). On the other hand, the gonadotrophin-dependent phase can be divided into recruitment of the preovulatory pool of follicles, selection of the ovulatory population and dominance. During these last steps the species-specific ovulation rate is determined (12 to 20 ovulations in the pig; Hunter *et al.*, 2004). The following section will address the specific characteristics of each of these phases.

Emergence or initial recruitment and preantral growth

Primordial follicles remain quiescent in the ovary until groups of follicles are recruited from the resting pool into the growing population. Most evidence suggests that gonadotrophins are unlikely to be a critical factor for initiating primordial follicle growth. First of all, in several species including the pig the gene for the follicle-stimulating hormone receptor (FSHR) is not expressed until the follicle reaches the primary or secondary stage of development (Tisdall *et al.*, 1995; Xu *et al.*, 1995; Yuan *et al.*, 1996, Oktay *et al.*, 1997). Moreover, FSH-knockout mice and hypophysectomized hamsters, rats and sheep all contain normally developing small preantral follicles (Kumar *et al.*, 1997; Hirshfield *et al.*, 1985; McNatty *et al.*, 1990, Wang and Greenwald, 1993). Similar to FSHR, lutenizing hormone receptor (LHCGR) in the pig is also expressed later during follicular development, and is detected only when the follicles reach the large preantral/small antral stages (Yuan *et al.*, 1996).

In addition, superstimulating doses of exogenous gonadotrophins do not appear to increase the rate of recruitment in the mouse, and chronic administration of gonadotrophins does not prematurely deplete the population of primordial follicles in the ovary (Danfour *et al.*, 1999). Another line of evidence supporting the concept that gonadotrophins are not involved in the initiation of primordial

follicle growth comes from *in vitro* experiments with bovine tissues. In these experiments, slices of ovarian cortex cultured in gonadotrophin-free media had an increased number of primary and small preantral follicles, corresponding to a decrease in the number of primordial follicles, suggesting the involvement of paracrine/autocrine factors rather than gonadotrophins in the initiation of primordial follicle growth (Wandji *et al.*, 1996, Braw-Tal and Yossefi, 1997).

Interestingly, follicular development in gilts treated with either the gonadotrophin-releasing hormone (GnRH) antagonist Antarelix to reduce plasma LH, or in hypophysectomized gilts which lacked both gonadotrophins, was comparable to the control animals until the follicles reached 2 to 4 mm (Driancourt *et al.*, 1995). A similar experiment has also been done in cattle using a GnRH agonist to decrease LH and eventually also plasma FSH concentration (Gong *et al.*, 1996 Webb and Armstrong, 1998). In these experiments, continuous administration of GnRH agonist led to a decrease in LH concentration and arrested follicular growth at around 7 to 9 mm. Prolonged administration of GnRH agonist then led to a fall in FSH concentration which caused the follicle to arrest at 4 mm. Altogether, these results suggest that, for the most part, the initiation of primordial follicle growth, as well as preantral and early antral development in livestock species, is independent of gonadotrophins.

However, evidence from Campbell *et al.* (2004) suggests that FSH could affect the development of sheep preantral follicles. In an autografting experiment, these authors showed that the ovarian cortex recovered from the grafted untreated animals, which were hypergonadotrophic (Hyper) because of the ovariectomy procedure, had reestablished a normal follicular hierarchy 2 months earlier than the autografted animal treated with GnRH agonist and oestradiol implants, which acted to suppress the hypothalamic-pituitary axis and thus keep the ewes hypogonadotrophic (Hypo). Moreover, plasma concentrations of inhibin (INH) A and oestradiol, as well as the rate of granulosa cell proliferation were higher in the Hyper ewes compared to the Hypo group. On the other hand, it is possible that the rate of ovarian revascularization after autografting was increased in the Hyper

sheep, therefore favoring the faster reinitiation of follicle development that was observed. This confounding effect will require further investigation. However, although preantral follicles may be largely independent of gonadotrophins, it is important to consider the potential for such follicles to be sensitive to gonadotrophic stimulation.

Finally, many intraovarian growth factors have been studied in order to understand how primordial follicles are initially recruited to grow, and also to gain insight on early (preantral) folliculogenesis. Among these factors, the Anti-Müllerian hormone, KIT/Kit Ligand, members of the transforming growth factor (TGF)- β superfamily, growth differentiation factor (GDF)-9 and bone morphogenetic protein (BMP)-15, and activin/follistatin are thought to be of great importance and have been actively studied in recent years (for detailed reviews on the role of these factors in early follicle growth see Fortune, 2003, Picton, 2000 and Trombly *et al.*, 2009). However, when compared to knowledge on the regulation of antral follicular growth, relatively little is known about the control of preantral growth. Experimental techniques allowing better primordial follicle isolation and *in vitro* culture will likely greatly help in understanding the initial phases of folliculogenesis.

Recruitment, selection and dominance

As mentioned in the previous section, porcine follicles can grow up to 2 mm in hypophysectomized and hypophyseal stalk-transected (HST) animals, and up to 4 mm in GnRH antagonist treated animals, suggesting that follicles become dependent on FSH at a diameter of around 2 mm and LH dependent at around 4 mm (Driancourt *et al.*, 1995, Kraeling *et al.*, 1986). Similarly, bovine follicles become dependent on FSH at around 4 mm and LH-dependent at 7 to 9 mm as shown by the absence of further follicular development after continuous GnRH agonist treatment (Gong *et al.*, 1996). Several physiological events occur during this period of gonadotrophin dependence. Therefore, the terms recruitment, selection and dominance have been used to identify the distinct processes leading to final follicular development.

Recruitment is defined as a gonadotrophin-dependent event during which a group of follicles gain the ability to respond to gonadotrophins and require gonadotrophins for continued growth (Ireland, 1987). Extensive data conclusively demonstrated that FSH is a key hormone for inducing recruitment in cattle. Firstly, a transient increase in plasma FSH is associated with the initiation of waves of follicular growth (Adams *et al.*, 1992). Moreover, in experiments where endogenous FSH secretion was blocked and exogenous FSH was injected, it was possible to show that decreased endogenous concentrations of FSH resulted in the disappearance of follicles larger than 4 mm, while exogenous FSH reinitiated recruitment (Crowe *et al.*, 2001, Webb *et al.*, 1999). It was also shown that increased expression of the steroidogenic enzymes cytochrome P450 side chain cleavage (CYP11A1) and cytochrome P450 aromatase (CYP19A1) in bovine granulosa cells, accompanying the transient rise in FSH, is associated with the recruitment process (Webb *et al.*, 1999). As a consequence, recruitment also increases the ability of bovine follicles to produce oestrogen.

In the pig, recruitment occurs between days 14 and 16 of the oestrous cycle, coinciding with luteolysis, and given the appropriate stimulation, a pool of approximately 50 follicles will develop (Foxcroft *et al.*, 1994, Hunter and Wiesak, 1990). Recruitment is characterized by the gradual transition of the antral follicle population from small to larger size follicle. As in cattle, it has been shown in the pig that exogenous administration of equine chorionic gonadotrophins (eCG or PMSG) to GnRH agonist-treated animals can reverse the inhibition of follicular development (Miller *et al.*, 1999). However, these data must be interpreted with care, since eCG contains both LH and FSH-like activity. Interestingly, in another experiment the same research group investigated the effect of FSH alone on follicular growth in GnRH agonist-treated animals (Picton *et al.*, 1999). As expected, the animals infused with FSH developed larger follicles than the animals treated with the GnRH agonist in which no follicle grew larger than 4 mm. Surprisingly, the animals infused with FSH developed many follicles of preovulatory size (> 6 mm). These results are not in agreement with the report of Driancourt *et al.* (1995) that showed that LH-deprived animals with normal FSH

levels grew follicles up to 4 mm only. This discrepancy in the experiments of Driancourt *et al.* (1995), and those of Miller *et al.* (1999) and Picton *et al.* (1999), in the size at which follicles arrest their growth might be due to the basal secretion of FSH found in the two latter experiments. Moreover, the results of Liu *et al.* (2000) suggest that follicles start to express the mRNA for the steroidogenic enzymes cytochrome P450 17 α -hydroxylase (CYP17A1) and CYP19A1 and also start to synthesize oestradiol once they reach approximately 2 mm in diameter. Therefore, similar to cattle, it seems that pig follicles gain the ability to produce oestradiol around the time of recruitment. Whether the recruitment process is responsible for the ability of the follicle to synthesize oestradiol, or the synthesis of oestradiol is necessary prior to recruitment, is difficult to determine and will require further investigation. However, taken together these results strongly support the hypothesis that FSH is of primary importance for the recruitment of growing follicles.

In contrast to recruitment, which seems to be a fairly well-defined process, follicle selection and dominance are closely linked. Although the concept of dominance has been first suggested in ruminant (monovulatory) species and may also apply to polyovulatory species such as the pig, slight adaptations to the concept may be necessary. First of all, the term selection is defined as a process whereby only a few of the recruited follicles are selected to escape atresia and survive to ovulate, while dominance can be defined as the mechanisms that the ovulatory population of follicles uses to survive in a environment suppressive to the growth of other follicles (Ireland, 1987).

It is generally accepted that healthy growing mammalian follicles increasingly produce oestradiol and inhibin, which in turn will act through a classical long negative feedback loop on the pituitary to regulate FSH secretion. Moreover, it has been shown that LH receptor mRNA increases, while FSH receptor mRNA decreases, as follicles develop from 2 mm to 6 mm in size (Liu *et al.*, 2000). Similarly, in an experiment using radiolabeled FSH and LH, Nakano *et al.* (1983) have shown that FSH binding decreased as the follicles grew from 1-

2 mm to 6-10 mm. In contrast, the LH signal was amplified as the follicles grew larger, due to the appearance of LH receptors on the granulosa cells of 6-10 mm follicles. These results strongly suggest that during selection, the follicles switch from FSH dependence to LH dependence. In addition, Liu *et al.* (2000) have shown that oestradiol concentrations in follicular fluid closely follow the expression pattern of LH receptors and mRNA for steroidogenic enzymes, suggesting that LH is essential to increase steroid production. This observation is supported by the results of Picton *et al.* (1999) in the pig, who found that although follicles stimulated with FSH could grow to preovulatory size, after 6 mm in diameter they were producing less oestradiol and testosterone than the follicles recovered from late follicular phase gilts. One of the possible hypotheses to explain the phenomenon of selection and dominance is that as the follicles grow under the influence of FSH they acquire more LH receptors. In turn, this allows the follicles to produce increasing amounts of oestrogen. In parallel, the growing follicles also produce more and more inhibin, which in combination with oestrogen, will act on the pituitary to reduce FSH release. This reduction in plasma FSH will cause the smaller follicles that are still highly dependent on FSH to undergo atresia, while the larger follicles possessing LH receptors on granulosa cells can survive FSH deprivation. The only remaining question concerns the fate of medium size follicles, which might still be partially dependent on FSH. One suggestion is that in polyovulatory species a portion of these follicles will be carried into the selected preovulatory population by the established dominant follicles and thus complete the ovulatory pool (Foxcroft *et al.*, 1994). This is supported by the observation that oestradiol can act in a paracrine manner to induce gonadotrophin receptors in smaller follicles (Richards *et al.*, 1976, Richards *et al.*, 1979, Rosenfeld *et al.*, 2001). This could allow the smaller follicles to survive with lower concentrations of FSH until they acquire LH receptors on the granulosa cells. Moreover, oestradiol has also been shown to inhibit granulosa cell apoptosis, which is the main mechanism associated with follicle atresia (Billig *et al.*, 1993, Rosenfeld *et al.*, 2001). Finally, it is important to consider that this hypothesis explaining the processes of selection and

dominance in the pig is an oversimplification since it does not take into account other factors such as the IGF systems and inhibin/activin/follistatin that can synergize with the gonadotrophins to modify the responsiveness of the follicle. However, it gives a general overview of how the gonadotrophins might be involved in this process.

EXTRAOVARIAN CONTROL OF FOLLICLE DEVELOPMENT

In the previous section, it was clearly established that antral follicles are dependent on the gonadotrophins (FSH and LH) for successful growth and ovulation. Therefore, the following section will address key information related to gonadotrophin production, regulation and the mechanisms of action of the gonadotrophins on the follicle.

Hypothalamus and pituitary gland

The hypothalamic-pituitary complex is responsible for the production of many hormones important for various physiological processes including control of mammalian reproductive function. The gonads or more specifically in the context of this review, the ovaries, are the primary targets of these reproductive hormones. Therefore, understanding the hypothalamic-pituitary-ovarian interactions necessary for the synthesis and release of these hormones, as well as their mechanisms of action and function in the follicle, is essential in order to better understand how these endocrine signals influence follicular development.

Hypothalamus

In addition to its production of oxytocin and vasopressin, the hypothalamus is involved in the control of the secretion of various hormones via different mechanisms specific for each hormone. The hypothalamus is generally defined as comprising the floor and walls of the third ventricle and as such is located at the base of the skull and is part of the central nervous system. It can be divided into many zones, which contain many nuclei formed by different groups

of neurons. Based on their morphology these neurons can be divided into the magnocellular neurons (going into the neurohypophysis) and the parvocellular neurons (affecting the adenohypophysis). Only the parvocellular neuronal products will be discussed in this review.

The anterior pituitary is irrigated by a network of capillaries that originate from the median eminence. This complex of hypophyseal portal vessels is responsible for the transfer of neuropeptides from the hypothalamus to the hypophysis where they will act on specific cells to trigger the release of the pituitary hormones. In the case of the gonadotrophins, the hypothalamus produces a decapeptide known as GnRH that will stimulate the gonadotrophs to secrete both LH and FSH. However, as discussed later, LH seems to be tightly linked to GnRH secretion while FSH is also regulated by other ovarian factors. Thyroid stimulating hormone (TSH) and adrenocorticotrophic hormone (ACTH) are also regulated in a similar manner, by a thyroid and a corticotrophin-releasing hormone that will be released into the portal vessels to act on the thyrotrophs and corticotrophs. On the other hand, growth hormone (GH) and prolactin (PRL) are under different regulatory mechanisms. First, GH is under the regulation of both a growth hormone releasing hormone (GHRH) that stimulates, and somatostatin that inhibits its secretion. Prolactin is under tonic inhibitory control by a signal that has been identified as dopamine. Therefore, in order for PRL to be released, dopamine secretion must be inhibited.

Pituitary gland

Firstly, the pituitary (also known as hypophysis) is located in the sella turcica of the sphenoid bone at the base of the skull and comprises an anterior lobe (adenohypophysis), intermediate lobe and the posterior lobe (neurohypophysis). Each lobe has a unique embryonic origin, acts as a separate endocrine organ, and is characterized by distinct cell populations, secretory products and regulatory mechanisms (Amar and Weiss, 2003).

The adenohypophysis is composed of large polygonal cells separated by an extensive network of capillaries. These cells produce six well-established hormones known as TSH, ACTH, FSH, LH, GH and PRL, which are described above. Each cell type was formerly classified based on the affinity of their cytoplasmic granules to various dyes (acidophils, basophils and chromophobes); however, based on modern microscopic techniques at least six cell populations are currently recognized (Somatotropes (GH), Lactotropes (PRL), Corticotrophs (ACTH), Thyrotrophs (TSH), Gonadotrophs (LH and FSH) and Null cells (secretory inactive)) (Amar and Weiss, 2003). In addition, the anterior lobe of the pituitary also produces pro-opiomelanocortin (POMC), a precursor glycoprotein that undergoes hydrolytic cleavages to generate corticotropin, β -lipotropin (β -LPH) and a small amount of β -endorphin (Amar and Weiss, 2003). Structurally ACTH, GH and PRL are simple polypeptides, whereas LH, FSH and TSH are glycoproteins composed of an α and β subunit. Within their respective secretory cells, these hormones are stored in granules that are released by exocytosis. When released into the circulation, these hormones will travel to and stimulate their respective target tissues (Amar and Weiss, 2003). The effects of ACTH, TSH, LH and FSH are mediated through G protein-coupled receptors via the second messenger cyclic adenosine monophosphate (cAMP), while GH and PRL receptors undergo dimerization before activating the intracellular cascades.

The intermediate lobe of the pituitary is composed mainly of agranular cells and, compared to the anterior pituitary, it is relatively avascular; however this lobe contains abundant innervation (Amar and Weiss, 2003). The intermediate lobe also produces POMC but in contrast to the anterior lobe, the products resulting from its hydrolytic cleavage are corticotrophin-like intermediate lobe peptide (CLIP), γ -lipotropin, β -endorphin and α - and β -melanotropin (MSH).

Finally, the posterior lobe of the pituitary is largely composed of axonal projections of neurosecretory cells originating in the hypothalamus. These axon terminals are closely apposed to blood vessels, allowing them to release their product into the bloodstream. The posterior pituitary secretes oxytocin and

vasopressin (also known as antidiuretic hormone or ADH). However, these hormones are synthesized in the cell bodies of the magnocellular neurons of the supraoptic and paraventricular nuclei of the hypothalamus and pass to the neurohypophysis via the hypothalamo-hypophyseal tract (Amar and Weiss, 2003). When released into the circulation, oxytocin will act on its target tissues via a G-protein coupled receptor that triggers an increase in the intracellular level of calcium, while ADH can act through three separate G-protein coupled receptors.

Mechanism of action of the gonadotrophins and their regulation

The gonadotrophins are the main hormones involved in follicular development since they enhance steroidogenic enzyme activity after interaction with their receptors. These interactions ultimately result in an increased synthesis and accumulation of steroids that are essential for further follicle development and for other physiological events important for reproduction. In this portion of the review, receptor localization, signal transduction and receptor mediated steroidogenesis will be discussed. Finally, the ovarian feedback mechanisms regulating the secretion of LH and FSH at the hypothalamic-pituitary level will be reviewed.

Receptor localization and signal transduction

When gonadotrophins are released from the pituitary they travel via the blood stream to reach the ovary, where they interact with specific, high-affinity, membrane receptors. Yuan *et al.* (1996) identified that FSHR mRNA in porcine follicles appears in the granulosa cells as early as the primary stage of development when the follicles possess only 1 to 2 layers of cells. FSHR is most strongly expressed in preantral and small antral follicles, while expression is suppressed in large antral follicles. On the other hand, LHCGR mRNA is first detected in the theca interna of large preantral-small antral follicles and expression in granulosa cells is only evident in medium-sized antral follicles and reaches maximal abundance in large antral follicles. These results are in agreement with the findings of Liu *et al.* (1998) who showed that FSHR mRNA is

expressed exclusively in the granulosa cells and whilst, it is strongly expressed in the small antral follicle stage (< 3mm), it is undetectable in large follicles (Liu *et al.*, 1998). In comparison, in follicles smaller than 3 mm, LHCGR mRNA was localized exclusively in theca interna but appeared later in the granulosa of large follicles.

In addition, an autoradiographic study has shown that radiolabelled FSH decreasingly bound to granulosa cells as the follicles grew from 1-2 mm to 6-10mm (Nakano *et al.*, 1983). In contrast, LH binding increased from the small to large follicles stages (Grant *et al.*, 1989, Nakano *et al.*, 1983). These results are in agreement with the appearance of LHCGR mRNA in the granulosa cells of medium follicles and explain the increase in LH binding observed in these experiments.

In order to trigger a response from the target cells (granulosa or theca cells), the binding of the gonadotrophins to the receptor must be transduced into an intracellular signal. As mentioned earlier, LH and FSH receptors are part of the G-protein coupled receptor family. The binding of the hormone to the receptor triggers the activation of a GTP-binding protein (G-protein). The G-protein then activates an adenylate cyclase, which will trigger the conversion of ATP into the second messenger cAMP. Cyclic AMP has been shown to activate some protein kinases such as protein kinase A (PKA), which leads to the expression of many genes including those encoding steroidogenic enzymes (Esbenshade *et al.*, 1990, Hunzicker-Dunn and Birnbaumer, 1985). These enzymes will ultimately convert cholesterol into physiologically active steroids that will be released into the follicular fluid and eventually into the peripheral circulation

Steroidogenesis

Binding of the gonadotrophins to their receptors initiates a series of intracellular cascades that lead to the activation of the steroidogenic enzymes, thus increasing steroid synthesis. Our current understanding of pig steroidogenesis

supports the two-cell, two-gonadotrophin model originally proposed for the rat (Armstrong *et al.*, 1979). According to this model, the theca cells respond to LH by synthesizing the androgen that is subsequently transferred to the granulosa cells where it is aromatized into oestrogen after FSH and LH stimulation. However, as discussed below, many peculiarities of pig steroidogenesis need to be emphasized.

First of all, it appears that in the pig both the theca and granulosa cells possess the ability to synthesize oestrogen and significantly contribute to oestradiol production. This is in contrast to the rat where only the granulosa cells participate to oestrogen production (Ainsworth *et al.*, 1990). Interestingly, the theca cells seem to possess the ability to synthesize oestrogen from cholesterol *in vitro*, while the granulosa cells need to be supplied with aromatizable androgen or be co-incubated with theca cells in order to produce oestradiol (Anderson *et al.*, 1979, Evans *et al.*, 1981, Haney and Schomberg, 1981, Stoklosowa *et al.*, 1982, Tsang *et al.*, 1982). Consistent with the previous statement, it was shown that the granulosa cells are the major site of progesterone synthesis but are unable to synthesize androgen *de novo*, while the theca cells are capable of producing large quantities of androgen (Channing and Tsafiriri, 1977, Evans *et al.*, 1981, Haney and Schomberg, 1981, Stoklosowa *et al.*, 1982, Tsang *et al.*, 1982). Evidence also suggests that granulosa cells could contribute to theca cell androgen production by supplying progesterone or a C₂₁ substrate (Lischinsky and Armstrong, 1983). Moreover, it was found that the ability of the theca cells to produce oestradiol is substantially less than that of the granulosa cells and is limited by the level of aromatase activity rather than substrate availability (Tsang *et al.*, 1985). In contrast, the ability of the granulosa cells to synthesize oestrogen seems to be limited by the availability of androgen precursors rather than enzyme activity. Therefore, it was suggested that as the follicles develop, the contribution of the granulosa cells to total oestrogen production increases, since extensive granulosa cell proliferation is associated with follicular growth (Daguet, 1978). Overall, our current knowledge of porcine steroidogenesis is summarized in Figure 2.4.

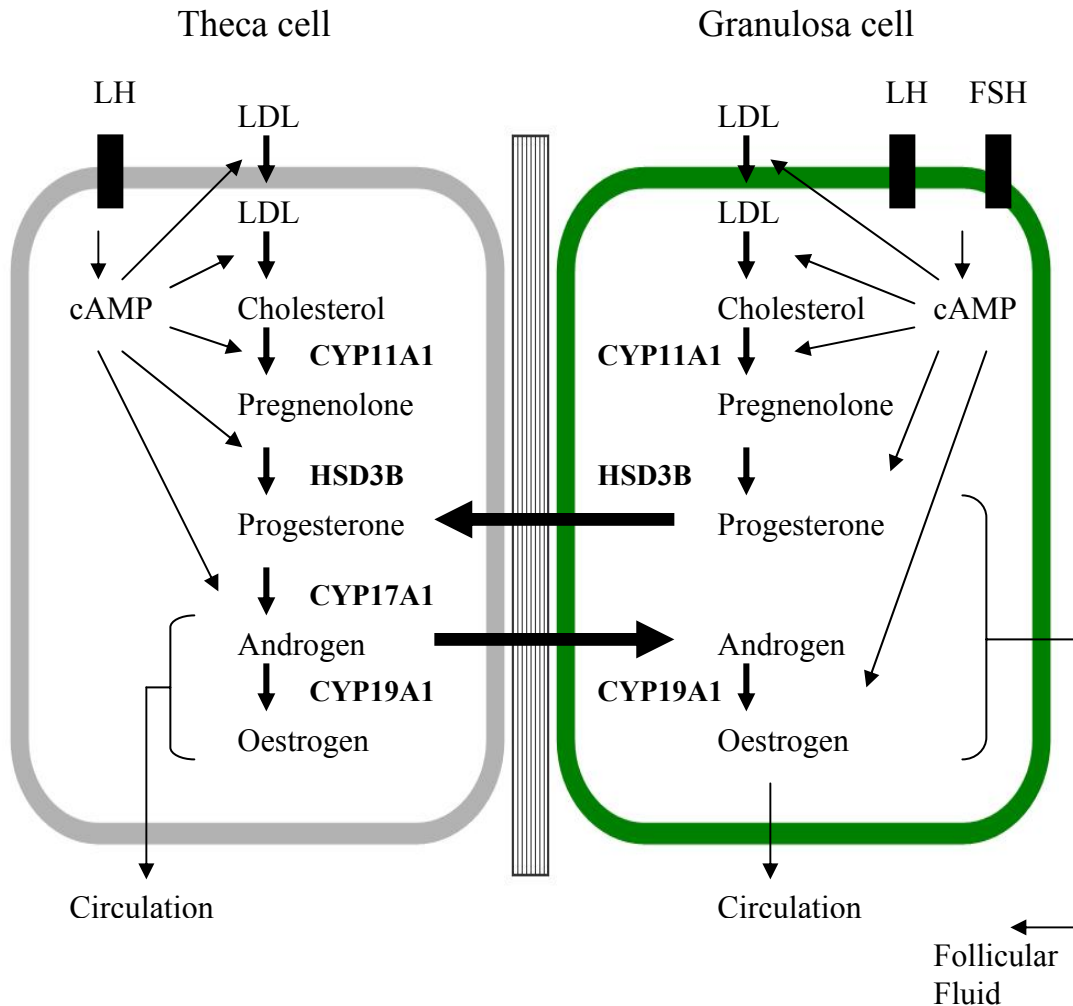


Figure 2.4 Schematic representation of the concept of cellular and hormonal interactions during pig follicular development. LDL = low density lipoprotein, cAMP = cyclic AMP, CYP11A1 = P450 side-chain cleavage, HSD3B = 3 β -hydroxysteroid dehydrogenase, CYP17A1 = 17 α -hydroxylase, CYP19A1 = P450 aromatase and ■ = receptor. Adapted from Ainsworth *et al.*, 1990.

Modulation of gonadotrophin secretion

In the previous sections, the control of the secretion of the gonadotrophins has been discussed and specific changes in LH and FSH secretion are critical for

normal follicle development. As illustrated in Figure 2.5, the hypothalamus secretes GnRH that acts on the gonadotrophs to stimulate both FSH and LH production and secretion. Once the gonadotrophins are released into the bloodstream, they interact with their receptors on the ovaries to trigger the production of steroids and other intraovarian factors such as inhibin. In turn, the steroid (principally oestradiol in the female) and inhibin will feedback to the hypothalamus and/or pituitary to regulate LH and FSH secretion.

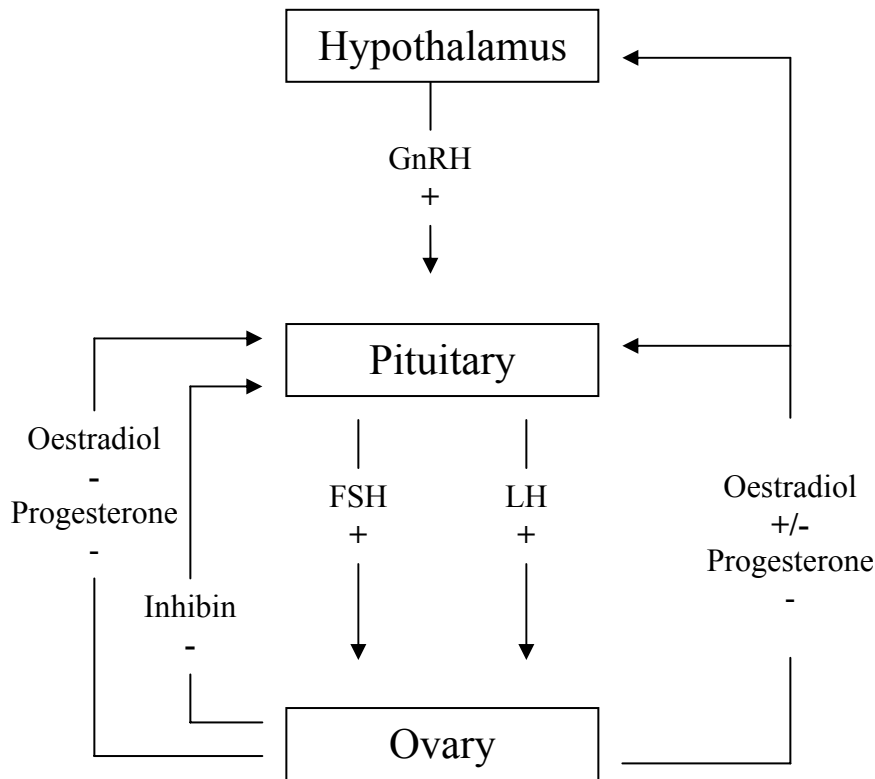


Figure 2.5 Schematic representation of the differential regulation of LH and FSH by ovarian peptides and steroids. + and – indicate stimulatory or inhibitory effects. Adapted from Foxcroft *et al.*, 1994.

Extensive evidence suggests that the ovaries play an important role in the differential regulation of gonadotrophin secretion and one of the most striking examples of the overall negative feedback loop comes from experiments using

ovariectomized animals. In this model, the removal of the ovaries triggers increased circulating concentrations of LH and FSH (Fonda *et al.*, 1983, Prunier and Louveau, 1997). Oestradiol has been shown to be principally involved in the negative feedback mechanisms involved in the control of LH secretion. However, its action on LH secretion can be biphasic since it has been shown to have an inhibitory effect in ovariectomized gilts, but when its level increases above a critical threshold it then turns into a positive signal to trigger the LH surge (Berardinelli *et al.*, 1984). It has also been suggested that oestradiol exerts its positive action on the central nervous system (Ford *et al.*, 2000, Kesner *et al.*, 1987, Kesner *et al.* 1989, Stickan *et al.*, 1999), as demonstrated by the absence of LH secretion by the pituitary of oestradiol-injected HST gilts (Ford *et al.*, 2000). Oestradiol's negative feedback effect could be mediated both via the pituitary by modulating pituitary sensitivity to GnRH and also via the hypothalamus by suppression of GnRH pulsatility (Foxcroft *et al.*, 1994). On the other hand, even if the long term synthesis of FSH by the gonadotrophs is dependent on GnRH, FSH seems to be mainly secreted through a constitutive pathway (McNeilly *et al.*, 2003). Evidence suggests that primarily inhibin, but also activin and follistatin are involved in the differential control of FSH secretion. However, only inhibin appears to be involved in the classic long-loop ovarian feedback mechanism, as shown by the absence of changes in the circulating levels of activin and follistatin after ovariectomy or during ovarian stimulation protocols (de Kretser and Phillips, 1998). Finally, progesterone has also been shown to modulate gonadotrophin secretions at the hypothalamic and pituitary level. However, since this review focuses mainly on the follicular phase, no further details of these modulatory effects of progesterone will be discussed.

At the pituitary level, many different mechanisms need to be taken into account to explain the differential synthesis/secretion of FSH and LH. As discussed previously, GnRH, steroids (mainly oestradiol in the female) and inhibin/activin/follistatin are the principal modulators of the gonadotrophins during folliculogenesis. As they interact with the gonadotrophs, they have been

shown to alter gene expression, mRNA stability, post-translational modifications and the secretion, potency and half-life of the gonadotrophins.

INTRAFOLLICULAR FACTORS CONTROLLING FOLLICLE DEVELOPMENT AND OOCYTE GROWTH

The previous two sections have established the importance of extragonadal factors in the regulation of ovarian follicle development. However, it has now become evident that intrafollicular interactions between the somatic cells and the oocyte, mediated through gap-junctional communication and by paracrine and autocrine signalling, are also essential for coordinating follicle and oocyte growth. Therefore, the following section will review our current knowledge on gap-junctional communication, focusing mainly on the exchange between the granulosa cells and the oocyte necessary for oocyte growth and for the maintenance of meiotic arrest. In addition, the role of several key local growth factors will also be reviewed.

Transzonal projections and gap junctions

The zona pellucida forms early during follicle development and could potentially disrupt the close association between the oocyte and the granulosa cells necessary for follicle development. However, the granulosa cells have developed a highly specialized network of channels within this barrier which maintain direct physical contact with the oocyte. The use of microscopy in conjunction with immunolabeling has permitted the visualization of these transzonal projections (TZP), but has also enabled the distinction between two populations of TZP, the actin- and microtubule-rich (Albertini and Barrett, 2003). Gap junctions are found at the end of these transzonal projections, allowing direct cytoplasm-to-cytoplasm exchange of small (<1-2 kDa) molecules including ions, metabolites and small peptides (Kidder and Mhawi, 2002, Gershons *et al.*, 2008) (Figure 2.6).

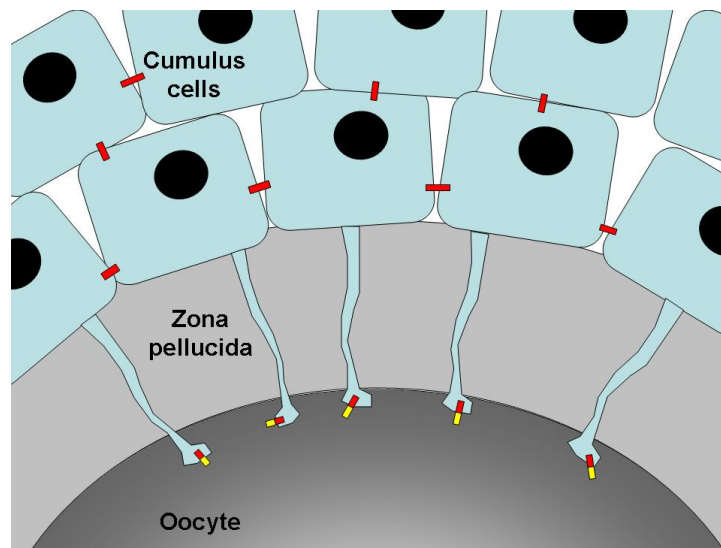


Figure 2.6 Schematic representation of the transzonal projections (TZP) with the proposed distribution of connexins (Cx) 37, 43 in the gap junctions of mouse cumulus-oocyte complexes. Adapted from Kidder and Mhawi, 2002.

■: Cx37 ■ Cx43

Gap junctions are composed of connexins (Cx) which are members of a large family of membrane proteins. At least 20 members of the connexin family have been identified in the mouse and human genome and most have a homologue in other species (Gershon *et al.*, 2008). The connexins vary greatly in size, ranging from 26 kDa (Cx26) to 60 kDa (Cx60) and are named accordingly. To form the channels, the connexins first organize themselves in hexamers, named the connexon, which is the fundamental unit of the gap junction. The subsequent docking between two connexons from neighbouring cells finally completes the formation of the gap junction. Given that most tissues and cell-types possess their own array of Cx and that gap junctions formed from different Cx possess different permeability and selectivity, it provides adjacent cells with the potential to exchange a variety of specific small molecules. For example, gap junction channels have been shown to be selective for different cyclic nucleotides and tracer dyes (Bevans *et al.*, 1998). However, evidence now suggests that assembly

of heteromeric connexons (i.e. connexons composed of different Cx) and heterotypic channels (i.e. channels formed from two different connexons) is possible, thus providing even greater versatility and specificity in the exchanges (Cottrell and Burt, 2005). As in other organs, many different connexins, including Cx26, Cx 32, Cx37 and Cx43 have been found in the mammalian ovary (Gershon *et al.*, 2008). In addition, porcine ovaries have also been shown to express Cx30.3 and Cx60 (Itahana *et al.*, 1996, Itahana *et al.*, 1998). However, Cx37 and Cx43 are the most abundant connexins in the ovary and their importance for follicle development and oocyte growth is undeniable (Figure 2.6). Therefore, they will be the focus of the following discussion.

Role of TZP and gap junctions

Little is known about the role of transzonal projections, except that they are involved in establishing a direct membrane-membrane contact between the oocyte and the surrounding granulosa cells allowing for the assembly of the gap junction. However, it was recently proposed that the TZP could also play an important role in paracrine signaling by mediating local delivery of certain growth factors into the perivitelline space and by facilitating receptor occupation (Albertini *et al.*, 2001). Some examples of this have been reported by Antczak and Van Blerkon (1997), who observed that leptin and STAT3 were delivered to the oocyte through TZP. In addition, the presence of the necessary machinery to transport paracrine factors to the extremity of the TZP and the involvement of external factors in the control of the TZP dynamics (uncoupling or closure of the channels), also reinforces their importance (Albertini *et al.*, 2001). However, much remains to be elucidated about the importance of transzonal projections in paracrine signaling.

Secondly, studies with knockout mice lacking connexin 37 and 43 have provided insights into the role of gap junctions during folliculogenesis and oogenesis. The connexin 37 knockout ablates the communication between the oocyte and the granulosa cells, but the mice are viable and function normally other than at late pre-antral stage of folliculogenesis (Simon *et al.*, 1997 and

Carabatsos *et al.*, 2000). At that point, null mutants failed to develop Graafian follicles which led to incomplete meiotic competence and to anovulation even after gonadotrophin stimulation. The uncoupling between the granulosa cells and the oocyte also caused the oocyte to arrest at 74% of its normal size, which is consistent with the role of the cumulus cell in transferring nutrients to the oocyte (Carabatsos *et al.*, 2000). Finally, the ovaries of the Cx37 null mutant were filled with structures similar to corpora lutea, indicating the importance of the gap junction in preventing luteinization (Simon *et al.*, 1997). In the case of the connexin 43 knockout mice, different results have been observed. First, very few germ cells are present in the ovary of the null mutant offspring; because Cx43 null mice die soon after birth from cardiac malfunction that precludes further studies on post-natal ovarian function (Reaume *et al.*, 1995, Juneja *et al.*, 1999). However, using organ culture or transplantation into immunocompromised mice, it was possible to show that follicular development in the Cx43 null mutant ovary was arrested before the formation of multiple layers of granulosa cells, indicating the important role of these gap junctions in granulosa cell proliferation (Juneja *et al.*, 1999, Ackert *et al.*, 2001). Moreover, reduced oocyte growth associated with incompetence and oocyte abnormality was also observed (Ackert *et al.*, 2001). The information obtained from these knockout models is limited to the developmental stage at which the absence of connexins becomes damaging. Therefore, the use of other *in vitro* models, as well as some creative *in vivo* experimental approaches, was also of great importance in revealing the importance of the gap junction communication in cumulus-oocyte complexes (COC).

Oocyte growth

Data obtained using *in vitro* models have suggested that the growth rate of mouse oocytes is correlated with the number of adherent granulosa cells (Brower and Schultz, 1982, Herlands and Schultz, 1984). Moreover, denuded mammalian oocytes take up amino acids, sugars and ribonucleosides very inefficiently compared to cumulus-enclosed oocytes, suggesting that the companion cells have

an important role to play in the transfer of nutrients to the oocyte (Heller and Schultz, 1980, Brower and Schultz, 1982, Colonna and Mangia, 1983 and Haghghat and Van Winkle, 1990). To further support this idea, it was shown that the human oocyte possesses only one glucose transporter while cumulus cells express four isoforms (Dan-Goor *et al.*, 1997). At the same time, it is also well known that pyruvate is the oocyte's preferred energy source (Eppig *et al.*, 1976). In contrast to the limited capacity of the oocyte to metabolize glucose, cumulus cells can efficiently transform glucose into pyruvate and transfer it to the oocyte (Donahue and Stern, 1968). From all these observations, it can be assumed that the cumulus cells take up the glucose from the environment, metabolize it into pyruvate and then transfer the pyruvate to the oocyte. This role of the cumulus cells can probably explain in part why the oocytes from the Cx37 null mice do not reach their normal size.

Meiotic arrest

Another important feature of the follicular environment is its ability to maintain the oocyte in meiotic arrest, as removal of the oocyte from the follicle leads to spontaneous meiotic resumption (Pincus and Enzmann, 1935). Therefore, it was originally proposed that the granulosa cells produce an oocyte meiotic inhibitor (OMI) that is transferred to the oocyte either by paracrine signaling or through the gap junctions. Several molecules have been proposed to be the OMI, including hypoxanthine (inhibitor of phosphodiesterase (PDE)) and cAMP (Eppig *et al.*, 1985 and Dekel, 1988). It has now become evident that cAMP plays a central role in maintaining the oocyte in meiotic arrest, since pharmacological manipulations that increase cAMP in the oocyte or inhibit the phosphodiesterases responsible for cAMP degradation in the oocyte prevent or delay spontaneous maturation (Reviewed in Conti *et al.*, 2002, Edry *et al.*, 2006). Similarly, injection of PKA into mouse oocytes inhibits meiotic resumption while the converse was observed following injection of the PKA inhibitor (PKI) (Bornslaeger *et al.*, 1986). Important progress has also been made in understanding how cAMP and PKA are linked to the inhibition of maturation

promoting factor (MPF) activity in mouse, rat and frog oocytes (Duckworth *et al.*, 2002, Han *et al.*, 2005, Kovo *et al.*, 2006, Newhall *et al.*, 2006). It is also apparent for the mouse and rat oocyte, that the preovulatory LH surge leads to a decrease in cAMP necessary for oocyte maturation (Aberdam *et al.*, 1987, Schultz *et al.*, 1983, Vivarelli *et al.*, 1983). However, the origin of the cAMP, as well as the mechanisms necessary for the modulation of cAMP level in the oocyte remains somewhat elusive.

Two main schools of thoughts can be found in the literature. The first and perhaps the most widely accepted model suggests that meiotic arrest is dependant on cell-to-cell interactions, involving the direct transfer of cAMP from the surrounding granulosa cells to the oocyte through gap junctions (Dekel, 1988, Eppig 1991). This model is supported by observations in the rat, in which stimulation of denuded oocytes (DO) with forskolin (an agonist of adenylyl cyclase) fails to induce an elevation in cAMP resulting in meiotic resumption, while similar stimulation of cumulus-enclosed oocytes results in an elevation in cAMP concentration and maintenance of meiotic arrest (Dekel *et al.*, 1984, Sherizly *et al.*, 1988). In this model, it is proposed that LH stimulation of the granulosa cells interrupts the gap-junctional communication between the oocyte and the somatic cell, leading to the drop in oocyte cAMP. However, this hypothesis has been questioned since some studies have found a lag between the initiation of meiotic resumption and the loss of gap-junctional communication (Eppig *et al.*, 1982, Moor *et al.*, 1980). However, Granot and Dekel (1994) have shown that although several hours are required for LH-induced inhibition of Cx43 translation, Cx43 phosphorylation was observed within 10 min of LH stimulation. More recently, mitogen-activated protein kinase (MAPK) was shown to be involved in LH-induced maturation of mouse follicle-enclosed oocytes (Su *et al.*, 2003). Interestingly, following LH stimulation, the somatic follicle cells activate MAPK, which was also found to induce Cx43 phosphorylation and cause the abolition of the gap-junctional communications between the oocyte and the cumulus cells (Sela-Abramovich *et al.*, 2005). Moreover, treating cumulus-enclosed oocytes with carbenoxolone (a blocker of gap junctions) leads to a

decrease in oocyte cAMP concentration and meiotic resumption without any associated changes in phosphodiesterase activity (Sela-Abramovich *et al.*, 2006). Together, these observations provide support for the hypothesis that the cumulus cells are essential for maintaining the oocyte in meiotic arrest by providing cAMP to the oocyte via the gap-junctions.

The second model suggests that the oocyte possesses the ability to produce sufficient cAMP to maintain meiotic arrest and that changes in the balance between cAMP synthesis and degradation within the oocyte are responsible for meiotic resumption. However, similar to the first model, it also embraces the importance of oocyte-somatic cell interactions. The first line of evidence to support this second model was that mouse and rat oocytes express active adenylyl cyclase and that oocytes deficient in adenylyl cyclase 3 precociously reinitiate meiosis (Horner *et al.*, 2003). Moreover, indirect inhibition of adenylyl cyclase activity through blockage of G proteins leads to meiotic resumption (Mehlmann *et al.*, 2002). Interestingly, it was proposed that G-protein coupled receptor 3 (GPR3), potentially stimulated by granulosa cell-derived signals, is necessary for maintaining meiotic arrest in mouse oocytes through the activation of G-protein (Mehlmann *et al.*, 2004, Mehlmann *et al.*, 2005a). From the same perspective, Vaccari *et al.* (2008) have recently shown that endogenous cAMP production in the oocyte is essential for meiotic arrest in the mouse. Using mouse oocytes defective for cAMP synthesis and degradation, the authors found that GPR3 and phosphodiesterase (PDE)-3A play a primary role in controlling oocyte cAMP concentrations without affecting the gap-junctional communication between the oocyte and cumulus cells. Although this experiment did not eliminate the possibility that some cAMP could diffuse through the gap-junction, the authors concluded that somatic cell-derived cAMP is not sufficient to compensate for the loss in oocyte cAMP production. Very recent evidence suggests that members of the epidermal growth factor (EGF) family play an important role in oocyte meiotic resumption and cumulus expansion following the endogenous LH surge (Park *et al.*, 2004). This finding demonstrated the possibility that the LH signal is transmitted from the LH-responsive granulosa cells to the oocytes and could also

eventually be linked to the sudden drop in endogenous oocyte cAMP levels required for meiotic resumption (see EGF family). This is an attractive alternative or even possibly coincidental mechanism, to the closure of the gap junctional communication hypothesized in the first model, which could further improve our understanding of oocyte meiotic resumption.

As in the rodent, cAMP and its modulation by adenylyl cyclase and PDE3 also appear critical for the regulation of meiotic resumption in the porcine oocyte (Laforest *et al.*, 2005). Laforest *et al.* (2005) showed that both cumulus-enclosed oocytes and denuded oocytes could be maintained in meiotic arrest using forskolin, suggesting that endogenous cAMP production by the oocyte is important. In addition, similar to the mouse and rat oocyte, the porcine oocyte appears to be the predominant site of PDE3A expression (Reinhardt *et al.*, 1995, Sasseville *et al.*, 2006, Tsafiriri *et al.*, 1996). Finally, gap-junctional communication in the porcine cumulus-oocyte complexes (COC) is under gonadotrophic regulation and appears to be lost coincident with oocyte germinal vesicle breakdown (GVBD) (Sasseville *et al.*, 2009). It is worth noting that evidence in the pig suggests that both intercellular communication between oocyte and cumulus cells, as well as endogenous cAMP production by the oocyte, appear to be involved in maintaining meiotic arrest.

Intrafollicular growth factors¹

Intraovarian factors are also extremely important regulators of follicle growth and act in a paracrine and autocrine manner to regulate cell function. In recent years, particular attention has been given to the transforming growth factor (TGF)- β superfamily, the vascular endothelial growth factor (VEGF) and other angiogenic factors, the insulin-like growth factor (IGF) system and the EGF/EGF-like peptide family because of their ability to fulfill many of the functions required for proper follicle growth. Therefore, the aim of this section will be to assess the localization of key local growth factors in the porcine follicle and

¹ A portion of this section has been published. Hunter MG and Paradis F 2009 Control of pig Reproduction VIII

describe their role in regulating cell proliferation and differentiation, steroidogenesis, angiogenesis, and apoptosis during antral follicle development as well as cumulus cell expansion and oocyte meiotic resumption during the periovulatory period in the pig.

Antral follicle development

TGF- β superfamily

The bone morphogenetic proteins (BMP) and associated receptors

The BMP subfamily represents a relatively large subset of the TGF- β superfamily. It is comprised of 8 ligands, namely BMP2, 3, 4, 5, 6, 7, 8, and 15 and, with the exception of BMP8, their expression has been reported in ovarian antral follicles of several species (Knight and Glister, 2006). These ligands are known to interact with at least 7 different receptors that can be separated into type 1 receptors including activin A receptor (ACVR) 1 (or ActRIA, ALK2), bone morphogenetic protein receptor (BMPR) 1A (or ALK3), BMPR1B (or ALK6), transforming growth factor β receptor (TGFB β) 1 (or ALK5) and type 2 receptors including BMPRII, ACVR2A and ACVR2B (Shimasaki *et al.*, 2004, Juengel and McNatty, 2005). For the purpose of this review, growth differentiation factor (GDF) 9 and its known receptors (TGFB β 1 and BMPRII) will also be included in this section.

In recent years, much attention has been given to members of this TGF- β subfamily because of their ability to mediate many important functions during follicle development including cell proliferation and differentiation, steroidogenesis, metabolism and apoptosis (Shimasaki *et al.*, 2004, Juengel and McNatty, 2005, Gilchrist *et al.*, 2008). Particular focus has been given to BMP6, BMP15 and GDF9 since they have been shown to be primarily derived from the oocyte and can mediate all of the aforementioned functions (Juengel and McNatty, 2005, Gilchrist *et al.*, 2008). Moreover, naturally occurring mutations in these factors or in their receptors have been shown to alter normal follicle development and impact ovulation rate. The presence of a functional BMP/GDF9

system in the porcine ovary has been demonstrated. Studies by Quinn *et al.* (2004a) and Brankin *et al.* (2005a) have reported the expression of several BMP's, GDF9 and their receptors in porcine antral follicles. However, their functions in the pig follicle remain unclear and require further investigation.

Oocyte-derived BMPs

Perhaps the first clue to the importance of oocyte-derived factors on the surrounding somatic cells came from el-Fouly *et al.* (1970), who showed that removal of the oocyte from rabbit antral follicles led to the premature luteinization of the follicle. Subsequently, oocyte-secreted factors have been clearly identified as modulators of granulosa cell luteinization, since the removal of the oocyte from the mouse, pig and cattle cumulus-oocyte complexes leads to increased progesterone production by the cumulus cells (Vanderhyden *et al.*, 1993, Coskun *et al.*, 1995 and Li *et al.*, 2000). Similarly, the addition of denuded oocytes to murine and porcine mural granulosa cells leads to a decrease in progesterone production (Gilchrist *et al.*, 2008, Coskun *et al.*, 1995, Brankin *et al.*, 2003a). This effect of the oocyte on progesterone production is believed to be, in part, associated with its ability to regulate the FSH-induced LH receptor and steroidogenic enzymes such as CYP11A1 (Eppig *et al.*, 1997, Diaz *et al.*, 2007). However, the role of oocyte-secreted factors is not limited to controlling luteinization or progesterone production, and extends to steroidogenesis in general. In mouse cumulus cells and pig mural granulosa cells, the oocyte has been shown to stimulate FSH-induced oestradiol production (Brankin *et al.*, 2003a, Vanderhyden *et al.*, 1993), while in pig cumulus cells and in bovine mural granulosa cells the oocyte suppresses oestradiol production (Coskun *et al.*, 1995, Glistler *et al.*, 2003). In addition, murine, porcine and bovine oocytes stimulate thymidine incorporation as an indicator of cell proliferation (Gilchrist *et al.*, 2003, Hickey *et al.*, 2004, Hickey *et al.*, 2005, Gilchrist *et al.*, 2006). Interestingly, porcine oocytes also increase granulosa and theca cell viability and bovine oocytes reduce cumulus cell apoptosis, likely contributing to increased cell numbers (Brankin *et al.*, 2003a, Hussein *et al.*, 2005). Moreover, mouse oocytes

also control cumulus cell metabolism, as shown by the downregulation of several glycolytic enzymes and an amino acid transporter in response to oocyectomy or oocyte removal (Sugiura *et al.*, 2005, Eppig *et al.*, 2005). Last, but not least, bovine oocyte-secreted factors have been shown to enhance oocyte developmental competence (Hussein *et al.*, 2006). The last two oocyte functions described above have yet to be described in a porcine model but the potential for similar effects on porcine cumulus cell metabolism and oocyte developmental competence should not be ignored.

Although the possibility exists that other oocyte factors play a role in fulfilling the above functions, BMP6, BMP15 and GDF9 have become central players in studies of regulation of ovarian follicle growth. There are two main reasons for this particular focus. First, these three ligands have been shown to be exclusively expressed in the oocyte of several species (Juengel and McNatty, 2005). Second, they have the ability to mediate most of the effects that the oocyte has on cell proliferation and differentiation, steroidogenesis, metabolism and apoptosis (Juengel and McNatty, 2005, Gilchrist *et al.*, 2008).

In the pig, similar to the other species, transcripts for *BMP6*, *BMP15* and *GDF9* are primarily expressed in the oocyte and are extremely abundant (Prochazka *et al.*, 2004, Brankin *et al.*, 2005a, Zhu *et al.*, 2008, Lee *et al.*, 2008). However, BMP6 and GDF9 mRNAs and/or proteins have also been detected, albeit at much lower levels, in ovarian somatic cells. This may indicate some species-specific specialized functions but may hint at potential functions for these factors in somatic cell interactions. Their receptors, BMPRI1A, BMPRI1B and BMPRII are expressed in all cell types in the antral follicle, demonstrating the possibility that these ligands modulate the function of cumulus and mural granulosa, and also the theca, cells (Quinn *et al.*, 2004a, Zhu *et al.*, 2008).

In vitro, BMP6 and BMP15 were found to regulate porcine granulosa and theca cell steroidogenic activity in a similar manner to the oocyte (Brankin *et al.*, 2003b, Quinn *et al.*, 2004b, Brankin *et al.*, 2005a, Brankin *et al.*, 2005b). In the

granulosa cells, BMP6 and BMP15 consistently inhibited progesterone production while increasing oestradiol production (Brankin *et al.*, 2003b, Brankin *et al.*, 2005a), whereas in the theca cells BMP6 suppressed androstenedione and progesterone production and BMP15 increased progesterone production (Quinn *et al.*, 2004b, Brankin *et al.*, 2005b). Recombinant GDF9 also decreased FSH-stimulated progesterone production in porcine granulosa cells and its effect was enhanced by androgen (Hickey *et al.*, 2005). Effects of GDF9 on theca cell steroidogenesis have not been investigated; however, bovine theca cell progesterone and androstenedione production decreased after GDF9 treatment (Spicer *et al.*, 2008). BMP6 and BMP15 have also been shown to increase theca cell viability, while BMP6 and GDF9, respectively were found to respectively stimulate theca and granulosa cell proliferation (Quinn *et al.*, 2004b, Brankin *et al.*, 2005a, Brankin *et al.*, 2005b, Hickey *et al.*, 2005). Finally, although it still remains to be shown in the pig, GDF9 increased bovine oocyte developmental competence and one cannot exclude the possibility for a similar effect on porcine oocytes. Interestingly, Li *et al.* (2008) reported that GDF9 mRNA and protein decrease gradually in COC during *in vitro* maturation. Although these changes are likely to be reflective of developmental changes occurring between the GV and MII stage oocyte, it is also tempting to hypothesize that this reduction in GDF9 could affect the developmental ability of those oocytes.

Somatic cell-derived BMPs

A role for the somatic cell-derived BMPs including BMP2, BMP4, BMP5 and BMP7 in ovarian function is supported by existing literature. However, as opposed to their counterparts that are derived from the oocyte, there is still only a paucity of information available in mammals and in pigs on their role during follicle development. Their localization in the ovary is perhaps the first clue that these molecules act as paracrine and autocrine modulators of ovarian functions. In the porcine follicle, BMP2 protein was expressed by the granulosa and theca cells throughout the follicular phase (Brankin *et al.*, 2005a). Also in the pig, expression of BMP4 mRNA has been reported in the oocyte and cumulus cells

and BMP4 and BMP5 mRNA were reported in the pig neonatal ovary (Shimizu *et al.*, 2004, Zhu *et al.*, 2008). In other species, BMP4 and BMP7 were reported to be expressed exclusively by the theca cells of rat and bovine antral follicles, while BMP5 was found exclusively in the granulosa cell of rat antral follicles (Erickson and Shimasaki, 2003, Glister *et al.*, 2004, Pierre *et al.*, 2005). As for the oocyte derived BMPs, every cell type in the follicle is a potential target for BMP2, -4, -5 and 7 since they signal through the same type I and type II receptors.

In the porcine antral follicle, only BMP2 has been tested for its ability to promote granulosa and theca cell steroidogenesis, and cell proliferation and viability (Brankin *et al.*, 2005a, b). Its action on the theca cells is remarkably similar to that of BMP6, as it reduces progesterone, androstenedione and oestradiol production. It also suppressed granulosa cell progesterone production in a dose-dependent manner. However, no effect on theca or granulosa cell proliferation or viability was observed. BMP5 was also found to stimulate rat granulosa cell proliferation while reducing progesterone production (Pierre *et al.*, 2005). Perhaps of more interest is the action of the theca cell-specific BMP4 and BMP7 on granulosa cell and theca cell function. In bovine granulosa cells, BMP4 and BMP7 caused an increase in both basal and IGF-1 stimulated oestradiol production, but they also stimulated inhibin A, activin A and follistatin production (Glister *et al.*, 2004). This is particularly interesting because follistatin, which is known to bind activin with high affinity, was also found to counteract the effect of many BMPs (Glister *et al.*, 2004 and Glister *et al.*, 2005). Other binding proteins including chordin and gremlin have also been reported to counteract the effect of specific BMP ligands (Glister *et al.*, 2005, Juengel and McNatty, 2005). This observation sheds some light on how the autocrine and paracrine BMP signaling pathways might be regulated in the ovarian follicle, but also introduces another level of complexity, demonstrating that the different TGF- β subfamilies interact with each other and also with other growth factor families (such as IGF-1). In addition to their involvement in granulosa cell functions, BMP-4 and BMP-7 have also been reported to decrease basal and LH-stimulated androstenedione production by the theca cells (Glister *et al.*, 2005). This effect is likely to occur

through the Smad 1-mediated decrease in CYP17A1 and also to a lesser extent, through decreases in CYP11A1, HSD3B and StAR expression. This observation has far reaching implications, since aberrations in the expression of BMP4 and BMP7 could be involved in hyperandrogenic dysfunction known to affect follicular development.

Overall, these observations illustrate the complexity of the BMPs/GDF9 system in the ovarian follicle and show that this system of growth factors is important for the regulation of porcine folliculogenesis. It is interesting to point out the intrinsic redundancy within the functions of the BMPs in steroidogenesis and cell proliferation which clearly illustrates that the bone morphogenetic proteins act in concert to prevent precocious luteinization of the follicle. These molecules also clearly promote cell proliferation and therefore directly affect follicle growth. Another interesting observation is that the oocyte appears to directly control the steroidogenic and metabolic activity of the cumulus cells, suggesting that the gradient of oocyte-derived BMPs is involved in establishing the cumulus cell versus mural granulosa cell phenotype. Finally, much remains to be learned about the mechanisms through which the BMPs mediate their functions and whether the observations *in vitro* can be extrapolated into *in vivo* models of antral follicular development.

TGF- β and associated receptors

The TGF- β subfamily comprises the three ligands TGFB1, TGFB2 and TGFB3 and two associated receptors, TGFBR1 (also known as ALK5) and TGFBR2 (ten Dijke and Hill, 2004, Juengel and McNatty, 2005). Betaglycan (also known as TGFBR3) has also been shown to be necessary for binding of TGFB2 in many cell types (ten Dijke and Hill, 2004). This family of genes has been extensively studied in several species and its ligands are known to be present and biologically active in ovarian follicles.

In porcine follicles, the theca interna appears to be the primary source of TGF- β (May *et al.*, 1996). As assessed by a proliferation assay using media

immunoneutralized with antibody raised against each TGF- β ligand, TGFB1 appears to account for most of the TGF- β bioactivity of the theca cells. Interestingly, *TGFB1* mRNA was localized to both the theca and granulosa cells of healthy antral follicles, however the protein could only be detected in the theca cells (Mulheron *et al.*, 1992, May *et al.*, 1996). Moreover, *TGFB2* mRNA could not be detected in the granulosa cells of small antral follicles (Mulheron *et al.*, 1992) and its expression in theca cells has yet to be reported in the pig. At this time, it is important to point out that significant differences have been observed between species relative to the expression of the TGF- β subfamily, preventing any extrapolation between species (see review of Juengel and McNatty, 2005). TGFB3 protein was exclusively present in the theca cells of antral follicles; however, as seen for TGFB1, mRNA expression was also detected in granulosa cells (Mulheron *et al.*, 1992, Steffl *et al.*, 2008). Finally, TGF- β bioactivity was found to increase with follicle size, and since TGFB1 seems to account for most of the effect of TGF- β , on cell proliferation, one can speculate that TGFB1 also increases with follicle size. Similarly, TGFB3 protein was most prominent in the theca cells of large antral follicles (May *et al.*, 1996, Steffl *et al.*, 2008).

The expression of the TGF- β receptors in the porcine ovary has been less extensively studied than their ligands. However, Goddard *et al.* (1995) reported that cultured granulosa cells expressed *TGFBRI*, *TGFBRII* and *TGFBRIII* mRNA and produce the protein for TGBBRI and TGFBRII. However, these results have to be interpreted with care since cultured granulosa cells tend to luteinize, especially when cultured with serum. Therefore, the results of the aforementioned experiment could also reflect the ability of the luteal cells to respond to the TGF- β ligand.

The effects of the TGF- β proteins on the ovarian cells have been mainly associated with cell proliferation and differentiation/steroidogenesis. Although most of the experiments were conducted *in vitro* using TGFB1, TGFB2 has also been shown to mediate similar effects (Juengel and McNatty, 2005). TGFB3 has not been extensively studied and its functions have yet to be understood. Initially,

TGFB1 and TGFB2 were tested for their ability to promote thymidine incorporation in porcine granulosa cells and were found to inhibit both basal- and growth factor-stimulated cell proliferation (Mondschein *et al.*, 1988). Similarly, May *et al.* (1994) found that TGFB1 attenuated granulosa cells (GC) proliferation, while having little effect on the theca cells. In addition, TGFB1 was shown to decrease both basal and FSH-stimulated aromatase activity, while the converse was observed in theca cells (Caubo *et al.*, 1989, Goddard *et al.*, 1995). TGFB1 was also shown to inhibit both basal and FSH-stimulated progesterone production in cultured granulosa cells and decreased both basal and LH- or dibutyryl(db)-cAMP stimulated progesterone production in cultured theca cells (Mondschein *et al.*, 1988, Caubo *et al.*, 1989, Engelhardt *et al.*, 1992, Kubota *et al.*, 1994). The inhibitory effect observed on theca cell progesterone production is believed to occur upstream of CYP11A1, since pregnenolone completely reversed the inhibitory effect of TGFB1 (Engelhardt *et al.*, 1992). TGFB1 and TGFB2 have been found to inhibit human chorionic gonadotrophin (hCG) binding in granulosa cells (Gitay-Goren *et al.*, 1993), suggesting that the TGF- β subfamily mediates the steroidogenic activity of the granulosa cells, and potentially of the theca cells, through direct regulation of the gonadotrophin receptors. On the other hand, TGFB1 has also been shown to interact with the IGF system in granulosa cells (Mondschein *et al.*, 1990), which in turn could indirectly influence the steroidogenic activity of those cells. Finally, the possibility that TGF- β ligands act directly on cholesterol transport cannot be excluded as a mechanism, since TGFB1 has been shown to downregulate StAR mRNA in a human theca-like cell line (Attia *et al.*, 2000). Such evidence has yet to be reported in the pig. Taken together, the observations that TGF- β bioactivity and that theca and granulosa cell-derived TGFBR1 mRNA increase with follicle size, combined with the effect of the TGF- β ligands on cell proliferation and differentiation, suggest that the TGF- β subfamily is important for modulating the rate of follicle growth while preventing precocious luteinization of the follicle.

Activin, inhibin and follistatin

The activin, inhibin and follistatin system is best known for its endocrine functions in the regulation of the hypothalamic-pituitary-ovarian axis, acting on FSH synthesis and secretion by the pituitary. However, they have also been shown in several species to act locally in the ovary, regulating follicle growth and modulating steroidogenesis. Interestingly, although it is one of the most studied families of ovarian growth factors, much remains to be learned about its role within the follicle.

Activin is a dimer composed of two β -subunits, β A- and β B-, yielding three possible combinations known as activin A, activin B and activin AB, while inhibin is formed by the dimerization of a common α -subunit and a β -subunit, yielding either inhibin A or B (Chapman *et al.*, 2004). Follistatin is a binding protein with high affinity for activin and is known to regulate activin bioavailability. Activin is known to signal through three receptors, namely ACVR1B (or ALK4), ACVR2A and ACVR2B, and although high affinity inhibin binding sites have been reported, no inhibin-specific receptors have been identified yet (Chapman *et al.*, 2002, Drummond *et al.*, 2002).

All three activin/inhibin subunit mRNAs, as well as follistatin mRNA, have been detected in porcine antral follicles (Li *et al.*, 1997, Van Den Hurk and Van De Pavert, 2001). Although the mRNA for both β -subunits was detected in the granulosa and theca cells of all follicle sizes, immunostaining for activin A revealed its presence in the granulosa cells, only a very weak signal in the theca cells of small antral follicle, while no signal could be detected in the theca cells of medium size antral follicles (Van Den Hurk and Van De Pavert, 2001). This observation suggests that the granulosa cells are the main source of activin or at least of activin A, which is consistent with the observations made in the rat where the β -subunits are confined to the granulosa cells (Meunier *et al.*, 1988). Intriguingly, activin A was also detected in close proximity to the oocyte

membrane although the mRNA for both subunits could not be detected in that cell type. In addition, Guthrie *et al.* (1997) reported the presence of inhibin in the follicular fluid of porcine antral follicles. Both activin and inhibin secretion has been shown to be stimulated by FSH and hCG in cultured granulosa cells, suggesting that the gonadotrophins regulate their temporal expression (Demura *et al.*, 1993). On the other hand, ACVR2A was detected in the granulosa and oocytes of small and medium size antral follicles, while it was only found in the theca cells of small antral follicles (Van Den Hurk and Van De Pavert, 2001). The expression of *ACVR1B* and *ACVR2B* has yet to be reported in the pig; however, in rat antral follicles *ACVR1B* mRNA was found in all cell types, while *ACVR2B* mRNA was localized to the oocyte and granulosa cells only (Drummond *et al.*, 2002). These results suggest that the oocyte, granulosa and theca cells are primary targets for activin and potentially inhibin. Interestingly, mRNA for the β -subunits and activin A could not be detected in porcine atretic follicles (Van Den Hurk and Van De Pavert, 2001).

Most studies investigating the activin/inhibin system in the ovary have described changes in mRNA or protein expression associated with particular follicle characteristics. In the bovine, a sharp increase in activin A was observed in 6 vs 2 mm follicles, suggesting a role for activin A during follicle selection (Glister *et al.*, 2006). Moreover, both human and bovine dominant follicles expressed inhibin α and β A subunits but not inhibin β B subunits, suggesting that inhibin A and activin A might play a role in the establishment of follicle dominance (Roberts *et al.*, 1993, Sisco and Pfeffer, 2007). Fewer studies have investigated the direct role of activin and inhibin on ovarian cell function but evidence points toward a role in regulating steroidogenesis. In both rat and bovine theca cells, activin was shown to decrease LH-stimulated androgen production. On the contrary, inhibin was found to increase both basal and LH-stimulated androstenedione in bovine theca cells and LH-stimulated androstenedione production in rat and sheep theca cells (Hsueh *et al.*, 1987, Wrathal and Knight, 1995, Campbell and Baird, 2001). Interestingly, inhibin was able to partially reverse the inhibitory effect of activin on rat theca cell androgen

production (Hsueh *et al.*, 1987). In porcine cultured granulosa cells, activin reduced both basal and FSH-stimulated oestradiol and progesterone production (Ford and Howard, 1997). In sheep granulosa cells, inhibin A had the opposite effect, increasing the FSH-stimulated oestradiol production (Campbell and Baird, 2001). The effects of activin on granulosa cell steroidogenesis, at least in the rat, are likely to be mediated by its ability to modulate the FSH receptor (Findlay and Drummond, 1999). In addition, activin has been shown to have a positive effect on bovine oocyte developmental competence, while the effect of inhibin was detrimental (Silva and Knight, 1998, Silva *et al.*, 1999). In the pig, activin was reported to have no effect on oocyte maturation (Coskun and Lin, 1994), however this study unfortunately did not investigate the developmental competence of the oocytes. Together, these observations suggest that a fine balance between activin and inhibin is required for proper steroidogenic activity of the ovarian follicle and for the acquisition of oocyte developmental competence.

IGF system

The IGF system has been extensively studied in several mammalian species over the years and has emerged as an important regulator of follicle growth. Indeed, the IGF system is known for both its endocrine actions, which are often associated with the metabolic status of the animal, and for its local paracrine and autocrine effects within the follicle on cell proliferation, steroidogenesis and apoptosis (Spicer and Echterkamp, 1995, Lucy *et al.*, 2001, Mazerbourg *et al.*, 2003, Spicer, 2004). In the context of this review, the local IGF system will be addressed. The IGF system is composed of two ligands, IGF1 and IGF2, as well as a type I and type II receptor, known as IGF1R and IGF2R (Mazerbourg *et al.*, 2003, Spicer, 2004). Importantly, it also includes more than six IGF binding proteins (IGFBP), including IGFBP1, -2, -3, -4, -5, -6, which bind to IGF1 and IGF2 with high affinity and are responsible for modulating their bioavailability (Mazerbourg *et al.*, 2003). Moreover, it is also well established that proteolytic degradation of IGFBP2, -4 and -5 by the protease pregnancy-

associated plasma protein-A (PAPP-A), plays an important role in regulating their actions in the follicle (Spicer, 2004).

Localization

The expression of the members of the IGF system in the ovarian follicle varies considerably between species. The reasons for those variations are still unclear, although it could be as a result of the different experimental techniques used to detect their expression and it most likely reflects species-specific differences in the pattern of follicular growth. In the pig, *IGF1* mRNA was localized to the granulosa and theca cells of follicles from 2 to 8 mm and its expression remained stable across all follicle categories (Liu *et al.*, 2000). Its protein, measured in the follicular fluid of the same follicle, showed a similar pattern of expression. On the other hand, *IGF2* mRNA was exclusively detected in the theca interna cells and in the ovarian stroma. The mRNA of their receptors (*IGF1R* and *IGF2R*) were also detected in all follicle categories but while *IGF1R* mRNA was expressed exclusively in the granulosa cell and remained unchanged as the follicle grew, *IGF2R* mRNA was detected in both cell compartments and increased in abundance in the granulosa of 8 mm preovulatory follicle post-LH surge (Liu *et al.*, 2000). Moreover, *IGFBP2* and *IGFBP4* mRNA were also present in the granulosa and theca cell of 2 to 8 mm pig follicle, but while *IGFBP2* mRNA expression decreased as the follicle grows, *IGFBP4* mRNA increased in large 8 mm post-LH surge preovulatory follicles (Liu *et al.*, 2000). In addition, Howard and Ford (1992) reported that follicular fluid *IGFBP2* also decreased as the follicle grew. The same authors measured follicular fluid *IGFBP3* and found that it remained unchanged as the follicle grows larger. This observation is in accordance with those of Wandji *et al.* (2000), who reported that *IGFBP3* mRNA was localized to both porcine granulosa and theca cells but did not change in abundance between different follicle sizes. *IGFBP5* mRNA was also detected in porcine granulosa cells as well as in the ovarian stroma but changes in its expression have not been investigated (Grimes *et al.*, 1994, Zhou *et al.*, 1996). *IGFBP1* has yet to be reported in the porcine ovary and although

IGFBP6 has been weakly detected in the follicular fluid, its localization within the follicle compartment, as well as the developmental changes in its expression, have yet to be determined (Shimasaki *et al.*, 1991). Finally, PAPP-A mRNA was found to increase in porcine granulosa cells as the follicle grows (Mazerbourg *et al.*, 2001). Large antral follicles also possess a higher IGFBP proteolytic activity than the smaller follicle, likely explained by the increased expression of PAPP-A (Besnard *et al.*, 1997).

Functions

As previously mentioned, the expression patterns of IGF1 and IGF1R remain unchanged during follicle growth. However, the IGFBPs, and more specifically IGFBP2 and IGFBP4, appear to be temporally regulated. This suggests that modulation of IGF1 bioavailability could play a determining role in IGF1 activity in the developing follicle. Several *in vitro* studies have clearly established that IGF, and perhaps even more specifically IGF1, are important factors that affect cell proliferation, steroidogenesis and apoptosis (Spicer and Echterkamp, 1995, Mazerbourg *et al.*, 2003). Firstly, IGF1 and IGF2 have been shown in numerous studies to stimulate porcine granulosa cell proliferation, as determined by thymidine incorporation studies or cell counts (Spicer and Echterkamp, 1995, Kolodziejczyk *et al.*, 2001). Kolodziejczyk *et al.* (2003) showed that the stimulatory effect of IGF1 is developmentally regulated, as thymidine incorporation was observed only in granulosa cells isolated from small and medium antral follicles but not in granulosa cells isolated from large follicles. This observation is also in accordance with a sheep study in which IGF1 stimulated proliferation of granulosa cells isolated from 1-3 mm follicles (Monniaux *et al.*, 1992). IGF1 also appears to stimulate theca cell proliferation, and this effect appears to be independent of follicle size (Kolodziejczyk *et al.*, 2001, Kolodziejczyk *et al.*, 2003). In addition, IGF1 and IGF2 have been shown to stimulate oestrogen synthesis by porcine granulosa and theca cells originating from various follicle sizes (Kolodziejczyk *et al.*, 2001, Kolodziejczyk *et al.*, 2003, see Spicer and Echterkamp, 1995 for review). Moreover, progesterone synthesis

by porcine granulosa cells and LH-stimulated androgen synthesis by theca cells are also stimulated by IGF1 and IGF2 (see Spicer and Echternkamp, 1995 review). However, perhaps the most interesting function of IGF1 signalling relates to its synergistic activity with FSH to enhance granulosa cell steroidogenesis (Baranao and Hammond, 1984). This is believed to occur through IGF modulation of the number and activity of gonadotrophin receptors (Lucy *et al.*, 2008) This observation is also supported by studies in IGF1 null-mice in which FSHR are severely reduced in number but are restored following supplementation with exogenous IGF1 (Zhou *et al.*, 1997). Finally, IGF1 has been shown to reduce porcine granulosa and cumulus cell apoptosis in culture and to promote FSH-stimulated synthesis of hyaluronic acid in cumulus-oocyte complexes (Nagyova *et al.*, 1999, Guthrie and Garret, 2001, Sirotkin *et al.*, 2002).

Altogether, these observations clearly illustrated that the IGF system is important for normal follicle function. However, further studies are necessary to establish how IGFs act within the follicle and how these actions are regulated through IGFBP and PAPP-A.

Angiogenic factors

Adequate vasculature is essential in all tissues to maintain sufficient blood flow to supply oxygen and nutrients, eliminate metabolic byproducts such as CO₂ and deliver hormones and other paracrine factors to the target cells. It is during embryonic development by a process known as vasculogenesis that blood vessels differentiate from endothelial precursors, establishing the general vasculature in the individual. Further vessel development in adult tissue occurs by intussusception and sprouting from existing vasculature by the process of angiogenesis. Although angiogenesis is a well-recognized hallmark of tumor development, it is generally limited in healthy adult tissues. The exception is the female reproductive tract, which undergoes continuous remodeling as part of the cyclic changes observed in the ovary and female reproductive tract during the oestrous or menstrual cycles, and during gestation. It is therefore not surprising

that angiogenesis and vasculature remodeling emerge as a critical component of follicle development and luteal function.

Angiogenesis usually consists of the breakdown of the basement membrane of existing vessels, followed by the migration of endothelial cells toward an angiogenic stimulus which, following cell proliferation, results in the establishment of new blood vessels. The creation of new blood vessels, along with their maintenance and the modulation of their permeability, is regulated by a variety of angiogenic factors. Although significant advances have been made in recent years in understanding the changes in follicle vasculature throughout the oestrous cycle; the factors responsible for these changes and the impacts of modulating follicle angiogenesis remain poorly understood.

Ovarian vasculature

In order to better comprehend how changes in follicular blood supply affect the normal functions and development of the ovarian follicle, it is imperative to understand the dynamic changes in ovarian and follicle vascularization occurring throughout the oestrous cycle. Numerous techniques have been described to monitor the progress of vascularization of the ovarian follicle. First, the use of ultrasonography in species with large and accessible ovaries such as the human, horse and cow, has allowed ovarian blood flow to be monitored, and has been used to demonstrate increases in blood flow to the cow preovulatory follicle (Acosta *et al.*, 2003). Another widely exploited technique involves the use of ovarian sections in which specific markers are used to stain endothelial cells (see review of Fraser, 2006). Finally, visualization of the vasculature using scanning electron microscopy of ovarian or follicle corrosion casts has allowed for a detailed morphological and quantitative analysis of the microvasculature in the ovary of rat, rabbit, cow and more recently the pig (Jiang *et al.*, 2002, Kanzaki *et al.*, 1982, Kitai *et al.*, 1985, Macchiarelli *et al.*, 1993, Murakami *et al.*, 1988, Yamada *et al.*, 1995).

In a study using scanning electron microscopy of porcine ovarian corrosion casts, Jiang *et al.* (2002) found that the vasculature of preantral follicles was minimal and was composed of only a few large capillaries. As the follicle progresses from small to medium antral follicle stage, the vasculature becomes arranged in a spherical mesh and evolves from being a single layer around the 500-700 μm follicle to being composed of three layers of vascular plexus around the 1-2 mm follicles. As the follicles grow to preovulatory size, only the density of the microvasculature increases compared to 1-2 mm antral follicles and these findings agree with the observations in rabbit and cow follicles and support the need for an increasing blood supply as healthy follicles grow larger (Kanzaki *et al.*, 1982, Kitai *et al.*, 1985, Yamada *et al.*, 1995). Increased accumulation of radiolabelled hCG into rhesus monkey large preovulatory follicles also confirmed the increase in blood supply in larger follicles (Zeleznik *et al.*, 1981). Interestingly, eCG has been found to increase the capillary density as follicles grow larger, while atretic follicles are generally associated with reduced or irregular vascularization (Hay *et al.*, 1976, Shimizu *et al.*, 2002). Finally, the vascular network that develops around each individual follicle is confined to the theca cell layer as the basement membrane prevents further progression into the granulosa cell layer which remains avascular until ovulation (see review of Fraser, 2006, Shimizu *et al.*, 2003a).

Localization and functions of angiogenic factors

Vascular endothelial growth factor

VEGFA was originally identified for its ability to promote proliferation of vascular endothelial cells but was also shown to induce changes in vascular permeability (see review of Stouffer *et al.*, 2001, Tamanini and Ambrogi, 2004, Yancopoulos *et al.*, 2000). At least 5 other VEGF family members have since been identified based on sequence homology and have been named consecutively from VEGF B to F. To date, 7 isoforms of VEGFA have also been identified in the human, and among those at least three (VEGF₁₂₁, VEGF₁₄₅ and VEGF₁₆₅) are soluble isoforms and two (VEGF₁₈₉ and VEGF₂₀₆) are membrane-bound (Stouffer

et al., 2001). Moreover, members of the VEGF family exert their functions mainly through a family of receptor tyrosine kinases including fms-related tyrosine kinase 1 (FLT1), also previously known as VEGFR1, and kinase insert domain receptor (KDR), formerly known as VEGFR2 and FLK1. Genetic ablation studies have established that both receptors are essential for VEGF signaling, as the absence of either receptor results in embryonic lethality (see review of Hanahan, 1997). However, deletion of each receptor results in distinct vascular deficiencies, as KDR null-mice lack both endothelial cells and a developing hematopoietic system, while the FLT1 null-mutant had abundant endothelial cells that did not assemble into functional vessels.

In the primate, VEGF mRNA and protein are absent from preantral follicles and become evident in the theca cells of antral follicles and in the granulosa cells of preovulatory follicles (Stouffer *et al.*, 2001). VEGFA concentrations in primate follicular fluid increase during the periovulatory period (Hazzard *et al.*, 1999). Similarly, VEGF was also shown to be absent from the granulosa and theca cells of rat preantral follicles. However, both granulosa and theca cells from early antral follicles weakly expressed VEGF, as did both cell types from preovulatory follicles, although the thecal layer stained more intensely (Abramovich *et al.*, 2009). The expression of KDR in early antral and preovulatory follicles followed a similar pattern of expression. To date, two VEGFA isoforms (VEGF120 and VEGF164) have been identified in the pig (Boonyaparakob *et al.*, 2003, Sharma *et al.*, 1995). Expression of both of these VEGFA isoforms was found in the granulosa and theca cells of small, medium and large follicles of prepubertal gilts, while their receptors were identified in the thecal layers (Barboni *et al.*, 2000, Shimizu *et al.*, 2002). Although these authors did not investigate the presence of the receptors in the granulosa cells, others have shown their presence in bovine granulosa cells (Greenaway *et al.*, 2004). Moreover, VEGFA was also detected in the follicular fluid from small, medium and large porcine antral follicles (Barboni *et al.*, 2000). The mRNA for both VEGFA isoforms in the granulosa cells (not in the theca cells), VEGFA in follicular fluid and the mRNA for both receptors in the theca cells of medium and

large gilts antral follicles, were up-regulated by eCG treatment, indicating the possibility for hormonal control (Barboni *et al.*, 2000, Shimizu *et al.*, 2002). Furthermore, VEGFA mRNA and protein in granulosa cells and follicular fluid sharply declines after hCG treatment (Barboni *et al.*, 2000). Another interesting aspect in the control of the expression of VEGF and its receptor is that hypoxia appears to be a key regulator. In both pigs and cattle, hypoxia has been found to significantly increase VEGF production (see review of Tamanini and Ambrogi, 2004). This is not the case in primates in which hypoxia had no effect on granulosa cell VEGF expression (Martinez-Chequer *et al.*, 2003). Moreover, FLT1 (VEGFR1) was found to respond to hypoxic conditions in the mouse (Gerber *et al.*, 1997). Finally, fasting also results in increased follicular fluid VEGF while its mRNA decreased in granulosa cells and increased in theca cells (Galeati *et al.*, 2003). It was proposed that modulation of follicle vasculature in times of famine would help in maximizing the transport of available nutrients to the follicular cells and potentially rescue the deprived growing follicles.

Most of the information on the role of vascular endothelial growth factors and their receptors in ovarian antral follicles comes from inhibition of the VEGF pathway using neutralizing antibodies, inhibitors of VEGF receptors, soluble VEGF receptors or VEGF traps, or alternatively through injection of VEGF in the ovary or follicle. Subcutaneous injection of VEGF trap during the follicular phase of the marmoset monkey cycle leads to a marked decrease in large follicles (Wulff *et al.*, 2002). This is accompanied by decreased proliferation of the theca and granulosa cells, decreased vascularization of the theca cells and increased atresia. Compensatory mechanisms were observed, as VEGF mRNA increased in the ovary of treated animals, while receptor expression decreased in the absence of stimulation. Moreover, intravenous injection of an antibody directed against KDR (VEGFR2) in the monkey decreased inhibin B production likely explaining the corresponding rise observed in FSH and LH secretion (Zimmermann *et al.*, 2002). It also significantly delayed the rise in oestradiol production and lengthened the follicular phase. Similar observations were also made by Fraser *et al.* (2005) using a VEGF trap system during the mid-follicular phase. In addition,

Mattioli *et al.* (2001) showed that follicular fluid VEGF levels in medium-sized antral follicles in the pig are correlated with the follicle's ability to produce oestradiol. Moreover, injection of VEGF gene fragments into the ovarian medulla of miniature gilts in combination with eCG treatment increased the number of preovulatory follicles as well as the capillary density in the theca cells (Shimizu *et al.*, 2003b). These observations were also accompanied by increased VEGF₁₂₀ and VEGF₁₆₄ mRNA expression in the granulosa cells and VEGFA content in the follicular fluid. A similar experiment in the rat has shown that injection of VEGF also promoted ovarian follicle development (Iijima *et al.*, 2005, Shimizu *et al.*, 2008). Collectively, these observations clearly suggest that modulation of angiogenesis during the early and mid-follicular phase affects follicle recruitment and/or selection. A consistent observation noted throughout these studies is that VEGF inhibition often results in increased circulating gonadotrophins. Finally, *in vitro* experiments have also revealed that VEGF affects granulosa cell proliferation, inhibiting proliferation in small follicles but stimulating proliferation in medium and large antral follicles (Grasselli *et al.*, 2002).

Angiopoietin

While vascular endothelial growth factors are of the utmost importance for the initiation of angiogenesis, formation of the vascular network and controlling vessel permeability, other factors are also required in the angiogenic process. Another important family of angiogenic factors, named angiopoietins (ANGPT), has been identified and an increasing number of studies have evaluated the role of this family in ovarian follicle development. Three ligands from the angiopoietin family have been identified in human and mouse, namely ANGPT1, ANGPT2 and ANGPT4 (also formerly known as ANG1, -2 and -4; see review of Stouffer *et al.*, 2001). These ligands bind to the same receptor tyrosine kinase named TEK (or TIE2). The importance of the angiopoietin family has become evident from studies of TEK knockout mice (see review of Hanahan, 1997). Interestingly, similar to the VEGF receptor knockout, the TEK null-mice die in utero but the phenotypic reasons are very different from that of mice lacking VEGF receptors.

While endothelial cells are present in normal numbers and the vasculature forms, the vessels remain immature, as determined by the lack of branching networks and organization, and evidence that the vessels are weak and prone to edema and hemorrhage. These observations suggest that the angiopoietin family, more specifically ANGPT1, is involved in recruiting peri-vascular cells that lead to vessel maturation and stabilization (Reviewed in Hanahan, 1997, Papertropoulos *et al.*, 1999). Moreover, studies on TEK signal transduction following stimulation with ANGPT ligands suggest that ANGPT1 induces receptor autophosphorylation while ANGPT2 does not (reviewed by Hanahan, 1997). Therefore, it was hypothesized that ANGPT1 binds to TEK to induce the recruitment and maintenance of the support cells necessary to maintain vessel integrity, while ANGPT2 binding prevents downstream signaling by ANGPT1, thereby loosening the matrix surrounding the blood vessels. In addition, it was further hypothesized that in the presence of other potent angiogenic factors such as VEGF, ANGPT2 would have a promoting effect on vasculaturization by allowing angiogenic factors to stimulate endothelial cell proliferation and migration. In the absence of angiogenic factors, ANGPT2 would destabilize the vessels to a point that would lead to degeneration of the vasculature.

In the rat ovary, ANGPT1 was detected exclusively in the theca cells of all follicles and showed a more intense immunostaining in the preovulatory follicle (Abramovich *et al.*, 2009). In comparison, ANGPT2 was very weakly expressed in the granulosa cells, while expression in the theca cells also increased with follicular size. The TEK receptor could not be detected in the granulosa cells but was stably expressed in the theca cells across all follicle categories studied. Similarly, Maisonpierre *et al.* (1997) detected ANGPT1 mRNA in the theca cells of all follicles while it also appears in the luteinizing granulosa cell during early CL formation. During early luteinization Maisonpierre *et al.* (1997) showed ANGPT2 mRNA expression near the front of invading vessels that successively appears in the theca cells of large preovulatory follicles and in the granulosa cell layer of luteinizing follicles. ANGPT2 was also found to increase dramatically in the granulosa cells of atretic follicles. In contrast, Hayashi *et al.* (2003 and 2004)

reported that ANGPT1, ANGPT2 and TEK mRNA were present in the theca and granulosa cells of bovine developing antral follicles. The authors showed that ANGPT 2 mRNA is decreasing in growing bovine follicles as they produce more oestradiol and that TEK mRNA expression remains unchanged between small and large antral follicles. Although the expression of ANGPT1 did not change in the theca cells of growing follicles, it peaked in the granulosa cells from larger antral follicles producing a considerable amount of oestradiol, however these changes were not statistically significant. Similarly, Shimizu *et al.* (2003c) found that ANGPT1 and ANGPT2 expression in granulosa cells decreased with increasing follicle diameter in prepubertal gilts, while TEK remained unaffected by follicle size. It is also important to note that, similar to VEGF, ANGPT1 and ANGPT2 are also affected by hypoxic conditions (reviewed by Stouffer *et al.*, 2001). Moreover, evidence for a role of ANGPT1 and ANGPT2 in the developing antral follicle is very scarce. First, Parborell *et al.* (2008) showed that intrabursal administration of ANGPT1 neutralizing antibody in the rat results in a reduction in the number of antral and preovulatory follicles and in increased atresia, supporting a role for ANGPT1 during antral follicle development. Hayashi *et al.* (2003) have also reported that ANGPT1 and ANGPT2 affect progesterone and oestradiol synthesis by bovine preovulatory follicles further illustrating the importance of the two ligands during follicle growth.

Other factors

Most studies focusing on angiogenesis in the developing follicle and corpus luteum have focused primarily on the vascular endothelial growth factor family and are now starting to evaluate the function of the angiopoietin family. However, a plethora of factors, each possessing different angiogenic properties, are expressed in the ovary; even though most of these other factors are not specific to endothelial cells and may exert pleiotropic effects on many different cell types. Among the factors that have the potential to influence angiogenesis in the ovarian follicle, hypoxia-inducible factor 1A (HIF1A) and angiogenin (ANG) are interesting candidates.

Hypoxia-inducible factor 1A

As mentioned earlier, hypoxia appears to impact the expression of VEGF and its receptors, as well as ANGPT1 and ANGPT2 expression. Oxygen tension in human and porcine follicular fluid is negatively correlated with follicle size, indicating that larger follicular cells are exposed to increased hypoxic conditions (Basini *et al.*, 2004, Fischer *et al.*, 1992). It is also well known that the transcription factor hypoxia inducible factor 1A (HIF1A) is induced during hypoxic conditions, thus promoting the expression of downstream target genes, including VEGF (reviewed by Semenza, 1998). Since the theca cells from antral follicles are generally well vascularized, they are less susceptible to hypoxia and one might predict HIF1A to be predominantly expressed in the granulosa cells. Immunolocalization studies in the primate ovary showed that HIF1A is weakly detected in the cytoplasm of theca cells, granulosa cells and oocytes from healthy follicles but HIF1A was abundant in the granulosa cell layer of atretic follicles (Duncan *et al.*, 2008). It was also expressed at a relatively low level in the preovulatory follicle with no clear nuclear staining being observed. However, at the time of ovulation, intense nuclear staining was observed in the granulosa cell layer. In contrast, a strong signal for HIF1A mRNA was detected in the granulosa cell layer of porcine small antral follicles via *in situ* hybridization (Boonyaparakob *et al.*, 2005). Unfortunately, although this study did not investigate expression further in the growing and preovulatory follicles, the authors did find that VEGF co-localized with HIF1A, further supporting a relationship between the two factors. The inhibition of VEGF in the primate ovary clearly up-regulated HIF1A expression in the granulosa cells (Duncan *et al.*, 2008), suggesting that, in response to the loss of VEGF and to the increasingly hypoxic conditions, HIF1A expression increases in an attempt to stimulate VEGF and angiogenesis. Importantly, HIF1A expression was also shown to be induced at low progesterone concentrations (10ng/ml) in cultured bovine granulosa cells, while higher progesterone concentrations appear to reduce its expression (Shimizu and Miyamoto, 2007). Luteinized human granulosa cells treated with hCG showed an increase expression in HIF1A concomitant with an increase in

VEGFA. These results suggest that although hypoxia influences VEGF expression through HIF1A, hormonal stimulation of HIF1A could also play an important role in controlling VEGF expression. This would provide another level of control over HIF1A, allowing for time-specific expression under limited hypoxic conditions.

Angiogenin

Angiogenin is a potent angiogenic factor originally purified from the media of cultured human colon adenocarcinoma cells but was later found in normal human and bovine serum (Bond *et al.*, 1988, Bond *et al.*, 1989, Fett *et al.*, 1985, Shapiro *et al.*, 1987). In addition, angiogenin mRNA was detected in several tumor cells and in the plasma of patients with various conditions including severe ovarian hyperstimulation syndrome and ovarian cancer (Aboulghar *et al.*, 1998, Chopra *et al.*, 1996, Li *et al.*, 1994, Montero *et al.*, 1998, Shimoyama *et al.*, 1996). Angiogenin has been associated with the oocyte and granulosa cells beginning with secondary follicles and was also detected in the theca cells of bovine antral follicles (Lee *et al.*, 1999), and its expression increased with the stage of follicle development. Moreover, angiogenin was detected in human granulosa cells and follicular fluid (Koga *et al.*, 2000), and its expression increased in cultured granulosa cells not only following hCG and cAMP stimulation but also under hypoxic conditions. More importantly, its expression was correlated with follicular fluid progesterone, suggesting that it may be particularly important in the periovulatory period. Finally, the findings of Malamitsi-Puchner *et al.* (2003) appear to support this hypothesis. In their study, higher human follicular fluid angiogenin was associated with a mature oocyte. As well, the abundance of follicular fluid angiogenin correlates with the abundance of VEGF, suggesting that the two factors might act in concert in the preovulatory follicle to modify the vasculature and ultimately affect oocyte maturation. However, at this point, it is impossible to rule out the possibility that angiogenin, VEGF or other factors also act directly on oocyte maturation.

Overall, the information presented in this section clearly indicates that the follicle vascular network is primarily established during antral follicle growth and then further develops along with other characteristics of later follicles. This is particularly interesting as it supports the observations that preantral follicle development is largely independent of exogenous gonadotrophic stimulation, and that larger follicles require an increased blood supply to limit hypoxia, provide metabolites and deliver the hormones necessary for further growth and development. It also provides strong evidence that defects in the follicle vasculature can have dramatic impacts on the normal development of healthy follicles. An overall schematic representation of intra-follicular growth factors and their role in the development of the antral follicle is presented in Figure 2.7.

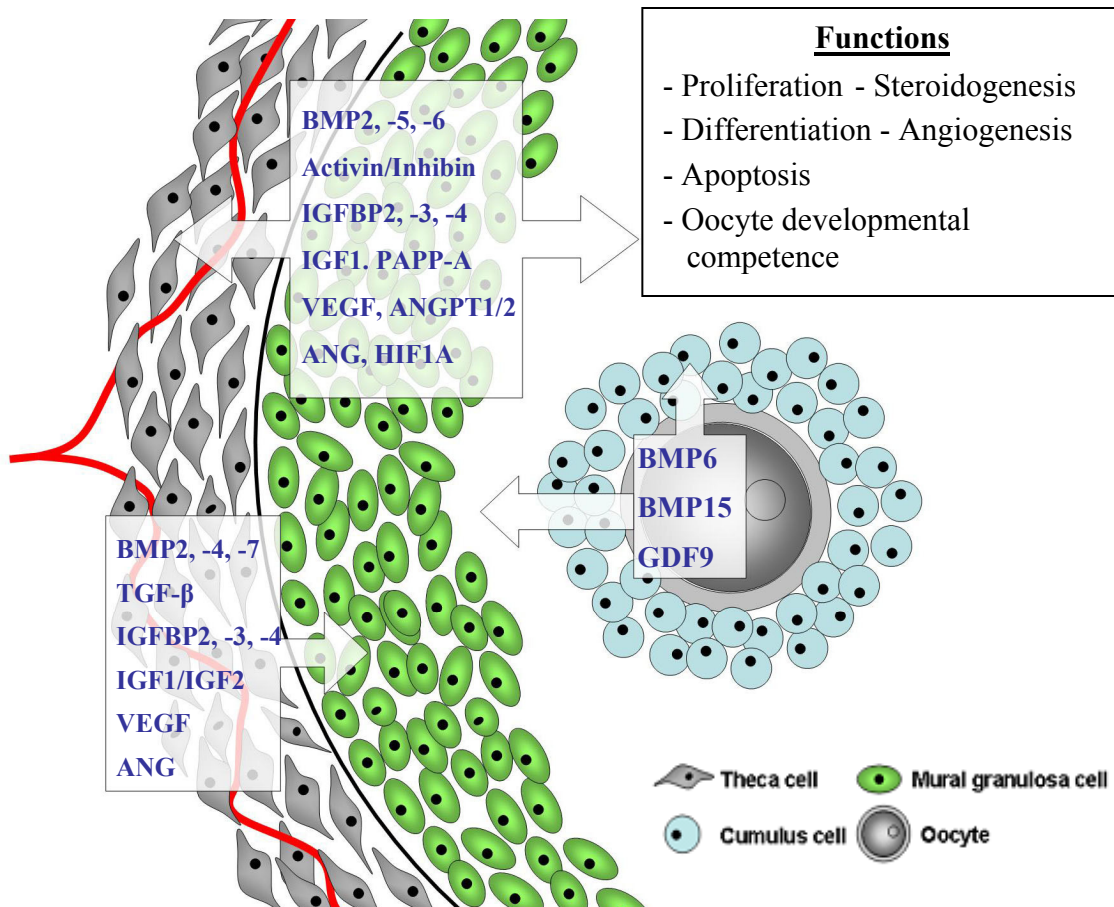


Figure 2.7 Schematic summary of the localization and functions of key local growth factors in the antral follicle.

Periovulatory period

Once the follicles are fully grown and the preovulatory population has been established, the oestradiol released by the follicle will provide a positive feedback signal to the hypothalamus and trigger the preovulatory LH surge which, in turn, will ultimately lead to the release of an oocyte. The series of events triggered by the LH surge and leading to ovulation consist of luteinization of the mural granulosa cell and theca cell, cumulus cell expansion and oocyte meiotic resumption (Richards *et al.*, 2002). Changes in the granulosa and theca cell compartments are predictable, as both cell types in the preovulatory follicle possess LH receptors. On the other hand, the quasi absence of LH receptor in the cumulus cells and oocyte is somewhat puzzling given the major biochemical and molecular events occurring in these two cell types after the LH surge. Gap-junctional communication between mural granulosa cells, cumulus cells and the oocyte has been postulated to propagate the signal from the LH responsive mural granulosa cells to the cumulus cells and oocyte, potentially through the modulation of the second messenger cAMP (Conti *et al.*, 2002, Mehlmann, 2005b) (see section on transzonal projections and gap junctions). However, more and more evidence suggests that paracrine signaling from the mural granulosa cells plays an important role in regulating cumulus cells and oocyte after the LH surge. Moreover, it has also become apparent, at least in the mouse, that the oocyte also mediates the cumulus cell's ability to respond to the preovulatory events. The TGF- β superfamily and the EGF/EGF-like ligands have attracted much interest because of their ability to fulfill these functions and will therefore be discussed in this section.

TGF- β superfamily

As mentioned earlier, the preovulatory LH surge triggers cumulus cell expansion which is caused by hyaluronic acid synthesis. This process is required for ovulation, since the inhibition of hyaluronic acid synthesis led to a marked reduction in ovulation (Chen *et al.*, 1993). In the mouse, removal of the oocyte from the cumulus-oocyte complex prevented the FSH-stimulated cumulus cell

expansion through inhibition of hyaluronic acid synthesis (Buccione *et al.*, 1990, Salustri *et al.*, 1990a). Similarly, addition of denuded oocytes to cultured mural granulosa cells induced the FSH-dependent synthesis of hyaluronic acid (Salustri *et al.*, 1990b). The oocyte factor responsible for cumulus cell expansion, named cumulus expansion-enabling factor (CEEF) was also shown to be only produced by fully grown mouse oocytes (Vanderhyden *et al.*, 1990). Paradoxically, although the pig oocyte has been shown to produce the CEEF and enable mouse cumulus cell expansion, it does not appear to be necessary for porcine cumulus cell expansion, or for hyaluronic acid synthesis (Prochazka *et al.*, 1991, Singh *et al.*, 1993a, Nagyova *et al.*, 1999). Similarly, bovine FSH-stimulated cumulus cells also undergo expansion in the absence of an oocyte (Ralph *et al.*, 1995). However, Prochazka *et al.* (1998) demonstrated that porcine cumulus and mural granulosa cells also produce the CEEF, as demonstrated by their ability to promote mouse cumulus cell expansion.

The identity of the CEEF still remains a controversial topic; however, BMP15 and GDF9 represent prime candidates to fulfill this function. First of all, GDF9 is a likely candidate because oocytes from GDF9 null mice are unable to stimulate FSH-induced cumulus expansion (Vanderhyden *et al.*, 2003). As well, the use of RNAi to knock-down the oocyte-derived GDF9 also prevented mouse cumulus expansion, and those oocytes failed to stimulate the expression of hyaluronan synthase 2 (HAS2) and prostaglandin-endoperoxide synthase 2 (PTGS2) necessary for hyaluronic acid synthesis (Gui and Joyce, 2005). Moreover, recombinant GDF9 has also been shown to promote mouse cumulus expansion and induce HAS2 expression (Elvin *et al.*, 1999, Dragovic *et al.*, 2005). Several lines of evidence suggest that BMP15 could also be involved in cumulus expansion. Firstly, BMP15 null mice have a decreased ovulation rate, while the BMP1B null mouse exhibited defects in cumulus expansion (Yan *et al.*, 2001, Yi *et al.*, 2001, Su *et al.*, 2004). In addition, the mature form of BMP15 appears during the periovulatory period in the mouse, following gonadotrophin stimulation (Yoshino *et al.*, 2006, Gueripel *et al.*, 2006). Unfortunately, recombinant BMP15 has yet to be tested for its ability to promote cumulus

expansion and hyaluronic acid synthesis and its related genes. In the pig, both BMP15 and GDF9 mRNA and protein were detected in the oocyte and GDF9 mRNA was also found in the surrounding cumulus and granulosa cells, convincingly demonstrating the potential for those cell types to promote cumulus cell expansion (Prochazka *et al.*, 2004, Lee *et al.*, 2008). As temporal expression of GDF9 mRNA did not increase prior to cumulus cell expansion, Prochazka *et al.* (2004) suggested that GDF9 might not be the porcine CEEF (Prochazka *et al.*, 2004). However, this observation does not preclude the possibility that post-translational modification or processing could regulate the bioactivity of GDF9. The direct effect of recombinant GDF9 or BMP15 on porcine cumulus expansion has yet to be reported but could shed light on how the ovulatory process is regulated in porcine follicles (Figure 2.8).

EGF, EGF-like peptide and receptors

The epidermal growth factor family includes many closely related proteins including EGF, amphiregulin (AREG), epiregulin (EREG) and betacellulin (BTC) (Conti *et al.*, 2006). These ligands signal through the EGF receptors, including EGFR (ErbB1), belonging to tyrosine kinase receptor family. The effect of EGF on cumulus and oocyte function in culture has been studied in all species and the roles of AREG, EREG and BTC is becoming increasingly documented in the mouse and in the pig.

In porcine follicles, EGF mRNA was detected in all cell types. However, the EGF protein appears to be primarily expressed in the mural granulosa cells, although it was also detected at much lower levels in the oocyte and cumulus cells (Singh *et al.*, 1995). The EGFR mRNA was found in all cell types in the antral follicle while its protein was detected in the cumulus and mural granulosa cells, as well as in the theca cells. However, no immunostaining was observed in the oocyte. This observation suggests that any effect of EGF on the oocyte would have to be mediated through the surrounding cumulus cells. The effects of epidermal growth factor on cumulus cell expansion and oocyte meiotic resumption have been extensively studied, and EGF potently stimulates mouse

and bovine cumulus cell expansion and evidence supports a similar role for EGF in the pig (Downs, 1989, Singh *et al.*, 1993b, Boland and Gosden, 1994, Lorenzo *et al.*, 1994, Ding and Foxcroft, 1994, Prochazka *et al.*, 2000). The ability of the porcine cumulus cell to undergo expansion increases as the follicle grows and can be explained by increased production and retention of hyaluronic acid by the cumulus cell of larger follicles (Prochazka *et al.*, 2000). Prochazka *et al.* (2003) also investigated whether differences in EGFR expression was the cause of this difference in hyaluronic acid synthesis but found no difference in receptor abundance. However, the ability of the receptor to become activated through tyrosine phosphorylation was greater in larger follicles, indicating increased responsiveness to EGF stimulation. In addition, EGF supplementation enhances oocyte nuclear maturation *in vitro* (Reed *et al.*, 1993, Singh *et al.*, 1993b, Ding and Foxcroft, 1994, Prochazka *et al.*, 2000). Oocyte developmental competence, as assessed by blastocyst development rate, was also found to be improved by addition of EGF to *in vitro* culture media (Abeydeera *et al.*, 1998). Consistent with the localization of the receptor, the effect of EGF on oocyte maturation has been shown to be mediated through the cumulus cell, as EGF had no direct effect on denuded oocytes (Li *et al.*, 2008). Moreover, these authors demonstrated that the effects of EGF on cumulus cell-mediated oocyte maturation occur through EGFR activation of MAPK and that phosphatidylinositol 3-kinase (PI3-kinase) was also involved. More recently, a group of EGF-like ligands, AREG, EREG and BTC have been found to mediate LH actions in the mouse follicle (Park *et al.*, 2004). The authors reported that mRNA for all three ligands were upregulated within 1-3 hours after hCG treatment and that they localized primarily, if not exclusively, to the mural granulosa cells. A recent study by Shimada *et al.* (2006) also reported the expression of these three ligands in COC. In addition, all three factors stimulated oocyte meiotic resumption *in vitro* in a whole follicle culture system and in a manner similar to LH (Park *et al.*, 2004). However, both EREG and AREG induced germinal vesicle breakdown (GVBD) in 2-3h, whereas hCG-induced GVBD took approximately 4h, suggesting that their effect is downstream of LH. A similar effect was also observed on cumulus cell expansion as LH- but

not AREG-, EREG- or BTC-stimulated cumulus cell expansion was abolished when COC rather than whole follicles were used, suggesting that LH regulation of cumulus cell expansion and oocyte meiotic resumption occur indirectly through mural granulosa cells. Moreover, the effects of the EGF-like ligands on the COC are also believed to occur via the cumulus cell, as denuded oocytes did not resume meiosis. Other convincing evidence for the involvement of these three factors in cumulus expansion was that all three EGF-like ligands induced transcript encoding HAS2, PTGS2 and TNFAIP6 in the same way as LH (Park *et al.*, 2004, Shimada *et al.*, 2006). Finally, the effect of AREG, EREG and BTC was shown to occur through the EGFR, since the EGFR kinase inhibitor AG1478 completely prevented their effects. Similar observations were made in porcine COC in which AREG and EREG were induced by FSH and LH (Yamashita *et al.*, 2007, Chen *et al.*, 2008). AREG also induced meiotic resumption in cultured porcine COC's and AG1478 inhibited both EGF- and AREG-stimulated cumulus expansion, suggesting that its activity occurred through the EGFR (Chen *et al.*, 2008). Another interesting aspect is that AREG and EREG are expressed as transmembrane precursors and require metalloprotease activity to be released and to activate the EGFR on the targeted cells (Peschon *et al.*, 1998, Dong *et al.*, 1999). In mouse embryonic cells, tumor necrosis factor (TNF) α -converting enzyme/A disintegrin and metalloprotease domain 17 (TACE or ADAM17) was the main metalloprotease involved in AREG and EREG cleavage (Sahin *et al.*, 2004). In cultured porcine COC, TACE/ADAM17 mRNA was induced by FSH and LH in a similar manner to that of AREG and EREG (Yamashita *et al.*, 2007). In addition, the activity of TACE/ADAM17 was induced by gonadotrophin supplementation. The used of selective and broad metalloprotease inhibitors prevented cumulus expansion, while the use of EGF completely reversed these inhibitory effects. From these results, the authors concluded that TACE/ADAM17 is required for the EGFR-mediated activation of cumulus cell expansion and oocyte meiotic maturation. Conti *et al.* (2006) proposed a model for LH regulation of the EGF network. It appears however that as opposed to his original model, in which only the mural granulosa cells produce AREG, EREG

and BTC, the cumulus cells are also expressing these ligands. Moreover, based on the observations from Yamashita *et al.* (2007), the TACE/ADAM17 metalloprotease is required for the release of the membrane bound EGF-like ligand and could explain the rapid stimulation of the EGFR following the LH surge (Figure 2.8). Finally, it remains to be established whether there is an interaction between the TGF- β and the EGF system in the regulation of the periovulatory events leading to ovulation.

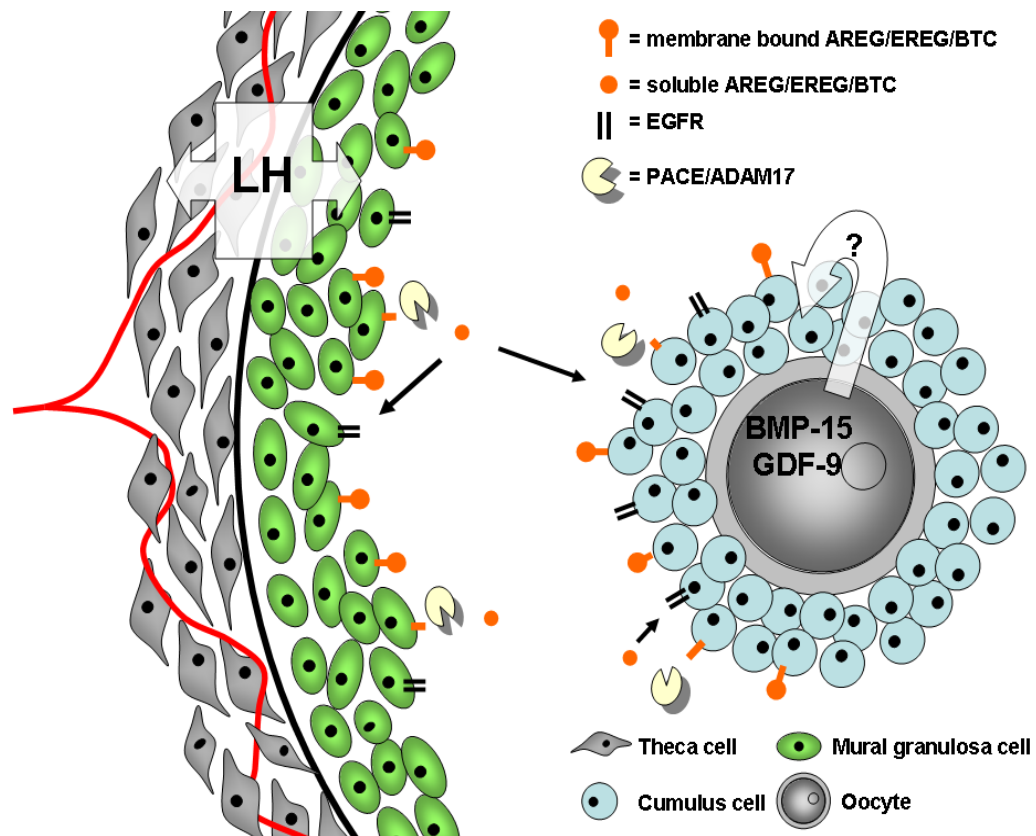


Figure 2.8 Schematic representation of the model proposed for LH-mediated cumulus expansion and oocyte meiotic resumption through stimulation of the EGF-like ligand. Adapted from Conti *et al.*, 2006.

Angiogenic factors

The importance of angiogenesis during antral follicle has been clearly established in previous sections. However, as follicles grow further and reach the preovulatory stage, the requirement for vascularization still exists. First, when follicular fluid oestradiol concentration reached a peak it must enter the circulatory system to provide feedback to the hypothalamus and pituitary and thus trigger the preovulatory LH surge. In turn, the release of gonadotrophins from the pituitary must reach the target cells inside the follicle to trigger ovulation. Moreover, as the oocyte is released and the basement membrane collapses, the luteinizing follicle must establish its vasculature to become a functional corpus luteum. Vascularization of the newly formed CL is very extensive as the CL requires one of the greatest blood flows of any tissue in the body (see review of Niswender and Nett, 1988).

Vascular endothelial growth factor

As previously mentioned, VEGF and its receptors FLT1 and KDR are expressed in the granulosa and theca cells of large antral follicle. However, in the pig follicle, VEGFA mRNA and protein in granulosa cells, and VEGF protein in follicular fluid sharply decline after hCG treatment, indicating that the vasculature required for the early luteal phase may be established before ovulation (Barboni *et al.*, 2000). Progesterone was shown to induce VEGF₁₂₀ mRNA expression in cow granulosa cells in culture but inhibited the expression of VEGF₁₆₄ (Shimizu and Miyamoto, 2007). This observation suggested that different VEGFA isoforms are regulated differently and potentially have different effects on follicle and CL vasculature. Moreover, direct injection of VEGF soluble receptor in the preovulatory follicle of the rhesus monkey led to ovulation failure, with the unruptured but luteinized follicles still containing their oocytes (Hazzard *et al.*, 2002). Interestingly, injection of a VEGF trap during the late follicular phase in the monkey results in the inhibition of the preovulatory rise in oestradiol and progesterone, as well as increased FSH and LH secretion. The treated animals failed to ovulate until the VEGF trap was eliminated from the system at which

time they resume normal ovarian activity. In addition, intra-follicular injection of soluble FLT1 into preovulatory follicles was shown to dose-dependently decrease plasma progesterone and inhibit ovulation in 50% of the animals (Xu *et al.*, 2005). It has been proposed that the effects of VEGF on vascular permeability could be involved in increasing gonadotrophin access to the preovulatory follicles and could be important for ovulation and later luteal functions (Koos *et al.*, 1995, Zeleznik *et al.*, 1981).

Angiopoietin

As reviewed earlier, ANGPT1, ANGPT2 and their receptor TEK are present in all antral follicles, including large preovulatory follicles, and appear to be essential for normal angiogenesis. However, evidence for a role of ANGPT1 or ANGPT2 during the periovulatory period is almost non-existent. However, Xu *et al.* (2005) have shown that intrafollicular injection of ANGPT2 into the preovulatory follicle around the time of the LH surge drastically reduces plasma progesterone concentrations. Interestingly, these animals also displayed abnormally high plasma oestrogen during the expected luteal phase. Finally, laparoscopic evaluation of the follicle from treated animals revealed the absence of ovulation. These results support the hypothesized negative role for ANGPT2 in the ovarian follicle. However, similar to the role of angiopoietin during the follicular phase, much remains to be learnt about these periovulatory mechanisms and the impact of disrupting these ligands in the preovulatory follicle and in the follicle to CL transition.

CONCLUSION

It is clear that follicle development is a long and dynamic process that relies on several endocrine signals, as well as an ever increasing number of intraovarian factors. It also appears that all ovarian cell compartments, including the oocyte itself, play critical roles during folliculogenesis, acting together to regulate angiogenesis, steroidogenesis, cell proliferation and differentiation, apoptosis, cumulus expansion and meiotic resumption, as well as modulating

oocyte developmental potential. Although our understanding of follicle growth has increased dramatically, there are still many unanswered questions, including how those factors interact together *in vivo* and why there appears to be so much redundancy in the functions of many growth factors. Finally, it is only through our understanding of the physiological mechanisms responsible for coordinating follicle development that further improvements in reproduction efficiency and sow management will be achieved.

REFERENCES

- Aberdam E, Hanski E & Dekel N** 1987 Maintenance of meiotic arrest in isolated rat oocytes by the invasive adenylate cyclase of *Bordetella pertussis*. *Biol Reprod* **36** 530-535.
- Abeydeera LR, Wang WH, Cantley TC, Rieke A, Prather RS & Day BN** 1998 Presence of epidermal growth factor during *in vitro* maturation of pig oocytes and embryo culture can modulate blastocyst development after *in vitro* fertilization. *Mol Reprod Dev* **51** 395-401.
- Aboulghar MA, Mansour RT, Serour GI, Elhelw BA & Shaarawy M** 1998 Elevated concentrations of angiogenin in serum and ascitic fluid from patients with severe ovarian hyperstimulation syndrome. *Hum Reprod* **13** 2068-2071.
- Abramovich D, Rodriguez Celin A, Hernandez F, Tesone M & Parborell F** 2009 Spatiotemporal analysis of the protein expression of angiogenic factors and their related receptors during folliculogenesis in rats with and without hormonal treatment. *Reproduction* **137** 309-320.
- Ackert CL, Gittens JE, O'Brien MJ, Eppig JJ & Kidder GM** 2001 Intercellular communication via connexin43 gap junctions is required for ovarian folliculogenesis in the mouse. *Dev Biol* **233** 258-270.
- Acosta TJ, Hayashi KG, Ohtani M & Miyamoto A** 2003 Local changes in blood flow within the preovulatory follicle wall and early corpus luteum in cows. *Reproduction* **125** 759-767.
- Adams GP, Matteri RL, Kastelic JP, Ko JC & Ginther OJ** 1992 Association between surges of follicle-stimulating hormone and the emergence of follicular waves in heifers. *J Reprod Fertil* **94** 177-188.
- Ainsworth L, Tsang BK, Downey BR & Marcus GJ** 1990 The synthesis and actions of steroids and prostaglandins during follicular maturation in the pig. *J Reprod Fertil Suppl* **40** 137-150.
- Albertini DF, Combelles CM, Benecchi E & Carabatsos MJ** 2001 Cellular basis for paracrine regulation of ovarian follicle development. *Reproduction* **121** 647-653.
- Albertini DF & Barrett SL** 2003 Oocyte-somatic cell communication. *Reproduction Suppl* **61** 49-54.
- Amar AP & Weiss MH** 2003 Pituitary anatomy and physiology. *Neurosurg Clin N Am* **14** 11-23, v.

Anderson LD, Schaerf FW & Channing CP 1979 Effects of follicular development on the ability of cultured porcine granulosa cells to convert androgens to oestrogens. *Adv Exp Med Biol* **112** 187-195.

Antczak M & Van Blerkom J 1997 Oocyte influences on early development: the regulatory proteins leptin and STAT3 are polarized in mouse and human oocytes and differentially distributed within the cells of the preimplantation stage embryo. *Mol Hum Reprod* **3** 1067-1086.

Armstrong DT, Goff AK & Dorrington JH 1979 Ovarian follicular development and function, Eds AR Midgley & WA Sadler. New York: Raven Press; pp 169-182.

Attia GR, Dooley CA, Rainey WE & Carr BR 2000 Transforming growth factor beta inhibits steroidogenic acute regulatory (StAR) protein expression in human ovarian thecal cells. *Molecular and Cellular Endocrinology* **170** 123-129.

Baranao JL & Hammond JM 1984 Comparative effects of insulin and insulin-like growth factors on DNA synthesis and differentiation of porcine granulosa cells. *Biochem Biophys Res Commun* **124** 484-490.

Barboni B, Turriani M, Galeati G, Spinaci M, Bacci ML, Forni M & Mattioli M 2000 Vascular endothelial growth factor production in growing pig antral follicles. *Biol Reprod* **63** 858-864.

Basini G, Bianco F, Grasselli F, Tirelli M, Bussolati S & Tamanini C 2004 The effects of reduced oxygen tension on swine granulosa cell. *Regul Pept* **120** 69-75.

Berardinelli JG, Ford JJ, Christenson RK & Anderson LL 1984 Luteinizing hormone secretion in ovariectomized gilts: effects of age, reproductive state and oestrogen replacement. *J Anim Sci* **58** 165-173.

Besnard N, Pisselet C, Monniaux D & Monget P 1997 Proteolytic activity degrading insulin-like growth factor-binding protein-2, -3, -4, and -5 in healthy growing and atretic follicles in the pig ovary. *Biol Reprod* **56** 1050-1058.

Bevans CG, Kordel M, Rhee SK & Harris AL 1998 Isoform composition of connexin channels determines selectivity among second messengers and uncharged molecules. *Journal of Biological Chemistry* **273** 2808-2816.

Bianco F, Basini G & Grasselli F 2005 Angiogenic activity of swine granulosa cells: effects of hypoxia and vascular endothelial growth factor Trap R1R2, a VEGF blocker. *Domest Anim Endocrinol* **28** 308-319.

Billig H, Furuta I & Hsueh AJ 1993 Estrogens inhibit and androgens enhance ovarian granulosa cell apoptosis. *Endocrinology* **133** 2204-2212.

- Black JL & Erickson BH** 1968 Oogenesis and ovarian development in the prenatal pig. *Anat Rec* **161** 45-55.
- Boland NI & Gosden RG** 1994 Effects of epidermal growth factor on the growth and differentiation of cultured mouse ovarian follicles. *J Reprod Fertil* **101** 369-374.
- Bond MD & Vallee BL** 1988 Isolation of bovine angiogenin using a placental ribonuclease inhibitor binding assay. *Biochemistry* **27** 6282-6287.
- Bond MD & Strydom DJ** 1989 Amino acid sequence of bovine angiogenin. *Biochemistry* **28** 6110-6113.
- Boonyaparakob U, Gadsby JE, Hedgpeth V, Routh P & Almond GW** 2003 Expression and localization of vascular endothelial growth factor and its receptors in pig corpora lutea during the oestrous cycle. *Reproduction* **126** 393-405.
- Boonyaparakob U, Gadsby JE, Hedgpeth V, Routh PA & Almond GW** 2005 Expression and localization of hypoxia inducible factor-1alpha mRNA in the porcine ovary. *Can J Vet Res* **69** 215-222.
- Bornslaeger EA, Mattei P & Schultz RM** 1986 Involvement of cAMP-dependent protein kinase and protein phosphorylation in regulation of mouse oocyte maturation. *Dev Biol* **114** 453-462.
- Brankin V, Mitchell MR, Webb B & Hunter MG** 2003a Paracrine effects of oocyte secreted factors and stem cell factor on porcine granulosa and theca cells *in vitro*. *Reprod Biol Endocrinol* **1** 55.
- Brankin V, Quinn RL, Webb R & Hunter MG** 2005a Evidence for a functional bone morphogenetic protein (BMP) system in the porcine ovary. *Domest Anim Endocrinol* **28** 367-379.
- Brankin V, Quinn RL, Webb R & Hunter MG** 2005b BMP-2 and -6 modulate porcine theca cell function alone and co-cultured with granulosa cells. *Domest Anim Endocrinol* **29** 593-604.
- Braw-Tal R & Yossefi S** 1997 Studies *in vivo* and *in vitro* on the initiation of follicle growth in the bovine ovary. *J Reprod Fertil* **109** 165-171.
- Brower PT & Schultz RM** 1982 Intercellular communication between granulosa cells and mouse oocytes: existence and possible nutritional role during oocyte growth. *Dev Biol* **90** 144-153.
- Buccione R, Vanderhyden BC, Caron PJ & Eppig JJ** 1990 FSH-induced expansion of the mouse cumulus oophorus *in vitro* is dependent upon a specific factor(s) secreted by the oocyte. *Dev Biol* **138** 16-25.

- Burger LL, Haisenleder DJ, Dalkin AC & Marshall JC** 2004 Regulation of gonadotropin subunit gene transcription. *J Mol Endocrinol* **33** 559-584.
- Cahill LP & Mauleon P** 1980 Influences of season, cycle and breed on follicular growth rates in sheep. *J Reprod Fertil* **58** 321-328.
- Campbell BK & Baird DT** 2001 Inhibin A is a follicle stimulating hormone-responsive marker of granulosa cell differentiation, which has both autocrine and paracrine actions in sheep. *J Endocrinol* **169** 333-345.
- Campbell BK, Telfer EE, Webb R & Baird DT** 2004 Evidence of a role for follicle-stimulating hormone in controlling the rate of preantral follicle development in sheep. *Endocrinology* **145** 1870-1879.
- Carabatsos MJ, Sellitto C, Goodenough DA & Albertini DF** 2000 Oocyte-granulosa cell heterologous gap junctions are required for the coordination of nuclear and cytoplasmic meiotic competence. *Dev Biol* **226** 167-179.
- Caubo B, Devinna RS & Tonetta SA** 1989 Regulation of Steroidogenesis in Cultured Porcine Theca Cells by Growth-Factors. *Endocrinology* **125** 321-326.
- Channing CP & Tsafiri A** 1977 Mechanism of action of luteinizing hormone and follicle-stimulating hormone on the ovary *in vitro*. *Metabolism* **26** 413-468.
- Chapman SC, Bernard DJ, Jelen J & Woodruff TK** 2002 Properties of inhibin binding to betaglycan, InhBP/p120 and the activin type II receptors. *Molecular and Cellular Endocrinology* **196** 79-93.
- Chen L, Russell PT & Larsen WJ** 1993 Functional significance of cumulus expansion in the mouse: roles for the preovulatory synthesis of hyaluronic acid within the cumulus mass. *Mol Reprod Dev* **34** 87-93.
- Chen X, Zhou B, Yan J, Xu B, Tai P, Li J, Peng S, Zhang M & Xia G** 2008 Epidermal growth factor receptor activation by protein kinase C is necessary for FSH-induced meiotic resumption in porcine cumulus-oocyte complexes. *J Endocrinol* **197** 409-419.
- Chopra V, Dinh TV & Hannigan EV** 1996 Angiogenin, interleukins, and growth-factor levels in serum of patients with ovarian cancer: correlation with angiogenesis. *Cancer J Sci Am* **2** 279-285.
- Colonna R & Mangia F** 1983 Mechanisms of amino acid uptake in cumulus-enclosed mouse oocytes. *Biol Reprod* **28** 797-803.
- Conti M, Andersen CB, Richard F, Mehats C, Chun SY, Horner K, Jin C & Tsafiri A** 2002 Role of cyclic nucleotide signaling in oocyte maturation. *Molecular and Cellular Endocrinology* **187** 153-159.

Conti M, Hsieh M, Park JY & Su YQ 2006 Role of the epidermal growth factor network in ovarian follicles. *Mol Endocrinol* **20** 715-723.

Coskun S & Lin YC 1994 Effects of transforming growth factors and activin-A on *in vitro* porcine oocyte maturation. *Mol Reprod Dev* **38** 153-159.

Coskun S, Uzumcu M, Lin YC, Friedman CI & Alak BM 1995 Regulation of cumulus cell steroidogenesis by the porcine oocyte and preliminary characterization of oocyte-produced factor(s). *Biol Reprod* **53** 670-675.

Cottrell GT & Burt JM 2005 Functional consequences of heterogeneous gap junction channel formation and its influence in health and disease. *Biochimica Et Biophysica Acta-Biomembranes* **1711** 126-141.

Crowe MA, Kelly P, Driancourt MA, Boland MP & Roche JF 2001 Effects of follicle-stimulating hormone with and without luteinizing hormone on serum hormone concentrations, follicle growth, and intrafollicular estradiol and aromatase activity in gonadotropin-releasing hormone-immunized heifers. *Biol Reprod* **64** 368-374.

Daguet MC 1978 Some aspects of final follicle growth in the sow. *Annl Biol Anim Biochim Biophys* **18** 1343-1349.

Dailey RA, Clark JR, Staigmiller RB, First NL, Chapman AB & Casida LE 1976 Growth of new follicles following electrocautery in four genetic groups of swine. *J Anim Sci* **43** 175-183.

Danfou MA, Picton HM, Leaf A & Gosden RG 1999 Impact of gonadotrophins treatment on the size of the ovarian follicle reserve. *J Reprod Fertil Abstr Series* **23** 62.

Dan-Goor M, Sasson S, Davarashvili A & Almagor M 1997 Expression of glucose transporter and glucose uptake in human oocytes and preimplantation embryos. *Hum Reprod* **12** 2508-2510.

de Kretser DM & Phillips DJ 1998 Mechanisms of protein feedback on gonadotropin secretion. *J Reprod Immunol* **39** 1-12.

Dekel N, Aberdam E & Sherizly I 1984 Spontaneous maturation *in vitro* of cumulus-enclosed rat oocytes is inhibited by forskolin. *Biol Reprod* **31** 244-250.

Dekel N 1988 Regulation of oocyte maturation. The role of cAMP. *Ann N Y Acad Sci* **541** 211-216.

Demura R, Suzuki T, Tajima S, Mitsuhashi S, Odagiri E & Demura H 1993 Activin and inhibin secretion by cultured porcine granulosa cells is stimulated by FSH and LH. *Endocr J* **40** 447-451.

- Diaz FJ, Wigglesworth K & Eppig JJ** 2007 Oocytes determine cumulus cell lineage in mouse ovarian follicles. *J Cell Sci* **120** 1330-1340.
- Ding J & Foxcroft GR** 1994 Epidermal growth factor enhances oocyte maturation in pigs. *Mol Reprod Dev* **39** 30-40.
- Donahue RP & Stern S** 1968 Follicular cell support of oocyte maturation: production of pyruvate *in vitro*. *J Reprod Fertil* **17** 395-398.
- Dong J, Opresko LK, Dempsey PJ, Lauffenburger DA, Coffey RJ & Wiley HS** 1999 Metalloprotease-mediated ligand release regulates autocrine signaling through the epidermal growth factor receptor. *Proc Natl Acad Sci U S A* **96** 6235-6240.
- Downs SM** 1989 Specificity of epidermal growth factor action on maturation of the murine oocyte and cumulus oophorus *in vitro*. *Biol Reprod* **41** 371-379.
- Dragovic RA, Ritter LJ, Schulz SJ, Amato F, Armstrong DT & Gilchrist RB** 2005 Role of oocyte-secreted growth differentiation factor 9 in the regulation of mouse cumulus expansion. *Endocrinology* **146** 2798-2806.
- Driancourt MA, Locatelli A & Prunier A** 1995 Effects of gonadotrophin deprivation on follicular growth in gilts. *Reprod Nutr Dev* **35** 663-673.
- Drummond AE, Le MT, Ethier JF, Dyson M & Findlay JK** 2002 Expression and localization of activin receptors, Smads, and beta glycan to the postnatal rat ovary. *Endocrinology* **143** 1423-1433.
- Duckworth BC, Weaver JS & Ruderman JV** 2002 G2 arrest in *Xenopus* oocytes depends on phosphorylation of cdc25 by protein kinase A. *Proc Natl Acad Sci U S A* **99** 16794-16799.
- Duncan WC, van den Driesche S & Fraser HM** 2008 Inhibition of vascular endothelial growth factor in the primate ovary up-regulates hypoxia-inducible factor-1alpha in the follicle and corpus luteum. *Endocrinology* **149** 3313-3320.
- Edry I, Sela-Abramovich S & Dekel N** 2006 Meiotic arrest of oocytes depends on cell-to-cell communication in the ovarian follicle. *Molecular and Cellular Endocrinology* **252** 102-106.
- el-Fouly MA, Cook B, Nekola M & Nalbandov AV** 1970 Role of the ovum in follicular luteinization. *Endocrinology* **87** 286-293.
- Elvin JA, Clark AT, Wang P, Wolfman NM & Matzuk MM** 1999 Paracrine actions of growth differentiation factor-9 in the mammalian ovary. *Mol Endocrinol* **13** 1035-1048.

- Engelhardt H, Tekpetey FR, Gore-Langton RE & Armstrong DT** 1992 Regulation of steroid production in cultured porcine thecal cells by transforming growth factor-beta. *Molecular and Cellular Endocrinology* **85** 117-126.
- Eppig JJ** 1976 Analysis of mouse oogenesis *in vitro*. Oocyte isolation and the utilization of exogenous energy sources by growing oocytes. *J Exp Zool* **198** 375-382.
- Eppig JJ** 1982 The relationship between cumulus cell-oocyte coupling, oocyte meiotic maturation, and cumulus expansion. *Dev Biol* **89** 268-272.
- Eppig JJ** 1991 Intercommunication between mammalian oocytes and companion somatic cells. *Bioessays* **13** 569-574.
- Eppig JJ, Ward-Bailey PF & Coleman DL** 1985 Hypoxanthine and adenosine in murine ovarian follicular fluid: concentrations and activity in maintaining oocyte meiotic arrest. *Biol Reprod* **33** 1041-1049.
- Eppig JJ, Wigglesworth K, Pendola F & Hirao Y** 1997 Murine oocytes suppress expression of luteinizing hormone receptor messenger ribonucleic acid by granulosa cells. *Biol Reprod* **56** 976-984.
- Eppig JJ, Pendola FL, Wigglesworth K & Pendola JK** 2005 Mouse oocytes regulate metabolic cooperativity between granulosa cells and oocytes: amino acid transport. *Biol Reprod* **73** 351-357.
- Erickson GF & Shimasaki S** 2003 The spatiotemporal expression pattern of the bone morphogenetic protein family in rat ovary cell types during the estrous cycle. *Reprod Biol Endocrinol* **1** 9.
- Esbenshade KL, Ziecik AJ & Britt JH** 1990 Regulation and action of gonadotrophins in pigs. *J Reprod Fertil Suppl* **40** 19-32.
- Evans G, Dobias M, King GJ & Armstrong DT** 1981 Estrogen, androgen, and progesterone biosynthesis by theca and granulosa of preovulatory follicles in the pig. *Biol Reprod* **25** 673-682.
- Fair T** 2003 Follicular oocyte growth and acquisition of developmental competence. *Anim Reprod Sci* **78** 203-216.
- Fett JW, Strydom DJ, Lobb RR, Alderman EM, Bethune JL, Riordan JF & Vallee BL** 1985 Isolation and characterization of angiogenin, an angiogenic protein from human carcinoma cells. *Biochemistry* **24** 5480-5486.
- Findlay JK & Drummond AE** 1999 Regulation of the FSH receptor in the ovary. *Trends in Endocrinology and Metabolism* **10** 183-188.

Fischer B, Kunzel W, Kleinstein J & Gips H 1992 Oxygen tension in follicular fluid falls with follicle maturation. *Eur J Obstet Gynecol Reprod Biol* **43** 39-43.

Fonda ES, Rampacek GB, Kraeling RR & Barb CR 1983 Serum luteinizing hormone in prepuberal gilts after ovariectomy or adrenalectomy. *J Anim Sci* **56** 1174-1179.

Ford JJ & Howard HJ 1997 Activin inhibition of estradiol and progesterone production in porcine granulosa cells. *J Anim Sci* **75** 761-766.

Ford JJ, Berardinelli JG, Christenson RK & Anderson LL 2000 Luteinizing hormone secretion as affected by hypophyseal stalk transection and estradiol-17beta in ovariectomized gilts. *Anim Reprod Sci* **63** 255-274.

Fortune JE 2003 The early stages of follicular development: activation of primordial follicles and growth of preantral follicles. *Anim Reprod Sci* **78** 135-163.

Foxcroft GR, Cosgrove JR, Ding J, Hofacker S & Wiesak T 1994 Reproductive function: Current concepts. In: Cole DJA, Wiseman J, Varley M (eds), Principles of Pig Science, Nottingham University Press; pp. 225-252.

Fraser HM, Wilson H, Rudge JS & Wiegand SJ 2005 Single injections of vascular endothelial growth factor trap block ovulation in the macaque and produce a prolonged, dose-related suppression of ovarian function. *J Clin Endocrinol Metab* **90** 1114-1122.

Fraser HM 2006 Regulation of the ovarian follicular vasculature. *Reprod Biol Endocrinol* **4** 18.

Galeati G, Spinaci M, Govoni N, Zannoni A, Fantinati P, Seren E & Tamanini C 2003 Stimulatory effects of fasting on vascular endothelial growth factor (VEGF) production by growing pig ovarian follicles. *Reproduction* **126** 647-652.

Gerber HP, Condorelli F, Park J & Ferrara N 1997 Differential transcriptional regulation of the two vascular endothelial growth factor receptor genes. Flt-1, but not Flk-1/KDR, is up-regulated by hypoxia. *Journal of Biological Chemistry* **272** 23659-23667.

Gershon E, Plaks V & Dekel N 2008 Gap junctions in the ovary: Expression, localization and function. *Molecular and Cellular Endocrinology* **282** 18-25.

Gilchrist RB, Morrissey MP, Ritter LJ & Armstrong DT 2003 Comparison of oocyte factors and transforming growth factor-beta in the regulation of DNA synthesis in bovine granulosa cells. *Molecular and Cellular Endocrinology* **201** 87-95.

Gilchrist RB, Ritter LJ, Myllymaa S, Kaivo-Oja N, Dragovic RA, Hickey TE, Ritvos O & Mottershead DG 2006 Molecular basis of oocyte-paracrine signalling that promotes granulosa cell proliferation. *J Cell Sci* **119** 3811-3821.

Gilchrist RB, Lane M & Thompson JG 2008 Oocyte-secreted factors: regulators of cumulus cell function and oocyte quality. *Hum Reprod Update* **14** 159-177.

Gitay-Goren H, Kim IC, Miggins ST & Schomberg DW 1993 Transforming growth factor beta modulates gonadotropin receptor expression in porcine and rat granulosa cells differently. *Biol Reprod* **48** 1284-1289.

Glister C, Groome NP & Knight PG 2003 Oocyte-mediated suppression of follicle-stimulating hormone- and insulin-like growth factor-induced secretion of steroids and inhibin-related proteins by bovine granulosa cells *in vitro*: possible role of transforming growth factor alpha. *Biol Reprod* **68** 758-765.

Glister C, Kemp CF & Knight PG 2004 Bone morphogenetic protein (BMP) ligands and receptors in bovine ovarian follicle cells: actions of BMP-4, -6 and -7 on granulosa cells and differential modulation of Smad-1 phosphorylation by follistatin. *Reproduction* **127** 239-254.

Glister C, Richards SL & Knight PG 2005 Bone morphogenetic proteins (BMP) -4, -6, and -7 potently suppress basal and luteinizing hormone-induced androgen production by bovine theca interna cells in primary culture: could ovarian hyperandrogenic dysfunction be caused by a defect in thecal BMP signaling? *Endocrinology* **146** 1883-1892.

Glister C, Groome NP & Knight PG 2006 Bovine follicle development is associated with divergent changes in activin-A, inhibin-A and follistatin and the relative abundance of different follistatin isoforms in follicular fluid. *J Endocrinol* **188** 215-225.

Goddard I, Hendrick JC, Benahmed M & Morera AM 1995 Transforming growth factor beta receptor expression in cultured porcine granulosa cells. *Molecular and Cellular Endocrinology* **115** 207-213.

Gong JG, Campbell BK, Bramley TA, Gutierrez CG, Peters AR & Webb R 1996 Suppression in the secretion of follicle-stimulating hormone and luteinizing hormone, and ovarian follicle development in heifers continuously infused with a gonadotropin-releasing hormone agonist. *Biol Reprod* **55** 68-74.

Gosden RG & Telfer E 1987 Numbers of follicles and oocytes in mammalian ovaries and their allometric relationships. *Journal of Zoology* **211** 169-175.

Gougeon A 1996 Regulation of ovarian follicular development in primates: facts and hypotheses. *Endocr Rev* **17** 121-155.

Granot I & Dekel N 1994 Phosphorylation and expression of connexin-43 ovarian gap junction protein are regulated by luteinizing hormone. *Journal of Biological Chemistry* **269** 30502-30509.

Grant SA, Hunter MG & Foxcroft GR 1989 Morphological and biochemical characteristics during ovarian follicular development in the pig. *J Reprod Fertil* **86** 171-183.

Grasselli F, Basini G, Bussolati S & Tamanini C 2002 Effects of VEGF and bFGF on proliferation and production of steroids and nitric oxide in porcine granulosa cells. *Reprod Domest Anim* **37** 362-368.

Greenaway J, Connor K, Pedersen HG, Coomber BL, LaMarre J & Petrik J 2004 Vascular endothelial growth factor and its receptor, Flk-1/KDR, are cytoprotective in the extravascular compartment of the ovarian follicle. *Endocrinology* **145** 2896-2905.

Greenwald GS & Moor RM 1989 Isolation and preliminary characterization of pig primordial follicles. *J Reprod Fertil* **87** 561-571.

Grimes RW, Barber JA, Shimasaki S, Ling N & Hammond JM 1994 Porcine ovarian granulosa cells secrete insulin-like growth factor-binding proteins-4 and -5 and express their messenger ribonucleic acids: regulation by follicle-stimulating hormone and insulin-like growth factor-1. *Biol Reprod* **50** 695-701.

Gueripel X, Brun V & Gougeon A 2006 Oocyte bone morphogenetic protein 15, but not growth differentiation factor 9, is increased during gonadotropin-induced follicular development in the immature mouse and is associated with cumulus oophorus expansion. *Biol Reprod* **75** 836-843.

Gui LM & Joyce IM 2005 RNA interference evidence that growth differentiation factor-9 mediates oocyte regulation of cumulus expansion in mice. *Biol Reprod* **72** 195-199.

Guthrie HD, Ireland JL, Good TE & Ireland JJ 1997 Expression of different molecular mass forms of inhibin in atretic and nonatretic follicles during the early luteal phase and altrenogest-synchronized follicular phase in pigs. *Biol Reprod* **56** 870-877.

Guthrie HD & Garrett WM 2001 Apoptosis during folliculogenesis in pigs. *Reprod Suppl* **58** 17-29.

Haghighat N & Van Winkle LJ 1990 Developmental change in follicular cell-enhanced amino acid uptake into mouse oocytes that depends on intact gap junctions and transport system Gly. *J Exp Zool* **253** 71-82.

Han SJ, Chen R, Paronetto MP & Conti M 2005 Wee1B is an oocyte-specific kinase involved in the control of meiotic arrest in the mouse. *Curr Biol* **15** 1670-1676.

Hanahan D 1997 Signaling vascular morphogenesis and maintenance. *Science* **277** 48-50.

Haney AF & Schomberg DW 1981 Estrogen and progesterone production by developing porcine follicles *in vitro*: evidence for estrogen formation by theca. *Endocrinology* **109** 971-977.

Hay MR, Cran DG & Moor RM 1976 Structural changes occurring during atresia in sheep ovarian follicles. *Cell Tissue Res* **169** 515-529.

Hayashi KG, Acosta TJ, Tetsuka M, Berisha B, Matsui M, Schams D, Ohtani M & Miyamoto A 2003 Involvement of angiotensin II system in bovine follicular development and atresia: messenger RNA expression in theca interna and effect on steroid secretion. *Biol Reprod* **69** 2078-2084.

Hayashi KG, Berisha B, Matsui M, Schams D & Miyamoto A 2004 Expression of mRNA for the angiotensin II system in granulosa cells during follicular development in cows. *J Reprod Dev* **50** 477-480.

Hazzard TM, Molskness TA, Chaffin CL & Stouffer RL 1999 Vascular endothelial growth factor (VEGF) and angiotensin II regulation by gonadotrophin and steroids in macaque granulosa cells during the peri-ovulatory interval. *Mol Hum Reprod* **5** 1115-1121.

Hazzard TM, Xu F & Stouffer RL 2002 Injection of soluble vascular endothelial growth factor receptor 1 into the preovulatory follicle disrupts ovulation and subsequent luteal function in rhesus monkeys. *Biol Reprod* **67** 1305-1312.

Heller DT & Schultz RM 1980 Ribonucleoside metabolism by mouse oocytes: metabolic cooperativity between the fully grown oocyte and cumulus cells. *J Exp Zool* **214** 355-364.

Herlands RL & Schultz RM 1984 Regulation of mouse oocyte growth: probable nutritional role for intercellular communication between follicle cells and oocytes in oocyte growth. *J Exp Zool* **229** 317-325.

Hickey TE, Marrocco DL, Gilchrist RB, Norman RJ & Armstrong DT 2004 Interactions between androgen and growth factors in granulosa cell subtypes of porcine antral follicles. *Biol Reprod* **71** 45-52.

Hickey TE, Marrocco DL, Amato F, Ritter LJ, Norman RJ, Gilchrist RB & Armstrong DT 2005 Androgens augment the mitogenic effects of oocyte-

secreted factors and growth differentiation factor 9 on porcine granulosa cells. *Biol Reprod* **73** 825-832.

Hirshfield AN 1985 Comparison of granulosa cell proliferation in small follicles of hypophysectomized, prepubertal, and mature rats. *Biol Reprod* **32** 979-987.

Horner K, Livera G, Hinckley M, Trinh K, Storm D & Conti M 2003 Rodent oocytes express an active adenylyl cyclase required for meiotic arrest. *Dev Biol* **258** 385-396.

Hsueh AJ, Dahl KD, Vaughan J, Tucker E, Rivier J, Bardin CW & Vale W 1987 Heterodimers and homodimers of inhibin subunits have different paracrine action in the modulation of luteinizing hormone-stimulated androgen biosynthesis. *Proc Natl Acad Sci U S A* **84** 5082-5086.

Hunter MG 2000 Oocyte maturation and ovum quality in pigs. *Rev Reprod* **5** 122-130.

Hunter MG & Wiesak T 1990 Evidence for and implications of follicular heterogeneity in pigs. *J Reprod Fertil Suppl* **40** 163-177.

Hunter MG, Robinson RS, Mann GE & Webb R 2004 Endocrine and paracrine control of follicular development and ovulation rate in farm species. *Anim Reprod Sci* **82-83** 461-477.

Hunter MG & Paradis F 2009 Intra-follicular regulatory mechanisms in the porcine ovary. *Control of Pig Reproduction VIII*.

Hunzicker-Dunn M & Birnbaumer L 1985 The involvement of adenylyl cyclase and cyclic AMP-dependent protein kinases in luteinizing hormone actions. In *Luteinizing Hormone Action and Receptors*, pp. 57-134. Ed M. Ascoli. CRC Press, Boca Raton.

Hussein TS, Froiland DA, Amato F, Thompson JG & Gilchrist RB 2005 Oocytes prevent cumulus cell apoptosis by maintaining a morphogenic paracrine gradient of bone morphogenetic proteins. *J Cell Sci* **118** 5257-5268.

Hussein TS, Thompson JG & Gilchrist RB 2006 Oocyte-secreted factors enhance oocyte developmental competence. *Dev Biol* **296** 514-521.

Iijima K, Jiang JY, Shimizu T, Sasada H & Sato E 2005 Acceleration of follicular development by administration of vascular endothelial growth factor in cycling female rats. *J Reprod Dev* **51** 161-168.

Ing NH 2005 Steroid Hormones Regulate Gene Expression Posttranscriptionally by Altering the Stabilities of Messenger RNAs. *Biol Reprod* **72** 1290-1296.

- Ireland JJ** 1987 Control of follicular growth and development. *J Reprod Fertil Suppl* **34** 39-54.
- Itahana K, Morikazu Y & Takeya T** 1996 Differential expression of four connexin genes, Cx-26, Cx-30.3, Cx-32, and Cx-43, in the porcine ovarian follicle. *Endocrinology* **137** 5036-5044.
- Itahana K, Tanaka T, Morikazu Y, Komatu S, Ishida N & Takeya T** 1998 Isolation and characterization of a novel connexin gene, Cx-60, in porcine ovarian follicles. *Endocrinology* **139** 320-329.
- Jiang JY, Macchiarelli G, Miyabayashi K & Sato E** 2002 Follicular microvasculature in the porcine ovary. *Cell Tissue Res* **310** 93-101.
- Juengel JL & McNatty KP** 2005 The role of proteins of the transforming growth factor-beta superfamily in the intraovarian regulation of follicular development. *Hum Reprod Update* **11** 143-160.
- Juneja SC, Barr KJ, Enders GC & Kidder GM** 1999 Defects in the germ line and gonads of mice lacking connexin43. *Biol Reprod* **60** 1263-1270.
- Kanzaki H, Okamura H, Okuda Y, Takenaka A, Morimoto K & Nishimura T** 1982 Scanning electron microscopic study of rabbit ovarian follicle microvasculature using resin injection-corrosion casts. *J Anat* **134** 697-704.
- Kesner JS, Kraeling RR, Rampacek GB & Johnson B** 1987 Absence of an estradiol-induced surge of luteinizing hormone in pigs receiving unvarying pulsatile gonadotropin-releasing hormone stimulation. *Endocrinology* **121** 1862-1869.
- Kesner JS, Estienne MJ, Kraeling RR & Rampacek GB** 1989 Luteinizing hormone and prolactin secretion in hypophysial-stalk-transected pigs given estradiol and pulsatile gonadotropin-releasing hormone. *Neuroendocrinology* **49** 502-508.
- Kidder GM & Mhawi AA** 2002 Gap junctions and ovarian folliculogenesis. *Reproduction* **123** 613-620.
- Kitai H, Yoshimura Y, Wright KH, Santulli R & Wallach EE** 1985 Microvasculature of preovulatory follicles: comparison of *in situ* and *in vitro* perfused rabbit ovaries following stimulation of ovulation. *Am J Obstet Gynecol* **152** 889-895.
- Knight PG & Glister C** 2006 TGF-beta superfamily members and ovarian follicle development. *Reproduction* **132** 191-206.

- Koga K, Osuga Y, Tsutsumi O, Momoeda M, Suenaga A, Kugu K, Fujiwara T, Takai Y, Yano T & Taketani Y** 2000 Evidence for the presence of angiogenin in human follicular fluid and the up-regulation of its production by human chorionic gonadotropin and hypoxia. *J Clin Endocrinol Metab* **85** 3352-3355.
- Kolodziejczyk J, Gregoraszczyk EL, Leibovich H & Gertler A** 2001 Different action of ovine GH on porcine theca and granulosa cells proliferation and insulin-like growth factors I- and II-stimulated estradiol production. *Reprod Biol* **1** 33-41.
- Kolodziejczyk J, Gertler A, Leibovich H, Rzasca J & Gregoraszczyk EL** 2003 Synergistic action of growth hormone and insulin-like growth factor I (IGF-I) on proliferation and estradiol secretion in porcine granulosa and theca cells cultured alone or in coculture. *Theriogenology* **60** 559-570.
- Koos RD** 1995 Increased expression of vascular endothelial growth/permeability factor in the rat ovary following an ovulatory gonadotropin stimulus: potential roles in follicle rupture. *Biol Reprod* **52** 1426-1435.
- Kovo M, Kandli-Cohen M, Ben-Haim M, Galiani D, Carr DW & Dekel N** 2006 An active protein kinase A (PKA) is involved in meiotic arrest of rat growing oocytes. *Reproduction* **132** 33-43.
- Kraeling RR, Barb CR & Rampacek GB** 1986 Ovarian response of the hypophysial stalk-transected pig to pregnant mare serum gonadotropin. *Domest Anim Endocrinol* **3** 177-183.
- Kubota T, Kamada S, Taguchi M & Aso T** 1994 Autocrine/paracrine function of transforming growth factor-beta 1 in porcine granulosa cells. *Hum Reprod* **9** 2118-2122.
- Kumar TR, Wang Y, Lu N & Matzuk MM** 1997 Follicle stimulating hormone is required for ovarian follicle maturation but not male fertility. *Nat Genet* **15** 201-204.
- Laforest MF, Pouliot E, Gueguen L & Richard FJ** 2005 Fundamental significance of specific phosphodiesterases in the control of spontaneous meiotic resumption in porcine oocytes. *Mol Reprod Dev* **70** 361-372.
- Lee HS, Lee IS, Kang TC, Jeong GB & Chang SI** 1999 Angiogenin is involved in morphological changes and angiogenesis in the ovary. *Biochem Biophys Res Commun* **257** 182-186.
- Lee GS, Kim HS, Hwang WS & Hyun SH** 2008 Characterization of porcine growth differentiation factor-9 and its expression in oocyte maturation. *Mol Reprod Dev* **75** 707-714.

- Li D, Bell J, Brown A & Berry CL** 1994 The observation of angiogenin and basic fibroblast growth factor gene expression in human colonic adenocarcinomas, gastric adenocarcinomas, and hepatocellular carcinomas. *J Pathol* **172** 171-175.
- Li MD, DePaolo LV & Ford JJ** 1997 Expression of follistatin and inhibin/activin subunit genes in porcine follicles. *Biology of Reproduction* **57** 112-118.
- Li R, Norman RJ, Armstrong DT & Gilchrist RB** 2000 Oocyte-secreted factor(s) determine functional differences between bovine mural granulosa cells and cumulus cells. *Biol Reprod* **63** 839-845.
- Li M, Liang CG, Xiong B, Xu BZ, Lin SL, Hou Y, Chen DY, Schatten H & Sun QY** 2008 PI3-kinase and mitogen-activated protein kinase in cumulus cells mediate EGF-induced meiotic resumption of porcine oocyte. *Domest Anim Endocrinol* **34** 360-371.
- Lischinsky A & Armstrong DT** 1983 Granulosa cell stimulation of thecal androgen synthesis. *Can J Physiol Pharmacol* **61** 472-477.
- Liu J, Aronow BJ, Witte DP, Pope WF & La Barbera AR** 1998 Cyclic and maturation-dependent regulation of follicle-stimulating hormone receptor and luteinizing hormone receptor messenger ribonucleic acid expression in the porcine ovary. *Biol Reprod* **58** 648-658.
- Liu J, Koenigsfeld AT, Cantley TC, Boyd CK, Kobayashi Y & Lucy MC** 2000 Growth and the initiation of steroidogenesis in porcine follicles are associated with unique patterns of gene expression for individual components of the ovarian insulin-like growth factor system. *Biol Reprod* **63** 942-952.
- Lorenzo PL, Illera MJ, Illera JC & Illera M** 1994 Enhancement of cumulus expansion and nuclear maturation during bovine oocyte maturation *in vitro* by the addition of epidermal growth factor and insulin-like growth factor I. *J Reprod Fertil* **101** 697-701.
- Lucy MC** 2008 Functional differences in the growth hormone and insulin-like growth factor axis in cattle and pigs: implications for post-partum nutrition and reproduction. *Reprod Domest Anim* **43 Suppl 2** 31-39.
- Lucy MC, Liu J, Boyd CK & Bracken CJ** 2001 Ovarian follicular growth in sows. *Reprod Suppl* **58** 31-45.
- Macchiarelli G, Nottola SA, Vizza E, Familiari G, Kikuta A, Murakami T & Motta PM** 1993 Microvasculature of growing and atretic follicles in the rabbit ovary: a SEM study of corrosion casts. *Arch Histol Cytol* **56** 1-12.

Maisonpierre PC, Suri C, Jones PF, Bartunkova S, Wiegand SJ, Radziejewski C, Compton D, McClain J, Aldrich TH, Papadopoulos N, Daly TJ, Davis S, Sato TN & Yancopoulos GD 1997 Angiopoietin-2, a natural antagonist for Tie2 that disrupts *in vivo* angiogenesis. *Science* **277** 55-60.

Malamitsi-Puchner A, Sarandakou A, Baka S, Hasiakos D, Kouskouni E & Creatsas G 2003 *In vitro* fertilization: angiogenic, proliferative, and apoptotic factors in the follicular fluid. *Ann N Y Acad Sci* **997** 124-128.

Manabe N, Goto Y, Matsuda-Minehata F, Inoue N, Maeda A, Sakamaki K & Miyano T 2004 Regulation mechanism of selective atresia in porcine follicles: regulation of granulosa cell apoptosis during atresia. *J Reprod Dev* **50** 493-514.

Manabe N, Matsuda-Minehata F, Goto Y, Maeda A, Cheng Y, Nakagawa S, Inoue N, Wongpanit K, Jin H, Gonda H & Li J 2008 Role of cell death ligand and receptor system on regulation of follicular atresia in pig ovaries. *Reprod Domest Anim* **43 Suppl 2** 268-272.

Martinez-Chequer JC, Stouffer RL, Hazzard TM, Patton PE & Molskness TA 2003 Insulin-like growth factors-1 and -2, but not hypoxia, synergize with gonadotropin hormone to promote vascular endothelial growth factor-A secretion by monkey granulosa cells from preovulatory follicles. *Biol Reprod* **68** 1112-1118.

Mattioli M, Barboni B, Turriani M, Galeati G, Zannoni A, Castellani G, Berardinelli P & Scapolo PA 2001 Follicle activation involves vascular endothelial growth factor production and increased blood vessel extension. *Biol Reprod* **65** 1014-1019.

May JV, Gotcher ED, Gangrade BK & Mau YH 1994 Secretion of Transforming Growth-Factor-Beta (Tgf-Beta) by Porcine Theca and Granulosa-Cells in-Vitro and Differential-Effects Upon Cell-Proliferation. *Endocrine* **2** 1045-1054.

May JV, Stephenson LA, Turzcynski CJ, Fong HW, Mau YH & Davis JS 1996 Transforming growth factor beta expression in the porcine ovary: evidence that theca cells are the major secretory source during antral follicle development. *Biol Reprod* **54** 485-496.

Mazerbourg S, Overgaard MT, Oxvig C, Christiansen M, Conover CA, Laurendeau I, Vidaud M, Tosser-Klopp G, Zapf J & Monget P 2001 Pregnancy-associated plasma protein-A (PAPP-A) in ovine, bovine, porcine, and equine ovarian follicles: involvement in IGF binding protein-4 proteolytic degradation and mRNA expression during follicular development. *Endocrinology* **142** 5243-5253.

- Mazerbourg S, Bondy CA, Zhou J & Monget P** 2003 The insulin-like growth factor system: a key determinant role in the growth and selection of ovarian follicles? a comparative species study. *Reprod Domest Anim* **38** 247-258.
- McGaughey RW, Montgomery DH & Richter JD** 1979 Germinal vesicle configurations and patterns of polypeptide synthesis of porcine oocytes from antral follicles of different size, as related to their competency for spontaneous maturation. *J Exp Zool* **209** 239-254.
- McNatty KP, Heath DA, Hudson N & Clarke IJ** 1990 Effect of long-term hypophysectomy on ovarian follicle populations and gonadotrophin-induced adenosine cyclic 3',5'-monophosphate output by follicles from Booroola ewes with or without the F gene. *J Reprod Fertil* **90** 515-522.
- McNeilly AS, Crawford JL, Taragnat C, Nicol L & McNeilly JR** 2003 The differential secretion of FSH and LH: regulation through genes, feedback and packaging. *Reprod Suppl* **61** 463-476.
- Mehlmann LM** 2005a Oocyte-specific expression of Gpr3 is required for the maintenance of meiotic arrest in mouse oocytes. *Dev Biol* **288** 397-404.
- Mehlmann LM** 2005b Stops and starts in mammalian oocytes: recent advances in understanding the regulation of meiotic arrest and oocyte maturation. *Reproduction* **130** 791-799.
- Mehlmann LM, Jones TL & Jaffe LA** 2002 Meiotic arrest in the mouse follicle maintained by a Gs protein in the oocyte. *Science* **297** 1343-1345.
- Mehlmann LM, Saeki Y, Tanaka S, Brennan TJ, Evsikov AV, Pendola FL, Knowles BB, Eppig JJ & Jaffe LA** 2004 The Gs-linked receptor GPR3 maintains meiotic arrest in mammalian oocytes. *Science* **306** 1947-1950.
- Meunier H, Cajander SB, Roberts VJ, Rivier C, Sawchenko PE, Hsueh AJW & Vale W** 1988 Rapid Changes in the Expression of Inhibin Alpha-Subunits, Beta-a-Subunits, and Beta-B-Subunits in Ovarian Cell-Types during the Rat Estrous-Cycle. *Molecular Endocrinology* **2** 1352-1363.
- Miller AT, Picton HM & Hunter MG** 1999 Suppression of ovarian activity in the gilt and reversal by exogenous gonadotrophin administration. *Anim Reprod Sci* **54** 179-193.
- Mondschein JS, Canning SF & Hammond JM** 1988 Effects of transforming growth factor-beta on the production of immunoreactive insulin-like growth factor I and progesterone and on [3H]thymidine incorporation in porcine granulosa cell cultures. *Endocrinology* **123** 1970-1976.

- Mondschein JS, Smith SA & Hammond JM** 1990 Production of insulin-like growth factor binding proteins (IGFBPs) by porcine granulosa cells: identification of IGFBP-2 and -3 and regulation by hormones and growth factors. *Endocrinology* **127** 2298-2306.
- Monniaux D & Pisselet C** 1992 Control of proliferation and differentiation of ovine granulosa cells by insulin-like growth factor-I and follicle-stimulating hormone *in vitro*. *Biol Reprod* **46** 109-119.
- Montero S, Guzman C, Cortes-Funes H & Colomer R** 1998 Angiogenin expression and prognosis in primary breast carcinoma. *Clin Cancer Res* **4** 2161-2168.
- Moor RM, Smith MW & Dawson RM** 1980 Measurement of intercellular coupling between oocytes and cumulus cells using intracellular markers. *Exp Cell Res* **126** 15-29.
- Morbeck DE, Esbenshade KL, Flowers WL & Britt JH** 1992 Kinetics of follicle growth in the prepubertal gilt. *Biol Reprod* **47** 485-491.
- Motlik J & Fulka J** 1986 Factors affecting meiotic competence in pig oocytes. *Theriogenology* **25** 87-95.
- Mulheron GW, Mulheron JG, Danielpour D & Schomberg DW** 1992 Porcine granulosa cells do not express transforming growth factor-beta 2 (TGF-beta 2) messenger ribonucleic acid: molecular basis for their inability to produce TGF-beta activity comparable to that of rat granulosa cells. *Endocrinology* **131** 2609-2614.
- Murakami T, Ikebuchi Y, Ohtsuka A, Kikuta A, Taguchi T & Ohtani O** 1988 The blood vascular wreath of rat ovarian follicle, with special reference to its changes in ovulation and luteinization: a scanning electron microscopic study of corrosion casts. *Arch Histol Cytol* **51** 299-313.
- Nagyova E, Prochazka R & Vanderhyden BC** 1999 Oocyectomy does not influence synthesis of hyaluronic acid by pig cumulus cells: retention of hyaluronic acid after insulin-like growth factor-I treatment in serum-free medium. *Biol Reprod* **61** 569-574.
- Nakano R, Sasaki K, Shima K & Kitayama S** 1983 Follicle-stimulating hormone and luteinizing hormone receptors on porcine granulosa cells during follicular maturation: an autoradiographic study. *Exp Clin Endocrinol* **81** 17-23.
- Newhall KJ, Criniti AR, Cheah CS, Smith KC, Kafer KE, Burkart AD & McKnight GS** 2006 Dynamic anchoring of PKA is essential during oocyte maturation. *Curr Biol* **16** 321-327.

Niswender GD & Nett TM 1988 The corpus luteum and its control. In: *The Physiology of Reproduction*, Eds: Knobil E, Neill JD, Ewing LL, Greewald GS, Market CL, Pfaff DW. Raven Press, New York; pp 489-525.

Oktay K, Briggs D & Gosden RG 1997 Ontogeny of follicle-stimulating hormone receptor gene expression in isolated human ovarian follicles. *J Clin Endocrinol Metab* **82** 3748-3751.

Papapetropoulos A, Garcia-Cardena G, Dengler TJ, Maisonpierre PC, Yancopoulos GD & Sessa WC 1999 Direct actions of angiopoietin-1 on human endothelium: evidence for network stabilization, cell survival, and interaction with other angiogenic growth factors. *Lab Invest* **79** 213-223.

Parborell F, Abramovich D & Tesone M 2008 Intrabursal administration of the antiangiopoietin 1 antibody produces a delay in rat follicular development associated with an increase in ovarian apoptosis mediated by changes in the expression of BCL2 related genes. *Biol Reprod* **78** 506-513.

Park JY, Su YQ, Ariga M, Law E, Jin SL & Conti M 2004 EGF-like growth factors as mediators of LH action in the ovulatory follicle. *Science* **303** 682-684.

Peschon JJ, Slack JL, Reddy P, Stocking KL, Sunnarborg SW, Lee DC, Russell WE, Castner BJ, Johnson RS, Fitzner JN, Boyce RW, Nelson N, Kozlosky CJ, Wolfson MF *et al.* 1998 An essential role for ectodomain shedding in mammalian development. *Science* **282** 1281-1284.

Picton, HM 2000 Activation of follicle development: The primordial follicle. *Theriogenology* **55**(6):1193-1210.

Picton HM, Miller AT & Hunter MG 1999 Effect of FSH infusion on follicle development in GnRH agonist-treated gilts. *J Reprod Fertil* **117** 249-257.

Pierre A, Pisselet C, Dupont J, Bontoux M & Monget P 2005 Bone morphogenetic protein 5 expression in the rat ovary: biological effects on granulosa cell proliferation and steroidogenesis. *Biol Reprod* **73** 1102-1108.

Pincus G & Enzmann EV 1935 The comparative behavior of mammalian eggs *in vivo* and *in vitro*: I. The activation of ovarian eggs. *J Exp Med* **62** 655-675.

Prochazka R, Nagyova E, Rimkevicova Z, Nagai T, Kikuchi K & Motlik J 1991 Lack of effect of oocyctectomy on expansion of the porcine cumulus. *J Reprod Fertil* **93** 569-576.

Prochazka R, Nagyova E, Brem G, Schellander K & Motlik J 1998 Secretion of cumulus expansion-enabling factor (CEEF) in porcine follicles. *Mol Reprod Dev* **49** 141-149.

- Prochazka R, Srsen V, Nagyova E, Miyano T & Flechon JE** 2000 Developmental regulation of effect of epidermal growth factor on porcine oocyte-cumulus cell complexes: nuclear maturation, expansion, and F-actin remodeling. *Mol Reprod Dev* **56** 63-73.
- Prochazka R, Kalab P & Nagyova E** 2003 Epidermal growth factor-receptor tyrosine kinase activity regulates expansion of porcine oocyte-cumulus cell complexes *in vitro*. *Biol Reprod* **68** 797-803.
- Prochazka R, Nemcova L, Nagyova E & Kanka J** 2004 Expression of growth differentiation factor 9 messenger RNA in porcine growing and preovulatory ovarian follicles. *Biol Reprod* **71** 1290-1295.
- Prunier A & Louveau I** 1997 Influence of ovariectomy on metabolic and endocrine parameters during sexual development in the female pig. *J Endocrinol* **154** 423-429.
- Quinn RL, Shuttleworth G & Hunter MG** 2004a Immunohistochemical localization of the bone morphogenetic protein receptors in the porcine ovary. *J Anat* **205** 15-23.
- Quinn RL, Brankin V, McGarr C, Webb R & Hunter MG** 2004b BMPs 2, 6 and 15 are regulators of porcine theca cell function *in vitro*. *Reproduction Abstract Ser* **31**:44
- Ralph JH, Telfer EE & Wilmut I** 1995 Bovine cumulus cell expansion does not depend on the presence of an oocyte secreted factor. *Mol Reprod Dev* **42** 248-253.
- Reaume AG, de Sousa PA, Kulkarni S, Langille BL, Zhu D, Davies TC, Juneja SC, Kidder GM & Rossant J** 1995 Cardiac malformation in neonatal mice lacking connexin43. *Science* **267** 1831-1834.
- Reed ML, Estrada JL, Illera MJ & Petters RM** 1993 Effects of epidermal growth factor, insulin-like growth factor-I, and dialyzed porcine follicular fluid on porcine oocyte maturation *in vitro*. *J Exp Zool* **266** 74-78.
- Reinhardt RR, Chin E, Zhou J, Taira M, Murata T, Manganiello VC & Bondy CA** 1995 Distinctive anatomical patterns of gene expression for cGMP-inhibited cyclic nucleotide phosphodiesterases. *J Clin Invest* **95** 1528-1538.
- Richards JS, Ireland JJ, Rao MC, Bernath GA, Midgley AR, Jr. & Reichert LE, Jr.** 1976 Ovarian follicular development in the rat: hormone receptor regulation by estradiol, follicle stimulating hormone and luteinizing hormone. *Endocrinology* **99** 1562-1570.

Richards JS, Jonassen JA, Rolfes AI, Kersey K & Reichert LE, Jr. 1979 Adenosine 3',5'-monophosphate, luteinizing hormone receptor, and progesterone during granulosa cell differentiation: effects of estradiol and follicle-stimulating hormone. *Endocrinology* **104** 765-773.

Richards JS, Russell DL, Ochsner S & Espey LL 2002 Ovulation: New dimensions and new regulators of the inflammatory-like response. *Annual Review of Physiology* **64** 69-92.

Roberts VJ, Barth S, el-Roeiy A & Yen SS 1993 Expression of inhibin/activin subunits and follistatin messenger ribonucleic acids and proteins in ovarian follicles and the corpus luteum during the human menstrual cycle. *J Clin Endocrinol Metab* **77** 1402-1410.

Rosenfeld CS, Wagner JS, Roberts RM & Lubahn DB 2001 Intraovarian actions of oestrogen. *Reproduction* **122** 215-226.

Sahin U, Weskamp G, Kelly K, Zhou HM, Higashiyama S, Peschon J, Hartmann D, Saftig P & Blobel CP 2004 Distinct roles for ADAM10 and ADAM17 in ectodomain shedding of six EGFR ligands. *J Cell Biol* **164** 769-779.

Salustri A, Yanagishita M & Hascall VC 1990a Mouse oocytes regulate hyaluronic acid synthesis and mucification by FSH-stimulated cumulus cells. *Dev Biol* **138** 26-32.

Salustri A, Ulisse S, Yanagishita M & Hascall VC 1990b Hyaluronic acid synthesis by mural granulosa cells and cumulus cells *in vitro* is selectively stimulated by a factor produced by oocytes and by transforming growth factor-beta. *Journal of Biological Chemistry* **265** 19517-19523.

Sasseville M, Cote N, Guillemette C & Richard FJ 2006 New insight into the role of phosphodiesterase 3A in porcine oocyte maturation. *BMC Dev Biol* **6** 47.

Sasseville M, Gagnon MC, Guillemette C, Sullivan R, Gilchrist RB & Richard FJ 2009 Regulation of gap junctions in porcine cumulus-oocyte complexes: contributions of granulosa cell contact, gonadotropins, and lipid rafts. *Mol Endocrinol* **23** 700-710.

Schultz RM, Montgomery RR, Ward-Bailey PF & Eppig JJ 1983 Regulation of oocyte maturation in the mouse: possible roles of intercellular communication, cAMP, and testosterone. *Dev Biol* **95** 294-304.

Sela-Abramovich S, Chorev E, Galiani D & Dekel N 2005 Mitogen-activated protein kinase mediates luteinizing hormone-induced breakdown of communication and oocyte maturation in rat ovarian follicles. *Endocrinology* **146** 1236-1244.

Sela-Abramovich S, Edry I, Galiani D, Nevo N & Dekel N 2006 Disruption of gap junctional communication within the ovarian follicle induces oocyte maturation. *Endocrinology* **147** 2280-2286.

Semenza GL 1998 Hypoxia-inducible factor 1: master regulator of O₂ homeostasis. *Curr Opin Genet Dev* **8** 588-594.

Shapiro R, Strydom DJ, Olson KA & Vallee BL 1987 Isolation of angiogenin from normal human plasma. *Biochemistry* **26** 5141-5146.

Sharma HS, Tang ZH, Gho BC & Verdouw PD 1995 Nucleotide sequence and expression of the porcine vascular endothelial growth factor. *Biochim Biophys Acta* **1260** 235-238.

Sherizly I, Galiani D & Dekel N 1988 Regulation of oocyte maturation: communication in the rat cumulus-oocyte complex. *Hum Reprod* **3** 761-766.

Shimada M, Hernandez-Gonzalez I, Gonzalez-Robayna I & Richards JS 2006 Paracrine and autocrine regulation of epidermal growth factor-like factors in cumulus oocyte complexes and granulosa cells: key roles for prostaglandin synthase 2 and progesterone receptor. *Mol Endocrinol* **20** 1352-1365.

Shimasaki S, Gao L, Shimonaka M & Ling N 1991 Isolation and molecular cloning of insulin-like growth factor-binding protein-6. *Mol Endocrinol* **5** 938-948.

Shimasaki S, Moore RK, Otsuka F & Erickson GF 2004 The bone morphogenetic protein system in mammalian reproduction. *Endocr Rev* **25** 72-101.

Shimizu T, Jiang JY, Sasada H & Sato E 2002 Changes of messenger RNA expression of angiogenic factors and related receptors during follicular development in gilts. *Biol Reprod* **67** 1846-1852.

Shimizu T, Kawahara M, Abe Y, Yokoo M, Sasada H & Sato E 2003a Follicular microvasculature and angiogenic factors in the ovaries of domestic animals. *J Reprod Dev* **49** 181-192.

Shimizu T, Jiang JY, Iijima K, Miyabayashi K, Ogawa Y, Sasada H & Sato E 2003b Induction of follicular development by direct single injection of vascular endothelial growth factor gene fragments into the ovary of miniature gilts. *Biol Reprod* **69** 1388-1393.

Shimizu T, Iijima K, Sasada H & Sato E 2003c Messenger ribonucleic acid expressions of hepatocyte growth factor, angiopoietins and their receptors during follicular development in gilts. *J Reprod Dev* **49** 203-211.

Shimizu T, Yokoo M, Miyake Y, Sasada H & Sato E 2004 Differential expression of bone morphogenetic protein 4-6 (BMP-4, -5, and -6) and growth differentiation factor-9 (GDF-9) during ovarian development in neonatal pigs. *Domest Anim Endocrinol* **27** 397-405.

Shimizu T, Berisha B, Schams D & Miyamoto A 2007 Expression of angiopoietin (ANPT)-1, ANPT-2 and their receptors in dominant follicles during periovulatory period in GnRH-treated cow. *Reprod Domest Anim* **42** 221-224.

Shimizu T & Miyamoto A 2007 Progesterone induces the expression of vascular endothelial growth factor (VEGF) 120 and Flk-1, its receptor, in bovine granulosa cells. *Anim Reprod Sci* **102** 228-237.

Shimizu T, Iijima K, Ogawa Y, Miyazaki H, Sasada H & Sato E 2008 Gene injections of vascular endothelial growth factor and growth differentiation factor-9 stimulate ovarian follicular development in immature female rats. *Fertil Steril* **89** 1563-1570.

Shimoyama S, Gansauge F, Gansauge S, Negri G, Oohara T & Beger HG 1996 Increased angiogenin expression in pancreatic cancer is related to cancer aggressiveness. *Cancer Res* **56** 2703-2706.

Silva CC & Knight PG 1998 Modulatory actions of activin-A and follistatin on the developmental competence of *in vitro*-matured bovine oocytes. *Biol Reprod* **58** 558-565.

Silva CC, Groome NP & Knight PG 1999 Demonstration of a suppressive effect of inhibin alpha-subunit on the developmental competence of *in vitro* matured bovine oocytes. *J Reprod Fertil* **115** 381-388.

Simon AM, Goodenough DA, Li E & Paul DL 1997 Female infertility in mice lacking connexin 37. *Nature* **385** 525-529.

Singh B, Zhang X & Armstrong DT 1993a Porcine oocytes release cumulus expansion-enabling activity even though porcine cumulus expansion *in vitro* is independent of the oocyte. *Endocrinology* **132** 1860-1862.

Singh B, Barbe GJ & Armstrong DT 1993b Factors influencing resumption of meiotic maturation and cumulus expansion of porcine oocyte-cumulus cell complexes *in vitro*. *Mol Reprod Dev* **36** 113-119.

Singh B, Rutledge JM & Armstrong DT 1995 Epidermal growth factor and its receptor gene expression and peptide localization in porcine ovarian follicles. *Mol Reprod Dev* **40** 391-399.

Sirotkin AV, Duksova J, Pivko J, Makarevich AV & Kubek A 2002 Effect of growth factors on proliferation, apoptosis and protein kinase A expression in cultured porcine cumulus oophorus cells. *Reprod Nutr Dev* **42** 35-43.

Sisco B & Pfeffer PL 2007 Expression of activin pathway genes in granulosa cells of dominant and subordinate bovine follicles. *Theriogenology* **68** 29-37.

Spicer LJ 2004 Proteolytic degradation of insulin-like growth factor binding proteins by ovarian follicles: a control mechanism for selection of dominant follicles. *Biol Reprod* **70** 1223-1230.

Spicer LJ & Echternkamp SE 1995 The ovarian insulin and insulin-like growth factor system with an emphasis on domestic animals. *Domest Anim Endocrinol* **12** 223-245.

Spicer LJ, Aad PY, Allen DT, Mazerbourg S, Payne AH & Hsueh AJ 2008 Growth differentiation factor 9 (GDF9) stimulates proliferation and inhibits steroidogenesis by bovine theca cells: influence of follicle size on responses to GDF9. *Biol Reprod* **78** 243-253.

Staton JM, Thomson AM & Leedman PJ 2000 Hormonal regulation of mRNA stability and RNA-protein interactions in the pituitary. *J Mol Endocrinol* **25** 17-34.

Steffl M, Schweiger M & Amselgruber WM 2008 Expression of transforming growth factor-beta3 (TGF-beta3) in the porcine ovary during the oestrus cycle. *Histol Histopathol* **23** 665-671.

Stickan F, Parvizi N & Elsaesser F 1999 Compensation by pulsatile GnRH infusions for incompetence for oestradiol-induced LH surges in long-term ovariectomized gilts and castrated male pigs. *J Reprod Fertil* **115** 333-339.

Stoklosowa S, Gregoraszczyk E & Channing CP 1982 Estrogen and progesterone secretion by isolated cultured porcine thecal and granulosa cells. *Biol Reprod* **26** 943-952.

Stouffer RL, Martinez-Chequer JC, Molskness TA, Xu F & Hazzard TM 2001 Regulation and action of angiogenic factors in the primate ovary. *Arch Med Res* **32** 567-575.

Su YQ, Denegre JM, Wigglesworth K, Pendola FL, O'Brien MJ & Eppig JJ 2003 Oocyte-dependent activation of mitogen-activated protein kinase (ERK1/2) in cumulus cells is required for the maturation of the mouse oocyte-cumulus cell complex. *Dev Biol* **263** 126-138.

Su YQ, Wu X, O'Brien MJ, Pendola FL, Denegre JN, Matzuk MM & Eppig JJ 2004 Synergistic roles of BMP15 and GDF9 in the development and function of the oocyte-cumulus cell complex in mice: genetic evidence for an oocyte-granulosa cell regulatory loop. *Dev Biol* **276** 64-73.

- Sugiura K, Pendola FL & Eppig JJ** 2005 Oocyte control of metabolic cooperativity between oocytes and companion granulosa cells: energy metabolism. *Dev Biol* **279** 20-30.
- Tamanini C & De Ambrogi M** 2004 Angiogenesis in developing follicle and corpus luteum. *Reprod Domest Anim* **39** 206-216.
- ten Dijke P & Hill CS** 2004 New insights into TGF-beta-Smad signalling. *Trends Biochem Sci* **29** 265-273.
- Tisdall DJ, Watanabe K, Hudson NL, Smith P & McNatty KP** 1995 FSH receptor gene expression during ovarian follicle development in sheep. *J Mol Endocrinol* **15** 273-281.
- Trombly DJ, Woodruff TK & Mayo KE** 2009 Roles for transforming growth factor beta superfamily proteins in early folliculogenesis. *Semin Reprod Med* **27** 14-23.
- Tsafri A, Chun SY, Zhang R, Hsueh AJ & Conti M** 1996 Oocyte maturation involves compartmentalization and opposing changes of cAMP levels in follicular somatic and germ cells: studies using selective phosphodiesterase inhibitors. *Dev Biol* **178** 393-402.
- Tsang BK, Moon YS & Armstrong DT** 1982 Estradiol-17 beta and androgen secretion by isolated porcine ovarian follicular cells *in vitro*. *Can J Physiol Pharmacol* **60** 1112-1118.
- Tsang BK, Ainsworth L, Downey BR & Marcus GJ** 1985 Differential production of steroids by dispersed granulosa and theca interna cells from developing preovulatory follicles of pigs. *J Reprod Fertil* **74** 459-471.
- Ulloa-Aguirre A, Maldonado A, Damian-Matsumura P & Timossi C** 2001 Endocrine regulation of gonadotropin glycosylation. *Arch Med Res* **32** 520-532.
- van den Hurk R & van de Pavert SA** 2001 Localization of an activin/activin receptor system in the porcine ovary. *Molecular Reproduction and Development* **60** 463-471.
- van den Hurk R & Zhao J** 2005 Formation of mammalian oocytes and their growth, differentiation and maturation within ovarian follicles. *Theriogenology* **63** 1717-1751.
- Vanderhyden BC, Caron PJ, Buccione R & Eppig JJ** 1990 Developmental pattern of the secretion of cumulus expansion-enabling factor by mouse oocytes and the role of oocytes in promoting granulosa cell differentiation. *Dev Biol* **140** 307-317.

- Vanderhyden BC, Cohen JN & Morley P** 1993 Mouse oocytes regulate granulosa cell steroidogenesis. *Endocrinology* **133** 423-426.
- Vanderhyden BC, Macdonald EA, Nagyova E & Dhawan A** 2003 Evaluation of members of the TGFbeta superfamily as candidates for the oocyte factors that control mouse cumulus expansion and steroidogenesis. *Reprod Suppl* **61** 55-70.
- Vivarelli E, Conti M, De Felici M & Siracusa G** 1983 Meiotic resumption and intracellular cAMP levels in mouse oocytes treated with compounds which act on cAMP metabolism. *Cell Differ* **12** 271-276.
- Wandji SA, Srsen V, Voss AK, Eppig JJ & Fortune JE** 1996 Initiation *in vitro* of growth of bovine primordial follicles. *Biol Reprod* **55** 942-948.
- Wandji SA, Gadsby JE, Simmen FA, Barber JA & Hammond JM** 2000 Porcine ovarian cells express messenger ribonucleic acids for the acid-labile subunit and insulin-like growth factor binding protein-3 during follicular and luteal phases of the estrous cycle. *Endocrinology* **141** 2638-2647.
- Wang XN & Greenwald GS** 1993 Hypophysectomy of the cyclic mouse. I. Effects on folliculogenesis, oocyte growth, and follicle-stimulating hormone and human chorionic gonadotropin receptors. *Biol Reprod* **48** 585-594.
- Webb R & Armstrong DG** 1998 Control of ovarian function; effect of local interactions and environmental influences on follicular turnover in cattle: a review. *Livestock Production Science* **53** 95-112.
- Webb R, Campbell BK, Garverick HA, Gong JG, Gutierrez CG & Armstrong DG** 1999 Molecular mechanisms regulating follicular recruitment and selection. *J Reprod Fertil Suppl* **54** 33-48.
- Wrathall JH & Knight PG** 1995 Effects of inhibin-related peptides and oestradiol on androstenedione and progesterone secretion by bovine theca cells *in vitro*. *J Endocrinol* **145** 491-500.
- Wulff C, Wilson H, Wiegand SJ, Rudge JS & Fraser HM** 2002 Prevention of thecal angiogenesis, antral follicular growth, and ovulation in the primate by treatment with vascular endothelial growth factor Trap R1R2. *Endocrinology* **143** 2797-2807.
- Xu Z, Garverick HA, Smith GW, Smith MF, Hamilton SA & Youngquist RS** 1995 Expression of follicle-stimulating hormone and luteinizing hormone receptor messenger ribonucleic acids in bovine follicles during the first follicular wave. *Biol Reprod* **53** 951-957.

Yamada O, Abe M, Takehana K, Hiraga T, Iwasa K & Hiratsuka T 1995 Microvascular changes during the development of follicles in bovine ovaries: a study of corrosion casts by scanning electron microscopy. *Arch Histol Cytol* **58** 567-574.

Yamashita Y, Kawashima I, Yanai Y, Nishibori M, Richards JS & Shimada M 2007 Hormone-induced expression of tumor necrosis factor alpha-converting enzyme/A disintegrin and metalloprotease-17 impacts porcine cumulus cell oocyte complex expansion and meiotic maturation via ligand activation of the epidermal growth factor receptor. *Endocrinology* **148** 6164-6175.

Yan C, Wang P, DeMayo J, DeMayo FJ, Elvin JA, Carino C, Prasad SV, Skinner SS, Dunbar BS, Dube JL, Celeste AJ & Matzuk MM 2001 Synergistic roles of bone morphogenetic protein 15 and growth differentiation factor 9 in ovarian function. *Mol Endocrinol* **15** 854-866.

Yancopoulos GD, Davis S, Gale NW, Rudge JS, Wiegand SJ & Holash J 2000 Vascular-specific growth factors and blood vessel formation. *Nature* **407** 242-248.

Yi SE, LaPolt PS, Yoon BS, Chen JY, Lu JK & Lyons KM 2001 The type I BMP receptor Bmpr1B is essential for female reproductive function. *Proc Natl Acad Sci U S A* **98** 7994-7999.

Yoshino O, McMahon HE, Sharma S & Shimasaki S 2006 A unique preovulatory expression pattern plays a key role in the physiological functions of BMP-15 in the mouse. *Proc Natl Acad Sci U S A* **103** 10678-10683.

Yuan W & Lucy MC 1996 Messenger ribonucleic acid expression for growth hormone receptor, luteinizing hormone receptor, and steroidogenic enzymes during the estrous cycle and pregnancy in porcine and bovine corpora lutea. *Domest Anim Endocrinol* **13** 431-444.

Zelevnik AJ, Schuler HM & Reichert LE, Jr. 1981 Gonadotropin-binding sites in the rhesus monkey ovary: role of the vasculature in the selective distribution of human chorionic gonadotropin to the preovulatory follicle. *Endocrinology* **109** 356-362.

Zhou J, Adesanya OO, Vatzias G, Hammond JM & Bondy CA 1996 Selective expression of insulin-like growth factor system components during porcine ovary follicular selection. *Endocrinology* **137** 4893-4901.

Zhou J, Kumar TR, Matzuk MM & Bondy C 1997 Insulin-like growth factor I regulates gonadotropin responsiveness in the murine ovary. *Mol Endocrinol* **11** 1924-1933.

Zhu G, Guo B, Pan D, Mu Y & Feng S 2008 Expression of bone morphogenetic proteins and receptors in porcine cumulus-oocyte complexes during *in vitro* maturation. *Anim Reprod Sci* **104** 275-283.

Zimmermann RC, Xiao E, Bohlen P & Ferin M 2002 Administration of antivasular endothelial growth factor receptor 2 antibody in the early follicular phase delays follicular selection and development in the rhesus monkey. *Endocrinology* **143** 2496-2502.

CHAPTER 3

GLOBAL TRANSCRIPT PROFILING IN CONJUNCTION WITH GENE ONTOLOGY ANNOTATION REVEALS THE SECRETOME OF THE PORCINE OOCYTE, GRANULOSA AND THECA CELLS DURING ANTRAL FOLLICLE DEVELOPMENT

INTRODUCTION

Ovarian follicle development in large domestic animals is a dynamic process that requires the initial recruitment of resting primordial follicles which then transition through the primary, secondary, antral and preovulatory stages of development. In the pig, follicular development occurs over approximately 100 days and through a process of recruitment and selection culminates in the ovulation of a subset of oocytes competent to undergo fertilization and embryonic development (Hunter *et al.*, 2000, Hunter *et al.*, 2004). Since ovulation rate and oocyte quality are important determinants of female reproductive efficiency, it is essential to understand the mechanisms regulating follicular growth and the role of endocrine and paracrine signals, metabolic factors and several local growth factors.

Nutritional manipulations have been shown to affect sow fertility and increased lactational catabolism in primiparous sows has detrimental consequences on embryo survival by day 30 of gestation in the subsequent litter (Foxcroft *et al.*, 1997). Nutritional restriction during the last week of gestation was also shown to exert detrimental effects on follicle and oocyte quality (Zak *et al.*, 1997). More recent studies established a relationship between the extent of protein catabolism during lactation and follicle quality in the sow (Yang *et al.*, 2000a, Clowes *et al.*, 2003a, Clowes *et al.*, 2003b). Interestingly, delaying breeding of primiparous sows until the second oestrus post-weaning results in

increased follicle maturity and increased embryo survival (Foxcroft *et al.*, 2007, Paradis *et al.*, 2009) ultimately leading to increased litter size (Clowes *et al.*, 1994). The mechanisms controlling such differences in follicle maturity are, therefore, of considerable practical significance.

The endocrine regulation of porcine follicular development has been studied extensively and, although the importance of local growth factors is well recognized (Hunter and Paradis, 2009), knowledge concerning the growth factor systems present in the ovary and their roles during follicle growth is limited. The development of large scale sequencing of cDNA libraries and microarray analysis strategies provide a rapid means of obtaining large amounts of information on the transcriptome and/or the differential regulation of genes expressed in the porcine ovary, follicle and oocyte (Agca *et al.*, 2006, Bonnet *et al.*, 2008a, Caetano *et al.*, 2003, Caetano *et al.*, 2004, Jiang *et al.*, 2004, Tosser-Klopp *et al.*, 1997, Whitworth *et al.*, 2005). The objectives of this study were 1) to use a combination of microarray analysis and gene ontology (GO) annotation to generate lists of oocyte, granulosa and theca cells transcript that encode secreted factors and their receptors, 2) to confirm the cell type localization of members of the insulin-like growth factor and the epidermal growth factor family identified by the microarray strategy, 3) to establish the temporal expression pattern of IGF1, IGF1R, IGFBP2, IGFBP4, IGFBP5, IGFBP6, PAPP-A, EGFR, AREG, EREG, BTC and ADAM17 during follicular development, and 4) to determine whether these growth factors and their receptors could play a role in creating the differences in follicle characteristics and embryo survival observed between the first and second post-weaning preovulatory wave of follicular development in primiparous sows. To our knowledge, this is the first study to investigate the profile of secreted growth factors and associated receptors expressed in each cell type present in porcine ovarian follicles. Co-localization and mRNA expression patterns of members of the IGF and EGF system during preovulatory follicle development are described in the pig and a critical role for AREG and EREG around the preovulatory LH surge *in vivo* is proposed.

MATERIALS AND METHODS

Chemicals and media

Unless otherwise stated all chemicals were obtained from Sigma-Aldrich (St-Louis, Mo, USA). The media used for washing the COCs and during follicle dissection was modified Tyrode lactate (TL)-HEPES medium supplemented with 0.1% (w/v) polyvinyl alcohol (PVA) (Funahashi *et al.*, 1997), 50 U/ml of penicillin and 50 µg/ml of streptomycin (Invitrogen, #15070-063, Burlington, ON, Canada). The phosphate-buffered saline pH 7.4 was composed of 137 mM NaCl, 2.7 mM KCl, 8.1 mM Na₂HPO₄ and 1.47 mM KH₂PO₄.

Animals

This experiment was conducted in accordance with the guidelines of the Canadian Council on Animal Care and with the approval of the University of Alberta, Faculty Animal Policy and Welfare Committee (Protocol #2005-40B). A total of 73 primiparous F1 sows, 35 cyclic gilts and 10 prepubertal gilts (Large White x Landrace, Hypor, Regina, SK, Canada) were used for follicle dissection and/or oocyte aspiration.

Primiparous sows: Within 48 h after farrowing, litter size was standardized to between 9 and 11 piglets through cross-fostering and routine piglet processing procedures (tail-docking, teeth clipping, ear notching and iron injection) were performed. During lactation, sows were offered fresh feed three times daily and permitted ad libitum access to fresh water. Sows were offered 3.5 kg of feed on the day of farrowing, and during the remainder of lactation, the amount of feed offered was increased by 0.5 kg daily until the sows daily consumption was exceeded by 0.5 kg. Sows were weaned 20.8 ± 3.2 (mean \pm stdev) days after farrowing and were randomly allocated to treatment (1st or 2nd cycle) at this time. After weaning, sows were moved to a common weaned-sow room, housed in individual sow stalls and fed to appetite twice daily until the day of euthanasia.

From the day after weaning, sows were actively heat-checked using fence-line boar contact twice daily (at 0800 and 1400). Onset of standing heat was designated as day 0 of the subsequent oestrous cycle. Sows were weighed on day 1, 6 and 13 of lactation, at weaning and at the time of euthanasia.

Sows whose ovaries were used for follicle dissection and/or oocyte aspiration were euthanized on day 1 (D1; n=5), 2 (D2; n=10) or 4 (D4; n=20) after weaning, or day 14 (D14; n=5), 16 (D16; n=10) or 20 (D20; n=23) after the 1st post-weaning oestrus. These time-frames correspond to the 1st and 2nd post-weaning preovulatory wave of follicular development and D1/D14 corresponds to the period of recruitment (R) of the growing cohort of follicles, D2/D16 corresponds to the mid-selection phase (MS) at which time follicles either keep growing or, if not selected, start to undergo atresia and D4/D20 corresponds to the final selection phase (FS) at which time the preovulatory follicle population has been established (Grant *et al.*, 1989, Hunter and Wiesak, 1990). The preovulatory follicle population from the final selection phase was further divided between the follicles in pre-LH surge (FS) or post-LH surge (FS/LH) stages based on follicular fluid oestradiol concentrations (see procedure below).

Cyclic gilts: The cyclic gilts were housed in individual stalls in a cyclic gilt room and were offered 2 kg of feed once daily until euthanasia. They were actively heat-checked using fence-line boar contact once daily. Onset of standing heat was designated as day 0 of the subsequent oestrous cycle. The cyclic gilts were weighed at the time of euthanasia.

Cyclic gilts used for follicle dissection and/or oocyte aspiration were euthanized on day 14 (D14; n=5), 16 (D16; n=10) or 20 (D20; n=20) after oestrus. Similar to the primiparous sows, these time-frames correspond to the period of recruitment (R) of the growing cohort of follicles (D14), to the mid-selection phase (MS) at which time follicles either keep growing or, if not selected, start to undergo atresia (D16) and to the final selection phase (FS) at which point the preovulatory follicle population has been established (D20) (Grant *et al.*, 1989,

Hunter and Wiesak, 1990). The preovulatory follicle population from the final selection phase was further divided between the follicles in pre-LH surge (FS) or post-LH surge (FS/LH) stages based on follicular fluid oestradiol concentrations (see procedure below).

Prepubertal gilts: The prepubertal gilts were housed in groups of 6-8 animals and were offered ad libitum access to feed. They were actively heat-checked using fence-line boar contact once daily starting at approximately 150 days of age and were euthanized before expressing their first oestrus at around 160-170 days of age.

The animals used in the experiments were euthanized on-site in a purpose-built necropsy facility according to the Swine Research and Technology Centre standard operating procedures. Prior to euthanasia, a single blood sample was collected into a 10 ml heparinized Vacutainer™ (Becton Dickinson, Franklin Lakes, NJ, USA) by jugular venipuncture, centrifuged at 1700 x g for 15 min at room temperature and the plasma was then stored at -20°C until assayed for plasma oestradiol concentration.

Tissue collection

Within 20 min after euthanasia, the ovaries of all animals were moved to an adjacent laboratory suite in 50 ml Falcon tube containing 0.9% (w/v) ice cold saline when the ovaries were intended for follicle dissection, or in 0.9% (w/v) warm saline when the ovaries were intended for oocyte aspiration. The ovaries from the 18 primiparous sows and 9 cyclic gilts intended for follicle dissection and oocyte aspiration were allocated as followed: for each phase of follicular development (R, MS and FS), 3 sows from each cycle group (1st or 2nd cycle) and 3 cyclic gilts were euthanized. The 3 prepubertal gilts intended for follicle dissection and oocyte aspiration were euthanized between 160 and 170 days of age. One ovary from each sow and gilt was chosen for follicle dissection and the other was used for oocyte aspiration. Both ovaries from the additional 55 primiparous sows, 26 cyclic gilts and 7 prepubertal gilts were used for oocyte

aspiration. Before processing the ovaries, the number and size of all visible follicles was recorded and the follicular fluid from the largest follicle(s) (1 to 3 pooled follicles depending on the volume recovered) of D4 and D20 animals was collected using an 18-gauge needle attached to a 1 ml disposable syringe. The follicular fluid was centrifuged for 5 min at 13 000 x g to remove any cellular debris, diluted 11-fold in M199 and stored at -20°C until assay of oestradiol or progesterone concentrations.

Follicle dissection: A total of 30 ovaries (prepubertal gilts n=3, cyclic gilts n=9, 1st cycle primiparous sows n=9 and 2nd cycle primiparous sows n=9), each originating from a different animal and representing each phase of follicular development, were sliced in half longitudinally and washed twice in ice cold PVA-TL-HEPES to remove blood contamination. The half ovaries were then placed into Petri dishes containing ice cold PVA-TL-HEPES and follicles representative of the population present on the ovary were dissected free of stromal tissue under a dissecting microscope using fine scissors and forceps. Intact dissected follicles were then placed into RNAlater (Ambion, Austin, TX, USA) to preserve RNA integrity during the remaining procedure. Depending on the size of the follicles, between 5 and 10 follicles were dissected within a 1-hour period. The intact follicles were then placed back into ice cold PVA-TL-HEPES and cut in half using a scalpel blade. The mural granulosa cells (MGC) were then gently scraped from the inner wall of the follicle hemisection using a fine glass loop and the oocytes were removed to ensure a pure MGC population. The MGC were transferred to a 1.5 ml microcentrifuge tube in ice cold media and centrifuged for 5 min at 200 x g at room temperature. The MGC pellets were washed twice with 1ml of ice cold PBS followed by centrifugation at 200 x g for 5 min. Following the last wash, the supernatant was removed and the cells were snap frozen in liquid nitrogen. The remaining follicle shells contained mainly theca cells (TC) and were vigorously agitated by repeated pipetting to ensure that all MGC were removed. The TC were then transferred to a 1.5 ml microcentrifuge tube in ice cold media and centrifuged for 5 min at 200 x g at room temperature. The TC pellets were washed twice with 1 ml of ice cold PBS

followed by centrifugation at 200 x g for 5 min. Following the last wash, the supernatant was removed and the cells were snap frozen in liquid nitrogen. The MGC and TC were finally stored at -80°C until RNA extraction.

Oocyte aspiration: Cumulus-oocyte complexes (COC) were collected from the remaining ovaries by aspiration using an 18-gauge needle attached to a 5 ml disposable syringe and the COC's from each animal were processed as a group. The COC's were transferred to a Petri dish containing 15 ml of warm PVA-TL-HEPES. The recovered COC's were washed three times in warm PVA-TL-HEPES to remove any cellular debris. The oocytes were then denuded by vortexing at low speed for 5 min in 150 µl of PBS in a 1.5 ml microcentrifuge tube. The denuded oocytes were observed under a dissecting microscope to ensure that they were free of cumulus cells and then washed twice in PBS before transfer to a fresh 1.5 ml microcentrifuge tube in a minimum volume of PBS and snap freezing on dry ice. The remaining cumulus granulosa cells (CGC) were transferred to a 1.5 ml tube and centrifuged for 5 min at 200 x g in a table top microcentrifuge. The pellets were washed twice with PBS followed by centrifugation at 200 x g for 5 min. Following the last wash, the supernatant was discarded and the cells were snap frozen on dry ice. The oocytes and the CGC were finally stored at -80°C until RNA extraction.

Radioimmunoassay (RIA)

Plasma oestradiol: Oestradiol concentrations were determined in all plasma samples in triplicate in a single RIA using the method of Yang *et al.* (2000b). Extraction efficiency was $63 \pm 4\%$ and estimated potencies were not corrected for recovery. Assay sensitivity, defined as 90 % of total binding, was 0.35 pg/ml. The intra-assay coefficient of variation (CV) was 9%.

Follicular fluid oestradiol: Follicle fluid (FF) oestradiol concentrations were quantified in a single RIA using a double antibody kit (Diagnostic Products Corporation # KE2D1, Diagnostic Products Corporation, Los Angeles, CA, USA) without extraction using the method of Paradis *et al.* (2009). The intra-assay CV for the single assay run was 5.7 %. Sensitivity estimated at 91 % of total binding

was 0.11 pg/tube, equivalent to 2.4 ng/ml. The recovery of a known amount of oestradiol when added to a sample of known potency was $94.5 \pm 2.7 \%$.

Follicular fluid progesterone: FF progesterone concentrations were quantified in a single RIA using the method of Mao *et al.* (2001). To ensure that all sample potencies were estimated from the linear part of the standard curve, the stored FF diluted 11-fold in TCM 199 was assayed both neat and further diluted five-fold in kit buffer. The sensitivity of the assay, defined as 88% of total binding, was 1.1 ng/ml. One sample fell below sensitivity. A control FF pool serially diluted showed parallelism to the standard curve. The intra-assay CV was 6.28%.

RNA isolation

Total RNA was extracted from the pooled CGC, MGC and TC of individual animals using TRIzol reagent (Invitrogen) following the manufacturer's instructions, with the following modification. The cells were thawed on ice directly in TRIzol and homogenized with a Polytron™. The homogenized samples were then incubated for 10 min at room temperature before further processing. The homogenized CGC and MGC originating from the same animals were then pooled together prior to the extraction and will be further referred to as granulosa cells (GC). The GC and TC total RNA was precipitated with 1/10 volume of 5M ammonium acetate, 1 volume of isopropanol and linear acrylamide (Ambion) was also added to the RNA as a carrier at a final concentration of 10 µg/ml. The total RNA was resuspended in nuclease free H₂O (Ambion) and was DNase treated using DNA-free™ (Ambion) following the manufacturer's instructions. The samples were quantified using the spectrophotometer ND-1000 (NanoDrop, Wilmington, DE, USA) and RNA integrity was evaluated on a 1 % (w/v) denaturing agarose gel. All samples were stored at -80°C until microarray analysis or cDNA synthesis. Oocyte total RNA was extracted from pools of between 15 (for D4 and D20 animals) and 200 (for D1, D14 and prepubertal animals) oocytes recovered from individual gilts or sows using the PicoPure RNA isolation kit (Arcturus, Mountain View, CA, USA)

following manufacturer's instructions. All samples were DNase treated as suggested in the protocol and the RNA was eluted in 30 μ l. Oocyte total RNA was stored at -80°C until use. Due to the large difference in the number of oocytes recovered between animals, the efficiency of RNA extraction and cDNA synthesis was monitored and was found to be consistent when ≥ 15 oocytes were used (data not shown).

Microarray analysis

For each cell type, a pool containing 1/3 of the total RNA from oocytes, granulosa or theca cells from each animal was used for the microarray experiment. In addition, for each cell type, two technical replicates were performed to ensure that the cDNA amplification, fragmentation, labelling and hybridization to the GeneChip were reproducible.

The RNA was sent to the Genomics Core in the Centre for Reproductive Biology at the Washington State University for processing and hybridization to the Affymetrix (Santa Clara, CA, USA) GeneChip® Porcine Genome Array. Two aliquots of 50 ng/ μ l of the pooled total RNA from each cell type were amplified using the Ovation® RNA Amplification System V2 (NuGen Technologies Inc., San Carlos, California, USA) according to the manufacturer's instruction. Briefly, the total RNA was reversed transcribed into double-stranded cDNA followed by linear cDNA amplification. Then, 3.75 μ g of amplified cDNA was fragmented and biotin labelled using the FL-Ovation™ cDNA Biotin Module V2 (Nugen Technologies Inc.) according to the manufacturer's instructions. Finally, 2.6 μ g of fragmented, biotin labeled amplified cDNA was then hybridized to the Affymetrix GeneChip® Porcine Genome Array. After the hybridization, the GeneChips® were washed and stained with the Affymetrix Fluidics Station 450 using the protocol FS450_0002 suggested by Affymetrix and scanned on the Affymetrix 3000GS scanner.

Microarray images were converted to the numerical data using the Affymetrix GeneChip Operating Software (GCOS) using a global scaling strategy

to produce a mean signal intensity of 125. In GCOS, the 11 perfect match and 11 mismatch oligonucleotides were used to determine the present and absent call, using a one-sided Wilcoxon's signed-rank test. Finally, files containing the signal intensity and the present/absent call for each probe sets were generated and the R^2 between the replicates of each cell type were calculated and were found to be ≥ 98 , indicating very high reproducibility.

Bioinformatics and gene ontology

The gene list from each cell type was visualized and in order for a transcript to be considered present, it had to be tagged as present and had to have a signal intensity higher than 50 in both technical replicates. The selected threshold of 50, was chosen based on background values (36-40) and was meant to be sufficiently stringent to exclude transcripts with low signal intensity which are the most likely to generate false positive identification. The files were then merged with annotation files specifically generated for the Affymetrix GeneChip® Porcine Genome Array and containing the putative identity of more than 80% of the primer probe set represented on the microarray (Tsai *et al.*, 2006). The annotated list of oocyte, GC and TC transcripts were then analysed in the gene ontology freeware GOTreePlus (<http://bioinformatics.cncresearch.org/GOTreePlus>) using the human gene ontology annotation file (www.geneontology.org/GO.current.annotations.shtml) and grouped using the gene ontology (GO) term extracellular region (GO:0005576) and receptor activity (GO:0004872).

Real-time RT-PCR

Oocyte, GC and TC total RNA, from the 18 primiparous sows used for follicle dissection and oocyte aspiration and from 10 additional primiparous sows use for oocyte aspiration only, was reverse transcribed with Superscript III reverse transcriptase (Invitrogen) according to the manufacturer's instructions, using a combination of 5 μ M oligo dT and 5 ng/ul of random hexamer. RNaseOUT (Invitrogen) was also added to the reaction at a concentration of 2 U/ μ l. The

cDNA synthesis was performed using 2 µg of GC and TC total RNA and with 10 µl of the oocyte total RNA. After reverse transcription, GC and TC cDNA were diluted to a concentration of 20 ng/µl and the oocyte cDNA to an equivalent of 0.25 oocytes/2µl with nuclease-free H₂O (Ambion).

Real-Time PCR was performed in duplicate using 20 ng of GC or TC cDNA, or the cDNA equivalent to 0.25 oocytes, in 96-well fast plates using the Taqman® Fast Universal PCR Master Mix and the ABI 7900HT thermocycler (Applied Biosystems (ABI), Foster City, CA, USA). The primers and Taqman-MGB probes (Table 4) were designed using the Primer Express® software v3.0 (Applied Biosystems) using species specific sequences found on GENBANK or were obtained from the Applied Biosystems library of porcine TaqMan® Gene Expression Assays. The amplification efficiency for each gene was determined using serial dilution of ovarian cDNA and was found to be $\geq 85\%$ for all genes (data not shown). Moreover, the amplification efficiency slopes for all genes were found to be similar. As reported by Bettegowda *et al.* (2006), cyclophilin (PPIA) was used as the endogenous control to correct for RNA extraction and reverse transcription efficiency within cell type. Cyclophilin transcript abundance was found to be stable within each cell type throughout the different stages of follicle development, confirming its utility as a good endogenous control. However, cyclophilin abundance differed between the cell types studied and limited the ability to compare statistically the abundance of each gene of interest (GOI) across cell types.

Statistical analysis

Real-time PCR data for the GOI were normalized against their respective means for cyclophilin using the Δ Ct method (Δ Ct = Ct_{GOI} – Ct_{cyclophilin}). The cycle threshold (Ct) is defined as the PCR cycle where the fluorescence reaches a determined threshold. Consequently, the Ct and corrected Ct (Δ Ct) value are inversely related to the copy number of the targeted gene initially present in the sample. For the analysis of the temporal changes in mRNA abundance, the Δ Ct values for all GOI were normally distributed except for IGF1, IGFBP5, IGFBP6,

EEREG and EGFR in the granulosa cell and IGF1R, IGFBP6, PAPP-A and TACE/ADAM17 in the oocyte which were RANK transformed and the analysis was performed on the transformed data. The individual ΔCt for each GOI were analysed using the MIXED procedure of SAS. The model for the experiment included phases and cycle as the independent variables. Differences between means were analyzed using a Least Significant Difference (LSD) test at a 95% confidence level. For ease of interpretation of the expression profiles the data were converted using the formula $2^{-(\Delta\text{Ct} - \Delta\text{Ct}_{\text{calibrator}})}$ and are expressed as relative mRNA abundance \pm SEM. The ΔCt value obtained for EREG in the granulosa and theca cell during the recruitment phase was used as the calibrator value for these cell types and the ΔCt value obtained for PAPP-A in the oocyte during the final selection phase was used as the calibrator value for the oocyte, thus maintaining the relative mRNA abundance for the GOI within cell types. Finally, correlations analyses were performed across all sows to determine relationships between the expression of each GOI and follicular fluid oestrogen, follicular fluid progesterone, plasma oestrogen concentration and follicle size.

RESULTS

Microarray quality and annotation

Oocyte, granulosa and theca cell cDNA was hybridized to the Affymetrix GeneChip® Porcine Genome Array that comprised 24,123 probe sets. Visual inspection of the scanned images revealed no artefacts and the average background values for the arrays ranged from 36 to 40, falling within the range of 20 to 100 typically observed by Affymetrix. Data quality assessment showed a “Percentage of Present call” ranging from 70% in the oocyte to 78% in the theca cells, suggesting that the overall quality of the sample was acceptable. Moreover, correlation analysis between the two technical replicates from each cell type showed a correlation coefficient of >0.98 for each cell type, illustrating the high degree of reproducibility between arrays. Using the Absent/Present call as well as

a selected threshold of 50, a list of 9141, 10589 and 10479 transcripts were considered expressed in the oocyte, granulosa and theca cells, respectively (data not shown). These are not all unique transcripts because a high degree of redundancy for many genes is observed on the array (i.e. the same gene is represented by multiple probe sets)

Although, the Affymetrix Porcine Genome Array contains a 24,123 probe set, only 10% of the probe set on the array has been annotated by Affymetrix (Tsai *et al.*, 2006). This is a particularly important issue because it limits the ability to interpret the data into physiologically relevant information. A more complete annotation file has recently been published by Tsai *et al.* (2006), allowing the putative identification of 19 675 (>80%) of the probe sets on the array. To ensure the validity of the annotation, 50 probe sets were randomly selected and their sequences were compared by BLAST against the NCBI non-redundant nucleotide collection database and the human genome databases. In all cases where the sequences were identified, the identities of the sequence determined by BLAST analysis were similar to the identity assigned by the annotation files, confirming the validity of the annotation file for our use.

Gene ontology clustering

Extracellular Region

Using the gene ontology freeware GOTreePlus and a human gene ontology annotation file, a list of 357, 466 and 609 transcripts clustering under the GO term Extracellular Region was generated for the oocyte, granulosa and theca cells, respectively from the total number of transcripts considered to be expressed on the Affymetrix array (Appendix 1: Supplemental table 3.3). For gene ontology, the GO term “extracellular region” is a broad node found under cellular component that includes several sub-nodes such as “extracellular space” and the assumption was that secreted factors should be found under the GO term “extracellular space”. However, preliminary analysis revealed that several factors, such as ZP2, ZP3, ZP4, IGFBP6 and INHBB, known to be secreted by the

follicular cells, were missing from the list using this more specific term. Therefore, it was decided to use the broader term extracellular space since a more complete list of secreted factors was observed under that term. Based on the transcripts represented on the array and the number considered to be expressed in each cell type, between 4 and 6% of the transcripts were localized to the extracellular region. Several families of genes were represented in the list. First, the zona pellucida sperm-binding proteins (ZP2, -3 and -4) were identified as being expressed exclusively in the oocyte. Although, this information is well known, it helps confirm the validity of the oocyte gene list used in this study. The transforming growth factor (TGF)- β superfamily, including BMP2, BMP4, BMP6, BMP15, GDF9, TGFB1, TGFB2, TGFB3, INHA, INHBA, INHBB and follistatin were well represented on the list, and BMP2 and BMP15 were detected exclusively in the oocyte, while GDF9 was detected in all three cell types, although its expression in the oocyte appeared to be much higher. Intriguingly, BMP6 was found in the granulosa and theca cells but was absent from the oocyte. TGFB1 and TGFB2 were present only in the theca cells, while TGFB3 was detected in granulosa and theca cells. The inhibin subunits (INHA, INHBA and INHBB) and follistatin were detected in the various cellular compartments of the follicle but appeared to be most abundant in the granulosa cells. Moreover, several members of the insulin-like growth factor family, including IGF1, IGFBP2, -3, -5, -6 and -7 as well as PAPP-A were present on the list. IGF1 was expressed only in the granulosa and theca cells, the expression of IGFBP in each cell type varied; PAPP-A was identified in all cell types. Members of the epidermal growth factor family, including EGF and AREG were also observed on the list. While EGF was detected in the oocyte and granulosa cells of the porcine antral follicle, AREG was exclusively expressed in the granulosa cell compartment. A plethora of other growth factors were also identified including many representative of the fibroblast growth factor (FGF) and the platelet-derived growth factor (PDGF) families.

Receptor Activity

A list of 298, 405 and 424 transcripts clustering under the GO term “Receptor Activity” was generated for the oocyte, granulosa and theca cells, respectively (Appendix 1: Supplemental table 3.4). The GO term “receptor activity” was selected since it is a relatively specific term that includes any gene product capable of combining with an extracellular or intracellular messenger to initiate a change in cell activity. Moreover, preliminary analysis showed that it included receptors that would be expected in the tissues analysed such as FSHR and LHCGR. Based on the transcripts represented on the array and the number considered to be expressed in each cell type, between 3 and 4% of the transcripts were identified as having receptor activity. First, while FSHR was detected specifically in the granulosa cells, LHCGR was detected in both granulosa and theca cells. As for the zona pellucida protein in the oocyte, the expression of FSH and LH receptor in the granulosa and theca cell help confirm the validity of the granulosa and theca cells gene list used in this experiment. Moreover, identification of receptors for the ligands identified in the previous section represents critical evidence supporting a role for these growth factors in the ovary, but also indicates which cell types are likely to be affected by the factors. Receptors belonging to the TGF- β superfamily included BMPR1A, BMPR1B, TGFBR2, TGFBR3, and several activin receptors (ACVR1, ACVR1B, ACVR2B) were identified. Although most of the receptors were expressed in all cell types, ACVR2B was detected exclusively in the granulosa and theca cells, TGFBR3 could only be identified in the theca cells. The IGF1 receptor was identified in the granulosa cells, and the EGF receptor was identified in both the granulosa and theca cells. Finally, the alpha and beta platelet-derived growth factor receptors were identified specifically in the theca cells, while the fibroblast growth factor receptors (FGFR1 and FGFR2) were detected in all cell types in the follicle. Together, the ligands and receptors identified using this strategy point to the activity of several growth factor systems in developing pig antral follicles.

Validation of transcript localization and abundance by real-time PCR

In the context of the present study, mRNA abundance of members of the IGF system (*IGF1*, *IGF1R*, *IGFBP2*, *IGFBP5*, *IGFBP6* and *PAPP-A*) and representatives of the epidermal growth factor family (*AREG* and *EGFR*) were further investigated by real-time PCR. Although *ADAM17* mRNA was below the detection threshold on the microarray, it was also selected for further real-time PCR analysis, as were *IGFBP4*, *EREG* and *BTC* mRNA, which were not represented on the porcine genome array but are important members of these two families and were of particular interest. Overall, the expression of members of the IGF and EGF family determined by real-time PCR analysis were for the most part consistent with the microarray analysis. The specific expression of *IGF1* and *IGFBP2* mRNA in granulosa and theca cells was confirmed by real-time PCR (Table 3.2; Figure 3.2A and 3.3A, B). Both techniques identified *PAPP-A* mRNA expression in the oocyte, granulosa and theca cells (Table 3.2; Figure 3.1, 3.2B and 3.3A) and abundant *IGFBP5* mRNA in the theca cells (Table 3.2; Figure 3.3A). Although *IGFBP5* expression was also detected in the granulosa cells by real-time PCR, its abundance was very low (Table 3.2; Figure 3.2A). Interestingly, further evaluation of the microarray signal intensity for *IGFBP5* mRNA in the granulosa cells revealed that it was slightly below 50, suggesting that the chosen arbitrary threshold was appropriate (data not shown). Expression of *IGFBP6* mRNA in the oocyte and theca cells identified by microarray was confirmed by real-time PCR (Figure 3.1 and 3.3A), however, minimal expression was also detected by real-time PCR in the granulosa cells (Figure 3.2A). *IGF1R* mRNA expression was intriguing since its presence in the granulosa cells was confirmed by both techniques, however its expression in the oocyte and theca cells was only observed by real-time PCR (Table 3.2; Figure 3.1, 3.2A and 3.3A). The expression of *AREG* mRNA which appeared by microarray to be specific to the granulosa cells was confirmed by real-time PCR, as its transcript in the theca cells was at the limit of detection of the real-time PCR, rising above the threshold on average around cycle 39 of 40 (Table 3.2; Figure 3.4A and 3.5). The specific expression of *EGFR* mRNA in the granulosa and theca cells was confirmed with

both techniques (Table 3.2; Figure 3.4A and 3.5). Finally, the results for *ADAM17* mRNA were somewhat surprising since its transcript could not be detected by microarray in any cell type but was found by real-time PCR to be expressed in the oocyte, granulosa and theca cells (Table 3.2; Figure 3.1, 3.4A and 3.5).

Real-time PCR-derived mRNA expression profiles during follicular development

In order to gain insight into the role of the IGF and EGF systems in the developing porcine follicle, the expression pattern of each ligand and receptor discussed previously was studied during follicle recruitment, mid-selection, and final selection before and after the preovulatory LH surge.

IGF system

IGF1 mRNA abundance in the granulosa cells was not affected by the stages of follicle development (Figure 3.2A). However, correlation analysis established positive relationships between *IGF1* and *IGFBP2* and *IGFBP5* mRNA abundance ($r = 0.59$, $P < 0.05$; $r = 0.76$, $P < 0.001$, respectively), and a negative relation between *IGF1* and *IGFBP6* mRNA abundance ($r = -0.69$, $P < 0.01$). *IGF1* mRNA abundance in the theca cells was affected by the stage of follicle growth and increased gradually from the recruitment to reach a peak at the final selection phase before and after the preovulatory LH surge ($P < 0.01$; Figure 3.3B). *IGF1* mRNA in the theca cells positively correlated with *IGF1R*, *IGFBP4*, *IGFBP5*, *IGFBP6*, *PAPP-A* mRNA and with follicle size ($r = 0.61$, $P < 0.01$; $r = 0.75$, $P < 0.001$; $r = 0.54$, $P < 0.05$; $r = 0.64$, $P < 0.01$; $r = 0.49$, $P < 0.05$ and $r = 0.68$, $P < 0.01$, respectively). Interestingly, *IGF1* mRNA abundance in the theca cells was also affected by the cycle of the animal ($P < 0.01$), and higher expression was observed in tissue recovered from follicles of the first preovulatory period after weaning (Figure 3.3B). *IGF1R* mRNA expression was very similar between the granulosa and theca cells, and was lower during the recruitment phase than the mid-selection and later phases of development ($P < 0.01$; Figure 3.2A and 3.3A).

In both cell types, *IGF1R* mRNA abundance was positively correlated with *IGFBP4* mRNA abundance ($r = 0.53$, $P < 0.05$ (GC); $r = 0.65$, $P < 0.01$ (TC)) and with follicle size ($r = 0.77$, $P < 0.001$ (GC); $r = 0.57$, $P < 0.05$ (TC)). In the theca cells, *IGF1R* mRNA abundance was also positively correlated with the mRNA abundance of *IGFBP5* and *IGFBP6* ($r = 0.69$, $P < 0.01$; $r = 0.78$, $P < 0.001$, respectively). In the oocyte, no change in *IGF1R* mRNA was observed (Figure 3.1). *IGFBP2* and *IGFBP4* mRNA had very similar expression patterns between the granulosa and theca cells, and with the exception of *IGFBP2* mRNA abundance in the granulosa cells that tended to be affected by the stage of follicle development ($P < 0.1$), no phase effects were observed for these IGFBP (Figure 3.2A and 3.3A). In contrast, *IGFBP5* mRNA abundance was affected by stage of follicle development in both granulosa and theca cells ($P < 0.05$; Figure 3.2A and 3.3A). In the granulosa cells, *IGFBP5* mRNA abundance was low and stable from the recruitment phase to the final selection phase but then decreased after exposure to the preovulatory LH surge. In contrast, in the theca cells, *IGFBP5* expression was low during the recruitment phase and generally increased during the later phases of development. *IGFBP6* mRNA abundance in the granulosa cells showed an opposite pattern to that of *IGFBP5* mRNA ($P < 0.05$; Figure 3.2A), whilst in the theca cell, *IGFBP6* mRNA tended to increase during follicle development ($P < 0.1$; Figure 3.3A). *IGFBP6* expression was constant in the oocyte during follicular growth (Figure 3.1). Finally, *PAPP-A* mRNA in the granulosa cells showed an interaction between the phase of follicle development and the cycle of the animal ($P < 0.05$; Figure 3.2B). Abundance during both the mid-selection phase and the final selection phase post-LH surge was lower in tissue recovered from sows during the second cycle of preovulatory follicle growth after weaning. In the theca cells, *PAPP-A* mRNA abundance showed only a tendency to be affected by the stage of follicular development, while in the oocyte its expression was found to be stable across all phases studied (Figure 3.1 and 3.3A).

EGF system

Evaluation of the changes in *EGFR* mRNA abundance in the granulosa cells showed that this receptor is stably expressed throughout the different phases of follicular development, while in the theca cells mRNA abundance was lower during the recruitment phase but increased during the mid-selection phase and remained high thereafter ($P < 0.01$; Figure 3.4A and 3.5). The expression of *AREG*, *EREG* and *BTC* mRNA was considered to be exclusive to the granulosa cells, as no expression was found in the oocyte and expression in the theca cells was at the limits of detection. Therefore, only the temporal expression of these genes in the granulosa cells will be discussed. *AREG* mRNA abundance was affected by the stage of follicular development ($P < 0.05$) and was low during the recruitment phase and then increased in the mid-selection phase where it remained high until the final selection phase after the preovulatory LH surge (Figure 3.4A). In contrast, expression of *EREG* mRNA did not change during any phase of follicle development (Figure 3.4A), however, a remarkable similarity between the expression profiles of the two genes was observed. In both cases, the variance during the final selection phase, before and after the LH surge, was extremely high, while almost no variance was observed in the recruitment and mid-selection phase. Further evaluation of *AREG* and *EREG* mRNA abundance in individual sows revealed two animals with particularly high expression for both genes (Figure 3.4B). Furthermore, the sow from the pre-LH final selection phase had high oestradiol and progesterone concentrations, while the sow from the final selection phase post-LH had the highest concentration of oestradiol among the animals from that phase, and also had a high concentration of progesterone (data not shown). This suggests that these two animals were the closest to the preovulatory LH surge and that *AREG* and *EREG* mRNA abundance could be promptly and transiently increased during that period. Moreover, abundance of *AREG* and *EREG* mRNA were positively correlated with each other ($r = 0.73$, $P < 0.001$) and also with follicle size ($r = 0.83$, $P < 0.01$; $r = 0.54$, $P < 0.05$, respectively) further supporting their importance in the large preovulatory follicle. Although *BTC* mRNA abundance was also affected by the stage of follicular

development ($P < 0.01$), its mRNA abundance was low during the recruitment phase, peaked during the mid-selection phase and returned to low levels during the final selection phase before and after exposure to the preovulatory LH surge (Figure 3.4A). Contrary to the relationship observed between *AREG* and *EREG* mRNA, *BTC* mRNA abundance showed a negative correlation with follicle size suggesting its importance earlier in follicle growth ($r = -0.51$, $P < 0.05$). Finally, *ADAMI7* mRNA abundance remained constant in the oocyte and granulosa cells during follicular development but showed a tendency to be affected by the stage of the follicle in the theca cells ($P < 0.1$; Figure 3.1, 3.4A and 3.5). Interestingly, in the granulosa cells, *ADAMI7* mRNA abundance positively correlated with *AREG* and *EREG* mRNA abundance ($r = 0.87$, $P < 0.001$; $r = 0.68$, $P < 0.01$, respectively), suggesting that co-expression of these genes in the developing follicle might be important.

DISCUSSION

It is becoming increasingly evident that modulation of follicular cell functions by local growth factors is essential for the coordination of follicle development (Gilchrist *et al.*, 2008, Hunter and Paradis, 2009, Juengel and McNatty, 2005, Knight and Glister, 2006, Webb *et al.*, 2007). However, our understanding of the plethora of growth factors and receptors present in the follicle throughout follicle development is still very limited. In order to gain insight into the local regulation of porcine antral follicle development, a strategy was used that combined microarray and gene ontology analysis. This allowed the generation of a list of oocyte, granulosa and theca cell transcripts containing the factors secreted by each cell type, as well as transcripts encoding receptors. In the context of the current experiment, the IGF and the EGF family of growth factors were identified as being expressed in the different cell types of the follicle. The validity of the secreted factors and receptors identified by microarray and gene ontology analysis were confirmed and their expression patterns during defined stages of preovulatory follicular development in the weaned sows was explored.

A common approach used in the study of gene expression in various tissue and cell types, including reproductive tissues, consists of selecting candidate genes from the existing literature that have either been shown to be important for specific cellular or tissue-specific functions in other species. Although this strategy has proven useful in many circumstances, it is also relatively limiting as there is no means of ensuring that the observations made in other species will apply to the model of interest. Another strategy that has been developed specifically to investigate the secretome of a particular cell type, is the use of signal-sequence trap. This strategy is based on the knowledge that proteins directed for secretion or anchoring to membranes contain specific target signal sequences necessary for their transport to the endoplasmic reticulum (von Heijne, 1990). Taking advantage of this characteristic it is possible to identify cDNA containing a signal sequence because of their ability to drive the secretion of a selection gene-encoded protein product in a genetically modified host. Using a signal-sequence trap method, Taft *et al.* (2002) studied the genes encoding secreted proteins in the mouse oocyte. Their results revealed 11 oocyte genes encoding secreted proteins and 23 transmembrane/membrane proteins likely to be involved in signal transduction. Importantly, several of the factors identified by Taft *et al.* (2002), including apolipoprotein E (APOE), BMP6, GDF9, crumbs protein homologue precursor 1 (CRB1), TPT1 and ZP2, were found on the lists generated in the current study and those that were not, had several related family members represented. Although this signal trap approach has allowed the identification of mouse oocyte factors likely to be involved in cell-to-cell communication, the number of candidate genes identified was limited and several important secreted factors such as BMP15, ZP1, and ZP3 were absent, suggesting the issues with efficiency of such an approach.

The advancement in microarray analyses now allows researchers to interrogate thousands of transcripts that are highly relevant to the model studied in a single experiment (Bonnet *et al.*, 2008b). This strategy was exploited by Pan *et al.* (2005) and allowed them to identify more than 140 secreted proteins potentially produced by the mouse oocyte. Using a combination of microarray

analysis and gene ontology annotation, we have identified over 500 unique genes from porcine oocyte, granulosa and theca cells whose products are believed to locate to the extracellular region and that are potentially involved in cell-to-cell communication. We have also identified a list of over 350 unique genes encoding receptor functions that are likely to be involved in the transduction of those signals. The rationale for generating a list of ligands and receptors was to ensure that the whole system was present in the follicle, increasing the likelihood that these factors would directly influence follicle development. Examination of the list of factors identified as localizing to the extracellular region revealed several members of the TGF- β superfamily, including BMP2, BMP4, BMP5, BMP6, BMP15, GDF9, TGFB1, TGFB2 and TGFB3. This is consistent with previous mouse literature where BMP5, BMP6, BMP15, GDF9, TGFB2 and TGFB3 were identified as being secreted by the oocyte (Pan *et al.*, 2005, Taft *et al.*, 2002). Importantly, we also report the expression of several receptors belonging to that family, including BMPRI1A and BMPRI1B, confirming the presence of a complete BMP system in the pig ovary as previously reported (Brankin *et al.*, 2005, Paradis *et al.*, 2009). The identification of several members of the TGF- β superfamily in our lists of growth factors is reassuring, particularly considering the recent findings that these molecules are key regulators of follicle growth in several species (Juengel and McNatty, 2005, Gilchrist *et al.*, 2008). We also identified several members of the IGF family including IGF1, IGF1R, several IGFBPs and the protease PAPP-A. Given the established importance of IGF1 for follicular cell functions (Mazerbourg *et al.*, 2003), these data confirm the value of the gene lists of growth factors and receptors that were generated. Finally, the identification of members of the EGF family, including EGFR and AREG, was of particular interest, especially in light of the fact that EGFR was exclusively found on the granulosa and theca cells, while AREG was specific to the granulosa cell. These factors have recently been shown to be important for LH-mediated cumulus cell expansion and oocyte meiotic resumption in mouse and porcine COCs *in vitro* (Chen *et al.*, 2008, Park *et al.*, 2004, Yamashita *et al.*, 2007) and could fulfil similar functions *in vivo*. Overall, these observations suggest that the microarray

and gene ontology approach described in the current study represents a powerful tool to determine the global expression of genes with a defined function or destination within each cell type of the ovarian follicle, permitting further characterization of the growth factors necessary for the coordination of folliculogenesis.

In most cases, confirmation of the localization of the selected candidate genes from the IGF and EGF system by real-time PCR analysis supported the results obtained by microarray, establishing the validity and usefulness of the list of growth factors and receptors generated for each cell type. However, in a few instances, such as for *IGF1R*, *IGFBP6* and *ADAM17* mRNA, discrepancies were observed, likely representing the potential pitfalls associated with microarray use. Our results clearly suggest that the detection of a transcript by microarray is generally indicative that the gene is expressed in that cell type, as confirmed in all cases by real-time PCR. However, absence of transcript detection by microarray does not always reliably eliminate the possibility that a gene is expressed in that particular cell type. This was the case for *IGF1R* mRNA which was not detected by microarray in the oocyte and theca cells but was by real-time PCR in both those cell types. This was also the case for *IGFBP6* mRNA in the granulosa cells. There are several possible explanations for these discrepancies. First, the differences in sensitivity between these techniques could allow real-time PCR to detect very low abundance transcripts that the microarray would likely have missed. It is also important to remember that the samples submitted to the microarray analysis were from a pool of tissues from animals of different level of maturity and different phases of follicular development. This could have led to the dilution of genes whose expression was transient in particular animals or phases of follicular development, thus limiting its detection by microarray. Since the real-time PCR analysis was performed on samples from individual sows, it increases the likelihood of detecting such transiently expressed genes in a particular group of animals. Furthermore, it is known from human and mouse data, that many transcripts possess alternative splicing variants which could also explain some of the differences between microarray and real-time PCR analysis.

In the human, *IGF1R* exists as two soluble variants that differ from the full length *IGF1R* in the 3' region. Since the Affymetrix genome arrays design is known to be biased toward the 3' end of the transcript (Tsai *et al.*, 2006), such similar splicing variants would likely have been missed if they exist in the pig. The scenario for ADAM17 would be different as its transcript was not detected in any cell type by microarray but was found to be expressed in the three cell types by real-time PCR analysis. In this situation it is important to consider that the amplification step used in the current experiment relies on the use of oligo dT during the reverse transcription step which upon binding to the poly A tail, located at the 3' extremity of the transcript, allows for the generation of cDNA. Since the Affymetrix genome arrays are biased towards the 3' end, this approach is likely to be inconsequential for most transcripts. However, in the case of longer transcripts in which the probe sets have been designed toward the 5' end, as is the case for ADAM17, it could dramatically reduce the likelihood of that transcript being detected by microarray. Collectively, these comparisons illustrate that although the use of high throughput technology represents an extremely powerful tool for the identification of hundreds of transcripts expressed in a particular context, it is important to be aware of the weaknesses and pitfalls of such techniques to avoid making any incorrect or incomplete assumptions.

In vitro studies have clearly established the importance of the IGF system for the modulation of follicular cell function, particularly regarding cell proliferation and steroidogenesis (Spicer and Echtenkamp, 1995, Mazerbourg *et al.*, 2003). Interestingly, Kolodziejczyk *et al.* (2003) showed that the stimulatory effect of IGF1 in the pig is developmentally regulated, as thymidine incorporation was observed only in granulosa cells isolated from small and medium antral follicles but not in granulosa cells isolated from large follicles. Moreover, although IGF1 also appears to stimulate theca cell proliferation, this effect appears to be independent of follicle size (Kolodziejczyk *et al.*, 2001, Kolodziejczyk *et al.*, 2003). IGF1 and IGF2 have been shown to stimulate oestrogen synthesis by porcine granulosa and theca cells originating from various follicle sizes (Kolodziejczyk *et al.*, 2001, Kolodziejczyk *et al.*, 2003, Spicer and

Echternkamp, 1995) and progesterone synthesis by porcine granulosa cells and LH-stimulated androgen synthesis by theca cells are also stimulated by IGF1 and IGF2 (Spicer and Echternkamp, 1995). Perhaps the most interesting function of IGF1, relates to its synergistic activity with FSH to enhance granulosa cell steroidogenesis (Baranao and Hammond, 1984). This is believed to occur through IGF modulation of the number of gonadotrophin receptors, as well as their activity (Lucy *et al.*, 2008). IGF1 has also been shown to reduce porcine granulosa and cumulus cell apoptosis in culture (Guthrie and Garret, 2001, Sirotkin *et al.*, 2002). However, the modulation of these functions *in vivo* remains somewhat unclear, partly because of the complexity of the IGF system's activity during follicle growth. The mRNA expression patterns observed in the current experiment clearly indicate the potential for IGF1 to modulate the aforementioned functions in granulosa and theca cells during preovulatory follicle development in weaned primiparous sows. First, *IGF1* and *IGF1R* mRNA were detected in both granulosa and theca cells, consistent with previous studies in the pig (Liu *et al.*, 2000, Yuan *et al.*, 1996, Zhou *et al.*, 1996). Also consistent with the study of Liu *et al.* (2000), IGF1 mRNA abundance in the granulosa cells did not change during follicular growth in weaned sows. However, in the current study *IGF1* mRNA expression in the theca cell was found to increase from the recruitment phase to the final selection phase and remained high after the preovulatory LH surge. This contrasts to the results of Liu *et al.* (2000) who reported no changes in IGF1 mRNA in the theca cells. Moreover, an effect of cycle on IGF1 mRNA abundance was observed in the theca cell. It could be speculated that the higher abundance observed in the tissues recovered from sows in the first phase of preovulatory follicle development after weaning (first cycle) reflects a higher dependence of those follicles on the gonadotrophins and thus would support the observation that the follicles from the second cycle preovulatory cohort are more mature (Foxcroft *et al.*, 2007, Paradis *et al.*, 2009). In addition, our results in granulosa and theca cells showed an increase in *IGF1R* mRNA abundance during the mid-selection phase and its abundance remained high in the remaining phases studied. In contrast, Liu *et al.* (2000) observed no change in *IGF1R* mRNA

abundance in either cell type. Furthermore, modulation of IGF1 bioavailability by the IGFBPs and the IGFBP protease PAPP-A could be important for regulating follicle cell function (Mazerbourg *et al.*, 2003). For example, elevation of IGFBP5 in ruminant follicles is often associated with atresia. Interestingly, Liu *et al.* (2000) reported that IGFBP2 decreased, while IGFBP4 increased, during porcine follicle growth. This observation was not validated in the current experiment, although there was a tendency for IGFBP2 in the granulosa cells to decrease in larger follicles. It could be suggested that by using a representative pool of follicles present on the ovary of each animal might have confounded such an effect, since it is possible that expression of the IGFBPs within the follicle population was different. Nevertheless, correlation analysis established strong relationships between granulosa and theca cell *IGF1* mRNA abundance and the mRNA abundance of several *IGFBPs* and *PAPP-A*, suggesting that IGF1 activity is tightly regulated during follicle growth. This observation also clearly illustrates the complexity of the interactions between IGF1, IGF1R and the IGFBPs. Only by gaining an insight into the affinity of each binding protein for IGF1, and by defining the role of each IGFBP in modulating IGF1 function, will it be possible to understand the complex regulation of the IGF system in the ovarian follicle.

The current results of the microarray and/or real-time PCR analysis also showed that the mRNA encoding for the EGF-like ligands, *AREG*, *EREG* and *BTC*, were specifically expressed in the granulosa cells of porcine antral follicles. This is consistent with observations in the mouse in which the three ligands were specifically expressed in the mural and cumulus granulosa cells (Park *et al.*, 2004, Shimada *et al.*, 2006). In addition, in the present study the abundance of *AREG* and *EREG* mRNA was found to dramatically increase in specific sows during the periods immediately preceding and following the endogenous preovulatory LH surge. This is in contrast to the mouse, where increased *AREG* and *EREG* mRNA abundance was observed only after hCG treatment (Park *et al.*, 2004, Shimada *et al.*, 2006). However, it is similar to the situation in eCG- and hCG-stimulated sows in which *AREG* and *EREG* mRNA increased after eCG treatment and remained high up to 12h post-hCG injection (Kawashima *et al.*, 2008). These

results suggest that the up-regulation of *AREG* and *EREG* mRNA observed in sow granulosa cells following exogenous gonadotrophin treatment also occur physiologically after exposure to endogenous gonadotrophins. *AREG* and *EREG* were shown to be important for LH-mediated cumulus cell expansion and oocyte meiotic resumption in mouse and porcine COCs *in vitro* (Chen *et al.*, 2008, Park *et al.*, 2004, Yamashita *et al.*, 2007) and the expression observed in the current study supports a similar role *in vivo*. Interestingly, in the mouse, *BTC* mRNA was also shown to be up-regulated by hCG stimulation and was found to stimulate cumulus cell expansion *in vitro* (Park *et al.*, 2004). However, in the current study, the mRNA encoding *BTC* was more abundantly expressed during the recruitment and mid-selection phases and decreased to very low levels during the periovulatory period. This observation suggests that, in contrast to the mouse, *BTC* may less be important for the ovulatory process in the pig; but may play a more significant role earlier in follicular growth. Moreover, the effects of the EGF-like ligands have been shown in both mouse and porcine COCs to occur through the cumulus cell EGFR (Chen *et al.*, 2008, Park *et al.*, 2004, Shimada *et al.*, 2006, Yamashita *et al.*, 2007). Kawashima *et al.* (2008) showed that exogenous administration of eCG and hCG to sows promoted increased expression of *EGFR* mRNA in the cumulus cells, whereas Prochazka *et al.* (2003) found very little change in EGFR in the cumulus and mural granulosa cells isolated from small and large follicles. Consistent with that study, our results showed that *EGFR* mRNA in the granulosa cells did not change between the different phases of follicular development. Regardless of the abundance of EGFR, Prochazka *et al.* (2003) also showed that the ability of the receptor to become activated through tyrosine phosphorylation was greater in larger follicles, indicating better responsiveness to EGF stimulation and suggesting that preovulatory follicles are likely to be primed to respond to the stimulation by EGF and EGF-like ligands. Finally, the EGF-like ligands are expressed as transmembrane precursors and require metalloprotease activity to be released and to activate the EGFR on the target cells (Peschon *et al.*, 1998, Dong *et al.*, 1999). In mouse embryonic cells, TNF α -converting enzyme (ADAM17) was the main

metalloprotease involved in AREG and EREG cleavage (Sahin *et al.*, 2004). In cultured porcine COCs, ADAM17 was shown to be essential for EGF-like ligand stimulation of EGFR and cumulus expansion (Yamashita *et al.*, 2007). In the current study, *ADAM17* mRNA abundance in the granulosa cells was found to be relatively stable across all phases of follicular development; however, a strong positive correlation between *ADAM17* mRNA abundance and *AREG* and *EREG* mRNA abundance was observed, suggesting that ADAM17 may be important for the EGF-like ligand activity.

In conclusion, the findings of the present study clearly demonstrate the presence of a complex signaling network of growth factors and receptors in the pig ovarian antral follicle. To our knowledge, this is the first study to provide such a detailed list of oocyte, granulosa and theca cell growth factors and receptors potentially involved in cell-to-cell communication in the developing ovarian follicle. Our results also demonstrate the changes in expression of several members of the IGF and EGF family during carefully defined stages of preovulatory follicle growth *in vivo* and suggest that amphiregulin and epiregulin, but not betacellulin, are important in the period immediately preceding and following the LH surge *in vivo*. Moreover, the results suggest that differences in IGF1 mRNA abundance between sows from the 1st and 2nd cycle could be responsible for creating the differences in follicle quality observed between those sows.

Table 3.1 Details of primers and probes used for Real-Time PCR

Gene	AC number	Primer	Sequence 5' --> 3' or assay ID	Product size	Annealing/Extension Temperature (°C)
AREG	NM_214376	ABI	Ss03384424_u1	92 bp	62
		Forward	GCCCTCGCCCTGGGTATA		
BTC	CU468060	Reverse	TCCTGGTTGAATTCCCATGTG	61 bp	62
		Probe	ATCCTTCACTGCGTTGTG		
		Forward	TTGGAGATCACCTACATGCAGAA		
EGFR	NM_214007	Reverse	GCGACCTCCTGAATGGTCTTT	65 bp	62
		Probe	AGCTACAACCTGTCTTT		
		Forward	GCTCTGCCTGGGTTTCCAT		
EREG	FP340229	Reverse	GGGATACAAGAAGGAATCACAGTTG	66 bp	62
		Probe	CTGCAAGCTGTTCTC		
		Forward	GCTGGTGGACGCTCTTCAGT		
IGF1	NM_214256	Reverse	CCTGTGGGCTTGTGAAATAAAA	63 bp	62
		Probe	CGTGTGCGGAGACAG		
IGF1R	NM_214172	ABI	Ss03394274_m1	76 bp	62
IGFBP2	NM_214003	ABI	Ss03393382_u1	71 bp	62

Gene	AC number	Primer	Sequence 5' --> 3' or assay ID	Product size	Annealing/Extension Temperature (°C)
IGFBP4	NM_001123129	ABI	Ss03387801_u1	76 bp	62
IGFBP5	NM_214099	ABI	Ss03382569_u1	118 bp	62
IGFBP6	NM_001100190	ABI	Ss03386322_u1	74 bp	62
PAPPA	AF421142	ABI	Ss03373446_m1	70 bp	62
PPIA	AY266299	Forward	AATGCTGGCCCCAACACA	56 bp	60
		Reverse	TCAGTCTTGGCAGTGCAAATG		
		Probe	ACGGTTCCCAGTTTT		
TACE/ADAM17	NM_001099926	ABI	Ss03386029_u1	63 bp	62

Table 3.2 Comparison of transcript localization for members of the insulin-like growth factor and epidermal growth factor family as determined by microarray and real-time PCR analysis.

Name	Symbol	Oocyte		Granulosa cell		Theca cell	
		MA	QPCR	MA	QPCR	MA	QPCR
Insulin-like growth factor IA precursor	IGF1	-	-	+	+	+	+
Insulin-like growth factor I receptor	IGF1R	-	+	+	+	-	+
Insulin-like growth factor binding protein 2	IGFBP2	-	-	+	+	+	+
Insulin-like growth factor binding protein 4	IGFBP4	na	-	na	+	na	+
Insulin-like growth factor binding protein 5	IGFBP5	-	-	+/-	+/-	+	+
Insulin-like growth factor binding protein 6	IGFBP6	+	+	-	+/-	+	+
Pregnancy-associated plasma protein-A	PAPPA	+	+	+	+	+	+
Epidermal growth factor receptor precursor	EGFR	-	-	+	+	+	+
Amphiregulin precursor	AREG	-	-	+	+	-	+/-
Epiregulin	EREG	na	-	na	+	na	+/-
Betacellulin	BTC	na	-	na	+	na	+/-
A disintegrin and metalloproteinase domain 17	ADAM17	-	+	-	+	-	+

MA: Microarray QPCR : Real-Time PCR

+ : Present; -: Absent; +/- : Low or Marginal expression ; na: not applicable

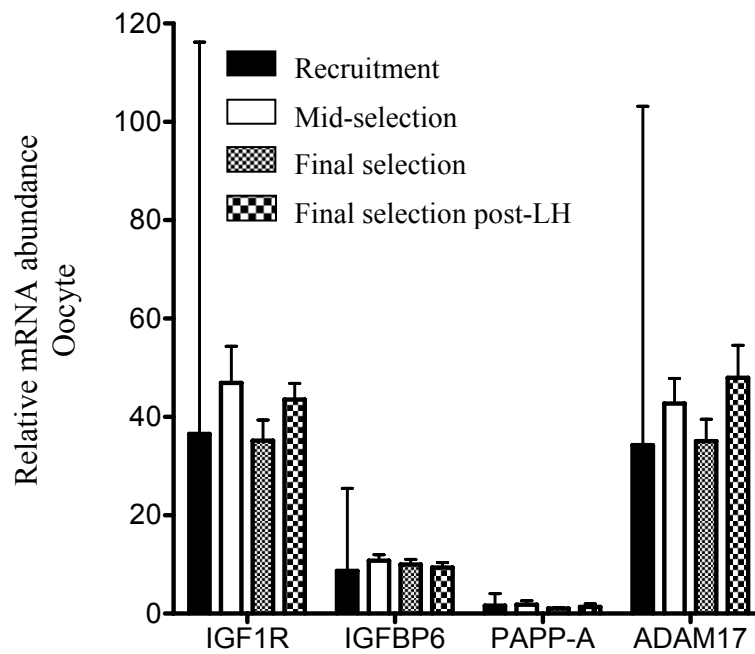


Figure 3.1 Quantification by real-time RT-PCR of *IGF1R*, *IGFBP6*, *PAPP-A* and *ADAM17* mRNA abundance in pig oocytes during recruitment (R; n=6), mid-selection (MS; n=6), final selection (FS; n=8) and final selection post-LH surge (FS/LH; n=8). Data are expressed as lsmeans of relative mRNA abundance \pm SEM.

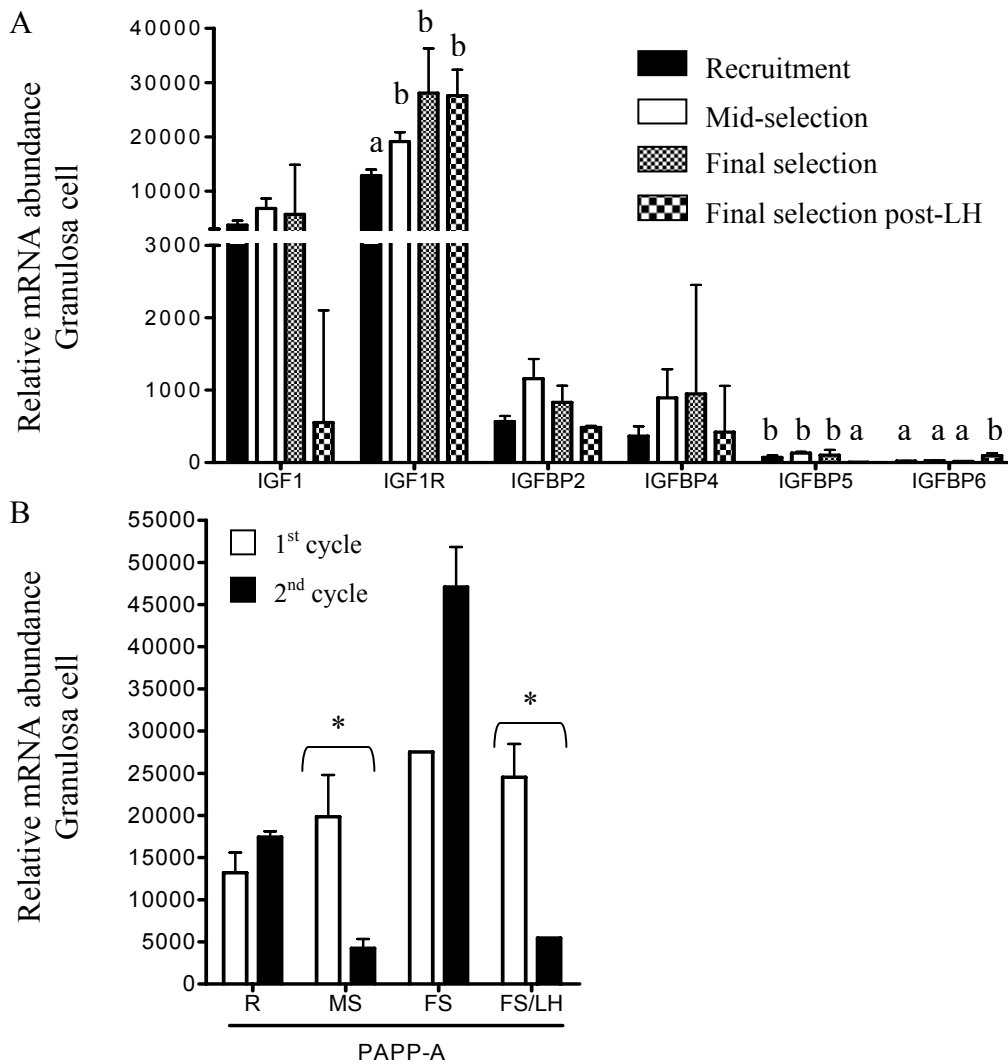


Figure 3.2 Quantification by real-time PCR of A) *IGF1*, *IGF1R*, *IGFBP2*, *IGFBP4*, *IGFBP5* and *IGFBP6* and B) *PAPP-A* mRNA abundance in pig granulosa cells during recruitment (R; n=6), mid-selection (MS; n=6) final selection (FS; n=3) and final selection post-LH (FS/LH; n=3). Data are expressed as means of relative mRNA abundance \pm SEM. Different letters within genes represent significant differences among phases (^{abc}P<0.05). *represents significant differences within phase between cycles (P<0.05).

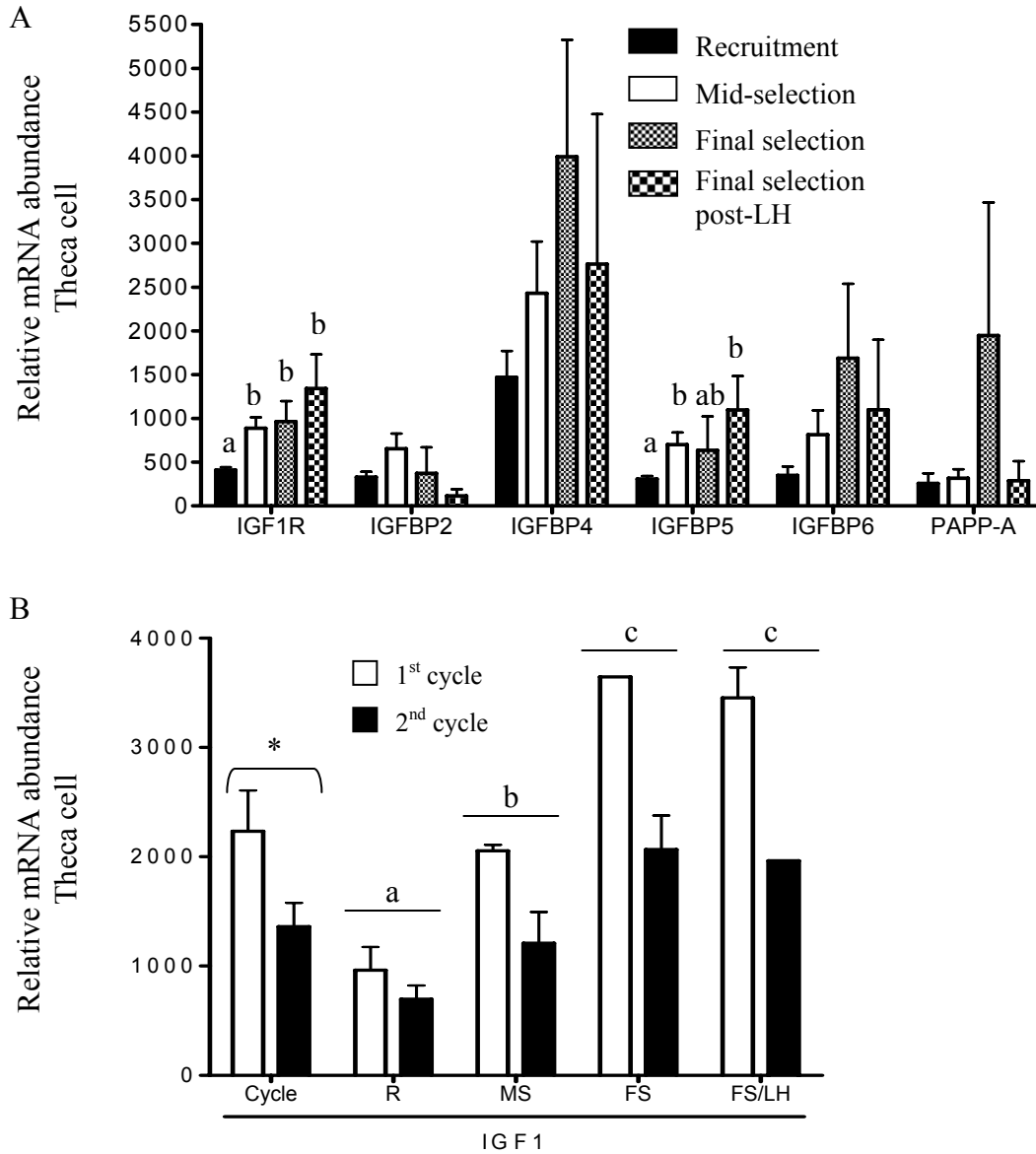


Figure 3.3 Quantification by real-time PCR of A) IGF1R, IGFBP2, IGFBP4, IGFBP5, IGFBP6 and PAPP-A and B) IGF1 mRNA abundance in pig theca cells during recruitment (R; n=6), mid-selection (MS; n=6) final selection (FS; n=3) and final selection post-LH (FS/LH; n=3). Data are expressed as means of relative mRNA abundance \pm SEM. Different letters within gene represent significant differences among phases (^{abc}P<0.05). * represents significant differences between 1st and 2nd cycle (P<0.05).

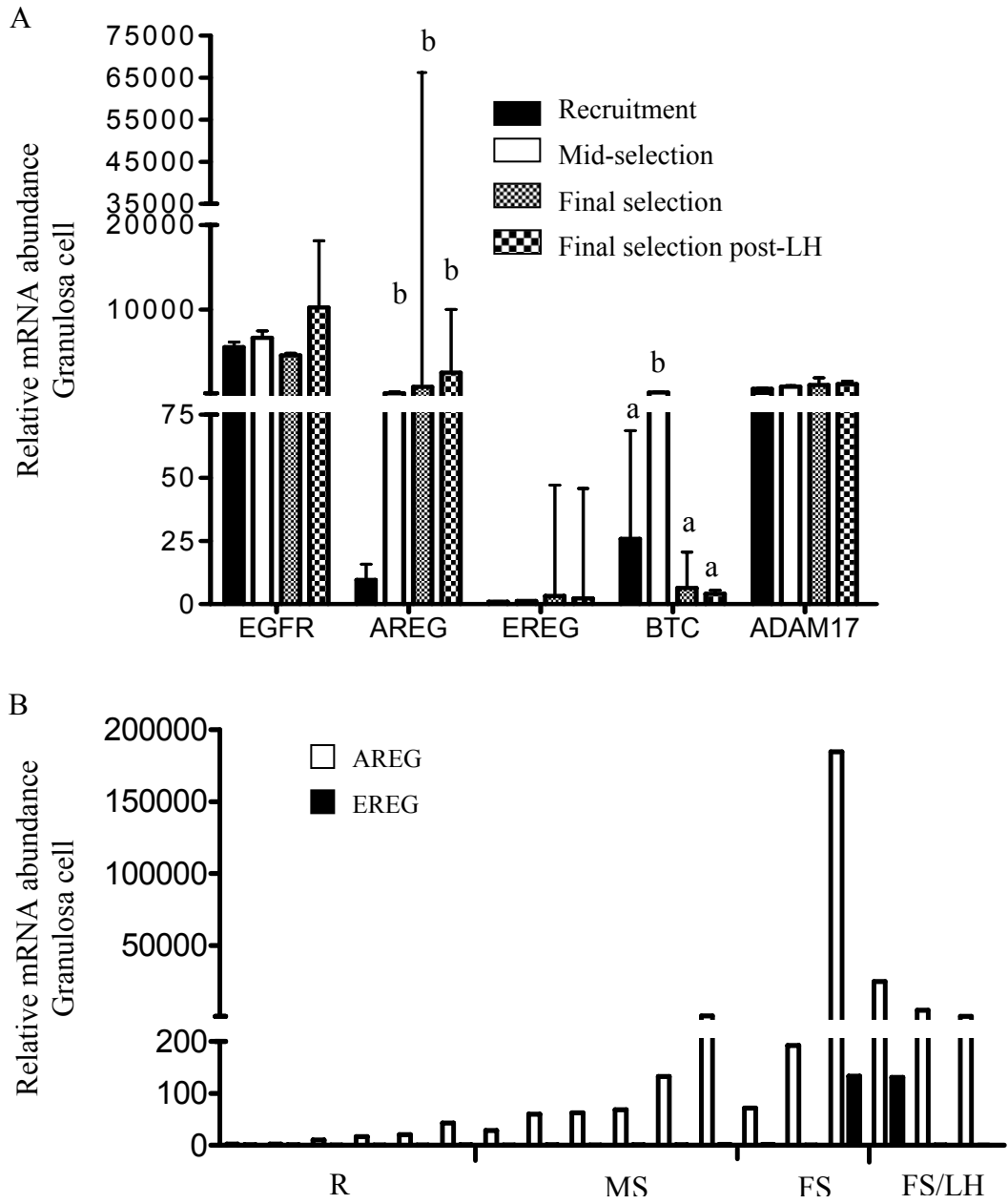


Figure 3.4 A) Quantification by real-time PCR of EGFR, AREG, EREG, BTC and ADAM17 mRNA abundance in pig granulosa cell during recruitment (R; n=6), mid-selection (MS; n=6) final selection (FS; n=3) and final selection post-LH (FS/LH; n=3). Data are expressed as means of relative mRNA abundance \pm SEM. Different letters within gene represent significant differences among phases ($P < 0.05$). B) AREG and EREG mRNA abundance in individual sows throughout follicular development.

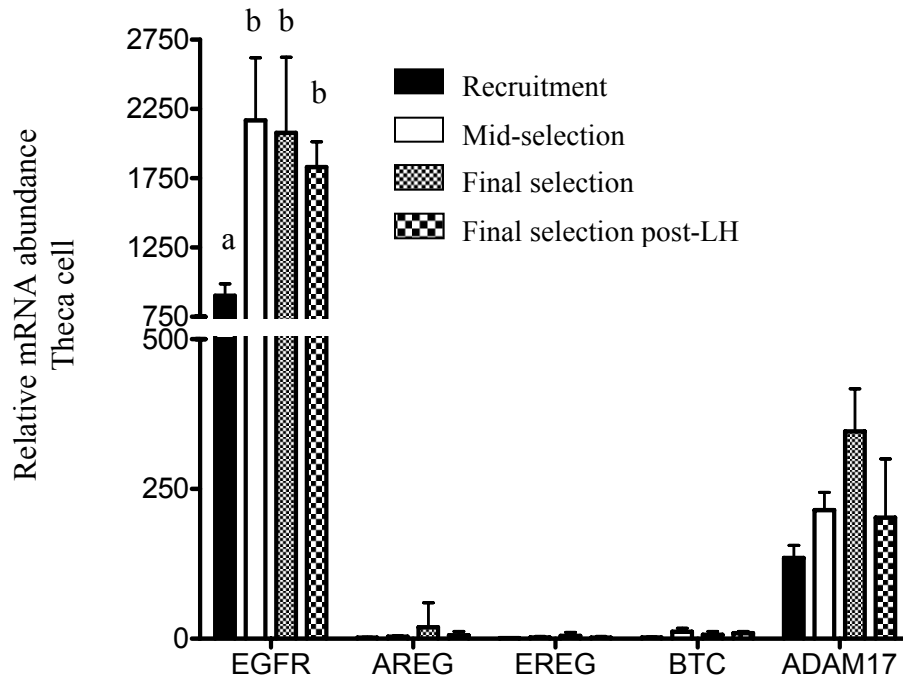


Figure 3.5 Quantification by real-time PCR of EGFR, AREG, EREG, BTC and ADAM17 mRNA abundance in pig theca cell during recruitment (R; n=6), mid-selection (MS; n=6) final selection (FS; n=3) and final selection post-LH (FS/LH; n=3). Data are expressed as means of relative mRNA abundance \pm SEM. Different letters within gene represent significant differences among phases ($P < 0.05$).

REFERENCES

- Agca C, Ries JE, Kolath SJ, Kim JH, Forrester LJ, Antoniou E, Whitworth KM, Mathialagan N, Springer GK, Prather RS & Lucy MC** 2006 Luteinization of porcine preovulatory follicles leads to systematic changes in follicular gene expression. *Reproduction* **132** 133-145.
- Baranao JL & Hammond JM** 1984 Comparative effects of insulin and insulin-like growth factors on DNA synthesis and differentiation of porcine granulosa cells. *Biochem Biophys Res Commun* **124** 484-490.
- Bonnet A, Le Cao KA, Sancristobal M, Benne F, Robert-Granie C, Law-So G, Fabre S, Besse P, De Billy E, Quesnel H, Hatey F & Tosser-Klopp G** 2008a *In vivo* gene expression in granulosa cells during pig terminal follicular development. *Reproduction* **136** 211-224.
- Bonnet A, Dalbies-Tran R & Sirard MA** 2008b Opportunities and challenges in applying genomics to the study of oogenesis and folliculogenesis in farm animals. *Reproduction* **135** 119-128.
- Brankin V, Quinn RL, Webb R & Hunter MG** 2005 Evidence for a functional bone morphogenetic protein (BMP) system in the porcine ovary. *Dom Anim Endocrinol* **28** 367-379.
- Caetano AR, Johnson RK & Pomp D** 2003 Generation and sequence characterization of a normalized cDNA library from swine ovarian follicles. *Mamm Genome* **14** 65-70.
- Caetano AR, Johnson RK, Ford JJ & Pomp D** 2004 Microarray profiling for differential gene expression in ovaries and ovarian follicles of pigs selected for increased ovulation rate. *Genetics* **168** 1529-1537.
- Chen X, Zhou B, Yan J, Xu B, Tai P, Li J, Peng S, Zhang M & Xia G** 2008 Epidermal growth factor receptor activation by protein kinase C is necessary for FSH-induced meiotic resumption in porcine cumulus-oocyte complexes. *J Endocrinol* **197** 409-419.
- Clowes EJ, Aherne FX & Foxcroft GR** 1994 Effect of delayed breeding on the endocrinology and fecundity of sows. *Journal of Animal Science* **72** 283-291.
- Clowes EJ, Aherne FX, Foxcroft GR & Baracos VE** 2003a Selective protein loss in lactating sows is associated with reduced litter growth and ovarian function. *Journal of Animal Science* **81** 753-764.

Clowes EJ, Aherne FX, Schaefer AL, Foxcroft GR & Baracos VE 2003b Parturition body size and body protein loss during lactation influence performance during lactation and ovarian function at weaning in first-parity sows. *Journal of Animal Science* **81** 1517-1528.

Dong J, Opresko LK, Dempsey PJ, Lauffenburger DA, Coffey RJ & Wiley HS 1999 Metalloprotease-mediated ligand release regulates autocrine signaling through the epidermal growth factor receptor. *Proc Natl Acad Sci U S A* **96** 6235-6240.

Foxcroft GR 1997 Mechanisms mediating nutritional effects on embryonic survival in pigs. *Journal of Reproduction and Fertility Suppl* **52** 47-61.

Foxcroft GR, Vinsky MD, Paradis F, Tse WY, Town SC, Putman CT, Dyck MK & Dixon WT 2007 Macroenvironment effects on oocytes and embryos in swine. *Theriogenology* **68 Suppl 1** S30-39.

Gilchrist RB, Lane M & Thompson JG 2008 Oocyte-secreted factors: regulators of cumulus cell function and oocyte quality. *Hum Reprod Update* **14** 159-177.

Guthrie HD & Garrett WM 2001 Apoptosis during folliculogenesis in pigs. *Reprod Suppl* **58** 17-29.

Hunter MG 2000 Oocyte maturation and ovum quality in pigs. *Rev Reprod* **5** 122-130.

Hunter MG, Robinson RS, Mann GE & Webb R 2004 Endocrine and paracrine control of follicular development and ovulation rate in farm species. *Anim Reprod Sci* **82-83** 461-477.

Hunter MG & Paradis F 2009 Intra-follicular regulatory mechanisms in the porcine ovary. *Control of Pig Reproduction VIII*. In press.

Jiang H, Whitworth KM, Bivens NJ, Ries JE, Woods RJ, Forrester LJ, Springer GK, Mathialagan N, Agca C, Prather RS & Lucy MC 2004 Large-scale generation and analysis of expressed sequence tags from porcine ovary. *Biol Reprod* **71** 1991-2002.

Juengel JL & McNatty KP 2005 The role of proteins of the transforming growth factor-beta superfamily in the intraovarian regulation of follicular development. *Human Reproduction Update* **11** 143-160.

Kawashima I, Okazaki T, Noma N, Nishibori M, Yamashita Y & Shimada M 2008 Sequential exposure of porcine cumulus cells to FSH and/or LH is critical for appropriate expression of steroidogenic and ovulation-related genes that impact oocyte maturation *in vivo* and *in vitro*. *Reproduction* **136** 9-21.

Knight PG & Glister C 2006 TGF-beta superfamily members and ovarian follicle development. *Reproduction* **132** 191-206.

Kolodziejczyk J, Gregoraszcuk EL, Leibovich H & Gertler A 2001 Different action of ovine GH on porcine theca and granulosa cells proliferation and insulin-like growth factors I- and II-stimulated estradiol production. *Reprod Biol* **1** 33-41.

Kolodziejczyk J, Gertler A, Leibovich H, Rzasa J & Gregoraszcuk EL 2003 Synergistic action of growth hormone and insulin-like growth factor I (IGF-I) on proliferation and estradiol secretion in porcine granulosa and theca cells cultured alone or in coculture. *Theriogenology* **60** 559-570.

Liu J, Koenigsfeld AT, Cantley TC, Boyd CK, Kobayashi Y & Lucy MC 2000 Growth and the initiation of steroidogenesis in porcine follicles are associated with unique patterns of gene expression for individual components of the ovarian insulin-like growth factor system. *Biol Reprod* **63** 942-952.

Lucy MC 2008 Functional differences in the growth hormone and insulin-like growth factor axis in cattle and pigs: implications for post-partum nutrition and reproduction. *Reprod Domest Anim* **43 Suppl 2** 31-39.

Mao J, Treacy BK, Almeida FR, Novak S, Dixon WT & Foxcroft GR 2001 Feed restriction and insulin treatment affect subsequent luteal function in the immediate postovulatory period in pigs: progesterone production in vitro and messenger ribonucleic acid expression for key steroidogenic enzymes. *Biol Reprod* **64** 359-367.

Mazerbourg S, Bondy CA, Zhou J & Monget P 2003 The insulin-like growth factor system: a key determinant role in the growth and selection of ovarian follicles? a comparative species study. *Reprod Domest Anim* **38** 247-258.

Pan H, O'Brien M J, Wigglesworth K, Eppig JJ & Schultz RM 2005 Transcript profiling during mouse oocyte development and the effect of gonadotropin priming and development *in vitro*. *Dev Biol* **286** 493-506.

Paradis F, Novak S, Murdoch G, Dyck MK, Dixon WT & Foxcroft GR 2009 Temporal regulation of BMP2, BMP6, BMP15, GDF-9, BMPR1A, BMPR1B, BMPR2 and TGF{beta}R1 mRNA expression in the oocyte, granulosa and theca cells of developing preovulatory follicles in the pig. *Reproduction* **138** 115-129.

Park JY, Su YQ, Ariga M, Law E, Jin SL & Conti M 2004 EGF-like growth factors as mediators of LH action in the ovulatory follicle. *Science* **303** 682-684.

Peschon JJ, Slack JL, Reddy P, Stocking KL, Sunnarborg SW, Lee DC, Russell WE, Castner BJ, Johnson RS, Fitzner JN, Boyce RW, Nelson N, Kozlosky CJ, Wolfson MF *et al.* 1998 An essential role for ectodomain shedding in mammalian development. *Science* **282** 1281-1284.

- Prochazka R, Kalab P & Nagyova E** 2003 Epidermal growth factor-receptor tyrosine kinase activity regulates expansion of porcine oocyte-cumulus cell complexes *in vitro*. *Biol Reprod* **68** 797-803.
- Sahin U, Weskamp G, Kelly K, Zhou HM, Higashiyama S, Peschon J, Hartmann D, Saftig P & Blobel CP** 2004 Distinct roles for ADAM10 and ADAM17 in ectodomain shedding of six EGFR ligands. *J Cell Biol* **164** 769-779.
- Shimada M, Hernandez-Gonzalez I, Gonzalez-Robayna I & Richards JS** 2006 Paracrine and autocrine regulation of epidermal growth factor-like factors in cumulus oocyte complexes and granulosa cells: key roles for prostaglandin synthase 2 and progesterone receptor. *Mol Endocrinol* **20** 1352-1365.
- Sirotkin AV, Dukesova J, Pivko J, Makarevich AV & Kubek A** 2002 Effect of growth factors on proliferation, apoptosis and protein kinase A expression in cultured porcine cumulus oophorus cells. *Reprod Nutr Dev* **42** 35-43.
- Spicer LJ & Echternkamp SE** 1995 The ovarian insulin and insulin-like growth factor system with an emphasis on domestic animals. *Domest Anim Endocrinol* **12** 223-245.
- Taft RA, Denegre JM, Pendola FL & Eppig JJ** 2002 Identification of genes encoding mouse oocyte secretory and transmembrane proteins by a signal sequence trap. *Biol Reprod* **67** 953-960.
- Tosser-Klopp G, Benne F, Bonnet A, Mulsant P, Gasser F & Hatey F** 1997 A first catalog of genes involved in pig ovarian follicular differentiation. *Mamm Genome* **8** 250-254.
- Tsai S, Cassady JP, Freking BA, Nonneman DJ, Rohrer GA & Piedrahita JA** 2006 Annotation of the Affymetrix porcine genome microarray. *Anim Genet* **37** 423-424.
- von Heijne G** 1990 The signal peptide. *J. Membrane Biol.* **115** 195-201.
- Webb R, Garnsworthy PC, Campbell BK & Hunter MG** 2007 Intra-ovarian regulation of follicular development and oocyte competence in farm animals. *Theriogenology* **68 Suppl 1** S22-29.
- Whitworth KM, Agca C, Kim JG, Patel RV, Springer GK, Bivens NJ, Forrester LJ, Mathialagan N, Green JA & Prather RS** 2005 Transcriptional profiling of pig embryogenesis by using a 15-K member unigene set specific for pig reproductive tissues and embryos. *Biol Reprod* **72** 1437-1451.
- Yamashita Y, Kawashima I, Yanai Y, Nishibori M, Richards JS & Shimada M** 2007 Hormone-induced expression of tumor necrosis factor alpha-converting enzyme/A disintegrin and metalloprotease-17 impacts porcine cumulus cell

oocyte complex expansion and meiotic maturation via ligand activation of the epidermal growth factor receptor. *Endocrinology* **148** 6164-6175.

Yang H, Foxcroft GR, Pettigrew JE, Johnston LJ, Shurson GC, Costa AN & Zak LJ 2000a Impact of dietary lysine intake during lactation on follicular development and oocyte maturation after weaning in primiparous sows. *Journal of Animal Science* **78** 993-1000.

Yang H, Pettigrew JE, Johnston LJ, Shurson GC, Wheaton JE, White ME, Koketsu Y, Sower AF & Rathmacher JA 2000b Effects of dietary lysine intake during lactation on blood metabolites, hormones, and reproductive performance in primiparous sows. *Journal of Animal Science* **78** 1001-1009.

Yuan W & Lucy MC 1996 Messenger ribonucleic acid expression for growth hormone receptor, luteinizing hormone receptor, and steroidogenic enzymes during the estrous cycle and pregnancy in porcine and bovine corpora lutea. *Domest Anim Endocrinol* **13** 431-444.

Zak LJ, Xu X, Hardin RT & Foxcroft GR 1997 Impact of different patterns of feed intake during lactation in the primiparous sow on follicular development and oocyte maturation. *Journal of Reproduction and Fertility* **110** 99-106.

Zhou J, Adesanya OO, Vatzias G, Hammond JM & Bondy CA 1996 Selective expression of insulin-like growth factor system components during porcine ovary follicular selection. *Endocrinology* **137** 4893-4901.

CHAPTER 4

TEMPORAL REGULATION OF BMP2, BMP6, BMP15, GDF9, BMPR1A, BMPR1B, BMPR2 AND TGFBR1 mRNA EXPRESSION IN THE OOCYTE, GRANULOSA AND THECA CELLS OF DEVELOPING PREOVULATORY FOLLICLES IN THE PIG²

INTRODUCTION

Ovarian follicular development in large domestic mammals is a long and intricate process that ultimately results in the ovulation of a subset of one or more oocytes potentially competent to support fertilization and embryonic development. Since ovulation rate and oocyte quality can be important determinants of reproductive efficiency, it is essential to understand the regulation of follicular growth leading to ovulation. It is now widely accepted that during the later phases of follicular growth, the processes of recruitment and selection establish a preovulatory follicle population characteristic of each species (Hunter *et al.*, 2004). At the onset of the follicular phase in the pig, a pool of approximately 50 follicles are recruited to actively grow, from which the preovulatory population of 12 to 20 follicles will be selected for ovulation (Foxcroft & Hunter 1985, Hunter *et al.*, 2004). These processes are closely regulated by endocrine and paracrine factors, including the gonadotrophins, metabolic factors and several local growth factors.

Nutritional manipulations modify sow fertility and increased lactational catabolism in primiparous sows has detrimental consequences for embryonic survival by Day 30 of gestation in the subsequent litter (Foxcroft, 1997). Nutritional restriction during the last week of lactation was also shown to exert detrimental effects on follicle and oocyte quality (Zak *et al.*, 1997). Using *in vitro* techniques, these authors demonstrated that 1) the oocytes recovered from the presumptive preovulatory follicles of feed-restricted sows were less capable of

² A version of this chapter has been published. Paradis F, Novak S, Murdoch GK, Dyck MK, Dixon WT & Foxcroft GR 2009. *Reproduction* 138:

undergoing nuclear maturation and 2) the follicular fluid obtained from the same follicles was less able to support nuclear maturation of pools of oocytes obtained from prepubertal gilts. Later studies established a relationship between the extent of protein catabolism during lactation and follicle quality in the sow (Yang *et al.*, 2000a, Clowes *et al.*, 2003a, Clowes *et al.*, 2003b). Interestingly, delaying breeding of primiparous sows until the second oestrus post-weaning results in an increase in litter size compared to animals bred at their first oestrus (Clowes *et al.*, 1994). This difference in litter size likely results from the increased embryo survival in the sows bred at their second post-weaning oestrus and potentially originates from differences in follicle maturity (size) during the periovulatory period (Foxcroft *et al.*, 2007). The mechanisms controlling such differences in follicular maturity are, therefore, of considerable practical significance.

Traditionally, studies investigating the control of follicular development have focused primarily on endocrine regulation by LH and FSH, and on local regulation involving IGF-1 and activin/inhibin/follistatin systems. However, the recent findings that the bone morphogenetic proteins (BMP) and growth differentiation factor 9 (GDF9) are key regulators of follicular development and might have a determinant role in establishing the ovulation quota, has raised an entirely new set of questions regarding the control of follicle/oocyte maturation (Shimasaki *et al.*, 2004, Juengel & McNatty 2005, Gilchrist *et al.*, 2008). This is especially true in the pig where there is a paucity of information available. Therefore, the objectives of this study were: 1) to confirm the presence and determine the localization of the ligands *BMP2*, *BMP6*, *BMP15*, *GDF9* and their receptors *BMPRIA*, *BMPR1B*, *BMPR2* and *TGFBR1* mRNA in developing preovulatory follicles in the pig, 2) to establish the temporal changes in mRNA abundance during the preovulatory wave of follicular development and 3) to determine whether these ligands and receptors could play a role in creating the differences in follicle characteristics observed between the 1st and 2nd post-weaning preovulatory wave of follicular development in primiparous sows. To our knowledge, this is the first experiment to report the spatial and temporal

changes in mRNA expression for these members of the TGF- β superfamily and their associated receptors in pig preovulatory follicles.

MATERIALS AND METHODS

Chemicals and media

Unless otherwise stated all chemicals were obtained from Sigma-Aldrich (St-Louis, Mo, USA). The media used for washing the COCs and during follicle dissection was modified Tyrode lactate (TL)-HEPES medium supplemented with 0.1% (w/v) polyvinyl alcohol (PVA) (Funahashi *et al.*, 1997), 50 U/ml of penicillin and 50 μ g/ml of streptomycin (Invitrogen, #15070-063, , Burlington, ON, Canada). The phosphate-buffered saline pH 7.4 was composed of 137 mM NaCl, 2.7 mM KCl, 8.1 mM Na₂HPO₄ and 1.47 mM KH₂PO₄.

Animals

This experiment was conducted in accordance with the guidelines of the Canadian Council on Animal Care and with the approval of the University of Alberta, Faculty Animal Policy and Welfare Committee (Protocol #2005-40B). A total of 28 primiparous F1 sows (Large White x Landrace, Hypor, Regina, SK, Canada) were used for follicle dissection and oocyte aspiration and an additional 9 sows were required for follicular fluid collection. Within 48 h after farrowing, litter size was standardized to between 9 and 11 piglets through cross-fostering and routine piglet processing procedures (tail-docking, teeth clipping, ear notching and iron injection) were performed. During lactation, sows were offered fresh feed three times daily and permitted ad libitum access to fresh water. Sows were offered 3.5 kg of feed on the day of farrowing, and during the remainder of lactation, the amount of feed offered was increased by 0.5 kg daily until the sows daily consumption was exceeded by 0.5 kg. Sows were weaned 20.8 ± 3.2 (mean \pm stdev) days after farrowing and were randomly allocated to treatment at this time. After weaning, sows were moved to a common weaned-sow room, housed in individual sow stalls and were fed to appetite twice daily until the day of euthanasia. From the day after weaning, sows were actively heat-checked using

fenceline boar contact twice daily (at 0800 and 1400). Onset of standing heat was determined as the midpoint between the time of first detection of standing oestrus and the last time that oestrus was detected. Similarly, the end of standing heat was calculated as the midpoint between the last time that signs of oestrus were detected and the first time after standing heat that no signs of oestrus were detected. Sows were weighed on day 1, 6 and 13 of lactation, at weaning and at the time of euthanasia.

Sows used for follicle dissection and oocyte aspiration were euthanized on day 1 (D1; n=3), 2 (D2; n=3) or 4 (D4; n=8) after weaning, or day 14 (D14; n=3), 16 (D16; n=3) or 20 (D20; n=8) after the 1st post-weaning oestrus. The additional 9 sows used for follicular fluid collection were euthanized on D2 (n=2), D14 (n=3) and D16 (n=4), respectively. These time-frames correspond to the 1st and 2nd post-weaning preovulatory wave of follicular development and D1/D14 corresponds to the period of recruitment (R) of the growing cohort of follicles, D2/D16 corresponds to the mid-selection phase (MS) at which time follicles either keep growing or, if not selected, start to undergo atresia and D4/D20 corresponds to the final selection phase (FS) where the preovulatory follicle population has been established (Grant *et al.*, 1989, Hunter and Wiesak, 1990). The preovulatory follicle population from the final selection phase was further divided between the follicles in pre-LH surge (FS) or post-LH surge (FS/LH) stages based on follicular fluid oestradiol concentrations (see procedure below). The sows used in the experiments were euthanized on-site in a purpose-built necropsy facility according to the Swine Research and Technology Centre standard operating procedures. Prior to euthanasia, a single blood sample was collected into a 10 ml heparinized Vacutainer™ (Becton Dickinson, Franklin Lakes, NJ, USA) by jugular puncture, centrifuged at 1700 x g for 15 min at room temperature and the plasma was then stored at -20°C until assayed for plasma oestradiol concentration.

Tissue collection

Within 20 min after euthanasia, the ovaries were moved to an adjacent laboratory suite in 50 ml Falcon tube containing 0.9% (w/v) warm saline when the

ovaries were intended for oocyte aspiration and follicular fluid collection, or in 0.9% (w/v) ice cold saline when the ovaries were intended for follicle dissection. The ovaries from the 28 sows intended for follicle dissection and/or oocyte aspiration were allocated as followed: for each phase of follicular development (R, MS and FS), 3 sows from each cycle group (1st or 2nd cycle) were euthanized. One ovary from each sow was chosen for follicle dissection and the other ovary was used for oocyte aspiration. In order to account for the low number of follicles present on the ovary of D4 and D20 animals and the risk of ovulation occurring, an additional 5 sows were allocated to each of these days. Both ovaries from these animals were used for oocyte aspiration. Before processing the ovaries, the number and size of all visible follicles was recorded and the follicular fluid from the largest follicle(s) (1 to 3 pooled follicles depending on the volume recovered) of D4 and D20 animals was collected using an 18-gauge needle attached to a 1 ml disposable syringe for assay of oestradiol concentration. An aliquot of follicular fluid from the D4 and D20 sows as well as the follicular fluid collected from the additional 9 sows was used for western blot analysis. The follicular fluid was centrifuged for 5 min at 13 000 x g to remove any cellular debris, diluted 11-fold in M199 and stored at -20°C for either assaying oestradiol concentrations or for western blot analysis.

Follicle dissection: A total of 18 ovaries, each originating from a different animal and representing each phase of follicular development, were sliced in half longitudinally and washed twice in ice cold PVA-TL-HEPES to remove blood contamination. The half ovaries were then placed into Petri dishes containing ice cold PVA-TL-HEPES and follicles representative of the population present on the ovary were dissected free of stromal tissue under a dissecting microscope using fine scissors and forceps. Intact dissected follicles were then placed into RNAlater (Ambion, Austin, TX, USA) to preserve RNA integrity during the remaining procedure. Depending on the size of the follicles, between 5 and 10 follicles were dissected within a 1-hour period. The intact follicles were then placed back into ice cold PVA-TL-HEPES and cut in half using a scalpel blade. One half of each follicle (hemisection) from an individual sow containing

granulosa and theca cells was transferred to a 1.5 ml microcentrifuge tube in ice cold media and centrifuged for 5 min at 200 x g at room temperature. The hemisections were washed twice with 1 ml of ice cold PBS followed by centrifugation at 200 x g for 5 min. Following the last wash, the supernatant was removed and the cells were snap frozen in liquid nitrogen. The hemisections were stored at -80°C until protein extraction. The mural granulosa cells (MGC) were then gently scraped from the inner wall of the remaining hemisection using a fine glass loop and the oocytes were removed to ensure a pure MGC population. The MGC were transferred to a 1.5 ml microcentrifuge tube in ice cold media and centrifuged for 5 min at 200 x g at room temperature. The MGC pellets were washed twice with 1ml of ice cold PBS followed by centrifugation at 200 x g for 5 min. Following the last wash, the supernatant was removed and the cells were snap frozen in liquid nitrogen. The remaining follicle shells contained mainly theca cells (TC) and were vigorously agitated by repeated pipetting to ensure that all MGC were removed. The TC were then transferred to a 1.5 ml microcentrifuge tube in ice cold media and centrifuged for 5 min at 200 x g at room temperature. The TC pellets were washed twice with 1 ml of ice cold PBS followed by centrifugation at 200 x g for 5 min. Following the last wash, the supernatant was removed and the cells were snap frozen in liquid nitrogen. The MGC and TC were finally stored at -80°C until RNA extraction.

Oocyte aspiration: Cumulus-oocyte complexes (COC) were collected from the remaining ovaries by aspiration using an 18-gauge needle attached to a 5 ml disposable syringe and the COC's from each sow were processed as a group. The COC's were transferred to a Petri dish containing 15 ml of warm PVA-TL-HEPES. The recovered COC's were washed three times in warm PVA-TL-HEPES to remove any cellular debris. The oocytes were then denuded by vortexing at low speed for 5 min in 150 µl of PBS in a 1.5 ml microcentrifuge tube. The denuded oocytes were observed under a dissecting microscope to ensure that they were free of cumulus cells and then washed twice in PBS before transfer to a fresh 1.5 ml microcentrifuge tube in a minimum volume of PBS and snap freezing on dry ice. The remaining cumulus granulosa cells (CGC) were

transferred to a 1.5 ml tube and centrifuged for 5 min at 200 x g in a table top microcentrifuge. The pellets were washed twice with PBS followed by centrifugation at 200 x g for 5 min. Following the last wash, the supernatant was discarded and the cells were snap frozen on dry ice. The oocytes and the CGC were finally stored at -80°C until RNA extraction.

Radioimmunoassay

Plasma oestradiol: Oestradiol concentrations were determined in all plasma samples in triplicate in a single RIA using the method of Yang *et al.* (2000b). Extraction efficiency was $63 \pm 4\%$ and estimated potencies were not corrected for recovery. Assay sensitivity, defined as 90 % of total binding, was 0.35 pg/ml. The intra-assay CV was 9%.

Follicular fluid oestradiol: Follicle fluid (FF) oestradiol concentrations were quantified in a single RIA using a double antibody kit (Diagnostic Products Corporation # KE2D1, Diagnostic Products Corporation, Los Angeles, CA, USA) without extraction, with the following modifications to the manufacturer's protocol. In-house oestradiol reference standards (17 β -Oestradiol, Sigma # E8875, Sigma-Aldrich) in PBS gel (0.1% (w/v) gelatin, Sigma #G2500, Sigma-Aldrich) buffer [phosphate buffered saline (PBS), containing 2.77 mM monobasic phosphate (Fisher # S369-500, Fisher Scientific, Nepean, ON, Canada), 7.22 mM dibasic phosphate (Fisher # 374B-500), 15 mM sodium azide (Fisher # S369-500) and 139 mM sodium chloride (BDH #ACS 783, BDH Inc., Toronto, Canada)], pH 7.0, were used, rather than the standards provided by the kit. Standards ranged from 0.1 to 50 pg per tube. The primary antiserum was reconstituted as directed by the manufacturer, but then further diluted 3-fold with distilled and deionised water to improve assay sensitivity. Centrifugation time was increased to 30 min to improve pelleting. The volume of sample taken to assay was 0.1 ml plus 0.1 ml PBS gel buffer. Serial dilutions with PBS gel buffer of a control FF pool diluted 11-fold in Medium 199 showed parallelism to the standard curve. Samples were assayed in triplicate in a single assay at two dilutions: FF diluted 11-fold in Medium 199 and FF further diluted 200-fold in PBS gel buffer for a final 2200-fold dilution. The intra-assay CV for the single

assay run was 10.2%. Sensitivity estimated at 95 % of total binding was 0.127 pg/tube, equivalent to 2.79 ng/ml for 11-fold diluted samples. The recovery of a known amount of oestradiol when added to a sample of known potency was 94.5 ± 2.7 %.

RNA isolation and Real-time RT-PCR

Total RNA was extracted from the pooled CGC, MGC and TC of individual animals using TRIzol reagent (Invitrogen) following the manufacturer's instructions, with the following modification. The cells were thawed on ice directly in Trizol and homogenized with a Polytron™. The homogenized samples were then incubated for 10 min at room temperature before further processing. The homogenized CGC and MGC originating from the same animals were then pooled together prior to the extraction and will be further referred to as granulosa cells (GC). The GC and TC total RNA was precipitated with 1/10 volume of 5M ammonium acetate, 1 volume of isopropanol and linear acrylamide (Ambion) was also added to the RNA as a carrier at a final concentration of 10 µg/ml. The total RNA was resuspended in nuclease free H₂O (Ambion) and was DNase treated using DNA-free™ (Ambion) following the manufacturer's instructions. The samples were quantified using the spectrophotometer ND-1000 (NanoDrop, Wilmington, DE, USA) and RNA integrity was evaluated on a 1 % (w/v) denaturing agarose gel. All samples were stored at -80°C until cDNA synthesis. Oocyte total RNA was extracted from pools of between 15 (for D4 and D20 animal) and 150 (for D1 and D14 animals) oocytes recovered from individual sows using the PicoPure RNA isolation kit (Arcturus, Mountain View, CA, USA) following manufacturer's instructions. All samples were DNase treated as suggested in the protocol and the RNA was eluted in 30 µl. Oocyte total RNA was stored at -80°C until use. Due to the large difference in the number of oocytes recovered between animals, the efficiency of RNA extraction and cDNA synthesis was tested and was found to be consistent when ≥ 15 oocytes were used (data not shown).

Oocyte, GC and TC total RNA was reverse transcribed with Superscript III reverse transcriptase (Invitrogen) according to manufacturer's instruction,

using a combination of 5 μ M oligo dT and 5 ng/ μ l of random hexamer. RNaseOUT (Invitrogen) was also added to the reaction at a concentration of 2 U/ μ l. cDNA synthesis was performed using 2 μ g of GC and TC total RNA and with 10 μ l of the oocyte total RNA. After reverse transcription, GC and TC cDNA were diluted to 20 ng/ μ l and the oocyte cDNA to an equivalent of 0.25 oocytes/2 μ l with nuclease-free H₂O (Ambion).

Real-Time PCR was performed in duplicate using 20 ng of GC or TC cDNA, or the cDNA equivalent to 0.25 oocytes, in 96-well fast plates using the Taqman® Fast Universal PCR Master Mix and the ABI 7900HT thermocycler (Applied Biosystems, Foster City, CA, USA). The primers and Taqman-MGB probes (Table 4.1) were designed using the Primer Express® software v3.0 (Applied Biosystems) using species specific sequences found on GENBANK. The amplification efficiency for each gene was determined using serial dilution of ovarian cDNA and was found to be $\geq 90\%$ for all genes (data not shown). Moreover, the amplification efficiency slopes for all 9 genes were found to be identical. As reported by Bettegowda *et al.* (2006), cyclophilin was used as the endogenous control to correct for RNA extraction and reverse transcription efficiency within cell type. Cyclophilin transcript abundance was found to be stable within each cell type throughout the different stages of follicle development, confirming its usefulness as a good endogenous control. However, cyclophilin abundance differed between the cell types studied and limited our ability to statistically compare the abundance of each gene of interest across cell types.

Western blot analysis

BMP15: Aliquots of follicular fluid (200 μ l) diluted 11-fold in M199 were precipitated using 3 volumes of ice cold acetone. The protein pellets were resuspended in 150 μ l of cell extraction buffer (Invitrogen) supplemented with 1mM PMSF (Sigma-Aldrich) and 5% (v/v) of protease inhibitor cocktail (Sigma-Aldrich) as recommended by the manufacturer. Protein concentration was determined by bicinchoninic acid (BCA) assay (Pierce, Rockford, IL, USA) according to the manufacturer's instructions and 7.5 μ g of follicular fluid protein

from each sample was resolved onto 12% SDS-PAGE gels. A control sample was also loaded on each gel to correct for interblot variability. The proteins were transferred at 4°C overnight at 150mA onto nitrocellulose membranes. The membranes were stained with Ponceau S to evaluate total protein loading and the image was acquired with an ImageScanner (GE Healthcare, Piscataway, NJ, USA). The membranes were blocked at room temperature for 1h in Tris-buffered saline containing 0.1% (v/v) Tween-20 (TBS-T) and 5% (w/v) nonfat dry milk. The membranes were then incubated for 1h with the primary anti-BMP15 antibody (sc-28911, Santa Cruz Biotechnology, Inc, Santa Cruz, CA, USA) using a 1:400 dilution in the blocking solution. Following the primary antibody, the membranes were washed three times for 5 min with the blocking solution and hybridized with the secondary antibody (HRP-conjugated donkey anti-rabbit, cat # 711-035-152, Jackson ImmunoResearch Laboratory, West Grove, PA, USA) diluted 1:10,000 in the blocking solution. The membrane was finally washed once for 15 min, followed by three 5-min washes in TBS-T.

BMPR1B: Hemisections from each animal were ground in liquid nitrogen and the proteins extracted on ice for 2h in cell extraction buffer supplemented with 1mM PMSF (Sigma-Aldrich) and 5% (v/v) of protease inhibitor cocktail (Sigma-Aldrich). The samples were then centrifuged at 18 000 x g for 10 min at 4°C to remove any insoluble material and protein concentration was determined by BCA assay (Pierce) according to the manufacturer's instructions. Immunoblotting was performed exactly as described for BMP15 with the following modifications. A total of 10 µg of protein from each sample was resolved onto 12% SDS-PAGE gels. The blocking solution used was TBS-T supplemented with 3% (w/v) nonfat dry milk and 5% (v/v) Donkey serum. The primary anti-BMPR1B antibody (sc-25455, Santa Cruz Biotechnology, Inc, Santa Cruz, CA, USA) was diluted 1:200 in the blocking solution and the secondary antibody (HRP-conjugated donkey anti-rabbit, cat # 711-035-152, Jackson ImmunoResearch Laboratory, West Grove, PA, USA) was diluted 1:20,000 in the blocking solution.

To ensure antibody specificity, preimmune rabbit IgG (Jackson ImmunoResearch, cat# 011-000-003) at a concentration identical to each primary antibody and the

secondary antibody alone were tested on follicular fluid and hemisection protein samples. Immunoreactive proteins were detected with ECL plus (GE Healthcare) and the images were acquired on a Typhoon Trio (GE Healthcare). Finally, the abundance of each immunoreactive protein, as well as a predetermined band stained with Ponceau S, was determined by densitometric analysis using the ImageQuant software (GE Healthcare).

Statistical analysis

The sow's reproductive data including weight, number of follicles per ovary, average size of the 3 largest follicles, plasma oestrogen and follicular fluid oestradiol concentrations were analysed using the MIXED procedure of SAS (SAS Institute Inc., Cary, NC). With the exception of the weight data that were normally distributed, all reproductive data were RANK transformed and the analysis was performed on the transformed data. The model for the experiment included phases of follicular development and cycle (1st and 2nd preovulatory wave after weaning) as the independent variables and sow as the random variable. Differences between means were analyzed using a Least Significant Difference (LSD) test at a 95% confidence level.

Real-time PCR data for the genes of interest (GOI) were normalized against their respective means for cyclophilin using the Δ Ct method (Δ Ct = Ct_{GOI} - Ct_{cyclophilin}). The cycle threshold (Ct) is defined as the PCR cycle where the fluorescence reaches a determined threshold. Consequently, the Ct and corrected Ct (Δ Ct) value are inversely related to the copy number of the targeted gene initially present in the sample. For the analysis of mRNA abundance between each GOI within day and within cell type, the Δ Ct values in the oocyte and granulosa cells were RANK transformed and the analysis was performed on the transformed data. The Δ Ct for each GOI were analysed using the MIXED procedure of SAS and the model for the experiment included GOI as the independent variables. Differences between means were analyzed using a Least Significant Difference (LSD) test at a 95% confidence level. For the analysis of the temporal changes in mRNA abundance, the Δ Ct values for all GOI were normally distributed except for BMPR1B in the granulosa cell which was RANK

transformed and the analysis was performed on the transformed data. The individual ΔCt for each GOI were analysed using the MIXED procedure of SAS. The model for the experiment included phases and cycle as the independent variables, and sow as the random variable. Since neither an effect of cycle nor an interaction between phase and cycle was found, the data were further analysed irrespective of cycle. Differences between means were analyzed using a Least Significant Difference (LSD) test at a 95% confidence level. For ease of interpretation of the expression profiles the data were converted using the formula $2^{-(\Delta\text{Ct} - \Delta\text{Ct}_{\text{calibrator}})}$ and are expressed as relative mRNA abundance \pm SEM. The ΔCt value obtained for BMP15 in the granulosa cell during the final selection phase post-LH surge was used as the calibrator value, thus maintaining the relative mRNA abundance for the GOI within and, to a limited extent, between cell type. Finally, correlations analyses were performed across all sows to determine relationships between the expression of each GOI and follicular fluid and plasma oestrogen concentration and follicle size.

Western blot data were corrected for loading differences using the abundance of a predetermined band from the total protein stain and then corrected for inter-blot variation using the abundance of each specific immunoreactive band from the loading control. The corrected data were analysed using the MIXED procedure of SAS (SAS Institute Inc., Cary, NC). The data for BMP15 band 2 were normally distributed, however, the data for BMP15 band 1 and 3 were log transformed and the data for BMP1B were RANK transformed and analyses were then performed using the transformed data. The model for BMP15 included only phase, while the model for BMP1B included phase, cycle and their interaction, as independent variables. Differences between means were analyzed using a Least Significant Difference (LSD) test at a 95% confidence level. Data are expressed as lsmeans of relative protein abundance \pm SEM.

RESULTS

Sow and follicle characteristics

The reproductive characteristics of the sows euthanized during the 1st and 2nd post-weaning preovulatory wave of follicular development were very similar. The average number of follicles observed per ovary, the range of follicle size observed and the concentration of follicular fluid oestradiol were not different between cycles (Table 4.2). As expected the sows euthanized during the 2nd post-weaning preovulatory wave of follicular development were heavier ($P \leq 0.01$). Although, overall, the average diameter of the 3 largest follicles was 0.5 mm larger ($P \leq 0.05$) in the 2nd preovulatory wave of follicle development, these sows had lower overall concentration of plasma oestrogen ($P \leq 0.05$). There were no interactions between cycle and stage of follicular development for any of the parameters studied; therefore, the data from both cycles were grouped to analyse the effect of stage of follicular development (Table 4.3). The number of follicles per ovary was lower during the final selection phase pre- and post-LH surge compared with the recruitment and mid-selection phase ($P \leq 0.001$). The average size of the 3 largest follicles showed a concomitant increase between the recruitment and the mid selection phase ($P \leq 0.05$) and was higher during the final selection phase pre- and post-LH surge when compared with the previous two phases ($P \leq 0.001$). Plasma oestrogen concentrations were low during the recruitment and mid-selection phases, increased during the final selection phase pre-LH surge and then declined in the post-LH surge period ($P \leq 0.001$). Finally, follicular fluid oestradiol concentrations were maximal in the pre-LH surge period and the subsequent decline in follicular fluid oestradiol ($P \leq 0.001$) was used to identify sows exposed to the preovulatory LH surge.

Gene localization and expression

With the exception of *BMP-6* which could not be detected in the granulosa cells with the current primer-probe set, the mRNA for the ligands *BMP2*, *BMP6*, *BMP15* and *GDF9* was present in every cell type throughout the different stages of follicular development (Table 4.4, Figure 4.1). Similarly, the transcripts for the receptors *BMPRIA*, *BMPR1B*, *BMPR2* and *TGFBR1* were also detected in all

three cell types and in every follicle class (Table 4.4, Figure 4.1). The oocyte was found to exhibit the highest transcript abundance for all ligands and the relative mRNA abundance for *BMP15* and *GDF9*, respectively, were 50-fold and 9-fold higher than *BMP6*, the next most abundant gene observed in the oocyte, and at least 110-fold and 18-fold higher than any other gene across all cell types (Figure 4.1). Although a statistical analysis across cell type was not possible because of the difference in endogenous control mRNA abundance, some of the differences observed in mRNA abundance between cell type (per example *BMP15* and *GDF9*) were so large that they could not be solely explained by the differences in cyclophilin mRNA abundance. In addition, the relative mRNA abundance of the various receptors also appears higher in the oocyte than in the granulosa and theca cells (Figure 4.1). Interestingly, the mRNA abundance for the receptors in granulosa and theca cells was, in most cases, higher than the ligands (Figure 4.1). Finally, no differences in mRNA localization or abundance were observed in the oocyte, GC or TC studied during the 1st vs 2nd preovulatory wave of follicle growth after weaning (Figure 4.2).

Oocyte mRNA expression profiles

Despite their abundance, little or no changes were observed in the mRNA abundance of the four ligands throughout the follicular phase (Figure 4.3A). *BMP15* was the only ligand whose transcript abundance was affected by the stage of follicular development ($P \leq 0.05$), with a 1.6-fold decrease in abundance between the recruitment phase and the final selection phase post-LH surge (Figure 4.3A). Interestingly, both *BMP15* and *GDF9* mRNA abundance were negatively correlated with the average size of the largest follicles ($r = -0.49$, $P \leq 0.01$ and $r = -0.38$, $P \leq 0.05$, respectively).

The expression of mRNA for the receptors *BMPRIA* and *BMPR1B* in the oocyte also remained constant across the different phases of follicle development (Figure 4.3B). In contrast, mRNA abundance for *BMPR2* and *TGFBR1* was affected by the stage of follicular development ($P \leq 0.05$) (Figure 4.3B). *BMPR2* mRNA increased by approximately 1.3-fold between the recruitment phase and the mid-selection phase and remained high thereafter. Oocyte-derived *TGFBR1*

showed a temporal mRNA expression profile dissimilar to that observed for any other gene, with relatively constant mRNA abundance during the recruitment and mid-selection phases, followed by a 1.6-fold fall in expression during both the final selection phase pre- and post-LH surge (Figure 4.3B). *TGFB β 1* mRNA abundance was negatively correlated with the average size of the largest follicles ($r = -0.48$, $P \leq 0.05$)

Granulosa cell mRNA expression profiles

In comparison to the oocyte, *BMP2*, *BMP15* and *GDF9* transcripts appeared to be much less abundant in the granulosa cells. Amongst the ligands, *GDF9* was the most abundant transcript in the granulosa cells with an average relative mRNA abundance 30-fold higher than *BMP15* which had the lowest abundance in this cell type (Figure 4.4A). Moreover, *BMP2* and *GDF9* mRNA abundance was affected by the stage of follicular development ($P \leq 0.05$ and $P \leq 0.01$, respectively) and both genes showed a similar temporal mRNA expression profile (Figure 4.4A). In the case of *BMP2*, a 3.3-fold increase in mRNA abundance was observed between the recruitment and mid-selection phases; mRNA abundance remained unchanged during the final selection phase but showed a tendency to decrease following the LH surge ($P = 0.08$) (Figure 4.4A). Interestingly, *BMP2* mRNA abundance also tended to be positively correlated with plasma oestrogen ($r = 0.4235$, $P = 0.08$). *GDF9* mRNA also increased 2.1-fold during the mid-selection phase, remained constant during the final selection phase and decreased 1.7-fold following exposure to the LH surge (Figure 4.4A). The abundance of *GDF9* mRNA in the granulosa cells obtained from large preovulatory follicles was strongly and positively correlated with follicular fluid oestradiol concentration ($r = 0.87$, $P \leq 0.05$).

The relative mRNA abundance for all receptors was found to be higher than those of the ligands. *BMP2* mRNA remained relatively constant in each follicle category; however, *BMP1A*, *BMP1B* and *TGFB1* mRNA were temporally regulated during follicular development ($P \leq 0.05$, $P \leq 0.01$ and $P \leq 0.01$, respectively) (Figure 4.4B). *BMP1A* mRNA abundance increased by 1.7-fold during the mid-selection phase, decreased to an intermediate level in the

preovulatory follicle population and was not affected by exposure to the LH surge (Figure 4.4B). *TGFBR1* expression showed a 2-fold increase during the mid-selection phase and remained high in the preovulatory follicles, even after exposure to the LH surge (Figure 4.4B). *TGFBR1* mRNA abundance was positively correlated with follicle size ($r = 0.54$, $P \leq 0.05$) and in the granulosa cells of the preovulatory population was strongly and negatively correlated with follicular fluid oestrogen ($r = -0.84$, $P \leq 0.05$). Finally, *BMPR1B* expression increased gradually over the first three phases of follicular development to peak during the final selection phase prior to the LH surge (Figure 4.4B). At that point, *BMPR1B* mRNA abundance was 7-fold higher than during the recruitment phase and 4-fold higher than during the mid-selection phase. Following exposure to the LH surge, *BMPR1B* expression fell to an intermediate level. *BMPR1B* mRNA abundance tended to be positively correlated with plasma oestrogen concentration ($r = 0.44$, $P = 0.07$) and was strongly and positively correlated with follicle size ($r = 0.73$, $P \leq 0.0001$).

Theca cell mRNA expression profiles

The mRNA for all four ligands was expressed in the theca cells and mRNA abundance was comparable to that found in the granulosa cells. Moreover, as with the granulosa cells, *GDF-9* was found to be the most abundant ligand mRNA in the theca cells, while *BMP-15* had the lowest expression (Figure 4.5A). Moreover, *BMP2*, *BMP6* and *GDF9* mRNA abundance in the theca cells were affected by the stage of follicular development ($P \leq 0.01$, $P \leq 0.01$ and $P \leq 0.05$, respectively). *BMP6* mRNA abundance increased 2.7-fold between the recruitment phase and the mid-selection phase, and remained high thereafter (Figure 4.5A). *BMP2* mRNA was also upregulated 2-fold during the mid-selection phase and then downregulated 2.1-fold post-LH surge (Figure 4.5A). *BMP2* mRNA abundance was positively correlated with plasma oestrogen concentration ($r = 0.56$, $P \leq 0.05$) and in the theca cells from the large preovulatory follicles a strong positive correlation was also observed with follicular fluid oestrogen concentration ($r = 0.94$, $P \leq 0.01$). Finally, *GDF9* mRNA abundance increased 2.3-fold from the recruitment phase to the mid-

selection phase and returned to an intermediate level in the theca cells of the preovulatory follicle population (Figure 4.5A).

Theca cell receptor *BMPR1B*, *BMPR2* and *TGFBR1* mRNA expression was also affected by the stage of follicular development ($P \leq 0.05$, $P \leq 0.05$ and $P \leq 0.01$, respectively) (Figure 4.5B). The temporal patterns of *BMPR1B* and *TGFBR1* expression paralleled those observed in the granulosa cells. *BMPR1B* mRNA abundance increased 3.6-fold during the final selection phase prior to the LH surge relative to the mRNA abundance observed during the mid-selection phase (Figure 4.5B). *BMPR1B* mRNA in the theca cells was also positively correlated with plasma oestrogen concentration ($r = 0.51$, $P \leq 0.05$) and with follicle size ($r = 0.71$, $P \leq 0.001$). *TGFBR1* mRNA expression showed a 1.7-fold increase in abundance during the mid-selection phase (Figure 4.5B) and also tended to be positively correlated with follicle size ($r = 0.45$, $P=0.063$). Finally, *BMPR2* mRNA expression increased 2.3-fold between the recruitment phase and the mid-selection phase (Figure 4.5B).

Western blot analysis

Western blot analysis of follicular fluid BMP15 revealed three immunoreactive bands located at ~65 kDa, ~55 kDa and ~25 kDa (Figure 4.6A). The three bands appeared to be specific, as the secondary antibody alone and the preimmune rabbit IgG did not produce any cross-reactivity (data not shown). Furthermore, the same bands were also detected using a different specific antibody directed against BMP15 (data not shown). These bands likely correspond to the uncleaved promature protein (~65 kDa), the cleaved proregion (~55 kDa) and the mature protein (~25 kDa) which correspond to the different forms of BMP15 recently reported in the mouse (McIntosh *et al.*, 2008). Densitometric analysis of each immunoreactive band showed that BMP15 protein abundance did not change between the different phases of follicular development studied (Figure 4.6A). In addition, western blot analysis for BMPR1B in follicle hemisections revealed one immunoreactive band located at ~45 kDa (Figure 4.6B). This band also appeared to be specific for BMPR1B, as the secondary antibody alone and the preimmune rabbit IgG did not produce any cross-reactivity

(data not shown). Densitometric analysis of BMPR1B confirmed that protein abundance peaked during the periovulatory period prior to the LH surge confirming the mRNA expression profile observed in both granulosa and theca cells (Figure 4.6B).

DISCUSSION

As members of the TGF- β superfamily, the BMPs and GDF9, and their receptors, have been shown to play important roles during mammalian folliculogenesis (Shimasaki *et al.*, 2004, Juengel & McNatty 2005, Gilchrist *et al.*, 2008). However, little information is available on the role of these genes during the preovulatory wave of follicular development. In order to better understand the physiological role of these genes in the developing porcine ovarian follicle and to assess their role in determining the differences in follicle quality observed between 1st and 2nd post-weaning preovulatory wave of follicle development, the expression pattern of four relevant ligands with their known receptors was determined by real-time PCR. In light of the real-time PCR results, the protein abundance for BMP15 in follicular fluid and its receptor, BMPR1B, in follicle hemisections were evaluated to confirm their potential role during the periovulatory period.

Few differences were observed between the 1st and 2nd post-weaning preovulatory wave of follicle development. However, consistent with the results of a previous experiment, follicle size was bigger during the 2nd wave of follicular development (Foxcroft *et al.*, 2007). Interestingly, no cycle by stages interactions were observed, suggesting that the members of the TGF- β superfamily investigated in the present study are unlikely to be involved in the differences in follicle maturity leading to the differences in embryo survival and litter size observed in this and/or in earlier studies in the weaned sows (Clowes *et al.*, 1994, Foxcroft *et al.*, 2007).

Notwithstanding this lack of differences between follicular “cycles”, our results showed that, with one exception, *BMP2*, *BMP6*, *BMP15* and *GDF9* mRNA were expressed in all three cell types throughout the follicular phase. The exception was *BMP6* mRNA expression which could not be detected in the granulosa cells using the current primer probe set. As anticipated, the oocyte was found to be the main site of transcription for all four ligands, with *BMP15* and *GDF9* being the most abundantly expressed genes in the oocyte. These results are for the most part consistent with previous studies done in the pig. Firstly, *GDF9* mRNA and protein were shown to be highly expressed in the oocyte of 3 to 5 mm follicles from immature gilts, but were also detected at lower abundance in the cumulus and mural granulosa cells (Prochazka *et al.*, 2004, Zhu *et al.*, 2008, Lee *et al.*, 2008). To our knowledge, no other studies in the pig have reported *GDF9* mRNA expression in the theca cells. However, in goat ovaries the *GDF9* protein was occasionally detected in the theca cells of follicles larger than 3mm (Silva *et al.*, 2005). This contrasts with the cow where *GDF9* mRNA could not be detected in the theca cells from small or large follicles (Spicer *et al.*, 2008). Brankin *et al.* (2005) reported a strong signal for *BMP2* and *BMP6* proteins in the oocyte of healthy 2 to 6 mm follicles from mature gilts, and *BMP2* was also detected in the granulosa and theca cells from the same follicles. Interestingly, these authors also reported *BMP6* expression in granulosa but not in theca cells. This discrepancy could be explained in part by the maturity of the animals used (gilts vs sows in our study) and/or the sensitivity and specificity of the detection technique (western blot vs real-time PCR in the present study). It is also probable that the differences in isolation techniques between the two studies might yield different theca cell populations (theca interna vs theca interna and externa in our experiment). Finally, Zhu and colleagues (2008) also detected *BMP6* mRNA in oocytes and cumulus cells from prepubertal gilts, whereas *BMP15* mRNA could be detected only in the oocyte and *BMP2* failed to produce a PCR amplicon in both the oocyte and its surrounding cumulus cells. Interestingly, despite the widespread interest in *BMP15* in other species, no other studies have investigated the localization of *BMP15* mRNA or the *BMP15* protein in porcine follicles. Our

results are consistent with the observations made in goat follicles in which *BMP15* mRNA and protein were found to be expressed in oocytes and granulosa cells of all antral follicles while *BMP15* mRNA was also detected in theca cells (Silva *et al.*, 2005). This is in contrast to mouse, rat, human and sheep follicles in which *BMP15* mRNA and/or BMP15 protein were localized exclusively to the oocyte (Dube *et al.*, 1998, Laitinen *et al.*, 1998, Aaltonen *et al.*, 1999, Galloway *et al.*, 2000, Juengel *et al.*, 2002, Erickson & Shimasaki 2003). Generally, our results confirm observations made in mouse, rat, human, sheep and goat follicles (Dube *et al.*, 1998, Laitinen *et al.*, 1998, Aaltonen *et al.*, 1999, Galloway *et al.*, 2000, Juengel *et al.*, 2002, Erickson & Shimasaki 2003, Glister *et al.*, 2004, Fatehi *et al.*, 2005, Silva *et al.*, 2005, Juengel *et al.*, 2006) and support the general conclusion that the oocyte is the primary source of BMP6, BMP15 and GDF9.

Interestingly, little change in ligand mRNA abundance were observed in the oocyte throughout the last week of follicular development. In contrast, although ligand expression in granulosa and theca cells was much lower than in the oocyte, in many cases their mRNA abundance was affected by the phase of follicular development. This is particularly intriguing, because BMP6, BMP15 and GDF9 are generally considered to be oocyte-derived ligands and BMP15 and GDF9 are exclusively expressed in the oocyte of most species (Juengel & McNatty 2005, Gilchrist *et al.*, 2008). One could suggest that the expression of these ligands in granulosa cells in the present experiment is due to a cross-contamination from oocytes. Although, it is not possible to firmly rule out a potential cross-contamination, the abundance of *BMP15* and *GDF9* mRNA observed in the oocyte and granulosa cells suggests otherwise. In the oocyte, *BMP15* mRNA was found to be approximately 6 times more abundant than *GDF9* mRNA, whilst the converse was true for expression in the granulosa cells. The same argument against a cross-contamination of the theca cells by the granulosa cells is supported by the relative abundance of *BMPRIA* and *BMPRIB* mRNA. On the other hand, the relatively low abundance and the changing expression of these ligands in the granulosa and theca cell could reflect phase-specific interactions between the granulosa and/or the theca cells populations necessary to

regulate their response to the follicle microenvironment. This has been suggested in rat in which the granulosa cell-derived *BMP6* mRNA is lost during the selection of the dominant follicle (Erickson & Shimasaki 2003). Knowing that BMP6 can prevent FSH action (Otsuka *et al.*, 2001a), the authors suggested that this loss of *BMP6* mRNA in granulosa cells may be necessary for FSH to affect the development of dominant follicles. Similar mechanisms have been shown for other members of the TGF- β superfamily such as BMP4 and BMP7, which can potentially suppress androgen production by bovine theca cells (Glister *et al.*, 2005). The major difference in this case is that BMP4 and BMP7 are theca cell-derived ligands. Although this hypothesis is attractive, the potential roles for the granulosa and theca cell-derived BMP2, BMP6, BMP15 and GDF9 have yet to be confirmed in any species, including the pig.

Our results also showed that the mRNA for the receptors of the TGF- β superfamily were detected in all three cell types and at every time point studied. Our findings confirmed observations made in the pig, sheep, goat and cow in which *BMPRIA*, *BMPRIB* and *BMPR2* mRNA and/or protein were expressed in the oocyte and in both granulosa and theca cells of antral follicles (Wilson *et al.*, 2001, Souza *et al.*, 2002, Glister *et al.*, 2004, Quinn *et al.*, 2004, Fatehi *et al.*, 2005, Silva *et al.*, 2005, Feary *et al.*, 2007). The only exception appears to be the rat follicle in which *BMPR2* mRNA could not be detected in the theca cells (Erickson & Shimasaki 2003). The expression of *TGFBRI* mRNA has only been studied in antral follicles of mouse, sheep and cow ovaries, and consistent with our findings, was expressed in the oocyte, granulosa and theca cells (Juneja *et al.*, 1996, Juengel *et al.*, 2004, Feary *et al.*, 2007, Jayawardana *et al.*, 2006). Similar to the observations made for the ligands in our study, the oocyte was found to abundantly express *BMPRIA*, *BMPRIB*, *BMPR2* and *TGFBRI* mRNA but little variation in mRNA abundance was observed between the different time points. On the other hand, the granulosa and theca cells were found to express the mRNA for each receptor at slightly lower levels than the oocyte. However, in both the granulosa cell and theca cell, three out of the four receptors showed at least a 1.7-fold change in mRNA abundance between time points.

The first general observation emerging from the current study is that pig oocytes produce high but relatively constant amounts of the TGF- β superfamily ligand mRNA during the follicular phase, while mRNA expression for the receptors was temporally regulated in the surrounding somatic cells. Based on the current concept that the oocyte regulates its own microenvironment by secreting soluble factors, it is tempting to hypothesize that the regulation of the type I and II receptor mRNA expression in the granulosa and theca cells plays a stage-dependent role in the interaction between the oocyte and its surrounding cells (Gilchrist and al., 2008). Consistent with our hypothesis, several other studies have shown that the receptors associated with the TGF- β superfamily are hormonally regulated. In bovine granulosa cells, oestrogen used alone and in combination with FSH has been shown to upregulate the expression of the activin receptor type I (*ALK2*), activin receptor type IIA (*ACVR2A*), *TGFBR1* (*ALK5*) and *BMPR2* mRNA (Shimizu *et al.*, 2006, Jayawardana *et al.*, 2006). Furthermore, FSH alone was shown to downregulate *TGFBR1* and *BMPR2* mRNA (Jayawardana *et al.*, 2006) and in a study using human granulosa-like tumour cell line (KGN) FSH upregulated *BMPR1A*, *BMPR1B*, *BMPR2* and *ACVR2A* (Miyoshi *et al.*, 2006). These results provide a basis for the temporal regulation of the receptor mRNA in porcine granulosa and theca cells and would explain the observed correlation between plasma oestrogen and *BMPR1B* mRNA abundance.

Each ligand of the TGF- β superfamily is known to signal through specific receptor complexes composed of a type I and type II serine-threonine kinase receptors. In the context of our study, *BMPR2* has been identified as one of the potential type II receptors involved in BMP2, BMP6, BMP15 and GDF9 signalling (Shimasaki *et al.*, 2004, Juengel & McNatty 2005). In addition, *BMPR1A* has been identified as a potential type I receptor for BMP2 and BMP6, *BMPR1B* has been found to be involved in BMP6 and BMP15 signalling and *TGFBR1* was identified as the receptor for GDF9 (Shimasaki *et al.*, 2004, Juengel & McNatty 2005). Given this information, the temporal changes in expression of each receptor in the ovarian follicle could be indicative of a functional role for its ligand(s) at a precise stage of follicular development.

In the context of recent literature, results from the present study on the expression pattern of *TGFBR1* mRNA in the granulosa and theca cell are consistent with a role for GDF9 in follicle selection. Spicer *et al.* (2008) reported that bovine theca cells isolated from small follicles were more responsive to GDF9 than their counterparts isolated from larger follicles, and that GDF9 stimulated proliferation, while inhibiting progesterone and androstenedione production, by the theca cells of small antral follicles. Similarly, building on the observations of Vitt *et al.* (2000) in the rat suggesting that GDF9 controls proliferation of granulosa cells, Shimizu *et al.* (2008) reported that intra-ovarian injection of GDF9 promoted the development of medium sized antral follicles. Collectively, these observations in other species suggest that GDF9 modulates aspects of granulosa and theca cell function important for follicle selection.

Finally, particularly in the context of the pig follicular development, the most interesting findings among our data are the pattern of *BMPR1B* mRNA and protein expression in granulosa and theca cells, along with that of *BMP15* mRNA in the oocyte and its protein in the follicular fluid. Firstly, in the oocyte, *BMP15* mRNA marginally decreased during the periovulatory period but no change in BMP15 protein abundance was observed in the follicular fluid. However, the upregulation of *BMPR1B* mRNA in the granulosa cells and theca cells during the same period, accompanied by a similar increase in BMPR1B protein in follicle hemisections, suggests that the oocyte-derived BMP15 may play a key role in the periovulatory period in the pig follicle. This is in accordance with the phenotype observed in the *Bmp15* null mice where no apparent defects in follicular development were observed; but ovulation rate was lower and the ovulated oocytes showed reduced developmental potential (Yan *et al.*, 2001, Su *et al.*, 2004). Interestingly, the *Bmpr1B* null mice exhibited defects in cumulus expansion which, in turn, prevented *in vivo* fertilization (Yi *et al.*, 2001). Moreover, recent results obtained in two different mouse studies showed that BMP15 is likely involved in cumulus expansion (Yoshino *et al.*, 2006, Gueripel *et al.*, 2006). Although, the precise timing was different, both studies showed that the mature form of BMP15 protein appeared in the periovulatory period following

gonadotrophin stimulation. This is in contrast to our study, in which levels of the mature form of BMP15 remained constant between the different phases of follicular development. However, as the current preovulatory follicle population was exposed to both LH and FSH, we hypothesized that the receptor rather than the ligand is subjected to regulation in the pig. The correlation observed between plasma oestrogen and BMPR1B mRNA abundance is another good indicator that this signalling pathway might be under the influence of FSH and/or LH.

In conclusion, the findings of the present study clearly demonstrate the presence of a complex signalling system within the porcine follicle involving members of the TGF- β superfamily and their associated receptors. To our knowledge, this is the first study to investigate the spatial and temporal regulation of those ligands and receptors during the final week of follicular development preceding ovulation in the pig. Our results clearly showed that what are generally considered to be oocyte-derived ligands, are also expressed in the granulosa and theca cells of pig follicles, potentially reflecting species-specific somatic cell interactions. Finally, although, additional studies will be required to further assess the exact role of these genes in the porcine follicle, this study provides strong evidence to support a role for BMP15 during ovulation.

Table 4.1 Details of primers and probes used for Real-Time PCR

Gene	AC number	Primer	Sequence 5' --> 3'	Product size	Annealing/Extension temperature (°C)
PPIA	AY266299	Forward	AATGCTGGCCCCAACACA	56 bp	60
		Reverse	TCAGTCTTGGCAGTGCAAATG		
		Probe	ACGGTTCCCAGTTTT		
BMP-2	AY669080	Forward	CCCCACGGAGGAGTTTATCA	59 bp	60
		Reverse	CCTGTGTCTGTTCCCCGAAAGA		
		Probe	CTCAGCAGAACTTC		
BMP-6	EU693015	Forward	CCAAACTTTTCTTATCAGCATTATCA	75 bp	62
		Reverse	TCCAACAGAAACAGGTCAGAGTCT		
		Probe	CTTACAGCAGCGTCAACA		
BMP-15	NM001005155	Forward	TTCCCAGAGGCCTGGAAGA	58 bp	60
		Reverse	GCCTTCCGCAAAGAAGAGA		
		Probe	TTTATGGCAAGAGACCC		
GDF-9	AY649763	Forward	ATGTGACGGCCATCCTTCAG	63 bp	60
		Reverse	CGATGGACATGTGAATCTCTCTCT		
		Probe	CCCTAGTGGTCTCCAAC		
BMPR1A	EU693016	Forward	GTGGATCTGGACTACCCTTGTTG	65 bp	60
		Reverse	TTGCCGAACCATCTGTATCTGT		
		Probe	TTCAGCGAACTATTGCCA		
BMPR1B	AY065994	Forward	TGGTTCCGAGAGACAGAAATATATCA	68 bp	60
		Reverse	GCAATGAAGCCCAAATGTTTT		
		Probe	ACAGTGTTGATGAGGCAT		
BMPR2	EU693017	Forward	GGGTCGGGTGAAAAGATCAA	60 bp	60
		Reverse	GCGCCACCGCTTAAGAGA		
		Probe	AAACGTGTGAAAACCTCCCTA		
TGFBR1	DQ519378	Forward	GTCTGCATCTCACTCATGTTGATG	67 bp	60
		Reverse	GCACTCGATGGTGAATGACTGT		
		Probe	TCTATATCTGCCATAACCG		

Table 4.2 Overall characteristics of the sows and follicles for each cycle irrespective of the phase of follicular development.

Cycle	Sow Weight (kg) ^{†*}	No. of follicles per ovary ^{†*}	Range of follicle size (mm) [†]	Average size of the 3 largest follicles (mm) ^{†*}	Plasma E2 concentration (pg/ml) ^{†*}	Follicular fluid E2 concentration (ng/ml)*	
						FS [‡]	FS post-LH [‡]
1 st	174 ± 5 ^a	26 ± 4	1-10	6.9 ± 0.3 ^a	13.0 ± 3.1 ^b	265 ± 57	15 ± 8
2 nd	189 ± 4 ^b	29 ± 5	1-10	7.4 ± 0.3 ^b	10.6 ± 4.3 ^a	466 ± 99	10 ± 2

[†] Represent the means for each cycle across all phases of follicular development (1st cycle n=14; 2nd cycle n=14)

[‡] Follicular fluid concentration measured during the final selection phase (FS) (1st cycle n=3; 2nd cycle n=5) and the final selection phase post-LH surge (FS post-LH) (1st cycle n=5; 2nd cycle n=3).

*Data are expressed as lsmean ± SEM. Different letters within column indicate significant difference (P ≤ 0.05).

Table 4.3 Characteristics of the sows and follicles from each stage of follicle development, irrespective of the cycle.

Stage of follicle development	No. of follicles per ovary ^{†*}	Range of follicle size (mm) ^{‡*}	Average size of the 3 largest follicles (mm)*	Plasma E2 concentration (pg/ml)*	Follicular fluid E2 concentration (ng/ml)*
Recruitment (n=6)	43 ± 4 ^b	1-6	5.0 ± 0.2 ^a	5.2 ± 1.1 ^b	NA
Mid-selection (n=6)	40 ± 2 ^b	1-7	5.9 ± 0.2 ^a	5.9 ± 1.6 ^b	NA
Final selection (n=8)	15 ± 1 ^a	3-10	8.8 ± 0.3 ^b	33.1 ± 2.4 ^c	365.5 ± 72.0 ^b
Final selection + LH (n=8)	11 ± 1 ^a	2-10	8.9 ± 0.2 ^b	3.2 ± 0.9 ^a	12.2 ± 4.8 ^a

[†] The number of follicles reported for the recruitment and mid-selection phase represents the total number of visible follicles, while the numbers reported for the final selection pre- and post-LH represent the number of healthy preovulatory follicles.

[‡] The range in follicle size reported represents the range of all visible follicles.

* Data are expressed as $\text{mean} \pm \text{SEM}$. Different letters within column indicate significant differences ($P \leq 0.05$).

NA = Not applicable

Table 4.4 Summary of the statistical analysis of oocyte, granulosa cell and theca cell mRNA abundance (ΔCt) at specific stages of follicular development.

Gene	Cell type	Stages of follicular development				P-value
		Recruitment	Mid-selection	Final selection	Final selection + LH	
BMP-2	Oocyte	5.18 ± 0.13	5.31 ± 0.13	5.14 ± 0.11	5.12 ± 0.12	NS
	Granulosa cell	11.63 ± 0.42 ^a	9.89 ± 0.42 ^b	9.14 ± 0.59 ^b	10.71 ± 0.59 ^{ab}	< 0.05
	Theca cell	9.25 ± 0.18 ^a	7.89 ± 0.18 ^b	7.65 ± 0.25 ^b	8.69 ± 0.25 ^a	< 0.001
BMP-6	Oocyte	2.42 ± 0.17	2.31 ± 0.17	2.14 ± 0.15	1.94 ± 0.19	NS
	Granulosa cell	ND	ND	ND	ND	ND
	Theca cell	9.82 ± 0.22 ^a	8.42 ± 0.22 ^b	8.88 ± 0.31 ^b	8.85 ± 0.31 ^b	< 0.01
BMP-15	Oocyte	-3.85 ± 0.16 ^a	-3.66 ± 0.16 ^a	-3.45 ± 0.14 ^{ab}	-3.19 ± 0.14 ^b	< 0.05
	Granulosa cell	13.66 ± 0.69	11.37 ± 0.69	13.38 ± 0.97	14.17 ± 0.97	NS
	Theca cell	11.19 ± 0.47	9.59 ± 0.47	9.77 ± 0.67	9.73 ± 0.67	NS
GDF-9	Oocyte	-1.15 ± 0.12	-0.97 ± 0.12	-0.98 ± 0.10	-0.74 ± 0.11	NS
	Granulosa cell	8.28 ± 0.18 ^a	7.18 ± 0.18 ^b	7.62 ± 0.25 ^b	8.39 ± 0.25 ^a	< 0.01
	Theca cell	8.47 ± 0.25 ^a	7.33 ± 0.25 ^b	7.67 ± 0.36 ^{ab}	7.62 ± 0.36 ^{ab}	< 0.05
BMPR1A	Oocyte	4.67 ± 0.12	4.64 ± 0.12	4.59 ± 0.11	4.49 ± 0.14	NS
	Granulosa cell	6.78 ± 0.15 ^a	6.00 ± 0.15 ^b	6.22 ± 0.22 ^{ab}	6.30 ± 0.22 ^{ab}	< 0.05
	Theca cell	6.37 ± 0.35	5.49 ± 0.35	5.82 ± 0.50	6.16 ± 0.50	NS
BMPR1B	Oocyte	3.41 ± 0.20	3.11 ± 0.20	3.17 ± 0.17	3.33 ± 0.22	NS
	Granulosa cell	5.17 ± 0.49 ^a	4.39 ± 0.49 ^b	2.36 ± 0.70 ^c	3.27 ± 0.70 ^{bc}	< 0.001
	Theca cell	9.75 ± 0.42 ^a	8.75 ± 0.42 ^a	6.90 ± 0.59 ^b	8.30 ± 0.59 ^{ab}	< 0.05
BMPR2	Oocyte	4.96 ± 0.11 ^a	4.56 ± 0.11 ^b	4.62 ± 0.11 ^b	4.38 ± 0.13 ^b	< 0.05
	Granulosa cell	6.34 ± 0.25	5.39 ± 0.25	5.51 ± 0.35	6.10 ± 0.35	NS
	Theca cell	7.58 ± 0.28 ^a	6.37 ± 0.28 ^b	6.56 ± 0.40 ^{ab}	6.56 ± 0.40 ^{ab}	< 0.05
TGFB1	Oocyte	5.39 ± 0.18 ^{bc}	5.24 ± 0.18 ^c	5.91 ± 0.17 ^a	5.88 ± 0.20 ^{ab}	< 0.05
	Granulosa cell	6.09 ± 0.19 ^a	5.20 ± 0.19 ^b	5.39 ± 0.27 ^b	4.74 ± 0.27 ^b	< 0.01
	Theca cell	7.21 ± 0.14 ^a	6.41 ± 0.14 ^b	6.41 ± 0.19 ^b	6.61 ± 0.19 ^b	< 0.01

NS = non-significant; ND = not detected

ΔCt are expressed as $\text{lsmean} \pm \text{SEM}$. Different letters within rows indicate significant differences ($P \leq 0.05$)

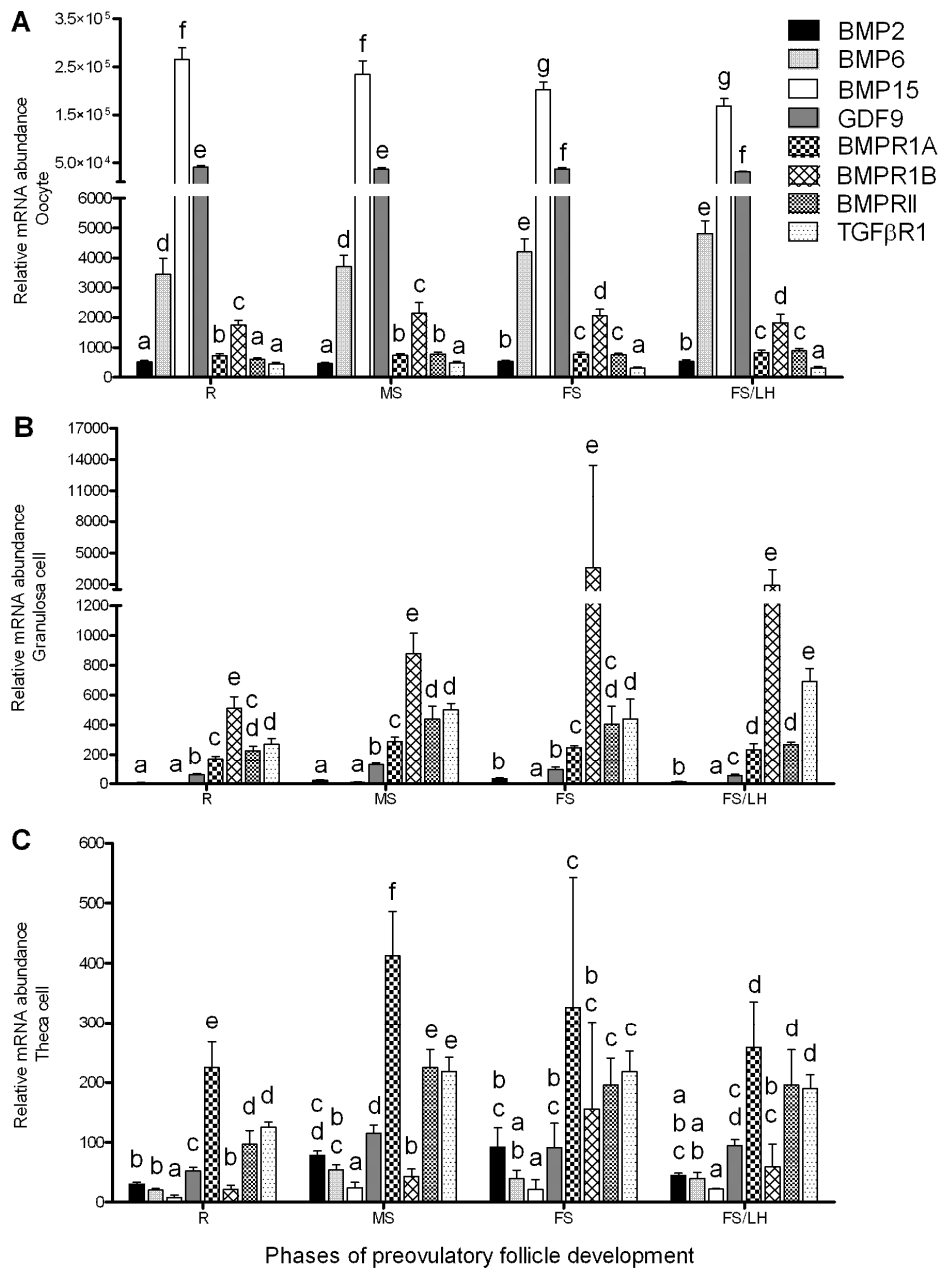


Figure 4.1: Comparison of *BMP2*, *BMP6*, *BMP15*, *GDF9*, *BMPRI1A*, *BMPRI1B*, *BMPRI2* and *TGFBR1* mRNA abundance in pig oocytes (A), granulosa cells (B) and theca cells (C) for each phase of preovulatory follicle development (recruitment (R), mid-selection (MS), final selection (FS) and final selection post-LH surge (FS/LH)), irrespective of cycle. Data are expressed as lmeans of relative mRNA abundance \pm SEM. Different letters between genes within phases represent significant differences ($P \leq 0.05$).

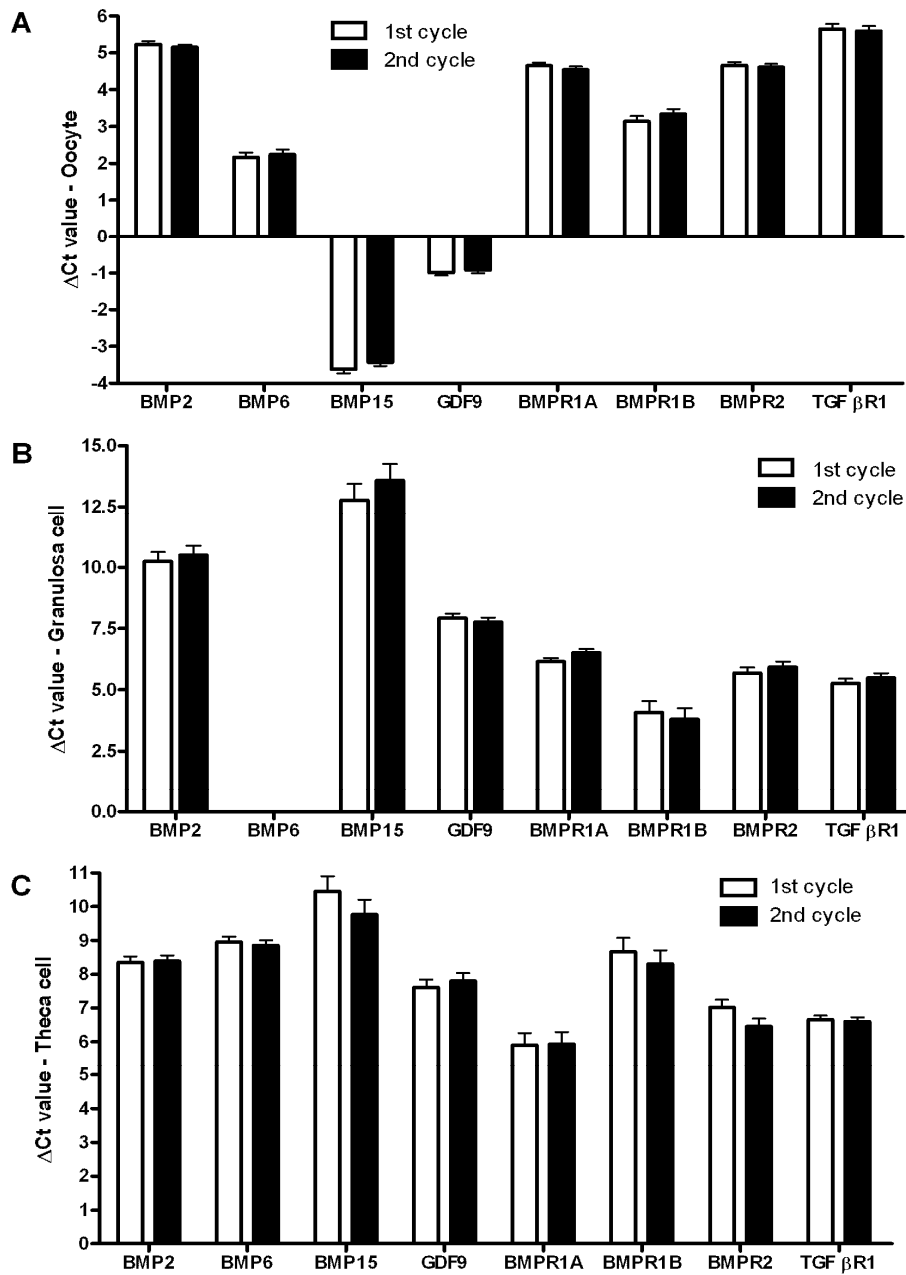


Figure 4.2: Quantification via real-time RT-PCR of *BMP2*, *BMP6*, *BMP15*, *GDF9*, *BMPRI1A*, *BMPRI1B*, *BMPRI2* and *TGFβR1* mRNA abundance in pig oocytes (A), granulosa cells (B) and theca cells (C) between 1st and 2nd cycle, irrespective of the phase of the cycle. The Δ Ct values are expressed as $\text{lsmeans} \pm \text{SEM}$.

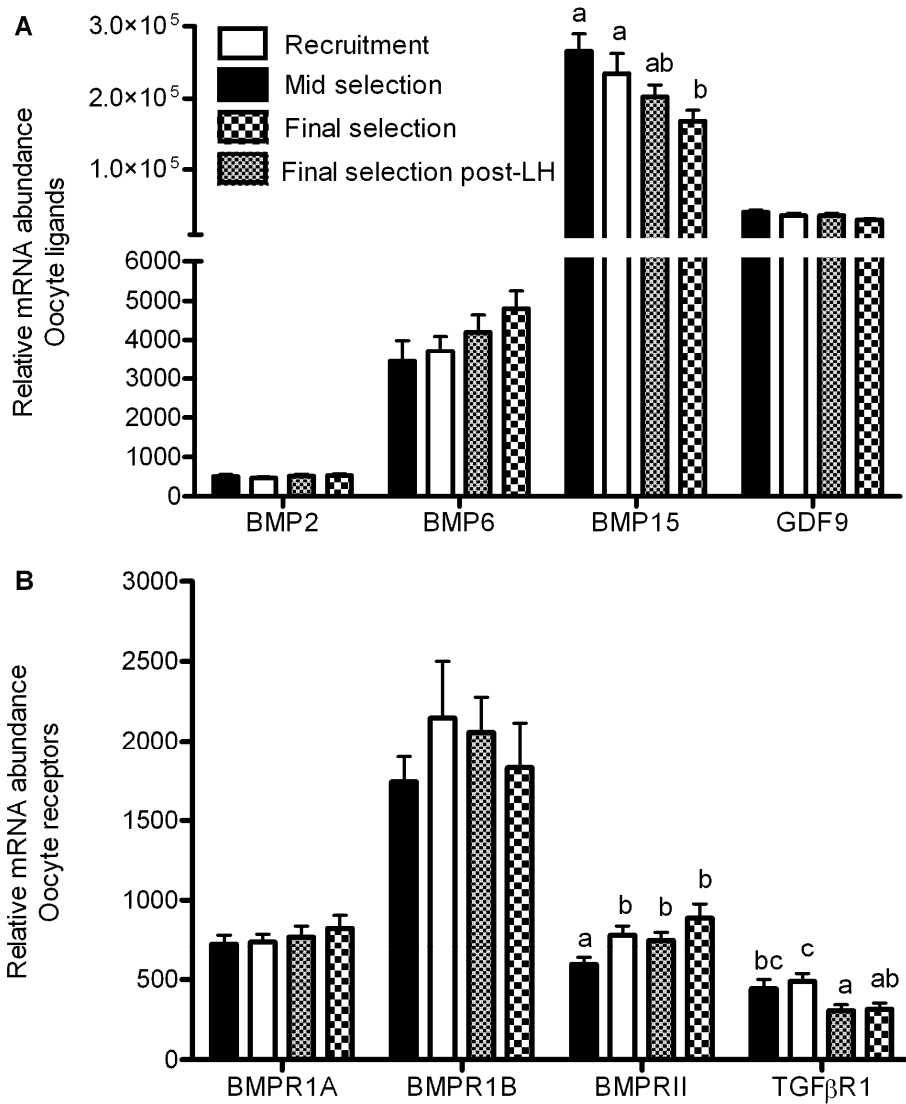


Figure 4.3: Quantification via real-time RT-PCR of A) *BMP2*, *BMP6*, *BMP15* and *GDF9* and B) *BMPRI1A*, *BMPRI1B*, *BMPRII* and *TGFβR1* mRNA abundance in pig oocytes during follicle recruitment (n=6), mid-selection (n=6), final selection (n=8) and final selection post-LH surge (n=8). Data are expressed as means of relative mRNA abundance \pm SEM for each phase, irrespective of cycle. Different letters within gene represent significant differences among phases ($P \leq 0.05^{a,b,c}$; $P \leq 0.01^{x,y,z}$).

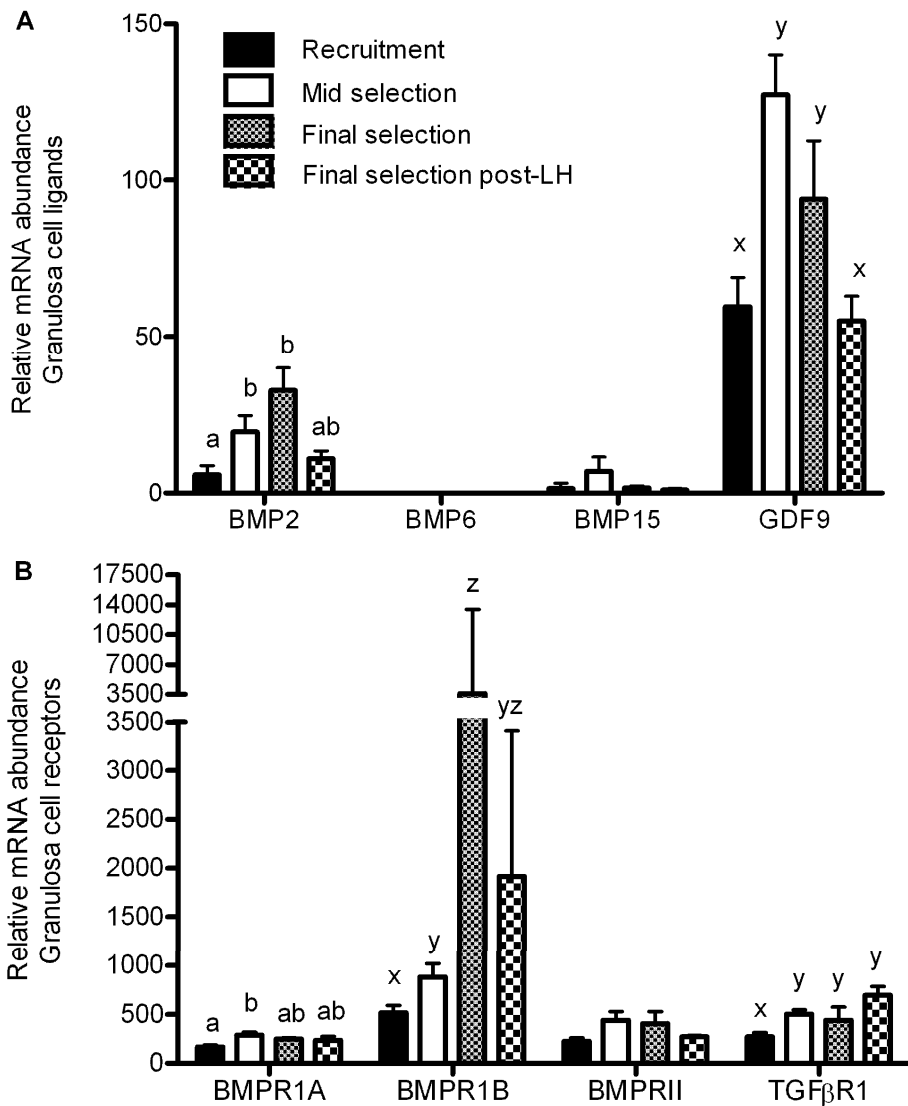


Figure 4.4: Quantification via real-time RT-PCR of A) *BMP2*, *BMP6*, *BMP15* and *GDF9* and B) *BMPRIA*, *BMPR1B*, *BMPRII* and *TGFβR1* mRNA abundance in pig granulosa cells during follicle recruitment (n=6), mid-selection (n=6), final selection (n=3) and final selection post-LH surge (n=3). Data are expressed as means of relative mRNA abundance ± SEM for each phase, irrespective of cycle. Different letters within gene represent significant difference among phases ($P \leq 0.05^{a,b,c}$; $P \leq 0.01^{x,y,z}$).

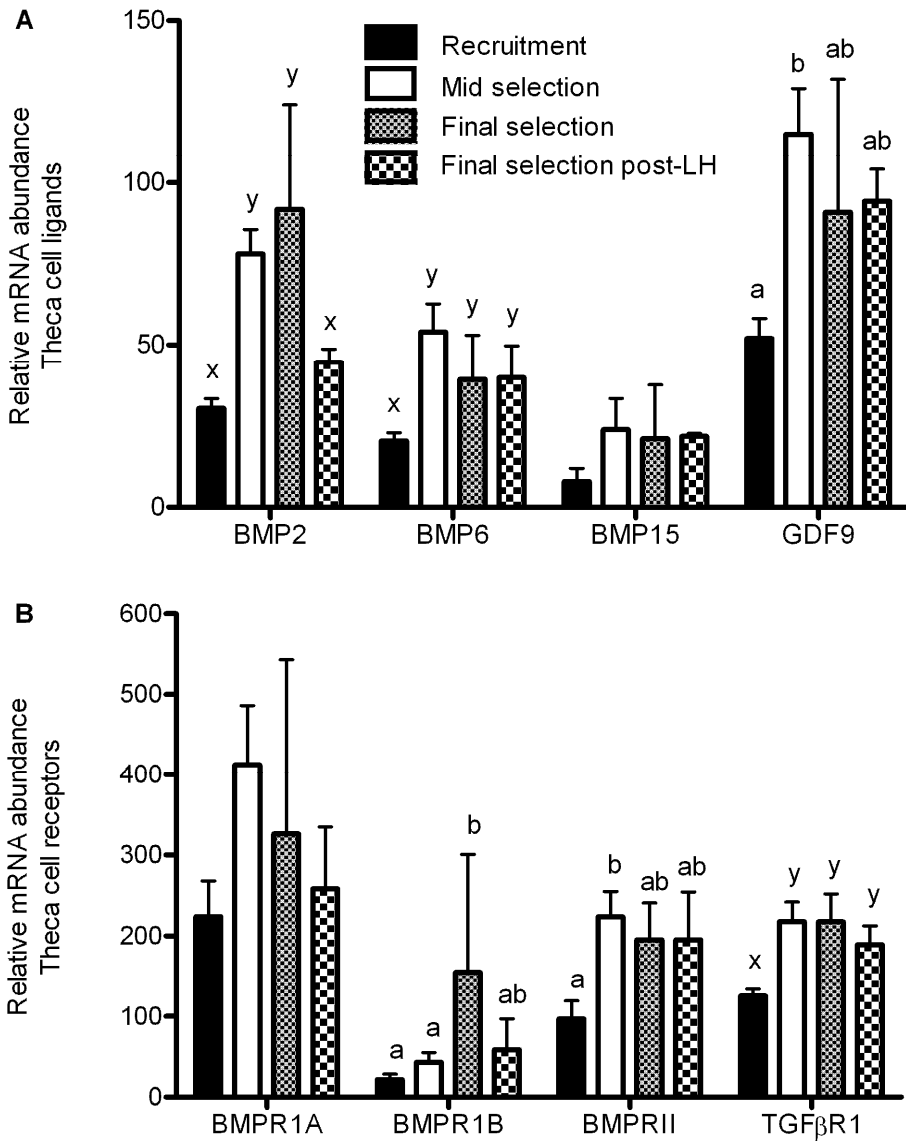


Figure 4.5: Quantification via real-time RT-PCR of A) *BMP2*, *BMP6*, *BMP15* and *GDF9* and B) *BMPR1A*, *BMPR1B*, *BMPR2* and *TGFBR1* mRNA abundance in pig theca cells during follicle recruitment (n=6), mid-selection (n=6), final selection (n=3) and final selection post-LH surge (n=3). Data are expressed as lsmeans of relative mRNA abundance \pm SEM for each phase, irrespective of cycle. Different letters within gene represent significant difference among phases ($P \leq 0.05^{a,b,c}$; $P \leq 0.01^{x,y,z}$).

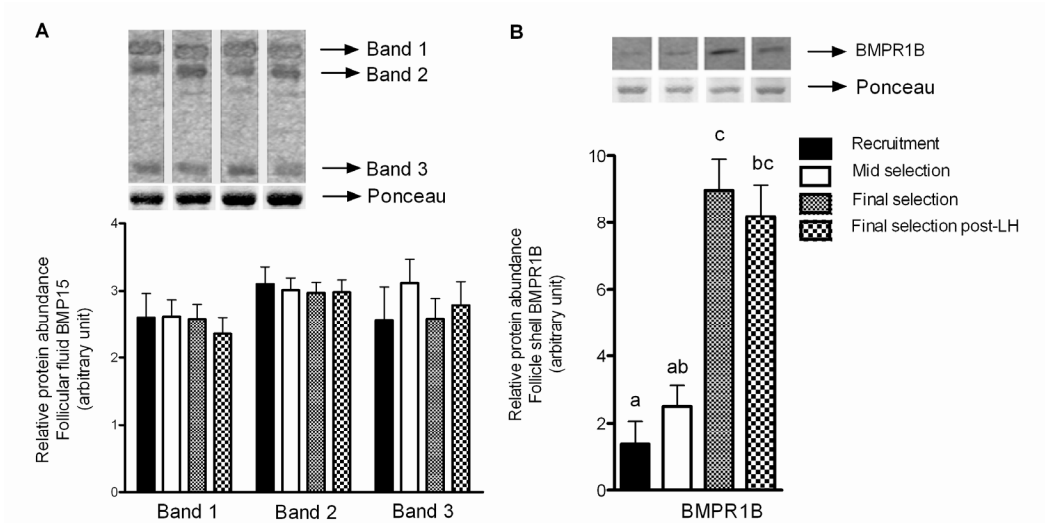


Figure 4.6: Western blot analysis for the presence of BMP15 in follicular fluid (A) and BMPR1B in follicle hemisections (B) during follicle recruitment (BMP15 n=3, BMPR1B n=6), mid-selection (BMP15 n=6, BMPR1B n=6), final selection (BMP15 n= 8, BMPR1B n=3) and final selection post-LH surge (BMP15 n=6, BMPR1B n=3). Relative protein abundance is expressed as $\text{lsmeans} \pm \text{SEM}$. Different letters represent significant differences among phases ($P \leq 0.05$).

REFERENCES

- Aaltonen J, Laitinen MP, Vuojolainen K, Jaatinen R, Horelli-Kuitunen N, Seppa L, Louhio H, Tuuri T, Sjoberg J, Butzow R, Hovatta O, Dale L & Ritvos O** 1999 Human growth differentiation factor 9 (GDF-9) and its novel homolog GDF-9B are expressed in oocytes during early folliculogenesis. *J Clin Endocrinol Metabol* **84** 2744-2750.
- Balemans W & Van Hul W** 2002 Extracellular regulation of BMP signaling in vertebrates: a cocktail of modulators. *Devel Biol* **250** 231-250.
- Brankin V, Quinn RL, Webb R & Hunter MG** 2005 Evidence for a functional bone morphogenetic protein (BMP) system in the porcine ovary. *Dom Anim Endocrinol* **28** 367-379.
- Bettegowda A, Patel OV, Ireland JJ & Smith GW** 2006 Quantitative analysis of messenger RNA abundance for ribosomal protein L-15, cyclophilin-A, phosphoglycerokinase, beta-glucuronidase, glyceraldehyde 3-phosphate dehydrogenase, beta-actin, and histone H2A during bovine oocyte maturation and early embryogenesis *in vitro*. *Mol Reprod Devel* **73** 267-278.
- Chang H, Brown CW & Matzuk MM** 2002 Genetic analysis of the mammalian transforming growth factor-beta superfamily. *Endocrine Rev* **23** 787-823.
- Clowes EJ, Aherne FX & Foxcroft GR** 1994 Effect of Delayed Breeding on the Endocrinology and Fecundity of Sows. *J Anim Sci* **72** 283-291.
- Clowes EJ, Aherne FX, Foxcroft GR & Baracos VE** 2003a Selective protein loss in lactating sows is associated with reduced litter growth and ovarian function. *J Anim Sci* **81** 753-764.
- Clowes EJ, Aherne FX, Schaefer AL, Foxcroft GR & Baracos VE** 2003b Parturition body size and body protein loss during lactation influence performance during lactation and ovarian function at weaning in first-parity sows. *J Anim Sci* **81** 1517-1528.
- Dube JL, Wang P, Elvin J, Lyons KM, Celeste AJ & Matzuk MM** 1998 The bone morphogenetic protein 15 gene is X-linked and expressed in oocytes. *Mol Endocrinol* **12** 1809-1817.
- Erickson GF & Shimasaki S** 2003 The spatiotemporal expression pattern of the bone morphogenetic protein family in rat ovary cell types during the estrous cycle. *Reprod Biol Endocrinol* **1** 9.

Fatehi AN, van den Hurk R, Colenbrander B, Daemen AJ, van Tol HT, Monteiro RM, Roelen BA & Bevers MM 2005 Expression of bone morphogenetic protein2 (BMP2), BMP4 and BMP receptors in the bovine ovary but absence of effects of BMP2 and BMP4 during IVM on bovine oocyte nuclear maturation and subsequent embryo development. *Theriogenology* **63** 872-889.

Feary ES, Juengel JL, Smith P, French MC, O'Connell AR, Lawrence SB, Galloway SM, Davis GH & McNatty KP 2007 Patterns of expression of messenger RNAs encoding GDF9, BMP15, TGFBR1, BMPR1B, and BMPR2 during follicular development and characterization of ovarian follicular populations in ewes carrying the Woodlands FecX2W mutation. *Biol Reprod* **77** 990-998.

Foxcroft GR & Hunter MG 1985 Basic physiology of follicular maturation in the pig. *J Reprod Fertil Suppl* **33** 1-19.

Foxcroft GR 1997 Mechanisms mediating nutritional effects on embryonic survival in pigs. *J Reprod Fertil Suppl* **52** 47-61.

Foxcroft GR, Vinsky MD, Paradis F, Tse WY, Town SC, Putman CT, Dyck MK & Dixon WT 2007 Macroenvironment effects on oocytes and embryos in swine. *Theriogenology* **68** S30-S39.

Funahashi H, Cantley TC & Day BN 1997 Synchronization of meiosis in porcine oocytes by exposure to dibutylryl cyclic adenosine monophosphate improves developmental competence following *in vitro* fertilization. *Biol Reprod* **57** 49-53.

Galloway SM, McNatty KP, Cambridge LM, Laitinen MPE, Juengel JL, Jokiranta TS, McLaren RJ, Luiro K, Dodds KG, Montgomery GW, Beattie AE, Davis GH & Ritvos O 2000 Mutations in an oocyte-derived growth factor gene (BMP15) cause increased ovulation rate and infertility in a dosage-sensitive manner. *Nat Genet* **25** 279-283.

Gilchrist RB, Lane M & Thompson JG 2008 Oocyte-secreted factors: regulators of cumulus cell function and oocyte quality. *Hum Reprod Update* **14** 159-177.

Glister C, Kemp CF & Knight PG 2004 Bone morphogenetic protein (BMP) ligands and receptors in bovine ovarian follicle cells: actions of BMP-4, -6 and -7 on granulosa cells and differential modulation of Smad-1 phosphorylation by follistatin. *Reproduction* **127** 239-254.

Glister C, Richards SL & Knight PG 2005 Bone morphogenetic proteins (BMP) -4, -6, and -7 potently suppress basal and luteinizing hormone-induced androgen production by bovine theca interna cells in primary culture: could ovarian hyperandrogenic dysfunction be caused by a defect in thecal BMP signaling? *Endocrinol* **146** 1883-1892.

Grant SA, Hunter MG & Foxcroft GR 1989 Morphological and Biochemical Characteristics during Ovarian Follicular Development in the Pig. *J Reprod Fertil* **86** 171-183.

Gueripel X, Brun V & Gougeon A 2006 Oocyte bone morphogenetic protein 15, but not growth differentiation factor 9, is increased during gonadotropin-induced follicular development in the immature mouse and is associated with cumulus oophorus expansion. *Biol Reprod* **75** 836-843.

Hunter MG, Robinson RS, Mann GE & Webb R 2004 Endocrine and paracrine control of follicular development and ovulation rate in farm species. *Anim Reprod Sci* **82-83** 461-477.

Hunter MG & Wiesak T 1990 Evidence for and implications of follicular heterogeneity in pigs. *J Reprod Fertil Suppl* **40** 163-177.

Jayawardana BC, Shimizu T, Nishimoto H, Kaneko E, Tetsuka M & Miyamoto A 2006 Hormonal regulation of expression of growth differentiation factor-9 receptor type I and II genes in the bovine ovarian follicle. *Reproduction* **131** 545-553.

Juengel JL, Hudson NL, Heath DA, Smith P, Reader KL, Lawrence SB, O'Connell AR, Laitinen MPE, Cranfield M, Groome NP, Ritvos O & McNatty KP 2002 Growth differentiation factor 9 and bone morphogenetic protein 15 are essential for ovarian follicular development in sheep. *Biol Reprod* **67** 1777-1789.

Juengel JL, Bibby AH, Reader KL, Lun S, Quirke LD, Haydon LJ & McNatty KP 2004 The role of transforming growth factor-beta (TGF-beta) during ovarian follicular development in sheep. *Reprod Biol Endocrinol* **2** 78.

Juengel JL & McNatty KP 2005 The role of proteins of the transforming growth factor-beta superfamily in the intraovarian regulation of follicular development. *Human Reprod Update* **11** 143-160.

Juengel JL, Reader KL, Bibby AH, Lun S, Ross I, Haydon LJ & McNatty KP 2006 The role of bone morphogenetic proteins 2, 4, 6 and 7 during ovarian follicular development in sheep: contrast to rat. *Reproduction* **131** 501-513.

Juneja SC, Chegini N, Williams RS & Ksander GA 1996 Ovarian intrabursal administration of transforming growth factor beta 1 inhibits follicle rupture in gonadotropin-primed mice. *Biol Reprod* **55** 1444-1451.

Laitinen M, Vuojolainen K, Jaatinen R, Ketola I, Aaltonen J, Lehtonen E, Heikinheimo M & Ritvos O 1998 A novel growth differentiation factor-9 (GDF-9) related factor is co-expressed with GDF-9 in mouse oocytes during folliculogenesis. *Mechanisms Devel* **78** 135-140.

Lee GS, Kim HS, Hwang WS & Hyun SH 2008 Characterization of porcine growth differentiation factor-9 and its expression in oocyte maturation. *Mol ReprodDevel* **75** 707-714.

McIntosh CJ, Lun S, Lawrence S, Western AH, McNatty KP & Juengel JL 2008 The proregion of mouse BMP15 regulates the cooperative interactions of BMP15 and GDF9. *Biol Reprod* **79** 889-896.

Miyoshi T, Otsuka F, Suzuki J, Takeda M, Inagaki K, Kano Y, Otani H, Mimura Y, Ogura T & Makino H 2006 Mutual regulation of follicle-stimulating hormone signaling and bone morphogenetic protein system in human granulosa cells. *Biol Reprod* **74** 1073-1082.

Otsuka F, Moore RK & Shimasaki S 2001a Biological function and cellular mechanism of bone morphogenetic protein-6 in the ovary. *J Biol Chem* **276** 32889-32895.

Otsuka F, Moore RK, Iemura S, Ueno N & Shimasaki S 2001b Follistatin inhibits the function of the oocyte-derived factor BMP-15. *Biochem Biophys Res Commun* **289** 961-966.

Prochazka R, Nemcova L, Nagyova E & Kanka J 2004 Expression of growth differentiation factor 9 messenger RNA in porcine growing and preovulatory ovarian follicles. *Biol Reprod* **71** 1290-1295.

Quinn RL, Shuttleworth G & Hunter MG 2004 Immunohistochemical localization of the bone morphogenetic protein receptors in the porcine ovary. *J Anat* **205** 15-23.

Shimasaki S, Moore RK, Otsuka F & Erickson GF 2004 The bone morphogenetic protein system in mammalian reproduction. *Endocrine Rev* **25** 72-101.

Shimizu T, Jayawardana BC, Nishimoto H, Kaneko E, Tetsuka M & Miyamoto A 2006 Involvement of the bone morphogenetic protein/receptor system during follicle development in the bovine ovary: Hormonal regulation of the expression of bone morphogenetic protein 7 (BMP-7) and its receptors (ActRII and ALK-2). *Mol Cell Endocrinol* **249** 78-83.

Shimizu T, Iijima K, Ogawa Y, Miyazaki H, Sasada H & Sato E 2008 Gene injections of vascular endothelial growth factor and growth differentiation factor-9 stimulate ovarian follicular development in immature female rats. *Fertil Steril* **89** 1563-1570.

Silva JR, van den Hurk R, van Tol HT, Roelen BA & Figueiredo JR 2005 Expression of growth differentiation factor 9 (GDF9), bone morphogenetic protein 15 (BMP15), and BMP receptors in the ovaries of goats. *Mol Reprod Devel* **70** 11-19.

Souza CJ, Campbell BK, McNeilly AS & Baird DT 2002 Effect of bone morphogenetic protein 2 (BMP2) on oestradiol and inhibin A production by sheep granulosa cells, and localization of BMP receptors in the ovary by immunohistochemistry. *Reproduction* **123** 363-369.

Spicer LJ, Aad PY, Allen DT, Mazerbourg S, Payne AH & Hsueh AJ 2008 Growth differentiation factor 9 (GDF9) stimulates proliferation and inhibits steroidogenesis by bovine theca cells: Influence of follicle size on responses to GDF9. *Biol Reprod* **78** 243-253.

Su YQ, Wu X, O'Brien MJ, Pendola FL, Denegre JN, Matzuk MM & Eppig JJ 2004 Synergistic roles of BMP15 and GDF9 in the development and function of the oocyte-cumulus cell complex in mice: genetic evidence for an oocyte-granulosa cell regulatory loop. *Devel Biol* **276** 64-73.

Vitt UA, Hayashi M, Klein C & Hsueh AJW 2000 Growth differentiation factor-9 stimulates proliferation but suppresses the follicle-stimulating hormone-induced differentiation of cultured granulosa cells from small antral and preovulatory rat follicles. *Biol Reprod* **62** 370-377.

Wilson T, Wu XY, Juengel JL, Ross IK, Lumsden JM, Lord EA, Dodds KG, Walling GA, McEwan JC, O'Connell AR, McNatty KP & Montgomery GW 2001 Highly prolific Booroola sheep have a mutation in the intracellular kinase domain of bone morphogenetic protein IB receptor (ALK-6) that is expressed in both oocytes and granulosa cells. *Biol Reprod* **64** 1225-1235.

Yan CN, Wang P, DeMayo J, DeMayo FJ, Elvin JA, Carino C, Prasad SV, Skinner SS, Dunbar BS, Dube JL, Celeste AJ & Matzuk MM 2001 Synergistic roles of bone morphogenetic protein 15 and growth differentiation factor 9 in ovarian function. *Mol Endocrinol* **15** 854-866.

Yang H, Foxcroft GR, Pettigrew JE, Johnston LJ, Shurson GC, Costa AN & Zak LJ 2000a Impact of dietary lysine intake during lactation on follicular development and oocyte maturation after weaning in primiparous sows. *J Anim Sci* **78** 993-1000.

Yang H, Pettigrew JE, Johnston LJ, Shurson GC, Wheaton JE, White ME, Koketsu Y, Sower AF & Rathmacher JA 2000b Effects of dietary lysine intake during lactation on blood metabolites, hormones, and reproductive performance in primiparous sows. *J Anim Sci* **78** 1001-1009.

Yi SE, LaPolt PS, Yoon BS, Chen JYC, Lu JKH & Lyons KM 2001 The type IBMP receptor Bmpr1B is essential for female reproductive function. *Proc Nat Acad Sci USA* **98** 7994-7999.

Yoshino O, McMahon HE, Sharma S & Shimasaki S 2006 A unique preovulatory expression pattern plays a key role in the physiological functions of BMP-15 in the mouse. *PNAS* **103** 10678-10683.

Zak LJ, Xu X, Hardin RT & Foxcroft GR 1997 Impact of different patterns of feed intake during lactation in the primiparous sow on follicular development and oocyte maturation. *J Reprod Fertil* **110** 99-106.

Zhu G, Guo B, Pan D, Mu Y & Feng S 2008 Expression of bone morphogenetic proteins and receptors in porcine cumulus-oocyte complexes during *in vitro* maturation. *Anim Reprod Sci* **104** 275-283.

CHAPTER 5

TEMPORAL EXPRESSION OF ANGIOGENIC FACTORS IN GRANULOSA AND THECA CELLS OF DEVELOPING PORCINE PREEVULATORY FOLLICLES AND THE POTENTIAL INVOLVEMENT OF ANGIOGENIN IN THE LUTEINIZING FOLLICLE

INTRODUCTION

Ovarian follicle development in the pig occurs over a period of approximately 100 days and results in the ovulation of a subset of oocytes potentially competent to develop after fertilization into viable embryos (Hunter *et al.*, 2000). Understanding the coordinated series of events leading to ovulation is therefore of prime importance, especially considering that ovulation rate and oocyte quality are important determinants of reproductive efficiency. In the pig, as in other species, it is now widely accepted that during the last week of follicular development, follicle recruitment and selection are responsible for establishing the preovulatory population characteristic of each species (Hunter *et al.*, 2004). It is also accepted that these processes are tightly regulated by a variety of endocrine signals, including the gonadotrophins, and by intrafollicular growth factors.

Nutritional restriction and increased catabolism during lactation in primiparous sows is detrimental to embryonic survival by day 30 of gestation in the subsequent litter and these effects are associated with changes in follicle and oocyte quality (Foxcroft, 1997, Zak *et al.*, 1997). Interestingly, delaying breeding of primiparous sows until the second oestrus post-weaning results in increased embryo survival and increased litter size, likely originating from differences in follicle maturity (size) observed in these animals (Clowes *et al.*, 1994, Foxcroft *et al.*, 2007, Paradis *et al.*, 2009). Understanding the molecular mechanisms underlying such differences is therefore of considerable practical significance.

In most tissues including the ovarian follicle, the establishment of an adequate blood supply is essential to ensure appropriate delivery of oxygen, nutrients and hormonal signals and for eliminating metabolic by-products such as CO₂. In the pig, the vasculature of the preantral follicle is minimal but, as the follicle progresses from a small to a large preovulatory follicle, the vasculature also increases dramatically (Jiang *et al.*, 2002). These findings corroborate the observations made in rabbit and cow follicles and support the concept that the blood supply increases as healthy follicles grow larger, while reduced or non-uniform vascularization is generally associated with atresia (Hay *et al.*, 1976, Kanzaki *et al.*, 1982, Kitai *et al.*, 1985, Yamada *et al.*, 1995). Finally, the vascular network that develops around each individual follicle is confined to the theca cell layer as the basement membrane prevents further progression into the granulosa cell layer, which remains avascular until the periovulatory period (Reviewed by Fraser, 2006, Shimizu *et al.*, 2003a). However, the granulosa cells are also thought to actively contribute to the development of the thecal vasculature by producing angiogenic factors that diffuse outside the follicle. The identification of angiogenic factors in the developing antral follicle of several species, as well as the reported detrimental effects caused by the disruption of the vasculature during follicular development, emphasizes the importance of understanding the molecular mechanisms responsible for the modulation of the follicular blood supply (Fraser, 2006, Stouffer *et al.*, 2001, Tamanini and De Ambrogi, 2004, Wulff *et al.*, 2002, Zimmermann *et al.*, 2002). Currently, little is known about the angiogenic process during preovulatory development in the pig.

Therefore, the objectives of this study were: 1) to generate a list of angiogenic transcripts expressed in the granulosa and theca cells of porcine developing follicles, 2) to confirm the localization of *VEGFA*, *FLT1*, *KDR*, *ANGPT1*, *ANGPT2*, *TEK*, *HIF1A* and *ANG* mRNA in the developing preovulatory follicle, 3) to establish their temporal expression patterns during follicular development and 4) to determine whether these angiogenic factors could play a role in creating the differences in follicle characteristics and eventual embryo survival observed between the first and second post-weaning preovulatory

waves of follicular development in primiparous sows. The results obtained demonstrate the co-localization and expression patterns of an array of angiogenic factors during porcine preovulatory follicle development *in vivo* and suggest a role for angiogenin in the luteinizing follicle.

MATERIALS AND METHODS

Chemicals and media

Unless otherwise stated all chemicals were obtained from Sigma-Aldrich (St-Louis, Mo, USA). The media used for washing the COCs and during follicle dissection was modified Tyrode lactate (TL)-HEPES medium supplemented with 0.1% (w/v) polyvinyl alcohol (PVA) (Funahashi *et al.*, 1997), 50 U/ml of penicillin and 50 µg/ml of streptomycin (Invitrogen, #15070-063, Burlington, ON, Canada). The phosphate-buffered saline pH 7.4 was composed of 137 mM NaCl, 2.7 mM KCl, 8.1 mM Na₂HPO₄ and 1.47 mM KH₂PO₄.

Animals

This experiment was conducted in accordance with the guidelines of the Canadian Council on Animal Care and with the approval of the University of Alberta, Faculty Animal Policy and Welfare Committee (Protocol #2005-40B). A total of 18 primiparous F1 sows (Large White x Landrace, Hypor, Regina, SK, Canada) were used for follicle dissection and an additional 26 sows were used for follicular fluid steroid analysis. Within 48 h after farrowing, litter size was standardized to between 9 and 11 piglets through cross-fostering and routine piglet processing procedures (tail-docking, teeth clipping, ear notching and iron injection) were performed. During lactation, sows were offered fresh feed three times daily and permitted ad libitum access to fresh water. Sows were offered 3.5 kg of feed on the day of farrowing, and during the remainder of lactation, the amount of feed offered was increased by 0.5 kg daily until the sows daily

consumption was exceeded by 0.5 kg. Sows were weaned 20.8 ± 3.2 (mean \pm stdev) days after farrowing and were randomly allocated to treatment at this time. After weaning, sows were moved to a common weaned-sow room, housed in individual sow stalls and were fed to appetite twice daily until the day of euthanasia. From the day after weaning, sows were actively heat-checked using fenceline boar contact twice daily (at 0800 and 1400). Onset of standing heat was determined as the midpoint between the time of first detection of standing oestrus and the last time that oestrus was detected. Similarly, the end of standing heat was calculated as the midpoint between the last time that signs of oestrus were detected and the first time after standing heat that no signs of oestrus were detected. Sows were weighed on day 1, 6 and 13 of lactation, at weaning and at the time of euthanasia.

Sows used for follicle dissection were euthanized on day 1 (D1; n=3), 2 (D2; n=3) or 4 (D4; n=3) after weaning, or day 14 (D14; n=3), 16 (D16; n=3) or 20 (D20; n=3) after the 1st post-weaning oestrus. The additional sows used for follicular fluid steroid analysis were euthanized on day 4 (D4; n=14) after weaning, or day 20 (D20; n=12) after the 1st post-weaning oestrus. These time-frames correspond to the 1st and 2nd post-weaning preovulatory wave of follicular development and D1/D14 corresponds to the period of recruitment (R) of the growing cohort of follicles, D2/D16 corresponds to the mid-selection phase (MS) at which time follicles either keep growing or, if not selected, start to undergo atresia and D4/D20 corresponds to the final selection phase (FS) where the preovulatory follicle population has been established (Grant *et al.*, 1989, Hunter and Wiesak, 1990). The preovulatory follicle population from the final selection phase was further divided between the follicles in pre-LH surge (FS) or post-LH surge (FS/LH) stages based on follicular fluid oestradiol concentrations (see procedure below). The sows used in the experiments were euthanized on-site in a purpose-built necropsy facility according to the Swine Research and Technology Centre standard operating procedures. Prior to euthanasia, a single blood sample was collected into a 10 ml heparinized Vacutainer™ (Becton Dickinson, Franklin Lakes, NJ, USA) by jugular venipuncture, centrifuged at 1700 x g for 15 min at

room temperature and the plasma was then stored at -20°C until assayed for plasma oestradiol concentration.

Tissue collection

Within 20 min after euthanasia, the ovaries were moved to an adjacent laboratory suite in 50 ml Falcon tube containing 0.9% (w/v) ice cold saline when the ovaries were intended for follicle dissection, or in 0.9% (w/v) warm saline when the ovaries were intended for follicular fluid collection. The ovaries from the 18 sows intended for follicle dissection and/or follicular fluid aspiration were allocated as followed: for each phase of follicular development (R, MS and FS), 3 sows from each cycle group (1st or 2nd cycle) were euthanized. One ovary from each sow was chosen for follicle dissection and the other ovary was used for follicular fluid aspiration. Moreover, the ovaries of the additional 26 sows were used for follicular fluid aspiration. Before processing the ovaries, the number and size of all visible follicles was recorded and the follicular fluid from the largest follicle(s) (1 to 3 pooled follicles depending on the volume recovered) of D4 and D20 animals was collected using an 18-gauge needle attached to a 1 ml disposable syringe for assay of oestradiol concentration. The follicular fluid was centrifuged for 5 min at 13 000 x g to remove any cellular debris, diluted 11-fold in M199 and stored at -20°C for either assaying oestradiol or progesterone concentrations.

Follicle dissection: A total of 18 ovaries, each originating from a different animal and representing each phase of follicular development, were sliced in half longitudinally and washed twice in ice cold PVA-TL-HEPES to remove blood contamination. The half ovaries were then placed into Petri dishes containing ice cold PVA-TL-HEPES and follicles representative of the population present on the ovary were dissected free of stromal tissue under a dissecting microscope using fine scissors and forceps. Intact dissected follicles were then placed into RNAlater (Ambion, Austin, TX, USA) to preserve RNA integrity during the remaining procedure. Depending on the size of the follicles, between 5 and 10 follicles were dissected within a 1-hour period. The intact follicles were then placed back into ice cold PVA-TL-HEPES and cut in half using a scalpel blade.

One half of each follicle (hemisection) from an individual sow containing granulosa and theca cells was transferred to a 1.5 ml microcentrifuge tube in ice cold media and centrifuged for 5 min at 200 x g at room temperature. The hemisections were washed twice with 1 ml of ice cold PBS followed by centrifugation at 200 x g for 5 min. Following the last wash, the supernatant was removed and the cells were snap frozen in liquid nitrogen. The hemisections were stored at -80°C until protein extraction. The mural granulosa cells (MGC) were then gently scraped from the inner wall of the remaining hemisection using a fine glass loop and the oocytes were removed to ensure a pure MGC population. The MGC were transferred to a 1.5 ml microcentrifuge tube in ice cold media and centrifuged for 5 min at 200 x g at room temperature. The MGC pellets were washed twice with 1ml of ice cold PBS followed by centrifugation at 200 x g for 5 min. Following the last wash, the supernatant was removed and the cells were snap frozen in liquid nitrogen. The remaining follicle shells contained mainly theca cells (TC) and were vigorously agitated by repeated pipetting to ensure that all MGC were removed. The TC were then transferred to a 1.5 ml microcentrifuge tube in ice cold media and centrifuged for 5 min at 200 x g at room temperature. The TC pellets were washed twice with 1 ml of ice cold PBS followed by centrifugation at 200 x g for 5 min. Following the last wash, the supernatant was removed and the cells were snap frozen in liquid nitrogen. The MGC and TC were finally stored at -80°C until RNA extraction.

Radioimmunoassay

Plasma oestradiol: Oestradiol concentrations were determined in all plasma samples in triplicate in a single RIA using the method of Yang *et al.* (2000b). Extraction efficiency was $63 \pm 4\%$ and estimated potencies were not corrected for recovery. Assay sensitivity, defined as 90 % of total binding, was 0.35 pg/ml. The intra-assay CV was 9%.

Follicular fluid oestradiol: Follicle fluid (FF) oestradiol concentrations were quantified in a single RIA using a double antibody kit (Diagnostic Products Corporation # KE2D1, Diagnostic Products Corporation, Los Angeles, CA, USA)

without extraction using the method of Paradis *et al.* (2009). The intra-assay CV for the single assay run was 5.7 %. Sensitivity estimated at 91 % of total binding was 0.11 pg/tube, equivalent to 2.4 ng/ml. The recovery of a known amount of oestradiol when added to a sample of known potency was 94.5 ± 2.7 %.

Follicular fluid progesterone: FF progesterone concentrations were quantified in a single RIA using the method of Mao *et al.* (2001). To ensure that all sample potencies were estimated from the linear part of the standard curve, the stored FF diluted 11-fold in TCM 199 was assayed both neat and further diluted five-fold in kit buffer. The sensitivity of the assay, defined as 88% of total binding, was 1.1 ng/ml. One sample fell below sensitivity. A control FF pool serially diluted showed parallelism to the standard curve. The intra-assay CV was 6.28%.

Microarray analysis

The microarray experiment has been previously described in Chapter 3. Briefly, a pool of total RNA from granulosa or theca cells isolated from animals of different maturity (prepubertal gilts, cyclic gilts, primiparous sows during the 1st and 2nd estrus post-weaning) and representing various important phases of follicle development (recruitment, mid-selection and final selection before and after the LH surge) was used for the experiment. In addition, for each cell type, two technical replicates were performed to ensure that the cDNA amplification, fragmentation, labelling and hybridization to the microarray were reproducible.

The RNA was sent to the Genomics Core in the Centre for Reproductive Biology at the Washington State University (Pullman, Washington) for processing and hybridization to the Affymetrix (Santa Clara, CA, USA) GeneChip® Porcine Genome Array. Two pools of 50 ng/ul of total RNA from each cell type were amplified using the Ovation® RNA Amplification System V2 (NuGen Technologies Inc., San Carlos, California, USA) and fragmented and biotin labelled using the FL-Ovation™ cDNA Biotin Module V2 (Nugen Technologies Inc.) according to manufacturer's instruction. Finally, 2.6 ug of fragmented,

biotin labeled amplified cDNA was then hybridized to the Affymetrix GeneChip® Porcine Genome Array.

The microarray image data were converted to numerical data using the Affymetrix GeneChip Operating Software (GCOS) using a global scaling strategy to produce a mean signal intensity of 125. In GCOS, the 11 perfect match and 11 mismatch oligonucleotides were used to determine present and absent call, using a one-sided Wilcoxon's signed-rank test. Finally, Excel files containing the signal intensity and the present/absent call for each probe sets were generated and the R^2 between the replicates of each cell type were calculated and were found to be ≥ 0.98 , indicating very high reproducibility.

Bioinformatics and gene ontology

The gene lists from each cell type were visualized and in order for a transcript to be considered present, it had to be tagged as present and have a signal intensity higher than 50 in both technical replicates. The arbitrary signal intensity of 50 was used to exclude the transcripts with very low signal intensity which are the most likely to be false positive identifications. The spreadsheets containing the gene lists were then merged with an annotation file specifically generated for the Affymetrix GeneChip® Porcine Genome Array and containing the putative identity of more than 80% of the primer probe set represented on the microarray (Tsai *et al.*, 2006). The annotated list of GC and TC transcripts were then analysed in the gene ontology freeware GOTreePlus (<http://bioinformatics.cnmcresearch.org/GOTreePlus>) using the human gene ontology annotation file (www.geneontology.org/GO.current.annotations.shtml) and grouped by the gene ontology (GO) term “angiogenesis” (GO:0001525).

RNA isolation and Real-time RT-PCR

Total RNA was extracted from the pooled CGC, MGC and TC of individual animals using TRIzol reagent (Invitrogen) following the manufacturer's instructions, with the following modification. The cells were thawed on ice directly in Trizol and homogenized with a Polytron™. The

homogenized samples were then incubated for 10 min at room temperature before further processing. The homogenized CGC and MGC originating from the same animals were then pooled together prior to the extraction and will be further referred to as granulosa cells (GC). The GC and TC total RNA was precipitated with 1/10 volume of 5M ammonium acetate, 1 volume of isopropanol and linear acrylamide (Ambion) was also added to the RNA as a carrier at a final concentration of 10 µg/ml. The total RNA was resuspended in nuclease-free H₂O (Ambion) and was DNase treated using DNA-free™ (Ambion) following the manufacturer's instructions. The samples were quantified using the spectrophotometer ND-1000 (NanoDrop, Wilmington, DE, USA) and RNA integrity was evaluated on a 1 % (w/v) denaturing agarose gel. All samples were stored at -80°C until cDNA synthesis.

GC and TC total RNA was reverse transcribed with Superscript III reverse transcriptase (Invitrogen) according to manufacturer's instruction, using a combination of 5 µM oligo dT and 5 ng/ul of random hexamer. RNaseOUT (Invitrogen) was also added to the reaction at a concentration of 2 U/µl. cDNA synthesis was performed using 2 µg of GC and TC total RNA. After reverse transcription, GC and TC cDNA were diluted to 20 ng/µl with nuclease-free H₂O (Ambion).

Real-Time PCR was performed in duplicate using 20 ng of GC or TC cDNA in 96-well fast plates using the Taqman® Fast Universal PCR Master Mix and the ABI 7900HT thermocycler (Applied Biosystems, Foster City, CA, USA). The primers and Taqman-MGB probes (Table 5.1) were designed using the Primer Express® software v3.0 (Applied Biosystems) using species specific sequences found in GENBANK. The amplification efficiency for each gene was determined using serial dilution of ovarian cDNA and was found to be $\geq 90\%$ for all genes (data not shown). Moreover, the amplification efficiency slopes for all 9 genes were found to be identical. As reported by Bettegowda *et al.* (2006), cyclophilin was used as the endogenous control to correct for RNA extraction and reverse transcription efficiency within cell type. Cyclophilin transcript abundance

was found to be stable within each cell type throughout the different stages of follicle development, confirming its usefulness as a good endogenous control. However, cyclophilin abundance differed between the cell types studied and limited our ability to compare the abundance of each gene of interest across cell types.

Statistical analysis

The sow's reproductive data including follicular fluid oestradiol and progesterone concentrations were analysed using the MIXED procedure of SAS (SAS Institute Inc., Cary, NC). Follicular fluid oestradiol and progesterone data were RANK and log transformed, and the analysis was performed on the transformed data. The model for the experiment included phase and cycle (1st and 2nd preovulatory wave after weaning) as the independent variables. Differences between means were analyzed using a Least Significant Difference (LSD) test at a 95% confidence level.

Real-time PCR data for the genes of interest (GOI) were normalized against their respective means for cyclophilin using the Δ Ct method (Δ Ct = Ct_{GOI} - Ct_{cyclophilin}). The cycle threshold (Ct) is defined as the PCR cycle where the fluorescence reaches a determined threshold. Consequently, the Ct and corrected Ct (Δ Ct) value are inversely related to the copy number of the targeted gene initially present in the sample. For the analysis of the temporal changes in mRNA abundance, the Δ Ct values for all GOI were normally distributed except for VEGFA, TEK and KDR in the granulosa cell which were RANK transformed and the analysis was performed on the transformed data. The individual Δ Ct for each GOI were analysed using the MIXED procedure of SAS. The model for the experiment included phases and cycle as the independent variables, and sow as the random variable. Differences between means were analyzed using a Least Significant Difference (LSD) test at a 95% confidence level. For ease of interpretation of the expression profiles the data were converted using the formula $2^{-(\Delta$ Ct - Δ Ct_{calibrator}) and are expressed as relative mRNA abundance \pm SEM. The Δ Ct value obtained for TEK in the granulosa cell during the mid-selection phase

was used as the calibrator value, thus maintaining the relative mRNA abundance for the GOI within and, to a limited extent, between cell types. Finally, correlation analyses were performed across all sows to determine relationships between the expression of each GOI and follicular fluid oestrogen, follicular fluid progesterone and plasma oestrogen concentration, as well as follicle size.

RESULTS

Identification of angiogenic factors from granulosa and theca cells

Using gene ontology annotation, a list of angiogenic factors expressed in the granulosa and theca cells of porcine antral follicles was generated from a global list of transcripts identified as being expressed in these cell types using the Affymetrix GeneChip Porcine Genome Array (See Chapter 3). The analysis revealed that 73 probe sets, representing 54 unique transcripts related to angiogenesis, were expressed in the granulosa cell (Table 5.2). Therefore, based on the 10589 probe sets considered to be expressed in the granulosa cells (ie identified as present and having a signal of ≥ 50 ; data not shown), less than 1% represented angiogenesis-related transcripts. Interestingly, the analysis also revealed that 86 probe sets, representing 65 unique angiogenesis-related transcripts, were expressed in the theca cells (Table 5.2). Again, according to the number of probe sets that were considered to be expressed in the theca cells (10479 probe sets), less than 1% represented angiogenesis-related factors. However, because of the high redundancy observed in several probe sets in both tissues, the percentage of angiogenic genes represented is likely higher in terms of unique transcripts. Among the factors identified, several members of the vascular endothelial growth factor (VEGF) family (3 and 4 members were identified in the granulosa and theca cells, respectively), including VEGFA, and several members of the angiopoietin (ANGPT) family (3 and 5 members were identified in the granulosa and theca cells respectively), including ANGPT1 and 2, were identified

in both the granulosa and theca cells. Based on these analyses, VEGFA and its two related receptors, as well as angiopoietin 1 and 2 and their related receptors, were selected for further real-time PCR analysis. Hypoxia-inducible factor 1a (HIF1A) and angiogenin (ANG) were also of interest and were selected for further analysis.

Assessment of transcript localization and abundance by real-time PCR

Real-time PCR analysis was first used to confirm the presence of selected angiogenic factors in the granulosa and theca cells identified with the microarray and to determine the relative abundance (within cell type) of these transcripts. Real-time PCR analysis revealed that *VEGFA* mRNA and mRNA of its receptors fms-related tyrosine kinase 1 (*FLT1*) and kinase insert domain receptor (*KDR*), were expressed in both granulosa and theca cells, confirming the microarray results (Figure 5.1A and 5.2A). *KDR* mRNA was found to be expressed exclusively in the theca cells, by microarray, and this was confirmed by real-time PCR. Although *KDR* mRNA was also detected by real-time PCR in granulosa cells, its abundance was very low (Figure 5.1B and 5.2C). In contrast, although *FLT1* mRNA was not detected in either cell type by microarray, it was shown by real-time PCR to be expressed in both granulosa and theca cells (Figure 5.1B and 5.2C). Similar to *KDR* mRNA, the abundance of *FLT1* mRNA in the granulosa cells was generally very low with the exception of the final selection phase after the LH surge when its expression increased dramatically (Figure 5.1B). Furthermore, *FLT1* mRNA expression in the theca cells was found to be relatively high compared to the other genes, which was not in agreement with the microarray data (Figure 5.2C). Angiopoietin 1 and 2 mRNA, as well as their receptor TEK tyrosine kinase (*TEK*) mRNA, were also detected in both granulosa and theca cells using real-time PCR. Although detection of *ANGPT1* mRNA in both granulosa and theca cells confirmed the microarray results, *ANGPT1* mRNA abundance in both granulosa and theca cells was very low (Figure 5.1A and 5.2A). Microarray analysis showed *TEK* mRNA to be expressed exclusively in the theca cells and although, this transcript was also detected by real-time PCR in

the granulosa cells, its abundance was extremely low, approaching the limit of detection (Figure 5.1B and 5.2C). Although microarray analysis indicated that ANGPT2 mRNA was considered to be exclusively expressed in the theca cell, expression was detected in both granulosa and theca cells by real-time PCR; however consistent with the microarray results, its expression was relatively high in theca cells and low in the granulosa cells (Figure 5.1A and 5.2A). Finally, HIF1A and ANG mRNA were localized to both cell types, as observed by microarray (Figure 5.1A and 5.2A, B). Overall, the cellular localization of 6 of the 8 genes studied and their relative expression levels are similar between the microarray and real-time PCR analyses.

Temporal granulosa and theca cell mRNA expression profiles

Real-time PCR analysis was also used to determine the temporal changes in mRNA abundance of the 8 angiogenic factors investigated in granulosa and theca cells. Interestingly, the mRNA expression pattern observed for each of the ligands (*VEGFA*, *ANGPT1*, *ANGPT2*, *ANG* and *HIF1A*) was very similar between the granulosa and theca cells (Figure 5.1A and 5.2A). *HIF1A* mRNA was the most abundant transcript in both cell types and although the effect of the stage of follicle development was only significant in the granulosa cells ($P < 0.01$), its expression profile was identical in the theca cell. *HIF1A* mRNA expression in granulosa cells increased from the recruitment to the mid-selection phase and although no statistical differences were observed between the mid-selection and the final selection phase, the mean abundance of *HIF1A* mRNA peaked during the final selection phase (Figure 5.1A). *HIF1A* mRNA abundance then dropped to its lowest level after the preovulatory LH surge. Interestingly, *HIF1A* mRNA abundance in the theca cells positively correlated with mRNA abundance for several other genes, including *VEGFA*, *FLT1*, *KDR*, *ANGPT1*, *TEK* ($r = 0.82$, $P < 0.001$ (*VEGFA*); $r = 0.86$, $P < 0.001$ (*FLT1*); $r = 0.75$, $P < 0.001$ (*KDR*); $r = 0.69$, $P < 0.01$ (*ANGPT1*) and $r = 0.50$, $P < 0.05$ (*TEK*) and *HIF1A* mRNA abundance in the granulosa cells also correlated positively with that of *VEGFA* ($r = 0.64$, $P < 0.01$). *HIF1A* mRNA abundance in the granulosa and theca cells was also

positively correlated with plasma oestrogen concentration ($r = 0.58$, $P < 0.01$; $r = 0.51$, $P < 0.01$, respectively).

The abundance of VEGFA mRNA in the granulosa and theca cells tended to be affected by the stage of follicle development ($P < 0.1$), and mean VEGFA mRNA abundance in both granulosa and theca cells was high during final selection phase and then fell during the final selection phase after the LH surge (Figures 5.1A and 5.2A). Interestingly, VEGFA mRNA abundance in the theca cells positively correlated with FLT1, KDR and HIF1A mRNA abundance ($r = 0.80$, $P < 0.001$; $r = 0.71$, $P < 0.001$ and $r = 0.82$, $P < 0.001$, respectively) and also positively correlated with HIF1A in the granulosa cells ($r = 0.64$, $P < 0.01$).

The angiopoietin ligands were also found to have very similar expression profiles in both cell types. ANGPT1 mRNA abundance increased ($P < 0.05$) from the recruitment to the final selection phase and then dropped during the final selection phase post-LH (Figure 5.1A and 5.2A). ANGPT1 mRNA abundance in the theca cells was positively correlated with its receptor (TEK) mRNA abundance ($r = 0.73$, $P < 0.01$). In contrast, ANGPT2 mRNA abundance was low during the recruitment phase, peaked during the mid-selection phase and then returned to lower abundance during the final selection phase pre- and post-LH surge (Figure 5.1A and 5.2A). In the theca cells, the abundance of ANGPT2 mRNA was positively correlated with VEGFA mRNA abundance ($r = 0.73$, $P < 0.01$). Finally, ANG mRNA abundance in granulosa cells was low during the recruitment phase but had already increased to its highest abundance by the mid-selection phase (Figure 5.1A). It then remained high in the final selection phase but returned to low abundance during the final selection phase after the LH surge. An interaction between phase of follicle development and first or second cycle was observed in the theca cells ($P < 0.05$). As shown on Figure 5.2B, angiogenin mRNA abundance did not change between the first and second cycle during the recruitment, mid-selection and final selection phase, however, its relative mRNA abundance during the final selection phase post-LH surge was higher ($P < 0.05$) in the second cycle.

In contrast to the ligands, the expression pattern of the receptor mRNA was relatively consistent within cell type but differed between the granulosa and theca cells. In granulosa cells, the mRNA abundance for *FLT1* and *TEK* remained mostly relatively unchanged during the recruitment, mid-selection and final selection phase but peaked during the final selection phase after the preovulatory LH surge (Figure 5.1B). In contrast, *KDR* mRNA abundance did not change dramatically but was slightly higher ($P < 0.05$) during the mid-selection and final selection phase (Figure 5.1B). In the theca cells, *KDR* mRNA was not affected by the stage of follicle development while *FLT1* mRNA tended ($P < 0.1$) to be affected by the stage of follicle development and reached peak abundance at the final selection phase of development (Figure 5.2C). Finally, *TEK* mRNA abundance increased from the recruitment phase to the mid-selection phase and remained constant until after the LH surge (Figure 5.2C).

Sow and follicle characteristics

As reported in Chapter 4, the reproductive characteristics of the sows euthanized during the 1st and 2nd post-weaning preovulatory wave of follicular development were very similar. However, the 3 largest follicles on the ovary of the sows euthanized during the 2nd post-weaning preovulatory wave of follicular development, irrespective of the phase of follicular development during which they were isolated, were approximately 0.5 mm larger. Although concentrations of follicular fluid oestradiol during the final selection phase appeared to be substantially higher in the sows studied at the 2nd cycle after weaning, this effect was not statistically significant in the subpopulation of animals used for that experiment. Further evaluation of follicular fluid oestradiol from the larger subset of sows in the current study established an effect of post-weaning cycle on follicular fluid oestradiol concentration in the pre-LH surge period (Table 5.3). After the preovulatory LH surge, follicular fluid oestradiol concentration fell to similar level in sows from the 1st and 2nd cycle. Analysis of follicular fluid progesterone concentration before and after the LH surge did not reveal any differences between the two groups of sows.

DISCUSSION

It is becoming increasingly evident that modulation of the follicle vasculature is essential for follicle development. The identification of several angiogenic factors in the developing antral follicle of different mammalian species, as well as the abnormalities observed in follicles deprived of specific factors, illustrates the importance of understanding the molecular mechanisms responsible for the modulation of the follicular blood supply (Fraser, 2006, Stouffer *et al.*, 2001, Tamanini and De Ambrogi, 2004). The vascular endothelial growth factor family and its receptors, as well as the angiopoietin family and its receptor, have been shown to be particularly important in the ovarian follicle of several species (Fraser, 2006, Stouffer *et al.*, 2001, Tamanini and De Ambrogi, 2004). In addition, hypoxia-inducible factor 1A and angiogenin also appear to be important in modulating the follicle vasculature (Lee *et al.*, 1999, Neeman *et al.*, 1997). Our results show that using a combination of microarray analysis and gene ontology annotation, these genes were all identified as being expressed in both the granulosa and theca cells of the porcine ovarian follicle. In order to gain insight into the physiological relevance of these genes in the developing pig antral follicle and to assess their role in determining the differences in follicle quality and embryo survival observed between the first and second post-weaning preovulatory wave of follicle development, their expression pattern in the granulosa cell and theca cells was assessed by real-time PCR.

At the outset, it is important to recognize that the follicular tissues recovered for analysis came from a well-defined *in vivo* experimental paradigm in which differences in follicle and oocyte maturity have been established as the likely cause of differences in subsequent fecundity in the sows (Clowes *et al.*, 1994, Foxcroft *et al.*, 2007, Paradis *et al.*, 2009, Zak *et al.*, 1997). Furthermore, the basis for exploring differences in gene expression in different sized follicles was based on the sequential recovery of follicles during the known preovulatory phase of follicle development, and follicular status was validated on the basis of

size and follicular fluid oestradiol concentration. Therefore, the biological relevance of the current data reported, in relation to the *in vivo* process of folliculogenesis in the sows, will be much greater than data reported from other studies with ovarian tissues obtained from prepubertal gilts subjected to exogenous gonadotrophin stimulation or other manipulations.

As an initial step in developing this study, the use of microarray analysis in combination with gene ontology annotation was extremely useful in identifying the angiogenic factors expressed in the granulosa and theca cells of pig antral follicle and revealed a list of 54 and 65 unique angiogenic transcripts for the granulosa and theca cells, respectively. In contrast to candidate gene studies based on selection of genes from the existing literature that may or may not be relevant to the species studied, the approach used in the current experiment allowed the generation of a large list of angiogenic transcripts, highly relevant to the pig. In addition, this approach also allowed the identification of families of genes that are represented by multiple members, as was the case for the vascular endothelial growth factor and the angiopoietin families. This increases the likelihood that these families mediate important functions in the follicle. A comparable approach was described by Pan *et al.* (2005), in which the authors explored their database to identify mouse oocyte factors related to cell cycle regulation, and others that could be involved in the acquisition of oocyte meiotic competence and oocyte-somatic cell interactions. Although, the remainder of their analysis was different, these authors used gene ontology to specifically target factors of interest and evaluate the changes in their expression pattern in the oocyte during follicle development.

Real-time PCR analysis based on our microarray results confirmed the cell type source of 6 of the 8 factors identified by microarray analysis and further evaluation of ANGPT2 and FLT1 mRNA reveal possible reasons for the discrepancies observed between the microarray results and the real-time PCR analysis. First, both genes possess transcript variants in the human and it is possible that variants also exist in the pig. Consequently, the primers used for

real-time PCR may detect different variants detected than the probe set used for the microarray analysis. In addition, *FLT1* mRNA is a very long transcript and since the cDNA amplification step prior to hybridization to the microarray relied on the use of oligo dT, it is also possible that the transcript was truncated, precluding its detection by microarray. The use of random hexamers in combination with oligo dT during the reverse transcription step could have eliminated this discrepancy during the real-time PCR analyses. However, for the most part, the observations made by real-time PCR confirmed those made by microarray and validated the usefulness of using microarray in combination with gene ontology annotation to identify an array of transcripts related to specific functions, in this case angiogenesis.

Moreover, the localization of *VEGFA*, *FLT1* and *KDR* mRNA are consistent with previous studies in which it was shown that the mRNA of two porcine isoforms of *VEGFA* localized to the granulosa and theca cells of small, medium and large prepubertal gilt follicles (Barboni *et al.*, 2000, Shimizu *et al.*, 2002). It was also shown that the receptors *FLT1* and *KDR* mRNA were present in the theca cells of the same follicle (Shimizu *et al.*, 2002). Unfortunately, the authors did not investigate the presence of the receptors in the granulosa cells, however *KDR* mRNA has been observed in bovine granulosa cells (Greenaway *et al.*, 2004). The expression patterns of *VEGF* mRNA observed in both cell types, as well as that of *FLT1* mRNA in the theca cell in the current experiment, are consistent with a role for VEGF during follicle development and suggest that *VEGFA* could play a predominant role in establishing the follicle vasculature necessary during follicle recruitment and selection, and for the maintenance of the vasculature in the preovulatory follicle population. This is consistent with observation in the marmoset monkey in which inhibition of VEGF during the follicular phase results in a marked decrease in the number of large follicles, accompanied by decreased granulosa and theca cell proliferation and decreased theca cell vasculature (Wulff *et al.*, 2002). Similarly, inhibition of *KDR* significantly delayed the rise in oestradiol production and lengthened the follicular phase in the rhesus monkey (Zimmermann *et al.*, 2002). Moreover,

injection of VEGF gene fragments into the ovarian medulla of miniature gilts in combination with eCG treatment resulted in a significant increase in the number of preovulatory follicles, as well as in the capillary density in the theca cells (Shimizu *et al.*, 2003a). The tendency for *VEGF* mRNA abundance to fall in the granulosa cells isolated during the final selection after the preovulatory LH surge is consistent with the results of Barboni *et al.* 2000, which showed that *VEGFA* mRNA and protein in the granulosa cell and the protein in the follicular fluid sharply decline after receiving a preovulatory dose of hCG. Interestingly, these observations are also consistent with the decline in follicular blood supply observed in the periovulatory period in the ewe (Murdoch *et al.*, 1983). Together, these observations suggest that VEGF is predominantly required for the establishment and maintenance of the follicle vasculature during the recruitment and selection of the preovulatory follicle population and perhaps during the very early stages of luteinisation, but that other factors might be more important for angiogenesis in the early corpus luteum. However, it is very interesting that the granulosa cells isolated during the final selection post-LH surge showed a marked increase in *FLT1* mRNA, suggesting that their responsiveness to VEGFA is increased. One could suggest that although the intrafollicular levels of VEGFA are decreasing after the LH surge, the previously avascular granulosa cells establish their own vasculature as part of the luteinization process. However, further experiments will be required to assess the physiological significance of this increase in *FLT1* mRNA abundance in the granulosa cells.

Our results also showed that mRNA for *ANGPT1*, *ANGPT2* and their receptor *TEK* were expressed in the granulosa and theca cells of developing porcine preovulatory follicles. This is consistent with results obtained in bovine follicles where the two ligands and their receptor mRNA were found in both granulosa and theca cells (Hayashi *et al.*, 2003, Hayashi *et al.*, 2004). It is also consistent with a study in prepubertal gilts in which *ANGPT1* and *ANGPT2* mRNA were expressed in the granulosa cells, and their receptor *TEK* mRNA was expressed in the theca cells (Shimizu *et al.*, 2003b). Unfortunately, these authors did not investigate the presence of either ligand mRNA in the theca cells, nor did

they investigate the presence of the receptor mRNA in the granulosa cells. The expression patterns for *ANGPT1*, *ANGPT2* and *TEK* mRNA observed in the current study suggest that the requirement for these factors changes during follicle development. First, *ANGPT1* mRNA was found to increase from the recruitment phase, when the ovary contains small antral follicles (3-5mm), to the final selection phase before the LH surge, when the ovary contains only large preovulatory follicles it then fell following the preovulatory LH surge. The positive correlation between *ANGPT1* mRNA abundance and *TEK* mRNA abundance in the theca cells suggests that the stimulatory effect of *ANGPT1* increases with follicular size and that *ANGPT1* becomes increasingly important during follicle selection and for maintenance of the preovulatory population. This is in accordance with the role of *ANGPT1* observed in the rat in which intrabursal injection of *ANGPT1* neutralizing antibody results in a reduction in the number of antral and preovulatory follicles (Parborell *et al.*, 2008). It is also consistent with the results of Hayashi *et al.* (2003), who showed that *ANGPT1* increased oestradiol and progesterone synthesis by the granulosa cells as the follicles grew to the preovulatory stage.

In contrast, *ANGPT2* mRNA abundance in both granulosa and theca cells peaked during the mid-selection phase, when the follicle population ranges from 3-7 mm in diameter and follicles will either be selected to grow and form the preovulatory population or will undergo atresia. Interestingly, *ANGPT2* was shown to antagonize the effect of *ANGPT1* through competitive binding with their receptor *TEK*, potentially leading to degenerative changes in the existing vasculature and to apoptosis (Hanahan, 1997, Maisonpierre *et al.*, 1997). It is possible that the increased expression of *ANGPT2* during the mid-selection phase reflects the increased follicular atresia generally observed in this category of follicles. The strong positive correlation observed between *ANGPT2* and *VEGFA* mRNA abundance in the theca cells is interesting, given the hypothesis of Hanahan (1997) that *ANGPT2* by itself would promote atresia but in the presence of other potent angiogenic factors such as VEGF, could favour the formation of new vasculature by destabilizing the matrix surrounding the blood vessel and thus

allowing the angiogenic factors to stimulate blood vessel formation. In the context of the current experiment, it is also likely that ANGPT2 is favouring angiogenesis in the follicles selected to form the preovulatory population by allowing VEGFA and/or other angiogenic factors to promote blood vessel growth. ANGPT1 would then stabilize the vasculature in the preovulatory follicle, as suggested by its increased expression during the final selection phase before the LH surge. Finally, as seen with *FLT1* mRNA, the granulosa cells isolated during the final selection post-LH surge showed a marked increase in *TEK* mRNA, suggesting that their responsiveness to ANGPTs is augmented. Again, as with VEGFA, this could indicate that although the intrafollicular levels of *ANGPT1* and *ANGPT2* mRNA are low after the LH surge, the previously avascular granulosa cells are establishing their own vasculature as part of the early process of luteinization. However, further experiments will also be required to assess the physiological significance of this increase in *TEK* mRNA abundance.

Another interesting finding in our experiment is the expression of the transcription factor *HIF1A* mRNA, which was detected in the granulosa and theca cells of all follicle categories and increased in granulosa cells from the recruitment to the final selection phase prior to the LH surge. HIF1A is a transcription factor that, under hypoxic conditions, drives the transcription of several genes, including VEGFA, thereby allowing the cell or tissue to adapt to those conditions (Milkiewicz *et al.*, 2006). Therefore, the changes observed in *HIF1A* mRNA expression in the current study suggest that as the follicles grow, the cells are exposed to increasingly hypoxic conditions. This is consistent with a study by Basini *et al.* (2004), who showed that oxygen tension in porcine follicular fluid is negatively correlated with follicle size. However, the most interesting aspect of *HIF1A* mRNA abundance is that it correlates strongly and positively with the mRNA abundance of several other factors. Indeed, in the theca cells, *HIF1A* mRNA abundance correlated with that of *VEGFA*, *FLT1* and *KDR*, as well as *ANGPT1* and *TEK*, while in the granulosa cells, *HIF1A* mRNA abundance correlated positively with *VEGFA* mRNA. These observations suggest that under increasingly hypoxic conditions, several angiogenic factors are

upregulated in the pig follicle, consistent with current literature suggesting that hypoxic conditions are known to induce VEGFA and ANGPT2 expression (Stouffer *et al.*, 2001). However, the potential for HIF1A to be modulated by the endocrine environment cannot be disregarded, particularly given that *HIF1A* mRNA abundance was positively correlated with plasma oestrogen concentrations, in the present study. This is in accordance with several other studies which showed that *HIF1A* mRNA in human luteinized granulosa cells is stimulated by hCG (Christenson and Stouffer, 1997, Fraser *et al.*, 2005, Koos, 1995, Laitinen *et al.*, 1997, Lee *et al.*, 1997, Neulen *et al.*, 1995, Ravindranath *et al.*, 1992, van den Driesche *et al.*, 2008). It is therefore likely that both hypoxia and the gonadotrophins are capable of stimulating *HIF1A* mRNA in the follicle, which ultimately modulates the expression of several other angiogenic factors necessary to establish and maintain the follicular vasculature.

Finally, as reported in the bovine follicle (Lee *et al.*, 1999), angiogenin was expressed in the granulosa and theca cells of all follicle categories. In the granulosa cells, the abundance of angiogenin mRNA peaked during the mid-selection and final selection phase, suggesting that it may act in concert with VEGFA and ANGPT1 to modulate angiogenesis during follicle selection and in the preovulatory follicle population. However, perhaps the most interesting finding of this experiment is the observed interaction between the phase of follicular development and the post-weaning cycle of the animal at the time of tissue recovery for angiogenin mRNA abundance in the theca cells. During the final selection phase following the preovulatory LH surge, ANG mRNA abundance was higher in theca cells recovered from the sow during the second cycle compared with those recovered during the first cycle after weaning. Coincidentally, the preovulatory follicle population prior to the LH surge isolated from the sows during the second cycle were more oestrogenic and were also larger (Foxcroft *et al.*, 2007, Paradis *et al.*, 2009), clearly illustrating differences in follicle maturity in sows during the first versus the second cycle of preovulatory follicle development. In addition, CL weights taken at day 9 after ovulation in similar experiment were found to be higher in the animal ovulating at

the second post-weaning estrus (Patterson *et al.*, unpublished observation). These observations offer a potential explanation for the increased embryo survival observed by day 30 of gestation in the animals bred during the second estrus post-weaning (Foxcroft *et al.*, 2007). Our original hypothesis was that increased angiogenin mRNA abundance in the luteinizing follicle would favour the development of more efficient corpora lutea, as suggested by the difference in CL weight at day 9 of gestation, which would ultimately provide better support for pregnancy. However, no differences in plasma progesterone were observed 60-72 hours after ovulation, suggesting that luteal efficiency may not be affected in those animals (Patterson *et al.*, unpublished observation). However, the most engaging hypothesis is that increased angiogenin expression in the follicle, perhaps as a reflection of follicle maturity, would lead to increased vasculature in the preovulatory follicle and in the early CL. In turn, this would lead to an earlier rise in progesterone which would allow for faster and more efficient priming of the oviduct and uterine environment, favouring early embryo development as discussed by Foxcroft *et al.* (2001). Moreover, increased follicle vasculature could also favour improved oocyte maturity, which would also improve the likelihood of successful embryo development. Several lines of evidence support this line of thinking. First, angiogenin is a potent angiogenic factor originally purified from human carcinoma cells (Fett *et al.*, 1985) and it is therefore probable that elevated expression of *ANG* mRNA also results in better vascularization of the preovulatory follicle. Secondly, angiogenin concentrations in the follicular fluid of women undergoing *in vitro* fertilization was found to correlate with oocyte maturity (Malamitsi-Puchner *et al.*, 2003). By analogy, better vascularization of the periovulatory follicle might favour the transfer of ovarian steroids into the sub-ovarian counter-current system in the pig. This would allow the oviduct to be exposed to high concentrations of steroids before the peripheral rise, enabling for faster exposure of the oviduct and uterus to progesterone, which together might ultimately impact embryo survival. Overall, these observations support the hypothesis that increased follicle vasculature in the periovulatory period would ultimately benefit embryo survival.

In conclusion, the present study clearly demonstrates the presence of a complex angiogenic system in the preovulatory porcine follicle. To our knowledge this is the first study to investigate the expression of these factors in the context of *in vivo* preovulatory follicle development in the pig. Our results clearly show that angiogenesis is developmentally regulated in the porcine follicle and that this regulation is species specific. Finally, although additional experiments will be required to assess the exact physiological relevance of the changes observed in angiogenin expression in the theca cells of preovulatory follicle after the LH surge, this study provides evidence to suggest that angiogenin is important in the periovulatory period and is potentially involved in modulating the differences in embryo survival linked to differences in the first and second post-weaning preovulatory wave of follicle development.

Table 5.1 Details of primers and probes used for Real-Time PCR

Gene	AC number	Primer	Sequence 5' --> 3'	Product size	Annealing/Extension Temperature (°C)
ANG	NM_001044573	Forward	TGGCTAAGGATGAAGACAGGTACA	64 bp	60
		Reverse	CCCTTTGGTTTGGCATCGTA		
		Probe	ACACTTCCTGACCCAGC		
ANGPT1	NM_213959	Forward	TTTCCTTTCCTTTCCTTCCCT	58 bp	60
		Reverse	TGGTTGCTGCACCCTATGTG		
		Probe	GCTGCCATTCTGAC		
ANGPT2	NM_213808	Forward	CCAGGTGTTAGTATCCAAGCAAAA	67 bp	60
		Reverse	CGTGGCAGTCACCAGTTGTT		
		Probe	TCCATCATTGAAGAACTAG		
FLT1	AY566244	Forward	CAACAGGACGGCAAAGACTACA	56 bp	60
		Reverse	CCGCTGTTGCTCGTCAGAA		
		Probe	CCCCCTCAACGCC		
HIF1A	NM_001123124	Forward	CCATGCCCCAGATTCAAGAT	64 bp	60
		Reverse	GGTGA ACTCTGTCTAGTGCTTCCA		
		Probe	CCAGCTAGTCCTTCTG		
KDR	EU714326	Forward	GGCTGCTTCTTGT CATCGTTCT	59 bp	60
		Reverse	CTTCAGTTCCCCTCCATTGG		
		Probe	CGGACCGTTAAGCGG		
PPIA	AY266299	Forward	AATGCTGGCCCCAACACA	56 bp	60
		Reverse	TCAGTCTTGGCAGTGCAAATG		
		Probe	ACGGTTCCCAGTTTT		
TEK	XM_001926034	Forward	CCCTCACCTGTAGAAGCCATCT	69 bp	60
		Reverse	GGCTCAGAAAACACATGACAAAGA		
		Probe	ATTTCA TTTGGTAATCTGA		
VEGFA	NM_214084	Forward	GCCCACTGAGGAGTTCAACATC	59 bp	60
		Reverse	GGCCTTGGTGAGGTTTGATC		
		Probe	CCATGCAGATTATGC		

Table 5.2 List of angiogenic factors expressed in the granulosa (GC) and theca (TC) cells of porcine antral follicles identified using the Affymetrix GeneChip Porcine Genome Array in combination with gene ontology annotation

Probe Set ID	Name	Gene Symbol	GenBank	raw signal	
				GC	TC
Ssc.9902.1.A1_at	Activin receptor type I precursor	ACVR1	BQ597961	207	309.35
Ssc.1718.1.S1_at	Angio-associated migratory cell protein	AAMP	CN160887	86.55	114.35
Ssc.11079.1.A1_at	Angiogenin precursor (Ribonuclease 5)	ANG	NM_213936.1	380.4	750
Ssc.4679.1.S1_at	Angiogenin precursor (Ribonuclease 5)	ANG	CN157788	182.45	219.25
Ssc.13805.1.S1_at	angiomin	AMOT	CN158845	68.25	196.35
Ssc.4753.1.A1_at	Angiopoietin 1 receptor precursor	TEK	CK451939		87.15
Ssc.16730.1.S1_at	Angiopoietin-1 precursor	ANGPT1	NM_213959.1	168.1	
Ssc.24374.1.S1_at	Angiopoietin-1 precursor	ANGPT1	CK452350	204.5	117.95
Ssc.6943.1.A1_at	Angiopoietin-1 precursor	ANGPT1	BF703917	86.3	
Ssc.240.1.S1_at	Angiopoietin-2 precursor (ANG-2)	ANGPT2	NM_213808.1		229.45
Ssc.28458.1.A1_at	Angiopoietin-related protein 3 precursor	ANGPTL3	CN025175	119.5	98.55
Ssc.17345.1.S1_at	Angiopoietin-related protein 4 precursor	ANGPTL4	AY307772.1	63.6	
Ssc.8980.1.A1_at	Angiopoietin-related protein 4 precursor	ANGPTL4	BI183736	441.5	466.65
Ssc.12241.1.A1_at	Annexin A2	ANXA2	CB471539	1720.25	1825.65
Ssc.11118.1.S1_at	ATP synthase beta chain, mitochondrial precursor	ATP5B	AJ458056	1697.65	1835.6
Ssc.18170.1.S1_at	ATP synthase beta chain, mitochondrial precursor	ATP5B	CF795803	488.95	559.95
Ssc.20283.1.S1_at	ATPase inhibitor, mitochondrial precursor	ATPIF1	CF792750	1072.2	1249
Ssc.6833.1.S1_at	B-cell translocation protein 1	BTG1	CB481644	839.9	526.7
Ssc.14003.1.S1_a_at	Beta-catenin	CTNNB1	NM_214367.1	769.2	774.95
Ssc.16690.1.S1_at	Bone morphogenetic protein 4 precursor	BMP4	CN159298		70.35
Ssc.12939.1.S1_at	Cadherin-13 precursor	CDH13	CK465596		99.85
Ssc.7268.1.A1_at	Chondromodulin-I precursor	LECT1	BQ598411	217.25	69.95
Ssc.16475.1.S1_at	Collagen alpha 3(IV) chain precursor	COL4A3	CB287584	980.4	557.15

Ssc.6900.1.A1_at	Collagen alpha 3(IV) chain precursor	COL4A3	BF711595	250.7	246.35
Ssc.8562.2.S1_a_at	Connective tissue growth factor precursor	CTGF	U83916.1		66.5
Ssc.8562.3.A1_at	Connective tissue growth factor precursor	CTGF	BI181686	879.2	1461.05
Ssc.9720.1.A1_at	CYR61 protein precursor	CYR61	CF365800	248.2	398.8
Ssc.27171.1.S1_at	Delta-like protein 4 precursor	DLL4	CN154752	105.75	
Ssc.1276.1.S1_at	DNA-binding protein inhibitor ID-1	ID1	CK464986	162.3	383.35
Ssc.120.1.S1_at	Endoglin precursor	ENG	NM_214031.1		281
Ssc.3231.1.S1_at	Endoribonuclease Dicer	DICER1	BX674333	57.5	
Ssc.3549.1.S1_at	Endothelial PAS domain protein 1	EPAS1	BI184638	557.1	888.95
Ssc.8965.1.A1_at	Endothelial PAS domain protein 1	EPAS1	BF708869		145.95
Ssc.4212.1.A1_at	ETS-domain protein	ELK3	CF363264		155.05
Ssc.26269.1.S1_at	Fibroblast growth factor-18 precursor	FGF18	BX922015	500.85	96.75
Ssc.29077.1.S1_at	GDP-fucose protein O-fucosyltransferase 1 precursor	POFUT1	CO948374	271.2	189.1
Ssc.6022.1.A1_at	GDP-fucose protein O-fucosyltransferase 1 precursor	POFUT1	BI402657	148.2	83.45
Ssc.6352.1.S1_at	Glutathione peroxidase 1	GPX1	NM_214201.1	337.75	464.9
Ssc.115.1.S1_s_at	Heme oxygenase 1	HMOX1	X60677.1	270.95	514.55
Ssc.24835.1.S1_at	Heparin-binding growth factor 1 precursor	FGF1	CK465956	169.65	94.8
Ssc.4271.1.S1_at	HIV-1 Tat interactive protein 2	HTATIP2	CK462444	701.7	413.45
Ssc.3428.1.S1_at	Homeobox protein	PKNOX1	CK451210	84.9	
Ssc.5542.1.A1_at	Hypoxia-inducible factor 1 alpha	HIF1A	CB480474	1433.1	897.5
Ssc.390.1.A1_at	Hypoxia-inducible factor 1 alpha	HIF1A	AJ439692.1	109.65	
Ssc.390.2.A1_at	Hypoxia-inducible factor 1 alpha	HIF1A	AY485675.1	113.4	
Ssc.390.2.S1_at	Hypoxia-inducible factor 1 alpha	HIF1A	AY485675.1	97.45	
Ssc.20.1.S1_at	Interleukin-18 precursor	IL18	AY450287.1		265.7
Ssc.8466.1.A1_at	Jagged 1 precursor	JAG1	BF704538	79.15	67
Ssc.9400.1.A1_at	Jagged 1 precursor	JAG1	CO943323	667.85	620.5
Ssc.13283.1.S1_at	Leptin receptor gene-related protein	LEPR	BI404777	81.9	
Ssc.816.1.S1_at	Leptin receptor gene-related protein	LEPR	CF790758	494.8	541.9
Ssc.734.1.S1_at	Matrix metalloproteinase-14 precursor	MMP14	NM_214239.1		111.85

Ssc.28514.1.S1_at	melanoma-associated chondroitin sulfate proteoglycan 4	CSPG4	CN069810	94.3	160.2
Ssc.11321.1.S1_at	Mitogen-activated protein kinase 7	MAPK7	CK449659	74.55	100.95
Ssc.17295.2.S1_at	Myosin heavy chain, nonmuscle type A	MYH9	BG381946	671.2	875.7
Ssc.17295.1.S1_at	Myosin heavy chain, nonmuscle type A	MYH9	CA781091	778.05	1589.85
Ssc.21222.1.A1_at	NADPH oxidase homolog 1	NOX1	CF789645	62.9	
Ssc.24810.1.A1_at	Neurofibromin	NF1	CK467609	254.55	367.2
Ssc.21862.1.A1_at	Neuropilin-2 precursor	NRP2	BG608506		109.15
Ssc.24899.1.S1_at	Neuropilin-2 precursor	NRP2	CK466196		145.75
Ssc.30598.1.A1_at	Neuropilin-2 precursor	NRP2	CO994833		95.95
Ssc.2695.1.S1_at	Nucleolin	NCL	AJ657247	442.5	517.25
Ssc.2695.2.S1_a_at	Nucleolin	NCL	BP157354	141.1	125.6
Ssc.10451.1.S1_at	Pigment epithelium-derived factor precursor	SERPINF1	BI181553		327.6
Ssc.9781.1.S1_at	Plasminogen activator inhibitor-1 precursor	SERPINE1	NM_213910.1	1370.85	717.55
Ssc.1551.1.S1_at	Plexin D1 precursor	PLXND1	AW485849		277.85
Ssc.12286.2.A1_at	Probable transcription factor PML	PML	BX926965		60.4
Ssc.9392.2.S1_at	Pro-epidermal growth factor precursor	EGF	BE013075	54.05	
Ssc.9392.3.A1_at	Pro-epidermal growth factor precursor	EGF	CF368947	84.45	
Ssc.10226.1.A3_at	ras homolog gene family, member B	RHOB	CN161862	1020.8	1306.85
Ssc.10226.2.A1_at	ras homolog gene family, member B	RHOB	BI185309	182.15	206.3
Ssc.5000.1.A1_at	Receptor protein-tyrosine kinase erbB-2 precursor	ERBB2	BI185975	321.75	346.45
Ssc.21264.1.A1_at	Receptor-type protein-tyrosine phosphatase mu precursor	PTPRM	AW437058		230.35
Ssc.27106.1.A1_at	Receptor-type protein-tyrosine phosphatase mu precursor	PTPRM	CN166740		70
Ssc.31029.1.A1_at	Receptor-type protein-tyrosine phosphatase mu precursor	PTPRM	CF175718	501.8	456.15
Ssc.13822.1.A1_at	Reticulon 4	RTN4	BM190281	122.4	90.6
Ssc.6865.1.S1_at	Reticulon 4	RTN4	CO991426	952.85	1020.2
Ssc.12877.1.A1_at	Rho GTPase activating protein 24	ARHGAP24	BI404040		68.8
Ssc.30055.1.A1_at	Runt-related transcription factor 1	RUNX1	CO949206	310.7	138.35

Ssc.13645.1.A1_at	Secretogranin II precursor	SCG2	BX676772	142.3	
Ssc.18947.1.A1_at	Serine protease inhibitor Kazal-type 5 precursor	SPINK5	CF364907	55.35	
Ssc.1577.1.S1_at	Serum response factor	SRF	CN156605	72.85	98.75
Ssc.5093.1.A1_at	SHC transforming protein 1	SHC1	CK450776	271.65	375.45
Ssc.14923.1.S1_at	Sphingosine kinase 1	SPHK1	BI184582	90.5	
Ssc.26221.1.S1_at	Stromal cell-derived factor 1 precursor	CXCL12	AY312066.1		113.2
Ssc.7243.1.A1_at	Stromal cell-derived factor 1 precursor	CXCL12	CO945718		394.4
Ssc.5330.1.A1_at	TGF-beta receptor type II precursor	TGFBR2	CK464325		703.35
Ssc.10406.1.A1_at	Thrombospondin 1 precursor	THBS1	BI400960		90.5
Ssc.924.1.A1_at	Thrombospondin 1 precursor	THBS1	CB470327		66.3
Ssc.924.2.A1_at	Thrombospondin 1 precursor	THBS1	BQ601960	475.7	1251.2
Ssc.924.3.A1_at	Thrombospondin 1 precursor	THBS1	BF710863		120.25
Ssc.20133.1.A1_at	Thy-1 membrane glycoprotein precursor	THY1	BX676685		386.4
Ssc.3566.2.A1_at	Transcription factor GATA-4	GATA4	CN159277	307.7	320.95
Ssc.15360.1.A1_a_at	Transcription factor SOX-18	SOX18	CK461722		378.2
Ssc.10287.1.A1_at	Transforming growth factor beta 2 precursor	TGFB2	BI400474		57.85
Ssc.1864.1.A1_a_at	Tumor necrosis factor receptor superfamily member Fn14 precursor	TNFRSF12A	BF710490	219.65	324.7
Ssc.1864.1.A1_at	Tumor necrosis factor receptor superfamily member Fn14 precursor	TNFRSF12A	BF710490	146.5	181.9
Ssc.15740.1.S2_at	Vascular endothelial growth factor A precursor	VEGF	CF789391	324	116.85
Ssc.12790.1.A1_at	Vascular endothelial growth factor C precursor	VEGFC	BI404162	269.75	338.95
Ssc.7152.1.A1_at	Vascular endothelial growth factor D precursor	FIGF	BX925296	588.7	534.5
Ssc.25045.1.S1_at	Vascular endothelial growth factor receptor 2 precursor	KDR	BI360137		257.55

Table 5.3 Steroidogenic activity of the follicles isolated during the final selection phase before and after the preovulatory LH surge from sows during the first or second preovulatory wave of follicular development after weaning.

Cycle	Follicular fluid OE2 concentration (ng/ml)		Follicular fluid P4 concentration (ng/ml)	
	FS	FS post-LH	FS	FS post-LH
First	227 ± 41 ^a	28 ± 43 ^c	379 ± 88	246 ± 44
Second	403 ± 37 ^b	8 ± 61 ^c	345 ± 75	183 ± 144

Data are expressed as $\text{mean} \pm \text{SEM}$. Different letters within steroid indicate significant differences ($P \leq 0.05$). Follicular fluid oestradiol (OE2) and progesterone (P4) concentrations were measured during the final selection (FS) phase (first cycle $n=9$; second cycle $n=11$) and the final selection phase post-LH (FS post-LH) (first cycle $n=8$, second cycle $n=4$).

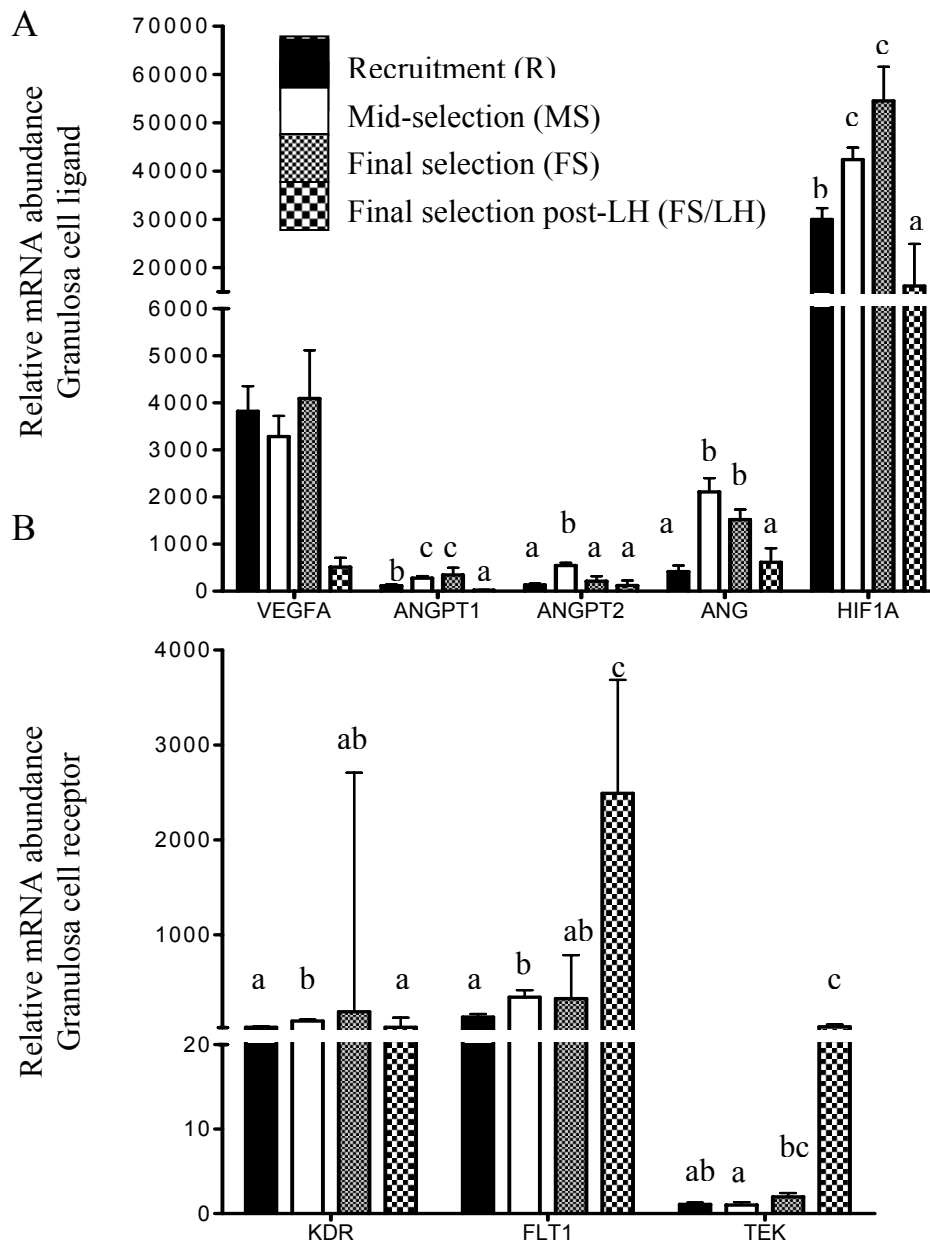


Figure 5.1 Quantification by real-time PCR of A) VEGFA, ANGPT1, ANGPT2, ANG and HIF1A and B) KDR, FLT1 and TEK mRNA abundance in pig granulosa cells during recruitment (n=6), mid-selection (n=6) final selection (n=3) and final selection post-LH (n=3). Data are expressed as means of relative mRNA abundance \pm SEM. Different letters within gene represent significant differences among phases ($P \leq 0.05$).

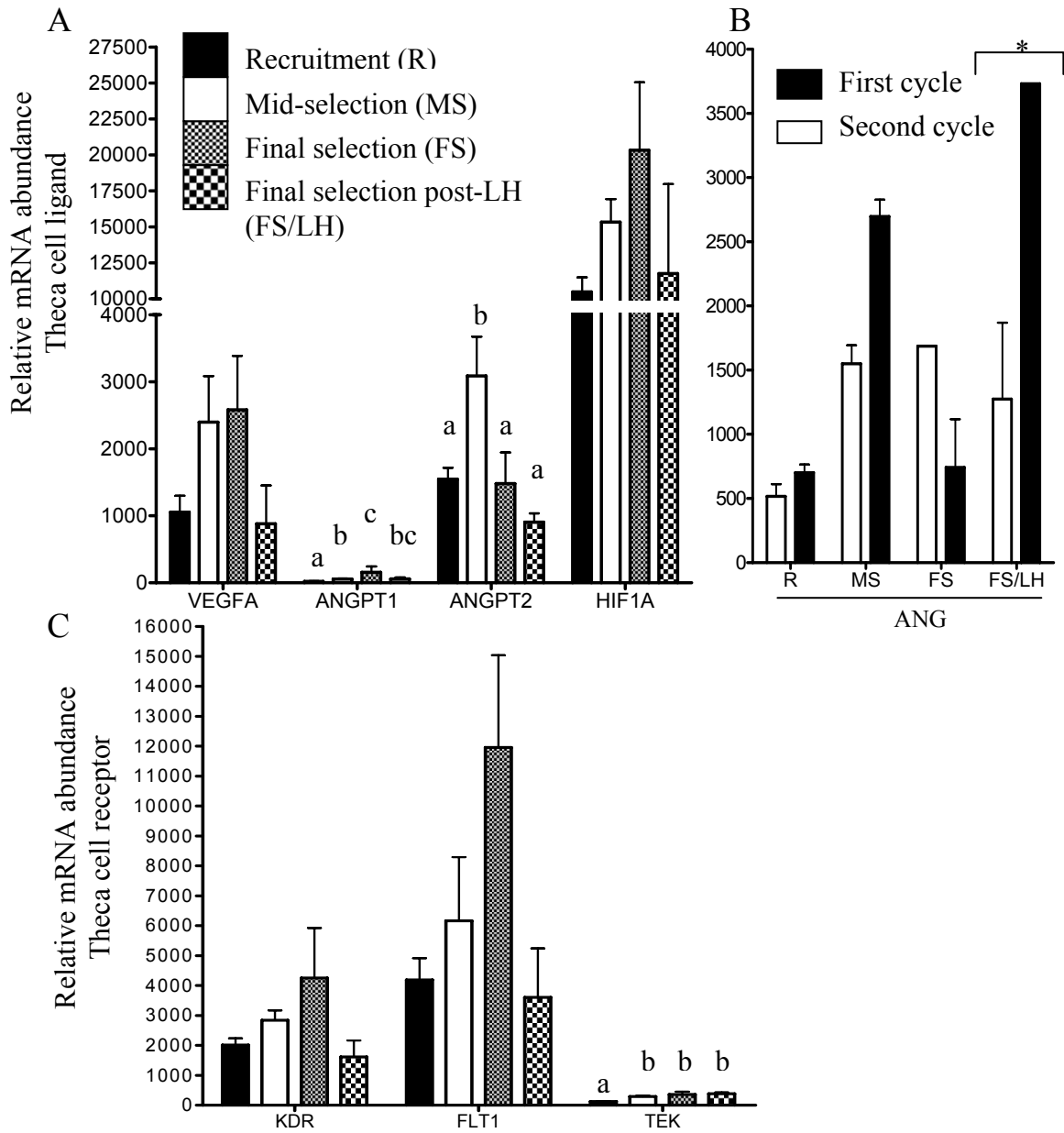


Figure 5.2 Quantification by real-time PCR of A) VEGFA, ANGPT1, ANGPT2 and HIF1A, B) ANG and C) KDR, FLT1 and TEK mRNA abundance in pig theca cell during recruitment (n=6), mid-selection (n=6) final selection (n=3) and final selection post-LH (n=3). Data are expressed as means of relative mRNA abundance \pm SEM. Different letters within gene represent significant differences among phases ($P \leq 0.05$). * Significant difference within phase between cycle ($P \leq 0.05$).

REFERENCES

- Almeida FR, Kirkwood RN, Aherne FX & Foxcroft GR** 2000 Consequences of different patterns of feed intake during the estrous cycle in gilts on subsequent fertility. *J Anim Sci* **78** 1556-1563.
- Ashworth CJ** 1991 Effect of pre-mating nutritional status and post-mating progesterone supplementation on embryo survival and conceptus growth in gilts. *Anim Reprod Sci* **26** 311-321.
- Barboni B, Turriani M, Galeati G, Spinaci M, Bacci ML, Forni M & Mattioli M** 2000 Vascular endothelial growth factor production in growing pig antral follicles. *Biol Reprod* **63** 858-864.
- Basini G, Bianco F, Grasselli F, Tirelli M, Bussolati S & Tamanini C** 2004 The effects of reduced oxygen tension on swine granulosa cell. *Regul Pept* **120** 69-75.
- Christenson LK & Stouffer RL** 1997 Follicle-stimulating hormone and luteinizing hormone/chorionic gonadotropin stimulation of vascular endothelial growth factor production by macaque granulosa cells from pre- and periovulatory follicles. *J Clin Endocrinol Metab* **82** 2135-2142.
- Clowes EJ, Aherne FX & Foxcroft GR** 1994 Effect of Delayed Breeding on the Endocrinology and Fecundity of Sows. *Journal of Animal Science* **72** 283-291.
- Fett JW, Strydom DJ, Lobb RR, Alderman EM, Bethune JL, Riordan JF & Vallee BL** 1985 Isolation and characterization of angiogenin, an angiogenic protein from human carcinoma cells. *Biochemistry* **24** 5480-5486.
- Foxcroft GR** 1997 Mechanisms mediating nutritional effects on embryonic survival in pigs. *Journal of Reproduction and Fertility Suppl* **52** 47-61.
- Foxcroft GR, Dixon WT, Treacey BK, Jiang L, Novak S, Mao J & Almeida FRCL** 2000 Insights into conceptus-reproductive tract interactions in the pig. *Proc Am Soc Anim Sci* **E37** 1-15.
- Foxcroft GR, Vinsky MD, Paradis F, Tse WY, Town SC, Putman CT, Dyck MK & Dixon WT** 2007 Macroenvironment effects on oocytes and embryos in swine. *Theriogenology* **68 Suppl 1** S30-39.
- Fraser HM, Bell J, Wilson H, Taylor PD, Morgan K, Anderson RA & Duncan WC** 2005 Localization and quantification of cyclic changes in the expression of endocrine gland vascular endothelial growth factor in the human corpus luteum. *J Clin Endocrinol Metab* **90** 427-434.

Fraser HM 2006 Regulation of the ovarian follicular vasculature. *Reprod Biol Endocrinol* **4** 18.

Greenaway J, Connor K, Pedersen HG, Coomber BL, LaMarre J & Petrik J 2004 Vascular endothelial growth factor and its receptor, Flk-1/KDR, are cytoprotective in the extravascular compartment of the ovarian follicle. *Endocrinology* **145** 2896-2905.

Hanahan D 1997 Signaling vascular morphogenesis and maintenance. *Science* **277** 48-50.

Hay MR, Cran DG & Moor RM 1976 Structural changes occurring during atresia in sheep ovarian follicles. *Cell Tissue Res* **169** 515-529.

Hayashi KG, Acosta TJ, Tetsuka M, Berisha B, Matsui M, Schams D, Ohtani M & Miyamoto A 2003 Involvement of angiotensin II system in bovine follicular development and atresia: messenger RNA expression in theca interna and effect on steroid secretion. *Biol Reprod* **69** 2078-2084.

Hayashi KG, Berisha B, Matsui M, Schams D & Miyamoto A 2004 Expression of mRNA for the angiotensin II system in granulosa cells during follicular development in cows. *J Reprod Dev* **50** 477-480.

Hazzard TM, Molskness TA, Chaffin CL & Stouffer RL 1999 Vascular endothelial growth factor (VEGF) and angiotensin II regulation by gonadotrophin and steroids in macaque granulosa cells during the peri-ovulatory interval. *Mol Hum Reprod* **5** 1115-1121.

Hazzard TM, Christenson LK & Stouffer RL 2000 Changes in expression of vascular endothelial growth factor and angiotensin-1 and -2 in the macaque corpus luteum during the menstrual cycle. *Mol Hum Reprod* **6** 993-998.

Hunter MG 2000 Oocyte maturation and ovum quality in pigs. *Rev Reprod* **5** 122-130.

Hunter MG, Robinson RS, Mann GE & Webb R 2004 Endocrine and paracrine control of follicular development and ovulation rate in farm species. *Anim Reprod Sci* **82-83** 461-477.

Jiang JY, Macchiarelli G, Miyabayashi K & Sato E 2002 Follicular microvasculature in the porcine ovary. *Cell Tissue Res* **310** 93-101.

Jindal R, Cosgrove JR & Foxcroft GR 1997 Progesterone mediates nutritionally induced effects on embryonic survival in gilts. *J Anim Sci* **75** 1063-1070.

Kanzaki H, Okamura H, Okuda Y, Takenaka A, Morimoto K & Nishimura T 1982 Scanning electron microscopic study of rabbit ovarian follicle microvasculature using resin injection-corrosion casts. *J Anat* **134** 697-704.

Kitai H, Yoshimura Y, Wright KH, Santulli R & Wallach EE 1985 Microvasculature of preovulatory follicles: comparison of *in situ* and *in vitro* perfused rabbit ovaries following stimulation of ovulation. *Am J Obstet Gynecol* **152** 889-895.

Koos RD 1995 Increased expression of vascular endothelial growth/permeability factor in the rat ovary following an ovulatory gonadotropin stimulus: potential roles in follicle rupture. *Biol Reprod* **52** 1426-1435.

Laitinen M, Ristimaki A, Honkasalo M, Narko K, Paavonen K & Ritvos O 1997 Differential hormonal regulation of vascular endothelial growth factors VEGF, VEGF-B, and VEGF-C messenger ribonucleic acid levels in cultured human granulosa-luteal cells. *Endocrinology* **138** 4748-4756.

Lee A, Christenson LK, Patton PE, Burry KA & Stouffer RL 1997 Vascular endothelial growth factor production by human luteinized granulosa cells *in vitro*. *Hum Reprod* **12** 2756-2761.

Lee HS, Lee IS, Kang TC, Jeong GB & Chang SI 1999 Angiogenin is involved in morphological changes and angiogenesis in the ovary. *Biochem Biophys Res Commun* **257** 182-186.

Maisonpierre PC, Suri C, Jones PF, Bartunkova S, Wiegand SJ, Radziejewski C, Compton D, McClain J, Aldrich TH, Papadopoulos N, Daly TJ, Davis S, Sato TN & Yancopoulos GD 1997 Angiopoietin-2, a natural antagonist for Tie2 that disrupts *in vivo* angiogenesis. *Science* **277** 55-60.

Malamitsi-Puchner A, Sarandakou A, Baka S, Hasiakos D, Kouskouni E & Creatsas G 2003 *In vitro* fertilization: angiogenic, proliferative, and apoptotic factors in the follicular fluid. *Ann N Y Acad Sci* **997** 124-128.

Mao J, Treacy BK, Almeida FR, Novak S, Dixon WT & Foxcroft GR 2001 Feed restriction and insulin treatment affect subsequent luteal function in the immediate postovulatory period in pigs: progesterone production *in vitro* and messenger ribonucleic acid expression for key steroidogenic enzymes. *Biol Reprod* **64** 359-367.

Milkiewicz M, Ispanovic E, Doyle JL & Haas TL 2006 Regulators of angiogenesis and strategies for their therapeutic manipulation. *Int J Biochem Cell Biol* **38** 333-357.

Murdoch WJ, Nix KJ & Dunn TG 1983 Dynamics of ovarian blood supply to periovulatory follicles of the ewe. *Biol Reprod* **28** 1001-1006.

Neeman M, Abramovitch R, Schiffenbauer YS & Tempel C 1997 Regulation of angiogenesis by hypoxic stress: from solid tumours to the ovarian follicle. *Int J Exp Pathol* **78** 57-70.

Neulen J, Yan Z, Raczek S, Weindel K, Keck C, Weich HA, Marme D & Breckwoldt M 1995 Human chorionic gonadotropin-dependent expression of vascular endothelial growth factor/vascular permeability factor in human granulosa cells: importance in ovarian hyperstimulation syndrome. *J Clin Endocrinol Metab* **80** 1967-1971.

Pan H, O'Brien M J, Wigglesworth K, Eppig JJ & Schultz RM 2005 Transcript profiling during mouse oocyte development and the effect of gonadotropin priming and development *in vitro*. *Dev Biol* **286** 493-506.

Paradis F, Novak S, Murdoch G, Dyck MK, Dixon WT & Foxcroft GR 2009 Temporal regulation of BMP2, BMP6, BMP15, GDF-9, BMPR1A, BMPR1B, BMPR2 and TGFBR1 mRNA expression in the oocyte, granulosa and theca cells of developing preovulatory follicles in the pig. *Reproduction*. **138** 115-129.

Parborell F, Abramovich D & Tesone M 2008 Intrabursal administration of the antiangiopoietin 1 antibody produces a delay in rat follicular development associated with an increase in ovarian apoptosis mediated by changes in the expression of BCL2 related genes. *Biol Reprod* **78** 506-513.

Ravindranath N, Little-Ihrig L, Phillips HS, Ferrara N & Zeleznik AJ 1992 Vascular endothelial growth factor messenger ribonucleic acid expression in the primate ovary. *Endocrinology* **131** 254-260.

Shimizu T, Jiang JY, Sasada H & Sato E 2002 Changes of messenger RNA expression of angiogenic factors and related receptors during follicular development in gilts. *Biol Reprod* **67** 1846-1852.

Shimizu T, Jiang JY, Iijima K, Miyabayashi K, Ogawa Y, Sasada H & Sato E 2003a Induction of follicular development by direct single injection of vascular endothelial growth factor gene fragments into the ovary of miniature gilts. *Biol Reprod* **69** 1388-1393.

Shimizu T, Iijima K, Sasada H & Sato E 2003b Messenger ribonucleic acid expressions of hepatocyte growth factor, angiopoietins and their receptors during follicular development in gilts. *J Reprod Dev* **49** 203-211.

Stouffer RL, Martinez-Chequer JC, Molskness TA, Xu F & Hazzard TM 2001 Regulation and action of angiogenic factors in the primate ovary. *Arch Med Res* **32** 567-575.

Tamanini C & De Ambrogi M 2004 Angiogenesis in developing follicle and corpus luteum. *Reprod Domest Anim* **39** 206-216.

Tsai S, Cassady JP, Freking BA, Nonneman DJ, Rohrer GA & Piedrahita JA 2006 Annotation of the Affymetrix porcine genome microarray. *Anim Genet* **37** 423-424.

van den Driesche S, Myers M, Gay E, Thong KJ & Duncan WC 2008 HCG up-regulates hypoxia inducible factor-1 alpha in luteinized granulosa cells: implications for the hormonal regulation of vascular endothelial growth factor A in the human corpus luteum. *Mol Hum Reprod* **14** 455-464.

Wulff C, Wilson H, Largue P, Duncan WC, Armstrong DG & Fraser HM 2000 Angiogenesis in the human corpus luteum: localization and changes in angiopoietins, tie-2, and vascular endothelial growth factor messenger ribonucleic acid. *J Clin Endocrinol Metab* **85** 4302-4309.

Wulff C, Wilson H, Wiegand SJ, Rudge JS & Fraser HM 2002 Prevention of thecal angiogenesis, antral follicular growth, and ovulation in the primate by treatment with vascular endothelial growth factor Trap R1R2. *Endocrinology* **143** 2797-2807.

Yamada O, Abe M, Takehana K, Hiraga T, Iwasa K & Hiratsuka T 1995 Microvascular changes during the development of follicles in bovine ovaries: a study of corrosion casts by scanning electron microscopy. *Arch Histol Cytol* **58** 567-574.

Zak LJ, Xu X, Hardin RT & Foxcroft GR 1997 Impact of different patterns of feed intake during lactation in the primiparous sow on follicular development and oocyte maturation. *Journal of Reproduction and Fertility* **110** 99-106.

Zimmermann RC, Xiao E, Bohlen P & Ferin M 2002 Administration of antivascular endothelial growth factor receptor 2 antibody in the early follicular phase delays follicular selection and development in the rhesus monkey. *Endocrinology* **143** 2496-2502.

CHAPTER 6

PORCINE PREEVULATORY GV OOCYTES SECRETE SOLUBLE FACTORS THAT MODULATE CUMULUS CELL PROTEIN EXPRESSION AND POTENTIALLY AFFECT THEIR STEROIDOGENIC ABILITY *IN VITRO*

INTRODUCTION

Ovarian follicle development in large domestic animals occurs over a relatively long period of time (~100 days in the pig) and requires a series of well coordinated events that results in the ovulation of a subset of one or more oocytes competent of undergoing fertilization and early embryonic development. Initially, the oocyte was considered to play a passive role in folliculogenesis, relying mainly on gonadotrophins and metabolic factors to stimulate the granulosa and theca cells which provided the necessary stimulus for oocyte growth and acquisition of developmental competence. However, it has recently become evident that the oocyte plays an active role during follicle development by secreting soluble factors that act on the surrounding somatic cells to modulate its own microenvironment (Gilchrist *et al.*, 2008, Hunter and Paradis, 2009, Juengel and McNatty, 2005). Perhaps the most convincing demonstration of the oocyte's role in controlling follicle development came from Eppig *et al.* (2002) who showed that reaggregated ovaries prepared with the ovarian somatic cells of newborn mice and either primary or secondary oocytes showed dramatic differences in the rate of follicle growth.

Indeed, in recent years, the oocyte has been shown to control several functions in the surrounding somatic cells that are essential for follicle development. The first evidence came from an early study in the rabbit demonstrating that removal of the oocyte from the follicle led to premature luteinization (el-Fouly *et al.*, 1970). Subsequently, the oocyte has been clearly shown to modulate granulosa cell luteinization, as the removal of the oocyte from

mouse, bovine and porcine cumulus-oocyte complexes leads to increased progesterone production by the remaining cumulus cells (Coskun *et al.*, 1995, Li *et al.*, 2000, Vanderhyden *et al.*, 1993) while addition of denuded oocytes to mouse, bovine and porcine mural granulosa cell has the opposite effect (Brankin *et al.*, 2003, Coskun *et al.*, 1995, Gilchrist *et al.*, 2008, Li *et al.*, 2000). Furthermore, evidence suggests that the oocyte controls steroidogenesis in a more general sense. In mouse cumulus cells and pig mural granulosa cells, the oocyte stimulated FSH-induced oestradiol production (Brankin *et al.*, 2003, Vanderhyden *et al.*, 1993), while in pig cumulus cells and in bovine mural granulosa cells the oocyte suppressed oestradiol production (Coskun *et al.*, 1995, Glister *et al.*, 2003). In addition, murine, porcine and bovine oocytes also stimulate cell proliferation, as shown by thymidine incorporation studies (Gilchrist *et al.*, 2003, Hickey *et al.*, 2004, Hickey *et al.*, 2005, Gilchrist *et al.*, 2006). Porcine oocytes increase granulosa and theca cell viability (Brankin *et al.*, 2003), while bovine oocytes reduce cumulus cell apoptosis and likely contribute to cell proliferation (Hussein *et al.*, 2005). Mouse oocytes have been shown to control cumulus cell metabolism as revealed by the down-regulation of several glycolytic enzymes and an amino acid transporter in response to oocyectomy or oocyte removal (Sugiura *et al.*, 2005, Eppig *et al.*, 2005). Interestingly, most of the aforementioned studies have used oocytes isolated from small and medium antral follicles and the effects observed have been generalized to fully grown oocytes, irrespective of the maturational status of the follicles from which they were isolated.

The objectives of this study were: 1) to determine the influence of the factors secreted by the porcine preovulatory oocyte on cumulus cell protein expression and 2) to investigate changes in the expression of candidate genes previously shown to be modulated by the oocyte. To our knowledge, this is the first study to investigate the effect of the porcine oocyte on protein and gene expression in the surrounding cumulus cells, and the first study in any species to utilize oocytes isolated from large oestrogenic preovulatory follicles prior to the LH surge.

MATERIALS AND METHODS

Chemicals and media

Unless otherwise stated all chemicals were obtained from Sigma-Aldrich (St-Louis, Mo, USA). The media used for washing the COCs and oocyctectomized cumulus cells (OOX) was modified Tyrode lactate (TL)-HEPES medium supplemented with 0.1% (w/v) polyvinyl alcohol (PVA) (Funahashi *et al.*, 1997), 50 U/ml of penicillin and 50 µg/ml of streptomycin (Invitrogen, #15070-063, , Burlington, ON, Canada). The phosphate-buffered saline (PBS) pH 7.4 was composed of 137 mM NaCl, 2.7 mM KCl, 8.1 mM Na₂HPO₄ and 1.47 mM KH₂PO₄. The modified M-199 (mM-199) media used for co-culture was Medium 199 with Earle's salts (Invitrogen # 31100-035) supplemented with 26 mM NaHCO₃, 0.91 mM sodium pyruvate, 0.1% PVA, 0.57 mM cysteine, 5 ug/ml insulin, 50 U/ml of penicillin and 50 µg/ml of streptomycin.

Animals

This experiment was conducted in accordance with the guidelines of the Canadian Council on Animal Care and with the approval of the University of Alberta, Faculty Animal Policy and Welfare Committee (Protocol #2005-40B). A total of 18 primiparous F1 sows (Large White x Landrace, Hypor, Regina, SK, Canada) were used for the temporal analysis of gene expression in the granulosa and theca cells as described by Paradis *et al.* (2009) and 20 primiparous F1 sows were used for the co-incubation experiment. Within 48 h after farrowing, litter size was standardized to between 9 and 11 piglets per sow through cross-fostering and routine piglet processing procedures (tail-docking, teeth clipping, ear notching and iron injection) were performed. During lactation, sows were offered fresh feed three times daily and permitted ad libitum access to fresh water. Sows were offered 3.5 kg of feed on the day of farrowing, and during the remainder of lactation the amount of feed offered was increased by 0.5 kg daily until the sows

daily consumption was exceeded by 0.5 kg. Sows were weaned 20.8 ± 3.2 (mean \pm stdev) days after farrowing. After weaning, sows were moved to a common weaned-sow room, housed in individual sow stalls and were fed to appetite twice daily until the day of euthanasia. From the day after weaning, sows were actively heat-checked using fenceline boar contact twice daily (at 0800 and 1400). Onset of standing heat was determined as the midpoint between the time of first detection of standing oestrus and the last time that oestrus was detected. Similarly, the end of standing heat was calculated as the midpoint between the last time that signs of oestrus were detected and the first time after standing heat that no signs of oestrus were detected. Sows were weighed on day 1, 6 and 13 of lactation, at weaning and at the time of euthanasia.

Five groups of four sows were euthanized on day 19 ± 1 after the 1st post-weaning oestrus. At this point the preovulatory follicle population has been established and the oocytes are presumably fully competent to undergo embryo development if fertilized. Follicular fluid oestradiol concentrations (see procedure below) was used to determine whether the follicles were exposed to the LH surge to ensure that the oocytes had not resumed meiosis. The sows used in the experiment were euthanized on-site in a purpose-built necropsy facility according to the Swine Research and Technology Centre standard operating procedures. Prior to euthanasia, a single blood sample was collected into a 10 ml heparinized Vacutainer™ (Becton Dickinson, Franklin Lakes, NJ) by jugular puncture, centrifuged at $1700 \times g$ for 15 min at room temperature and the plasma was then stored at -20°C until assayed for plasma oestradiol concentration.

Sow oocyte collection and culture

Within 1 hour after euthanasia, the sows' ovaries were transported to the laboratory in 50 ml conical tubes containing 0.9% (w/v) warm saline supplemented with antibiotic and antimycotic. Before processing the ovaries, the number and size of all visible follicles was recorded and the follicular fluid from the largest follicle(s) of the D19 animals was collected using an 18-gauge needle attached to a 1 ml disposable syringe for assay of oestradiol concentrations.

Cumulus-oocyte complexes (COC) were collected from both ovaries by aspiration using an 18-gauge needle attached to a 5 ml disposable syringe and the COC's from each sow were processed as a group. The COC's were selected and transferred into a Petri dish containing 15 ml of warm PVA-TL-HEPES. The recovered COC's were washed three times in warm PVA-TL-HEPES to remove any cellular debris. The oocytes were then denuded by vortexing at low speed for 5 min in 200 μ l of PBS in a 1.5 ml microcentrifuge tube. The denuded oocytes (DOs) were observed under a dissecting microscope to ensure that they were intact and free of cumulus cells and then washed three times in 5 ml of warm PVA-TL-HEPES to remove free cumulus cells. Groups of 17-20 DOs from individual animals were then transferred to 36 μ l droplets of culture media under mineral oil for a final concentration of \sim 0.5 DOs/ μ l. The culture media used was composed of mM199 (see Chemicals and Media) supplemented with 10ug/ml of porcine FSH (pFSH) and porcine LH (pLH) ((Folltropin-V and Lutropin-V, Bioniche Animal Health Canada Inc., Belleville, Ontario Canada) and 20 μ M of the phosphodiesterase PDE3 inhibitor cilostamide (BIOMOL International, L.P., # PD-125, Plymouth Meeting, PA, USA). The denuded oocytes were then cultured for an initial 6-h period at 5% CO₂ in a humidified atmosphere at 38.5°C to condition the culture media prior to adding the OOX.

Gilt COC collection and oocytectomy

Gilt ovaries were collected from a commercial slaughterhouse and transported to the laboratory within 2h of collection in a thermoflask containing 0.9% (w/v) warm saline supplemented with antibiotic and antimycotic. The cumulus-oocyte complexes (COCs) were collected by aspiration of 2-6 mm follicles with an 18-gauge needle attached to a 10 ml disposable syringe into a 50 ml conical tube. The COCs were allowed to sediment for 10 min at room temperature and the supernatant was discarded. The pellet was washed twice in warm PVA-TL-HEPES and then transferred into a Petri dish containing 15 ml of warm PVA-TL-HEPES. COCs with at least 2 layers of compact cumulus cells completely surrounding the oocyte were selected and washed an additional 3

times in PVA-TL-HEPES. The oocytes were microsurgically removed from the COC as described by Buccione *et al.* (1990) with the following modification. The oocyte cytoplasm was removed by aspiration with an enucleation pipet rather than by suction through the holding pipe, as this technique was found to cause less damage to the porcine cumulus cells following oocyte removal. The resulting oocyte removed cumulus cells (OOX) were examined under a microscope and OOX with less than 5% of oocyte cytoplasm remaining were used in the subsequent co-incubation. The OOX were then washed three times in mM199 preincubated at 5% CO₂ in a humidified atmosphere at 38.5°C and transferred by groups of 16 into 36 µl droplets of culture media under mineral oil with or without oocytes. The OOX with and without oocyte were then incubated for 22h at 5% CO₂ in a humidified atmosphere at 38.5°C. A total of 8 droplets were used per replicate of which 4 contained 16 OOX without oocytes and 4 contained 16 OOX with the DOs from an individual sow. The co-cultures were repeated 5 times using the same conditions.

After 22h of culture, the OOX from each individual culture droplet were washed twice in 5 ml of warm PBS before being transferred into their own 1.5 ml microcentrifuge tube containing 1 ml of warm PBS. The OOX were centrifuged for 5 min at 8000 x g at room temperature and the supernatant was discarded. The OOX pellet was then snap frozen on dry ice and stored at -80°C. The denuded oocytes were fixed for at least 24h in ethanol:acetic acid (3:1) before being stained for 15 min with a solution of 25 µg/ml of Hoechst 33258 in 100% ethanol. The slides were destained for approximately 10 min in a solution of 20% (v/v) glycerol and the nuclear status of the DOs was then evaluated under a microscope to ensure that the oocyte remained arrested at the germinal vesicle (GV) stage during culture.

Radioimmunoassay

Plasma oestradiol: Oestradiol concentrations were determined in all plasma samples in triplicate in a single RIA using the method of Yang *et al.* (2000).

Extraction efficiency was 72.4 ± 0.6 % and estimated potencies were not corrected for recovery. Assay sensitivity, defined as 86 % of total binding, was 0.35 pg/ml. The intra-assay CV was 5%.

Follicular fluid oestradiol: Follicle fluid (FF) oestradiol concentrations were quantified in a single RIA using a double antibody kit (Diagnostic Products Corporation # KE2D1, Diagnostic Products Corporation, Los Angeles, CA, USA) without extraction using the method of Paradis *et al.* (2009). The intra-assay CV for the single assay run was 5.7 %. Sensitivity estimated at 91 % of total binding was 0.1 pg/tube, equivalent to 2.4 ng/ml. The recovery of a known amount of oestradiol when added to a sample of known potency was 94.5 ± 2.7 %.

2-D gel electrophoresis and data analysis

Using follicle size and follicular fluid oestradiol concentration as a measure of follicle maturity, 3 groups of 16 OOX incubated with DOs originating from large preovulatory sow follicles prior to the LH surge, and their counterpart OOX incubated without DOs were selected from 3 of the 5 replicate cultures to be resolved on 2-dimensional gel electrophoresis. The remaining 2 replicates had less than 2 animals (groups of DOs) that satisfied our criteria and therefore could not be used for 2-dimensional gel analysis. Six Immobiline™ DryStrips pH 3-10, 7 cm were rehydrated overnight with 150 µl of rehydration solution (7M Urea, 2M Thiourea, 4% Chaps, 1.2% (v/v) DeStreak reagent (GE Healthcare, Piscataway, NJ) and 0.8% (v/v) IPG buffer pH 3-10 (GE Healthcare)). The three groups of 16 OOX from each replicate incubated with or without DOs were solubilized in 35 µl of sample buffer (7M Urea, 2M Thiourea, 4% Chaps, 20mM TCEP and 0.8% (v/v) IPG buffer pH 3-10 (GE Healthcare) for 2h at room temperature, vortexing occasionally. For each replicate, the OOX incubated alone or with DOs were pooled to obtain the amount of protein equivalent to 48 OOX and the samples were centrifuged 5 min at 14000 x g at room temperature. The supernatant was transferred to a fresh 1.5 ml microcentrifuge tube without disturbing the pellets and the volume was adjusted to 125 µl with sample buffer containing a trace of bromophenol blue.

The samples were simultaneously applied to the Immobiline™ DryStrips by anodic cup loading and the isoelectric focusing was performed overnight on an Ettan IPGphor apparatus (GE Healthcare). The program used for the isoelectric focusing was comprised of 100V for 10h, 300V for 4h, 1000V gradient for 30 min, 5000V gradient for 1.5h and 5000V to 5000Vhrs to reach a total of ~13 500 Vhrs. After focusing the Immobiline™ DryStrips were equilibrated 15 min in 5 ml of SDS equilibration buffer (6M Urea, 75 mM Tris-HCl pH 8.8, 29.3% (v/v) glycerol, 2% (w/v) SDS and a trace of bromophenol blue) with 10 mg/ml of dithiothreitol followed by 15 min in 5 ml of SDS equilibration buffer with 25 mg/ml of Iodoacetamide. The equilibrated strips were loaded onto 10% (w/v) SDS-PAGE gel (8 x 10 cm) to separate the proteins according to their molecular weight and the gels were fixed overnight in 50% (v/v) methanol. The gels were visualized using SYPRO Ruby protein stain according to the manufacturer's instructions (BioRad, Hercules, CA) and the images were captured on a Typhoon Trio (GE Healthcare) at 550 V, high sensitivity and 100 microns resolution. A total of 6 gels, comprising 3 gels representing OOX cultured alone and 3 gels representing OOX co-cultured with DOs were obtained. However, only the gels from 2 replicates were submitted to the final analysis since both gels from the third replicate showed incomplete isoelectric focusing.

Gel images were processed and analyzed using the Progenesis SameSpot software (Nonlinear dynamics, Newcastle Upon Tyne, UK) and each spot was manually verified to ensure proper matching. A total of > 600 spots were matched across the 4 gels and the individual spot intensities were normalized with the total spot volume from the gel of origin.

Preparative 2-D gel for protein identification

Cumulus cells originating from 500 COCs, cultured in the same conditions as the OOX, were resolved on 2-dimensional gel electrophoresis to obtain a preparative gel for protein excision and sequencing. The cumulus cells were solubilised in 75 ul of sample buffer (7M Urea, 2M Thiourea, 4% Chaps, 5mM TCEP) for 2h at room temperature, vortexing occasionally. The sample was

centrifuged for 10 min at 18000 x g at room temperature and the supernatant was transferred to a fresh tube containing 265 μ l of rehydration solution (7M Urea, 2M Thiourea, 4% Chaps, a touch of bromophenol blue) supplemented with DeStreak reagent and IPG buffer pH 3-10 (GE Healthcare) to obtain a final concentration of 1.2 % (v/v) and 0.8% (v/v), respectively. An Immobiline™ DryStrips pH 3-10, 18 cm was rehydrated overnight with 340 μ l of sample and subjected to isoelectric focusing on an Ettan IPGphor apparatus (GE Healthcare). The program used for the isoelectric focusing comprised a 250V gradient for 1h, 500 V for 1h, 1000V gradient for 8h, 1000V for 2h, 4000V gradient for 4h, 8000V gradient for 2h and 8000V to 16000Vhrs for a total of \sim 46000 Vhrs. After focusing the Immobiline™ DryStrips were equilibrated for 15 min in 5 ml of SDS equilibration buffer (6M Urea, 75 mM Tris-HCl pH 8.8, 29.3% (v/v) glycerol, 2% (w/v) SDS and a trace of bromophenol blue) with 10 mg/ml of dithiothreitol followed by 15 min in 5 ml of SDS equilibration buffer with 25 mg/ml of Iodoacetamide. The equilibrated strips were loaded onto 10% (w/v) SDS-PAGE gels (16 x 20 cm) to separate the proteins according to their molecular weight and the gels were fixed overnight in 50% (v/v) methanol. The gels were visualized using Colloidal Blue protein stain according to manufacturer's instruction (GE Healthcare) and the image was captured on a 14-bit scanner (Imagescanner, GE Healthcare). The image from the preparative gel was matched to the images from the analytical gels. The proteins found to be differentially expressed and showing \geq 1.2 fold changes were manually excised from the preparative and analytical gels and sent to a mass spectrometry facility for further processing and identification (Centre Genomique du Quebec, Sainte-Foy, Canada).

Protein identification by LC-MSMS

Tryptic digestions of the proteins were performed on a MassPrep liquid handling robot (Waters, Mississauga, Canada) according to the manufacturer's specifications and using sequencing grade modified trypsin (Promega, Madison, WI). Peptide extracts were separated by online reversed-phase nanoscale capillary LC and analyzed by electrospray MS (ES MS/MS) using a LTQ linear ion trap

mass spectrometer (Thermo Electron, San Jose, CA, USA) equipped with a nanoelectrospray ion source (Thermo Electron, San Jose, CA, USA). Peptide separation took place within a PicoFrit column BioBasic C18, 10 cm x 0.075 mm internal diameter (New Objective, Woburn, MA, USA) with a linear gradient from 2 % to 50 % solvent B (acetonitrile, 0.1 % formic acid) in 30 min, at 200 nl/min. Mass spectra were acquired using data-dependent acquisition mode (Xcalibre software, version 2.0). Each full-scan mass spectrum (400–2000 m/z) was followed by collision-induced dissociation of the seven most intense ions. The dynamic exclusion function was enabled (30 s exclusion), and the relative collisional fragmentation energy was set to 35 %.

Interpretation of Tandem MS Spectra

All MS/MS samples were analyzed using Mascot (Matrix Science, London, UK; version 2.2.0). The database used to search tryptic peptides was the mammalian protein database Uniref_100_14_Mammalia_40674. Fragment and parent ion monoisotopic mass tolerances were 0.5 Da and 2.0 Da, respectively. The iodoacetamide derivative of cysteine was specified as a fixed modification and methionine oxidations were specified as variable modifications. Two missed cleavages were allowed.

Criteria for protein identification

Scaffold (version Scaffold_2.1.03, Proteome Software Inc., Portland, OR) was used to validate MS/MS based peptide and protein identifications. Peptide identifications were accepted if they could be established at greater than 95.0 % probability as specified by the Peptide Prophet algorithm (Keller *et al.*, 2002). Protein identifications were accepted if they could be established at greater than 95.0 % probability and contained at least 2 unique identified peptides. Protein probabilities were assigned by the Protein Prophet algorithm (Nesvizhskii *et al.*, 2003). Proteins that contained similar peptides and could not be differentiated based on MS/MS analysis alone were grouped to satisfy the principles of parsimony.

RNA isolation and Real-time RT-PCR

Total RNA was extracted from 6 remaining pairs of 16 OOX incubated alone or with DOs using the PicoPure RNA isolation kit (Arcturus, Mountain View, CA, USA) following manufacturer's instructions. All samples were DNase treated as suggested in the manufacturer's protocol; the RNA was eluted in 11 μ l and quantified using the spectrophotometer ND-1000 to ensure adequate recovery (NanoDrop, Wilmington, DE, USA). OOX total RNA was reverse transcribed with Superscript III reverse transcriptase (Invitrogen) according to manufacturer's instruction, using a combination of 5 μ M oligo dT and 5 ng/ μ l of random hexamer. RNaseOUT (Invitrogen) was also added to the reaction at a concentration of 2 U/ μ l. cDNA synthesis was performed using approximately 200ng of OOX total RNA and following the reverse transcription, the cDNA was diluted to the equivalent of 1 ng/ μ l with nuclease-free H₂O (Ambion).

Real-Time PCR was performed in duplicate using 1 ng of cDNA from OOX or from 20 ng of cDNA from granulosa cells (granulosa cell collection and processing is described in Paradis *et al.*, 2009) in 96-well fast plates using the Taqman® Fast Universal PCR Master Mix and the ABI 7900HT thermocycler (Applied Biosystems, Foster City, CA, USA). The primers and Taqman-MGB probes (Table 6.1) were designed using the Primer Express® software v3.0 (Applied Biosystems) using sequences found on GENBANK or ordered from the porcine TaqMan® Gene Expression Assays library (Applied Biosystems). The amplification efficiency for each gene, determined using serial dilution of ovarian cDNA, was found to be $\geq 90\%$ for all genes and the slopes for all 9 genes were found to be identical (data not shown). Cyclophilin was used as the endogenous control to correct for RNA extraction and reverse transcription efficiency and its transcript abundance was found to be stable between treatments, confirming its validity as an endogenous control.

Statistical analysis

Real-time PCR data for the genes of interest (GOI) were normalized against their respective means for cyclophilin using the ΔCt method ($\Delta\text{Ct} = \text{Ct}_{\text{GOI}} - \text{Ct}_{\text{cyclophilin}}$). The cycle threshold (Ct) is defined as the PCR cycle where the fluorescence reaches a determined threshold. Consequently, the Ct and corrected Ct (ΔCt) value are inversely related to the copy number of the targeted gene initially present in the sample. For the analysis of mRNA abundance between OOX cultured alone or with DO, the ΔCt values for all GOI were normally distributed and the individual ΔCt for each GOI were analysed using the MIXED procedure of SAS. The model for the experiment included treatment as the independent variables, and sow as the random variable. Differences between means were analyzed using a Least Significant Difference (LSD) test at a 95% confidence level. For the analysis of the temporal changes in FSHR and HSD3B mRNA abundance in granulosa cells, the ΔCt values for the GOI were RANK transformed for normality and the analysis was performed on the transformed data. The individual ΔCt for each GOI were analysed using the MIXED procedure of SAS. The model for the experiment included phase as the independent variables. Differences between means were analyzed using a Least Significant Difference (LSD) test at a 95% confidence level. For ease of interpretation of the expression profiles the data were converted using the formula $2^{-(\Delta\text{Ct} - \Delta\text{Ct}_{\text{calibrator}})}$ and are expressed as relative mRNA abundance \pm SEM. The highest expression (lowest ΔCt) for each GOI was used as the calibrator value and the corresponding ΔCt is expressed as a relative abundance to that value. Finally, correlation analysis was performed to determine the nature of the relationships between FSHR mRNA abundance and that of YWHAH mRNA.

RESULTS

Phenotypic characteristics of OOX after culture

Visual assessment of the appearance of the OOX following 22h of culture in the presence or absence of denuded preovulatory oocytes did not reveal any particular phenotype (Figure 6.1). Interestingly, OOX diameter, used as a measure of expansion, was identical between OOX cultured alone and OOX cultured with oocytes (data not shown). On a scale from 0 to 4, where 0 is no expansion and 4 is full expansion, OOX incubated with or without denuded oocytes both scored 1 after 22h of culture (Figure 6.1). Moreover, the number of potentially atretic OOX, as assessed by morphological characteristics including cell attachment to the dish and appearance/colour of the cytoplasm, did not indicate any differences between the two groups (Figure 6.1). The nuclear status of the denuded oocytes used for the co-culture was also assessed after 22h of culture using Hoechst 33258 staining to ensure that the oocyte remained arrested at the germinal vesicle stage and did not resume meiosis. Evaluation of oocyte nuclear maturation confirmed that more than 95% of the oocytes remained arrested at the germinal vesicle stage (GV) (data not shown), validating the effectiveness of cilostamide in preventing meiotic resumption and confirming that the effects observed were emanating from fully grown preovulatory GV oocytes. Finally, follicular fluid oestradiol and plasma oestradiol, as well as the average size of the three largest follicles, were used to determine that the sow oocytes used in the experiment were derived from large oestrogenic preovulatory follicles (Table 6.2).

Protein profiling and identification

More than 600 protein spots were matched across the 4 gels of which 14 proteins were found to be differentially expressed by OOX incubated with and without denuded oocytes. Interestingly, 9 of the 14 differentially expressed proteins were up-regulated in OOX incubated without DOs (Figure 6.2A, B and Table 6.3). The magnitude of the upregulation ranged from 1.2-fold for protein

spot 20 to 2.7-fold for protein spot 2 (Figure 6.2B and Table 6.3). Conversely, only 5 of the 14 proteins were downregulated in OOX incubated without oocytes and the magnitude of the downregulation observed was generally lower, ranging between 1.1 and 1.2 fold-changes (Figure 6.2A, C and Table 6.3).

To determine the identity of the protein spots differentially expressed between OOX cultured alone or with denuded oocytes, the spots were excised from the gel and sent for identification by LC-MSMS. The identity of all the proteins spots, with the exception of protein spot 18, was successfully determined (Table 6.3). Protein spot #18 could not be effectively visualized on the analytical gel for excision and could not be accurately matched to the preparative gel and therefore was not sent for identification. In addition, after analysis of the peptides identified for each protein spot, 5 proteins could not be effectively matched to a single protein and may have contained a mixture of proteins. Consequently, the identities of the two most probable identifications are provided (Table 6.3 : Spot 6, 12, 19, 22, 27). The likelihood that these protein spots correspond to specific proteins was assessed based on the number of unique peptides identified, the percentage of protein coverage and the comparison between the observed and the predicted molecular weight and isoelectric point.

Real-Time PCR analysis

Concomitant with the protein analysis, real-time PCR was performed to determine if changes in mRNA abundance for several genes involved in apoptosis, proliferation, metabolism and steroidogenesis in granulosa and cumulus cells was affected by co-culture with oocytes. Culturing the OOX with or without oocytes did not affect mRNA abundance for the apoptosis related gene BCL2-associated X protein (*BAX*) and B-cell CLL/lymphoma 2 (*BCL2*), the cell proliferation marker cyclin D2 (*CCND2*), or the phosphofructokinase (*PFKP*) and lactate dehydrogenase A (*LDHA*) genes, known for their involvement in metabolism (Figures 6.3A, B and C, respectively). The mRNA abundance for several genes involved in steroidogenesis was also evaluated (Figure 6.4A). Although, luteinizing hormone receptor (*LHCGR*), steroidogenic acute regulatory

protein (*STAR*) and cytochrome P450 aromatase (*CYP19A1*) mRNA abundance was not affected by the co-culture of OOX with oocyte, follicle stimulating hormone receptor (*FSHR*) and 3 β -hydroxysteroid dehydrogenase (*HSD3B*) mRNA abundance changed depending on whether the OOX were cultured in the presence or absence of denuded oocytes. Interestingly, while the presence of denuded oocytes decreased *FSHR* mRNA by more than 25% in cultured OOX ($P<0.05$), the expression of *HSD3B* mRNA increased by almost 40% ($P<0.05$). Interestingly, 14-3-3 η (*YWHAH*) mRNA expression also tended to decrease in OOX cultured with oocytes in a similar way to the protein ($P=0.08$) and a strong positive correlation between *YWHAH* mRNA and *FSHR* mRNA abundance was found (Figure 6.4B, C; $R=0.75$, $P<0.01$).

To better comprehend the basis for the changes observed in *FSHR* and *HSD3B* mRNA abundance in OOX incubated with denuded preovulatory oocytes, real-time PCR analysis was performed to determine the temporal changes in mRNA abundance for these genes in granulosa cells during antral follicle development. Abundance of *FSHR* mRNA was higher ($P<0.05$) in granulosa cells from smaller follicles (3-6mm), taken during the recruitment and mid-selection phase than in large preovulatory follicles recovered before and after the LH surge (Figure 6.5A). The expression of *HSD3B* in the granulosa cells showed the opposite pattern; mRNA abundance was low in smaller follicles during the recruitment and mid-selection phase but substantially increased ($P<0.05$) during the periovulatory period prior and after the LH surge (Figure 6.5B).

DISCUSSION

Although it has been clearly shown that the oocyte secretes soluble factors that act on the neighbouring somatic cells to modulate their functions, much of the evidence has come from rodent models or sheep and cow studies (Gilchrist *et al.*, 2008, Juengel and McNatty, 2005). Consequently, our understanding of the role

of the porcine oocyte during follicle growth is limited. It also remains to be established whether fully grown oocytes originating from different follicle categories of known physiological status (small, medium and large antral follicles) exhibit different abilities to modulate their environment. In order to better understand how the porcine oocyte affects its environment, a well established *in vitro* model developed by Buccione *et al.* (1990), involving microsurgical removal of the oocyte from the cumulus oocyte complex, was used. In addition, using a combination of proteomic and real-time PCR techniques, the effect of preovulatory porcine oocytes on protein and gene expression in the oocyctomized cumulus cell (OOX) was assessed.

Morphological evaluation of the OOX after 22 hours of culture revealed no obvious differences in their diameter and it was concluded that the porcine preovulatory oocyte had no effect on cumulus cell expansion. However, as most of the expansion observed in porcine cumulus-oocyte complexes (COC) cultured *in vitro* generally occurs during the last 22 hours of a 44-hour culture period, the 22-hour culture period used in the present study may not be optimal for evaluating effects on cumulus expansion. Although this lack of an effect of the oocyte on cumulus expansion is different from results obtained with the mouse oocyte, in which FSH-stimulated hyaluronic acid synthesis and cumulus cell expansion, it is consistent with other studies in the pig (Buccione *et al.*, 1990, Salustri *et al.*, 1990a). Although the pig oocyte has been shown to secrete the cumulus expansion enabling factors (CEEF) similar to those produced by the mouse oocyte, the oocyte does not appear to be necessary for porcine cumulus cell expansion, nor for hyaluronic acid synthesis (Prochazka *et al.*, 1991, Singh *et al.*, 1993, Nagyova *et al.*, 1999). Similarly, bovine FSH-stimulated cumulus cells also undergo expansion in the absence of oocytes (Ralph *et al.*, 1995). Interestingly, Prochazka *et al.* (1998) demonstrated that porcine cumulus and mural granulosa cells also secrete the CEEF, as demonstrated by their ability to promote mouse cumulus cell expansion, providing a rationale for why the porcine oocyte may not be absolutely essential in that process. Moreover, the overall morphological appearance of the OOX, including attachment to the culture dish

and appearance and colour of the cytoplasm, did not suggest a higher incidence of atresia in the OOX incubated in the absence of denuded oocytes. This was reflected in the real-time PCR analysis of *BAX* (pro-apoptotic) and *BCL2* (anti-apoptotic) mRNA abundance which were not affected by culture with or without denuded oocytes. In contrast, Hussein *et al.* (2005) reported that bovine oocytes prevent apoptosis in OOX and that this effect is achieved by modulation of *BAX* and *BCL2* expression in the cumulus cells.

Based on the 2-D gel analysis, 14 proteins were found to be differentially expressed between the OOX incubated with and without denuded oocytes. Given that over 600 protein spots were matched across the gels, less than 2% of the proteins appear to be affected, suggesting that the effects on the OOX were specific and do not reflect global changes in protein expression. This result is also consistent with that reported by Eppig *et al.* (1997), who showed that few differences were observed in the global pattern of protein synthesis between mural granulosa cells cultured with and without oocytes. Interestingly, 9 of the 14 proteins identified in this study were up-regulated in the OOX cultured without oocytes and the extent of the upregulation was more substantial than the down-regulation observed in the remaining 5 proteins. These results suggest that the oocyte has a predominantly suppressive effect on protein expression in the cumulus cells. This observation is in accordance with the current concept in the mouse suggesting that the oocyte is responsible for maintaining the cumulus cell phenotype and that removal of the oocyte from the cumulus oocyte complexes leads to up-regulation of several mural granulosa cells markers in the cumulus cells, such as LHCGR, CYP11A1 and hematopoietic progenitor cell antigen CD34 (CD34) (Diaz *et al.*, 2007, Eppig *et al.*, 1997). It could also be suggested that the differences observed between the suppressive and stimulatory effects of the oocyte only reflect the differences in the time required for protein synthesis, compared to that of protein turnover. However, irrespective of the mechanisms responsible for the observed differences in protein up- and down-regulation following co-incubation with oocytes, these results are in accordance with the

findings that fully mature pig oocytes are essential for maintaining the cumulus cell phenotype.

Interestingly, the protein showing the largest degree of upregulation in the OOX cultured without denuded oocytes was identified by LC-MSMS as being 14-3-3 protein eta (14-3-3 η or YWHAH). The 14-3-3 proteins are part of a large family of highly conserved acidic proteins originally identified in the brain (Van Hemert *et al.*, 2001). The family is comprised of at least 7 mammalian isoforms (β , γ , ϵ , ζ , η , σ , τ) that have been shown to interact with over 100 cellular proteins. Although many of their functions remain unknown, the 14-3-3 proteins have been shown to be involved in cell division, apoptosis and cell signaling (Van Hemert *et al.*, 2001). Interestingly, the 14-3-3 protein can modulate various signal transduction pathways involving several different receptors. First, 14-3-3 η has been shown to interact with a variety of nuclear receptors including the glucocorticoid receptor, androgen receptor, estrogen receptor 1 and 2 (ESR1 and ESR2) and thyroid hormone receptor α (THRA) (Haendler *et al.*, 2001, Wakui *et al.*, 1997, Zilliagus *et al.*, 2001). In addition, 14-3-3 ϵ has been shown to interact with insulin like growth factor 1 receptor (IGF1R) and insulin receptor substrate 1 (IRS1); however, as for ESR1 and 2 and THRA, the importance of this interaction for the activity of each receptor remains to be determined (Craparo *et al.*, 1997). Finally, it is also particularly interesting that the 14-3-3 protein family (14-3-3 τ) was shown to interact with FSHR (Cohen *et al.*, 2004). Its role on FSHR signal transduction appears to be inhibitory, since overexpression of 14-3-3 τ in HEK 293 cells stably expressing FSHR, decreases intracellular levels of cAMP following FSH stimulation. Overall, these results suggest that the 14-3-3 proteins are modulating signal transduction for various receptors and their interaction with FSHR is extremely interesting in the context of the present study.

Although the exact mechanism for the action of the 14-3-3 proteins on FSHR signal transduction and cAMP production is largely unknown, one could suggest that affecting cAMP production would modulate the activity of protein kinase A, which ultimately would result in changes in transcriptional activity. Moreover, the 14-3-3 proteins were also previously known as protein kinase C

inhibitor (KCIP-1) because of their ability to inhibit protein kinase C (PKC) (Toker *et al.*, 1992). Interestingly, PKC signaling pathways have been shown to be involved in FSH-mediated oocyte maturation and epidermal growth factor receptor activation by PKC is essential for that process in mouse and porcine COC (Chen *et al.*, 2008, Downs *et al.*, 2001, Down and Chen, 2008, Fan *et al.*, 2004, Jin *et al.*, 2006, Lu *et al.*, 2001, Su *et al.*, 1999). These observations are extremely interesting since our results showed that culturing oocyctomized cumulus cells in the presence of denuded oocytes led to a marked reduction in *FSHR* mRNA abundance and correlation analysis revealed a strong positive relationship between *FSHR* and *14-3-3 η* mRNA abundance, suggesting that the expression of these two genes may be closely linked. Moreover, the known inhibitory role of the 14-3-3 proteins on PKC, as well as their potential to modulate PKA, suggests potential mechanisms for modulating FSH action in the granulosa cells. Altogether, this experimental evidence suggests that preovulatory porcine oocytes act on the cumulus cells to modulate their responsiveness to FSH.

Perhaps the most intriguing finding of this study is the antagonistic effect of the porcine preovulatory oocyte on *FSHR* and *HSD3B* mRNA abundance in the oocyctomized cumulus cells. Denuded GV oocytes isolated from large oestrogenic preovulatory follicles prior to the LH surge down-regulated *FSHR* mRNA while up-regulating *HSD3B* mRNA. Interestingly, no effects were observed on *LHCGR* mRNA or on *STAR* and *CYP19A1* mRNA abundance. These observations are somewhat puzzling since these effects have either not been previously reported in the literature or contradict results from most existing studies. First, *LHCGR* mRNA was shown to be upregulated in FSH-stimulated mouse oocyctomized cumulus cells, while addition of denuded oocytes to mural granulosa cells had the opposite effect (Eppig *et al.*, 1997). In our study, the presence or absence of oocytes did not affect *LHCGR* mRNA abundance in OOX, but rather modulated *FSHR* mRNA abundance and also potentially altered its activity via regulation of the 14-3-3 proteins. One could suggest that the effects on *LHCGR* observed in the study by Eppig *et al.* (1997) resulted from the indirect modulation of *FSHR* by the oocyte, since FSH is known to induce *LHCGR*.

However, the authors showed that this effect occurred downstream of FSHR activation and cAMP production (Eppig *et al.*, 1998). However, since FSHR signal transduction can occur through various protein kinases pathways including PKC, the possibility exists that the mouse oocyte also modulates the activity of FSHR. On the other hand, Otsuka *et al.* (2001) reported that BMP15, a known oocyte-derived ligand, suppressed FSHR in rat granulosa cells isolated from small antral follicles. This observation clearly indicates that, as observed in our experiment, the rat oocyte can also modulate FSHR activity. In addition, our findings suggest that the preovulatory porcine oocyte increases *HSD3B* mRNA abundance. Since *HSD3B* is the enzyme responsible for the conversion of pregnenolone into progesterone and the porcine granulosa cells do not possess the enzyme *CYP17A1* necessary to convert progesterone to androgen, the increase in *HSD3B* mRNA observed in the cumulus cells is likely contributing to increased progesterone production. Interestingly, this observation contrasts previous studies in mouse, bovine and porcine granulosa cells in which the oocyte has generally been shown to have a suppressive effect on progesterone production (Brankin *et al.*, 2003, Coskun *et al.*, 1995, Gilchrist *et al.*, 2008, Li *et al.*, 2000, Vanderhyden *et al.*, 1993). However, all of the above studies have used oocytes from small and medium (3-6 mm) antral follicles in contrast to the preovulatory oocytes used in the present study.

In order to better comprehend the physiological relevance of these changes in *FSHR* and *HSD3B* mRNA abundance and that of 14-3-3 η protein and mRNA observed in the oocyctomized cumulus cells incubated with and without preovulatory porcine oocyte, we evaluated the temporal expression pattern of *FSHR* and *HSD3B* mRNA in porcine granulosa cells during the follicular phase. Our results clearly showed that *FSHR* mRNA abundance is high during the recruitment and mid-selection phase when only small and medium antral follicles are present on the ovary, and its expression was dramatically reduced during the final selection phase prior to and after the LH surge at a time where the preovulatory population has been established and comprises only large antral follicles. In contrast, *HSD3B* mRNA abundance was found to be very low in

small- and medium-sized antral follicles but increased substantially in the large preovulatory follicle population before and after the LH surge. Our results are consistent with conclusions from the existing literature that show *FSHR* mRNA decreasing as the follicle is growing and transitioning from FSH to LH dependence at the same time as *HSD3B* mRNA is increasing in preparation for ovulation (Yuan *et al.*, 1996). Interestingly, the oocyctomized cumulus cells used in the current study were isolated from small-medium antral follicles from prepubertal gilt ovaries that are still dependent on FSHR expression are not likely to express HSD3B. By comparison, the oocytes originated from large oestrogenic preovulatory sow follicles in which FSHR has normally been down-regulated and HSD3B expression has increased in preparation for ovulation. This strongly suggests that oocyte modulation of cumulus cell steroidogenesis is developmentally regulated in the pig, allowing the oocyte to change the follicular environment to adapt for the specific requirements of each stage of follicle growth. There are already several lines of evidence to suggest that the influence of the oocyte on the surrounding somatic cell changes as the follicle develops. For example, Eppig *et al.* (2002) showed that primary and secondary oocytes affect the rate of follicle development differently. Moreover, mouse oocytes progressing to metaphase II gradually lose their mitogenic inducing ability on the granulosa cells (Gilchrist *et al.*, 2001). Similarly, Eppig *et al.* (1997) have shown that the ability of the oocyte to suppress LHCGR mRNA abundance in the mouse granulosa cell is developmentally regulated, since fully grown oocytes potently suppress LHCGR mRNA, while growing oocytes isolated from preantral follicles and maturing oocytes were less capable of suppressing LHCGR expression. Nevertheless, this is the first study to suggest that developmental regulation also occurs within fully grown oocytes depending on the size and maturational status of the follicle from which they are isolated.

The up-regulation of phosphoglycerate mutase (PGAM1) in OOX cultured with denuded oocytes represents another compelling finding. PGAM1 is a glycolytic enzyme that catalyzes the interconversion of 2- and 3-phosphoglycerate and changes in its abundance and/or activity could potentially modulate levels of

glycolysis. Mouse oocytes have also been shown to positively regulate cumulus cell metabolism by modulating several glycolytic enzymes (Sugiura *et al.*, 2005, Eppig *et al.*, 2005). In the current experiment, mRNA abundance for phosphofructokinase (PFKP) and lactate dehydrogenase A (LDHA), two essential enzymes in metabolism, were not differentially regulated in OOX cultured with or without denuded oocytes, suggesting that the glycolytic ability of the OOX is not regulated by the oocyte. However, changes in the activity of this enzyme could also modify the quantity of glucose 6-phosphate available for the pentose-phosphate pathway (PPP): this is indispensable for maintaining the levels of NADPH in the cell, necessary for downstream biosynthetic pathways such as steroid synthesis, and also for protecting the cells against oxidative damage by maintaining the level of reduced glutathione (Shalom-Barak and Knaus, 2002). Unfortunately, it was not possible to design an efficient primer-probe set to evaluate the consequences of the imposed treatment on glucose 6-phosphate dehydrogenase (G6PD) mRNA abundance, which is the rate limiting enzyme in the pentose phosphate pathway.

Finally, several other proteins were found to be differentially expressed between OOX cultured alone or with denuded oocytes. The role of many of these proteins in the ovary remains largely unknown while others have the potential to affect a very broad range of functions. It is therefore very difficult to speculate as to what their functions might be in the context of the present study.

In conclusion, the findings of the present study clearly demonstrate that the porcine preovulatory oocyte secretes soluble factors that act on the surrounding cumulus cells to modulate protein and gene expression. Our results suggest that the effect of the fully grown GV oocyte is developmentally regulated, allowing the oocyte to modulate the follicular environment to adapt to the specific requirements of each stage of follicle growth. To our knowledge, this is the first study to investigate the role of the porcine oocyte on the cumulus cell global protein expression and it is the first study investigating the role of the preovulatory oocyte on mammalian cumulus cell functions. Additional studies are needed to further elucidate the nature of the interaction between FSHR and

14-3-3 protein and to assess the potential roles of other proteins identified in this study

Table 6.1 Details of primers and probes used for Real-Time PCR

Gene	AC number	Primer	Sequence 5' --> 3' or assay ID	Product size	Annealing/ Extension Temperature (°C)
BAX	AJ606301	Forward	CCCCCGAGAAGTCTTTTTTCC	56 bp	62
		Reverse	TGAAGTTGCCGTCAGCAAAC		
		Probe	AGTGGCGGCCGAAA		
BCL2	AB271960	Forward	CGCTGGGAGAACAGGGTATG	66 bp	60
		Reverse	TGCGACAGCTTATAGTGGATGTACT		
		Probe	AACCGGGAAATAGTG		
CCND2	NM_214088	ABI	Ss03382534_s1	97 bp	62
CYP19A1	NM_214429	Forward	GTGCCTTTTGCCAGCATTG	61 bp	60
		Reverse	AATTCCAAACCAAGAGAAGAAAGC		
		Probe	AGTCCTGCTGCTCACT		
FSHR	NM_214386	Forward	TCACAGTGAGGAACCCCAACA	64 bp	60
		Reverse	GCCATACGCTTGGCGATCT		
		Probe	TGTCCTCCTCTAGTGACACC		
HSD3B1	NM_001004049	Forward	CGTCCTGACACACAACCTCCAA	59 bp	60
		Reverse	CCACGTTGCCGACGTAGAC		
		Probe	TTCTCCAGAGTCAACCC		
LDHA	SDU07178	Forward	TCACAAACAGGTGGTGGACAGT	62 bp	62
		Reverse	CCCAGGACGTGTAGCCTTTC		
		Probe	CTTATGAGGTGATCAAAC		

Gene	AC number	Primer	Sequence 5' --> 3' or assay ID	Product Size	Annealing/Extension Temperature (°C)
LHCGR	NM_214449	Forward	TGGAGCTGAAGGAGAATGCA	56 bp	60
		Reverse	CCCTCGGAAGGCGTCAT		
		Probe	ACCTGAAGAAGATGCAC		
PFKP	AK238519	Forward	AGGCTCCATTCTTGGGACAA	59 bp	60
		Reverse	CCGCAATGTCCTCCAGGTACT		
		Probe	ACGCACGCTTCCT		
PPIA	AY266299	Forward	AATGCTGGCCCCAACACA	56 bp	60
		Reverse	TCAGTCTTGGCAGTGCAAATG		
		Probe	ACGGTTCCCAGTTTT		
STAR	NM_213755	Forward	GGGACGAGGTGCTGAGTAAAGT	59 bp	60
		Reverse	CACCTCCAGCCGGAACAC		
		Probe	ATCCCAGATGTGGGCAA		
YWHAH	XM_001928076	Forward	GGGCGATTACTACCGCTACCT	63 bp	62
		Reverse	TCAACCACGCTGTTTTTCTTCTC		
		Probe	CCGAGGTGGCTTC		

Table 6.2 Characteristics of the sows and preovulatory follicles (POF) from which oocytes were isolated.

Sow Weight (kg)	Nos. POF per sow	Average size of the 3 largest follicles (mm)	Plasma E2* concentration (pg/ml)	Follicular fluid E2* concentration (ng/ml)
170 ± 10	21 ± 2	8.4 ± 0.9	25 ± 12	141 ± 67

Data are expressed as means ± sd

* E2: oestradiol

Table 6.3 Identity of the proteins identified by LC-MSMS that were differentially expressed between oocyctectomized cumulus cells (OOX) incubated alone or with denuded oocytes (DO) isolated from large oestrogenic sow follicles prior to the LH surge.

Spot #	↑↓ in OOX w/o DOs (fold change)	Protein name (symbol)	Accession #	Observed MW (kDa)/pI	Theoretical MW (kDa)/pI	# of unique Peptides (% coverage)
2	↑ (2.7)	14-3-3 protein eta (Protein AS1) (YWHAH)	UPI0000EB0531	28 / 4	28 / 4.8	21 (60)
3	↑ (2.1)	Nucleophosmin (NPM1)	P06748	38 / 4	33 / 4.6	10 (39)
4	↑ (1.8)	Prolyl 4-hydroxylase, beta subunit (P4HB)	P05307	60 / 4.5	57 / 4.7	15 (32)
5	↑ (1.7)	Translationally-controlled tumor protein (TCTP)	P13693	23 / 4.5	20 / 4.8	6 (31)
6.1	↑ (1.7)	Eukaryotic translation initiation factor 3 subunit I	Q9QZD9	38 / 5	36 / 5.4	15 (53)
6.2		Calponin-3	Q32L92	38 / 5.5	36 / 5.7	15 (43)
12.1	↑ (1.4)	Eukaryotic translation initiation factor 3 subunit I	Q9QZD9	38 / 5	36 / 5.4	11 (49)
12.2		Calponin-3	Q32L92	38 / 5.5	36 / 5.7	11 (37)
17	↑ (1.3)	Heterogeneous nuclear ribonucleoprotein Q (hnRNP Q)	O60506	70 / 7.5	60-68 / 8.5	10 (22)
19.1		Eukaryotic initiation factor 4A-I (EIF4A1)	P60842	45 / 5	46 / 5.3	10 (31)
19.2	↓ (1.2)	cAMP-dependent protein kinase type I-alpha regulatory subunit	P07802	45 / 5	43 / 5.3	7 (24)
20	↑ (1.2)	Rho GDP-dissociation inhibitor 1 (ARHGDI1)	P19803	26 / 5	23 / 5	8 (43)
22.1	↓ (1.2)	Highly similar to T-complex protein 1 subunit epsilon	UPI00015601FB	62 / 5.7	59 / 5.5	25 (48)
22.2		Procollagen-proline 2-oxoglutarate-4-dioxygenase	A1X898	62 / 5.7	61 / 5.7	19 (40)
23	↓ (1.15)	Phosphoglycerate mutase 1 (PGAM1)	P18669	27 / 7	29 / 6.7	20 (78)
25	↓ (1.1)	Neutral alpha-glucosidase AB (GANAB)	P79403	110 / 5.7	107 / 5.5	46 (56)
27.1		Eukaryotic initiation factor 4A-I (EIF4A1)	P60842	43 / 5	46 / 5.3	16 (42)
27.2	↓ (1.1)	cAMP-dependent protein kinase type I-alpha regulatory subunit	P07802	43 / 5	43 / 5.3	6 (22)

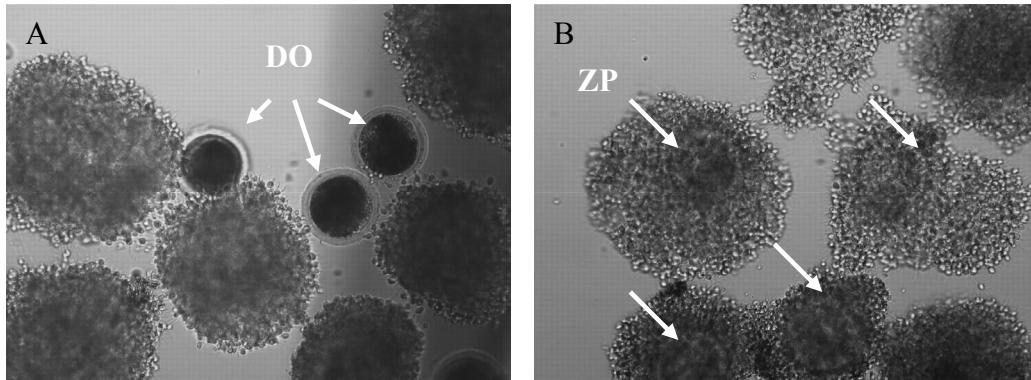


Figure 6.1 Morphological appearance of the oocytectomized cumulus cells (OOX) after 22h of culture with (A) and without (B) denuded oocytes (DO) isolated from large oestrogenic sow follicles prior to the LH surge. In the focal plane used to capture image B, the zona pellucidae (ZP) from which the oocyte has been aspirated are clearly visible. In image A, in which the focal plane capture clear images of the DOs, the empty ZP are less obvious.

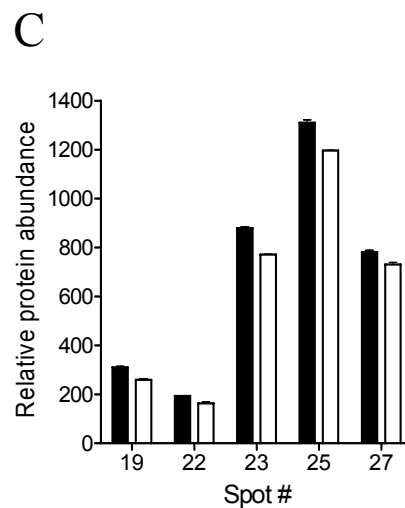
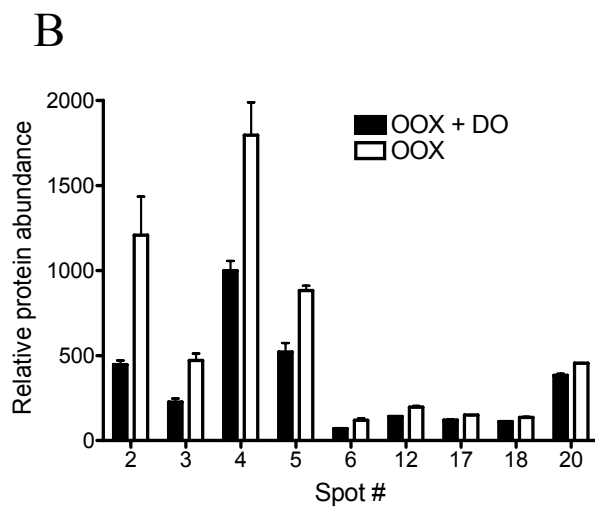
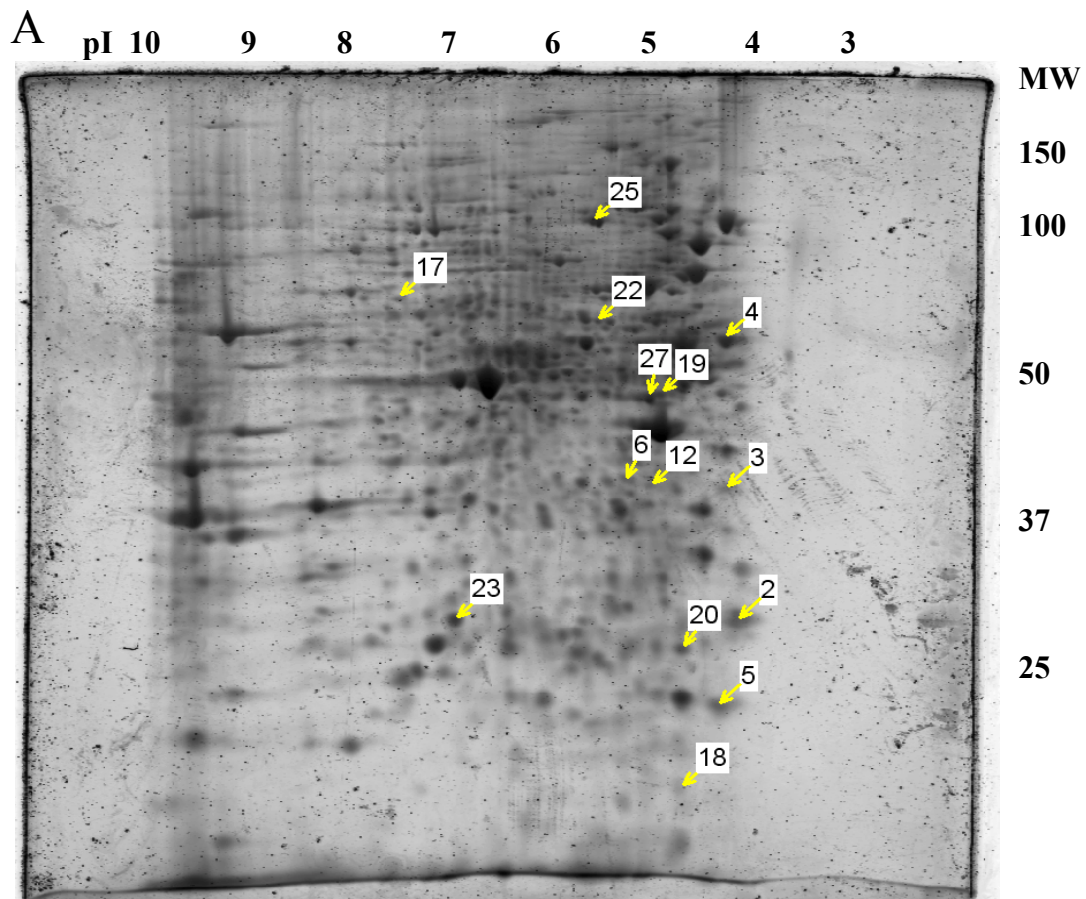


Figure 6.2 Representative 2-dimensional gel of proteins from a pool of 48 OOX incubated without oocytes. Protein spot numbers identify proteins differentially expressed between treatments (A). The proteins found to be up- and down-regulated in OOX culture alone are shown in B and C, respectively.

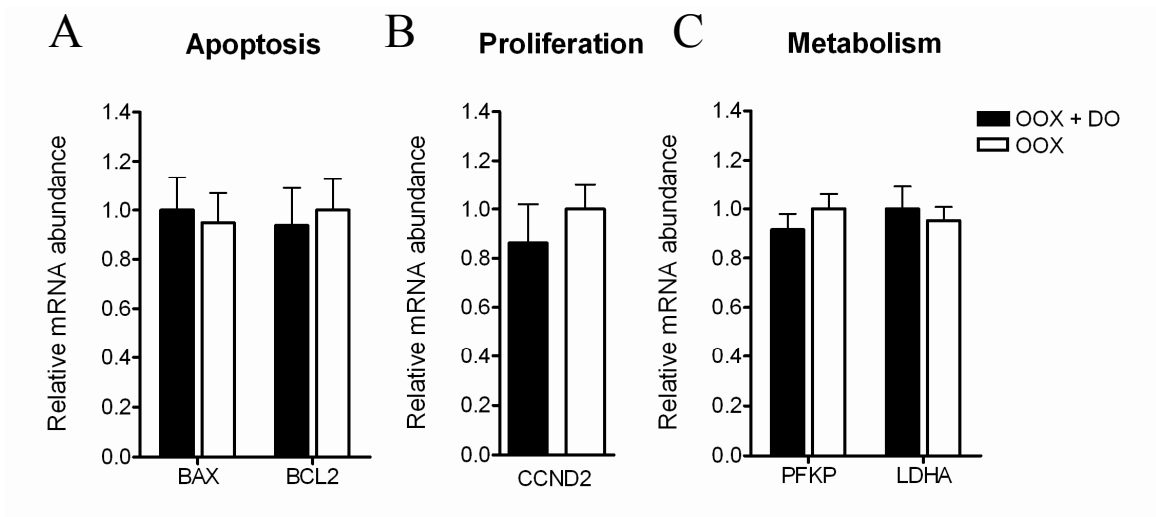


Figure 6.3 Quantification via real-time RT-PCR of the mRNA of genes involved in A) Apoptosis, B) Proliferation and C) Metabolism in pig oocyctomized cumulus cells after 22h of culture with (n=6) and without (n=6) denuded oocytes isolated from large oestrogenic sow follicles prior to the LH surge. Data are expressed as lsmeans of relative mRNA abundance \pm SEM.

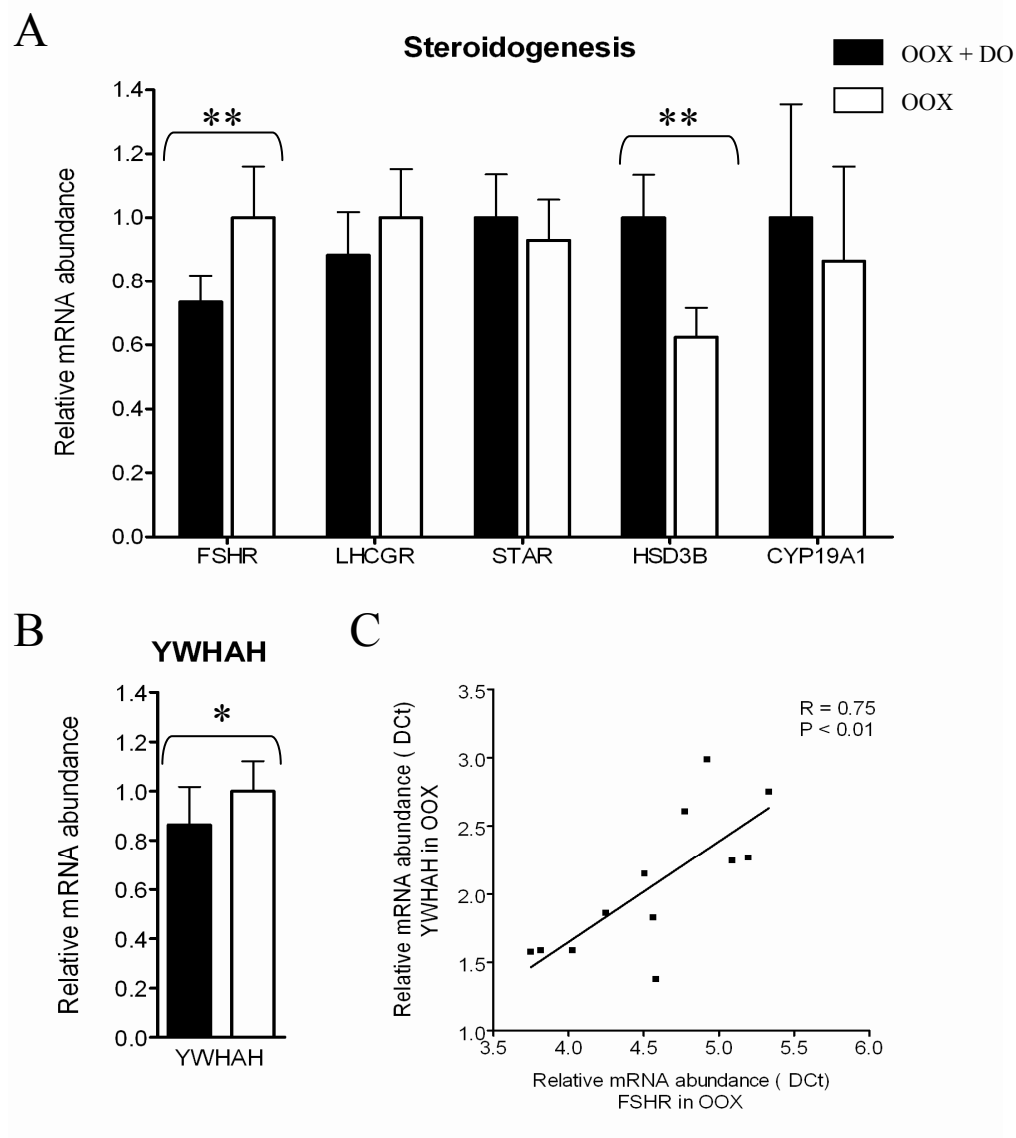


Figure 6.4 Quantification via real-time RT-PCR of A) the mRNA of genes involved in Steroidogenesis and B) YWHAH mRNA in pig oocyctectomized cumulus cells after 22h of culture with (n=6) and without (n=6) denuded oocytes isolated from large oestrogenic sow follicles prior to the LH surge. Data are expressed as means of relative mRNA abundance \pm SEM. The asterisks indicates differences within gene between treatment ($P \leq 0.05$ ** and $P \leq 0.1$ *). C) Correlation analysis between FSHR and YWHAH mRNA abundance (Δ Ct).

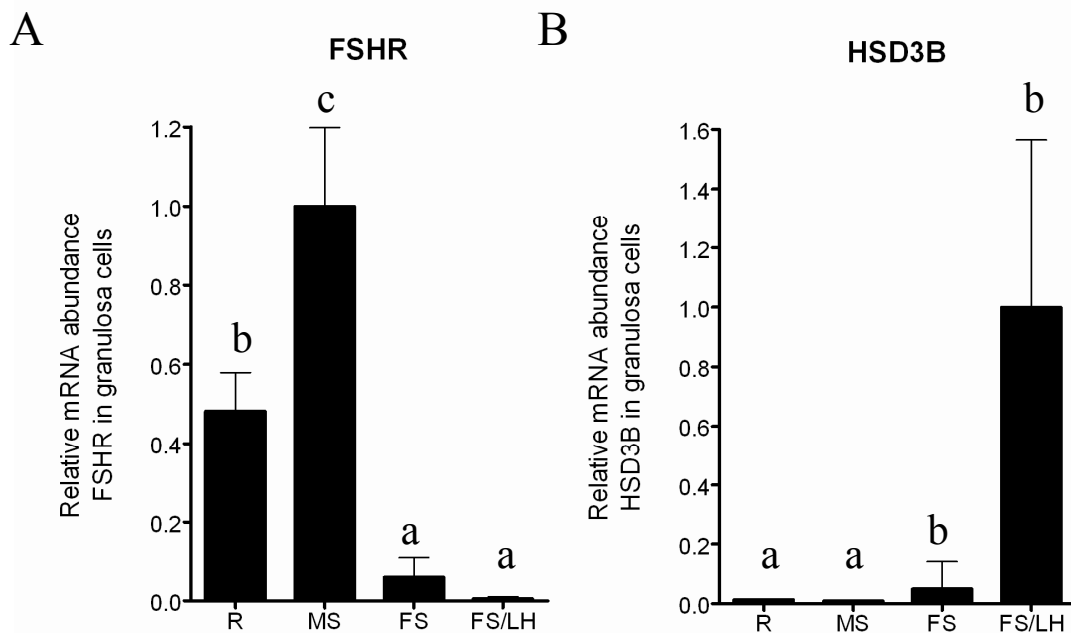


Figure 6.5 Quantification via real-time RT-PCR of A) *FSHR* mRNA B) *HSD3B* mRNA abundance in pig granulosa cells during follicle recruitment (R; n=6), mid-selection (MS; n=6), final selection (FS; n=3) and final selection post-LH surge (FS/LH; n=3). Data are expressed as means of relative mRNA abundance \pm SEM for each phase, irrespective of cycle. Different letters within gene represent significant difference among phases ($P \leq 0.05^{a,b,c}$).

REFERENCES

- Bommer UA & Thiele BJ** 2004 The translationally controlled tumour protein (TCTP). *Int J Biochem Cell Biol* **36** 379-385.
- Brankin V, Mitchell MR, Webb B & Hunter MG** 2003 Paracrine effects of oocyte secreted factors and stem cell factor on porcine granulosa and theca cells *in vitro*. *Reprod Biol Endocrinol* **1** 55.
- Buccione R, Vanderhyden BC, Caron PJ & Eppig JJ** 1990 FSH-induced expansion of the mouse cumulus oophorus *in vitro* is dependent upon a specific factor(s) secreted by the oocyte. *Dev Biol* **138** 16-25.
- Chen X, Zhou B, Yan J, Xu B, Tai P, Li J, Peng S, Zhang M & Xia G** 2008 Epidermal growth factor receptor activation by protein kinase C is necessary for FSH-induced meiotic resumption in porcine cumulus-oocyte complexes. *J Endocrinol* **197** 409-419.
- Cohen BD, Nechamen CA & Dias JA** 2004 Human follitropin receptor (FSHR) interacts with the adapter protein 14-3-3tau. *Mol Cell Endocrinol* **220** 1-7.
- Coskun S, Uzumcu M, Lin YC, Friedman CI & Alak BM** 1995 Regulation of cumulus cell steroidogenesis by the porcine oocyte and preliminary characterization of oocyte-produced factor(s). *Biol Reprod* **53** 670-675.
- Craparo A, Freund R & Gustafson TA** 1997 14-3-3 (epsilon) interacts with the insulin-like growth factor I receptor and insulin receptor substrate I in a phosphoserine-dependent manner. *J Biol Chem* **272** 11663-11669.
- Diaz FJ, Wigglesworth K & Eppig JJ** 2007 Oocytes determine cumulus cell lineage in mouse ovarian follicles. *J Cell Sci* **120** 1330-1340.
- Downs SM, Cottom J & Hunzicker-Dunn M** 2001 Protein kinase C and meiotic regulation in isolated mouse oocytes. *Mol Reprod Dev* **58** 101-115.
- Downs SM & Chen J** 2008 EGF-like peptides mediate FSH-induced maturation of cumulus cell-enclosed mouse oocytes. *Mol Reprod Dev* **75** 105-114.
- el-Fouly MA, Cook B, Nekola M & Nalbandov AV** 1970 Role of the ovum in follicular luteinization. *Endocrinology* **87** 286-293.
- Eppig JJ, Wigglesworth K, Pendola F & Hirao Y** 1997 Murine oocytes suppress expression of luteinizing hormone receptor messenger ribonucleic acid by granulosa cells. *Biol Reprod* **56** 976-984.

Eppig JJ, Wigglesworth K & Pendola FL 2002 The mammalian oocyte orchestrates the rate of ovarian follicular development. *Proc Natl Acad Sci U S A* **99** 2890-2894.

Eppig JJ, Pendola FL, Wigglesworth K & Pendola JK 2005 Mouse oocytes regulate metabolic cooperativity between granulosa cells and oocytes: amino acid transport. *Biol Reprod* **73** 351-357.

Fan HY, Huo LJ, Chen DY, Schatten H & Sun QY 2004 Protein kinase C and mitogen-activated protein kinase cascade in mouse cumulus cells: cross talk and effect on meiotic resumption of oocyte. *Biol Reprod* **70** 1178-1187.

Gilchrist RB, Ritter LJ & Armstrong DT 2001 Mouse oocyte mitogenic activity is developmentally coordinated throughout folliculogenesis and meiotic maturation. *Dev Biol* **240** 289-298.

Gilchrist RB, Morrissey MP, Ritter LJ & Armstrong DT 2003 Comparison of oocyte factors and transforming growth factor-beta in the regulation of DNA synthesis in bovine granulosa cells. *Mol Cell Endocrinol* **201** 87-95.

Gilchrist RB, Ritter LJ, Myllymaa S, Kaivo-Oja N, Dragovic RA, Hickey TE, Ritvos O & Mottershead DG 2006 Molecular basis of oocyte-paracrine signalling that promotes granulosa cell proliferation. *J Cell Sci* **119** 3811-3821.

Gilchrist RB, Lane M & Thompson JG 2008 Oocyte-secreted factors: regulators of cumulus cell function and oocyte quality. *Hum Reprod Update* **14** 159-177.

Glister C, Groome NP & Knight PG 2003 Oocyte-mediated suppression of follicle-stimulating hormone- and insulin-like growth factor-induced secretion of steroids and inhibin-related proteins by bovine granulosa cells *in vitro*: possible role of transforming growth factor alpha. *Biol Reprod* **68** 758-765.

Haendler B, Schuttke I & Schleuning WD 2001 Androgen receptor signalling: comparative analysis of androgen response elements and implication of heat-shock protein 90 and 14-3-3eta. *Mol Cell Endocrinol* **173** 63-73.

Hickey TE, Marrocco DL, Gilchrist RB, Norman RJ & Armstrong DT 2004 Interactions between androgen and growth factors in granulosa cell subtypes of porcine antral follicles. *Biol Reprod* **71** 45-52.

Hickey TE, Marrocco DL, Amato F, Ritter LJ, Norman RJ, Gilchrist RB & Armstrong DT 2005 Androgens augment the mitogenic effects of oocyte-secreted factors and growth differentiation factor 9 on porcine granulosa cells. *Biol Reprod* **73** 825-832.

- Hunter MG & Paradis F** 2009 Intra-follicular regulatory mechanisms in the porcine ovary. *Control of pig Reproduction VIII*
- Hussein TS, Froiland DA, Amato F, Thompson JG & Gilchrist RB** 2005 Oocytes prevent cumulus cell apoptosis by maintaining a morphogenic paracrine gradient of bone morphogenetic proteins. *J Cell Sci* **118** 5257-5268.
- Jin S, Zhang M, Lei L, Wang C, Fu M, Ning G & Xia G** 2006 Meiosis activating sterol (MAS) regulate FSH-induced meiotic resumption of cumulus cell-enclosed porcine oocytes via PKC pathway. *Mol Cell Endocrinol* **249** 64-70.
- Juengel JL & McNatty KP** 2005 The role of proteins of the transforming growth factor-beta superfamily in the intraovarian regulation of follicular development. *Hum Reprod Update* **11** 143-160.
- Li R, Norman RJ, Armstrong DT & Gilchrist RB** 2000 Oocyte-secreted factor(s) determine functional differences between bovine mural granulosa cells and cumulus cells. *Biol Reprod* **63** 839-845.
- Lu Z, Xia G & Zhang J** 2001 Protein kinase C, rather than protein kinase A is involved in follicle-stimulating hormone-mediated meiotic resumption of mouse cumulus cell-enclosed oocytes in hypoxanthine-supplemented medium. *Mol Cell Endocrinol* **182** 225-232.
- Nagyova E, Prochazka R & Vanderhyden BC** 1999 Oocyectomy does not influence synthesis of hyaluronic acid by pig cumulus cells: retention of hyaluronic acid after insulin-like growth factor-I treatment in serum-free medium. *Biol Reprod* **61** 569-574.
- Okuwaki M** 2008 The structure and functions of NPM1/Nucleophsmin/B23, a multifunctional nucleolar acidic protein. *J Biochem* **143** 441-448.
- Otsuka F, Yamamoto S, Erickson GF & Shimasaki S** 2001 Bone morphogenetic protein-15 inhibits follicle-stimulating hormone (FSH) action by suppressing FSH receptor expression. *J Biol Chem* **276** 11387-11392.
- Paradis F, Novak S, Murdoch G, Dyck MK, Dixon WT & Foxcroft GR** 2009 Temporal regulation of BMP2, BMP6, BMP15, GDF-9, BMPR1A, BMPR1B, BMPR2 and TGFBR1 mRNA expression in the oocyte, granulosa and theca cells of developing preovulatory follicles in the pig. *Reproduction*. **138** 115-129.
- Prochazka R, Nagyova E, Rimkevicova Z, Nagai T, Kikuchi K & Motlik J** 1991 Lack of effect of oocyectomy on expansion of the porcine cumulus. *J Reprod Fertil* **93** 569-576.

Prochazka R, Nagyova E, Brem G, Schellander K & Motlik J 1998 Secretion of cumulus expansion-enabling factor (CEEF) in porcine follicles. *Mol Reprod Dev* **49** 141-149.

Ralph JH, Telfer EE & Wilmut I 1995 Bovine cumulus cell expansion does not depend on the presence of an oocyte secreted factor. *Mol Reprod Dev* **42** 248-253.

Salustri A, Yanagishita M & Hascall VC 1990a Mouse oocytes regulate hyaluronic acid synthesis and mucification by FSH-stimulated cumulus cells. *Dev Biol* **138** 26-32.

Singh B, Zhang X & Armstrong DT 1993 Porcine oocytes release cumulus expansion-enabling activity even though porcine cumulus expansion *in vitro* is independent of the oocyte. *Endocrinology* **132** 1860-1862.

Su YQ, Xia GL, Byskov AG, Fu GD & Yang CR 1999 Protein kinase C and intracellular calcium are involved in follicle-stimulating hormone-mediated meiotic resumption of cumulus cell-enclosed porcine oocytes in hypoxanthine-supplemented medium. *Mol Reprod Dev* **53** 51-58.

Sugiura K, Pendola FL & Eppig JJ 2005 Oocyte control of metabolic cooperativity between oocytes and companion granulosa cells: energy metabolism. *Dev Biol* **279** 20-30.

Toker A, Sellers LA, Amess B, Patel Y, Harris A & Aitken A 1992 Multiple isoforms of a protein kinase C inhibitor (KCIP-1/14-3-3) from sheep brain. Amino acid sequence of phosphorylated forms. *Eur J Biochem* **206** 453-461.

van Hemert MJ, Steensma HY & van Heusden GP 2001 14-3-3 proteins: key regulators of cell division, signalling and apoptosis. *Bioessays* **23** 936-946.

Vanderhyden BC, Cohen JN & Morley P 1993 Mouse oocytes regulate granulosa cell steroidogenesis. *Endocrinology* **133** 423-426.

Wakui H, Wright AP, Gustafsson J & Zilliacus J 1997 Interaction of the ligand-activated glucocorticoid receptor with the 14-3-3 eta protein. *J Biol Chem* **272** 8153-8156.

Yang H, Pettigrew JE, Johnston LJ, Shurson GC, Wheaton JE, White ME, Koketsu Y, Sower AF & Rathmacher JA 2000 Effects of dietary lysine intake during lactation on blood metabolites, hormones, and reproductive performance in primiparous sows. *J Anim Sci* **78** 1001-1009.

Yuan W, Lucy MC & Smith MF 1996 Messenger ribonucleic acid for insulin-like growth factors-I and -II, insulin-like growth factor-binding protein-2, gonadotropin receptors, and steroidogenic enzymes in porcine follicles. *Biol Reprod* **55** 1045-1054.

Zilliacus J, Holter E, Wakui H, Tazawa H, Treuter E & Gustafsson JA 2001 Regulation of glucocorticoid receptor activity by 14--3-3-dependent intracellular relocalization of the corepressor RIP140. *Mol Endocrinol* **15** 501-511.

CHAPTER 7

GENERAL DISCUSSION AND CONCLUSIONS

Mammalian ovarian follicle development is a well-coordinated orchestration of morphological, cellular and molecular changes that result in the production of a subset of oocytes competent of being fertilized and developing into embryos. Female fertility is therefore dependent on the ability of the follicle and oocyte to develop normally. This is important in the livestock industry where maximizing female reproductive efficiency is essential for productivity. As described in Chapter 2, antral follicle development is known to require sequential exposure to FSH and LH in order to transition to the preovulatory stage of development. It is also becoming apparent that the production of intrafollicular factors is essential for the local coordination of follicle and oocyte growth (Hunter and Paradis, 2009). Several families of growth factors, including the TGF- β superfamily, the IGF and EGF families, and angiogenic factors, are produced locally by the granulosa and theca cells and have been shown to affect the follicular environment. Historically, the oocyte was believed to play a passive role during folliculogenesis, relying mainly on the growth factors and metabolites produced by the granulosa and theca cells to grow and acquire developmental competence. In recent years, this concept has evolved dramatically and it became clear that the oocyte produces soluble growth factors (Juengel and McNatty, 2005, Gilchrist *et al.*, 2008). Several of these belong to the TGF- β superfamily and are responsible for modulating surrounding cell function and coordinating follicle growth (Eppig *et al.*, 2002, Matzuk *et al.*, 2002). The objective of the series of experiments described herein was to gain insight on the local regulation of preovulatory follicle development in the pig.

The origin of the animals and tissues used in the study of ovarian follicle development is an aspect that is too often ignored or regarded as being of minor significance in the literature. The materials used in the current studies were recovered *ex vivo* from gilts and sows of known reproductive status. Using a combination of follicular size, plasma progesterone and oestradiol concentrations, as well as follicular fluid oestradiol concentrations in large preovulatory follicles, it was possible to accurately allocate the follicles recovered from each animal to their developmental phase with respect to the process of recruitment, mid-selection and final selection. It was also possible to further categorize the large preovulatory follicle population as having been exposed or not to the preovulatory surge of luteinizing hormone. The basis for exploring changes in gene expression was to determine the potential involvement of several growth factors in those processes *in vivo*. Moreover, the use of a well-defined *in vivo* experimental paradigm, in which differences in follicle and oocyte maturity have been established as the likely cause of differences in subsequent fecundity in the sows, allowed the evaluation of involvement of local growth factors during normal versus suboptimal follicle and oocyte development (Clowes *et al.*, 1994, Foxcroft *et al.*, 2007, Paradis *et al.*, 2009, Zak *et al.*, 1997). The biological relevance of the data reported with respect to the normal process of folliculogenesis *in vivo* in the sows, will therefore be much greater than data reported from studies with ovarian tissues obtained from prepubertal gilts subjected to exogenous gonadotrophin stimulation or from *in vitro* studies using poorly defined abattoir material.

The limitations and obstacles associated with cellular and molecular studies in the pig is another important aspect to consider when considering the findings of current research. Too often, this aspect is not considered and the expectations for porcine studies are similar to those using human or rodent models. However given the differences in the information and research tools available, one should recognize the difficulties in meeting such expectations. Firstly, in contrast to the human and other model organisms, including the mouse and rat, that have a fully sequenced and annotated genome, sequencing of the porcine genome is only partially complete. Therefore, the information regarding

pig-specific genomic or mRNA sequences on public databases is still limited. For example, when the expression of the TGF- β superfamily members was evaluated in the present studies, the sequence information for porcine BMP6, BMPR1A and BMPR2 mRNA was unavailable. Through design of PCR primers based on sequence homology between human, mouse and rat, it was possible to obtain partial coding sequences for these genes, which then allowed the design of porcine-specific primer-probe sets for real-time PCR analysis. Secondly, the availability of porcine-specific antibodies is also extremely limited and validation of changes in protein expression most often requires the use of cross-reacting human or mouse antibodies. Unfortunately, these antibodies do not always function with porcine samples and often it is not possible to confirm associations between changes in protein expression and the changes in mRNA abundance observed. This was the case for porcine angiogenin mRNA which was shown to be more abundant in the theca cells during the final selection phase after the LH surge in the sows from the 2nd cycle post-weaning. Four different antibodies failed to detect angiogenin in porcine tissues or fluids that should have contained it. Therefore, it was impossible to determine if the change in mRNA abundance observed was reflected in a similar change in protein abundance.

The study presented in Chapter 3 describes the use of a microarray to identify the growth factors and receptors expressed in the oocyte, granulosa and theca cells. This experiment clearly demonstrates the value of using microarray in combination with gene ontology annotation to identify factors associated with a specific localization or functions. The list that was obtained from that experiment included a vast array of growth factors and receptors relevant to porcine follicle development. Interestingly, several of these factors were previously identified as being secreted by the mouse oocyte, further confirming the significance of these findings (Taft *et al.*, 2002, Pan *et al.*, 2005). This approach proved to be much more efficient than the previously reported signal sequence trap strategy, which relies on the presence of a signal sequence in the cDNA to identify the secreted factors. This latter strategy was employed by Taft *et al.* (2002) to describe the mouse oocyte secretome and yielded only a limited number of potential secreted

factors. Indeed this was the original strategy that we intended to use to identify the porcine oocyte, granulosa and theca cell secreted factors. However, several technical difficulties, mainly related to cloning of the cDNAs into the yeast shuttle vector necessary to identify the cDNA containing a signal sequence, significantly delayed the progress of the studies and prevented completion of this experimental approach. Failure to implement the signal sequence trap approach ultimately led to the use of microarray strategy which proved to be extremely useful.

The temporal changes in mRNA abundance for several growth factor families were determined during follicle development, more specifically during the recruitment, mid-selection and final selection phase. The expression patterns of some of the most interesting candidate genes are summarized in Figure 7.1 and changes in their mRNA abundance at specific times during follicle growth are indicative of their potential involvement in that process. In Chapter 4, GDF9 mRNA abundance was found to remain relatively stable in the oocyte throughout follicle growth. Since the oocyte appears to be the main site for GDF9 production in the follicle, it is likely that similar patterns of expression could be expected for the presence of the protein in follicular fluid. The expression of its receptor TGFBR1 was found to increase concomitantly in the granulosa and theca cells during the mid-selection phase, suggesting that GDF9 could be important for the selection and maintenance of the preovulatory population. Recent *in vitro* studies in cattle support these observations as GDF9 was found to stimulate proliferation of theca cells isolated from smaller follicles and to a greater extent, those isolated from larger follicles (Spicer *et al.*, 2008). In addition, intra-ovarian injection of GDF9 gene fragments promoted the development of medium-sized antral follicles in the rat (Shimizu *et al.*, 2008).

The pattern of expression of the angiogenic factors VEGFA, ANGPT1 and ANGPT2, and the transcription factor HIF1A, reported in Chapter 5 also suggests that development of the follicular vasculature at specific times during follicle development is important for follicle growth. The specific timing for the up-regulation of each factor is of particular interest, especially in light of the

antagonistic effect of ANGPT1 and ANGPT2 (reviewed by Hanahan, 1997). ANGPT2 mRNA is known to destabilize the vasculature but it has been hypothesized that, in the presence of other potent angiogenic factors, it would be favourable for vascular development. In contrast, in the absence of other stimulating factors, ANGPT2 would have a degenerative influence. The higher mRNA abundance of ANGPT2 observed during the mid-selection phase could therefore be indicative of a higher incidence of atresia during that period. However, in light of the constant expression of VEGFA during follicle development, it could also indicate the initiation of blood vessel development in the selected follicle. Moreover, ANGPT1 is known to stabilize blood vessels and the increased expression observed during the mid-selection and final selection phases suggests that it is involved in the maintenance of a healthy preovulatory follicle population. Finally, an increase in HIF1A mRNA expression during follicle growth is a potential indicator of the increased hypoxic conditions present in larger follicles. The strong relationships observed between *HIF1A* mRNA and ANGPT1 and VEGFA mRNA suggest the potential for this transcription factor to regulate the expression of those genes.

IGF1 has long been known to modulate granulosa and theca cell functions. *In vitro* studies have clearly established its involvement in modulating granulosa and theca cell proliferation and steroidogenesis (Spicer and Echterkamp, 1995, Mazerbourg *et al.*, 2003). In the current experiments, the expression of *IGF1* mRNA in the granulosa cells remained stable across all stages of follicle development whereas the expression of its receptor in granulosa cells increased during the mid-selection phase. Since increased cell proliferation and steroidogenic activity is expected in the selected follicle, IGF1 is likely to be important in mediating those effects in the granulosa cells. The expression of *IGF1* mRNA in the theca cells is very different, as it increases gradually from the recruitment to the final selection phase, indicating that its effect would be predominantly exerted in the large preovulatory follicle. The expression of IGF1R in theca cells is somewhat consistent with this hypothesis since it increases during the mid-selection phase and remains high in the selected preovulatory

population. The current data suggests IGF1 could be responsible for the increased steroidogenic activity of theca cells that is expected in larger follicles. It was also observed that the expression of the IGF1BPs is highly variable, demonstrating the complexity of the regulation of IGF1 activity in the follicle. Throughout the stages studied, *IGF1* mRNA in the theca cells of the sows from the 1st post-weaning cycle of preovulatory development was consistently higher than that of the 2nd cycle. We hypothesized that the less mature follicles present in the sows from the 1st cycle require higher IGF1 stimulation to increase proliferation and responsiveness to the gonadotrophins to carry those follicles into the preovulatory population.

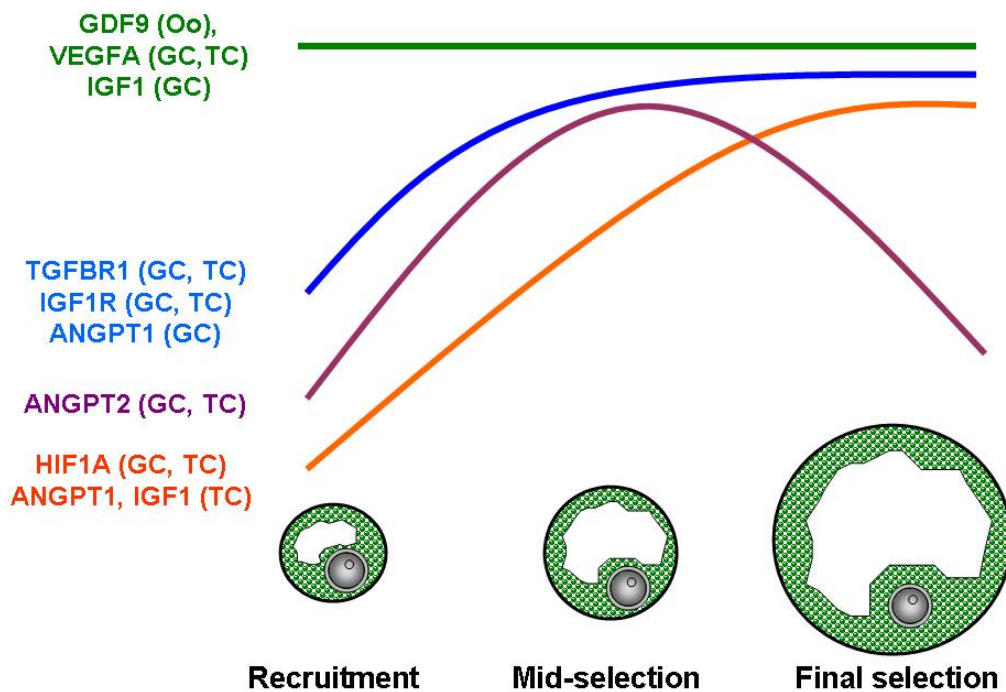


Figure 7.1 Schematic representation of the temporal regulation of growth factors and receptors mRNA in the oocyte (Oo), granulosa (GC) and theca (TC) cells during the recruitment, mid-selection and final selection phase that are potentially involved in each specific phase of follicular development.

Perhaps the most interesting findings from the series of studies described in this thesis involve the molecular events occurring during the period

immediately preceding or following the LH surge in the pig preovulatory follicle population. First, the up-regulation of BMPR1B in the preovulatory follicle population described in Chapter 4 is coincident with the up-regulation of AREG and EREG observed during the same period in Chapter 3 (Figure 7.2). These results suggest that at the time of the preovulatory LH surge *in vivo*, modulation of these factors could be essential for initiating the succession of events leading to ovulation. In the mouse, there is evidence for a role for BMP15 in the ovulatory process. First, BMP15 null-mice exhibited a lower ovulation rate accompanied with reduced oocyte developmental competence (Su *et al.*, 2004, Yan *et al.*, 2001). Knockout mice for the BMP15 receptor, BMPR1B, also presented defects in cumulus expansion and decreased fertilization rates (Yi *et al.*, 2001). In addition, the mature form of BMP15 was also shown to appear in the preovulatory follicle population either just before or after hCG treatment (Gueripel *et al.*, 2006, Yoshino *et al.*, 2006). Furthermore, BMP15 in the mouse is considered to be oocyte specific and the mouse oocyte is also involved in FSH-stimulated cumulus cell expansion, suggesting that the oocyte-derived BMP15 might be involved in that process. Similarly, AREG and EREG have been shown to be involved in LH-mediated cumulus cell expansion and oocyte meiotic resumption in the mouse (Park *et al.*, 2004). Available evidence supports a similar role in the pig as eCG and hCG stimulation has been shown to induce AREG and EREG mRNA expression in sow granulosa cells (Kawashima *et al.*, 2008) and both factors are capable of inducing cumulus cell expansion and oocyte meiotic resumption *in vitro* (Chen *et al.*, 2008, Yamashita *et al.*, 2007).

Another important event occurring around the preovulatory LH surge is the transition of the cells from oestradiol to progesterone secretion. Modulation of *FSHR* and *HSD3B* mRNA by the preovulatory porcine oocyte described in Chapter 6 suggests that the oocyte is involved in mediating this transition (Figure 7.2). This observation has important implications since most studies describing the role of the oocyte on surrounding cells have been performed using oocytes isolated from medium-sized follicles and the results have been generalized to all oocytes from antral follicles. This further emphasizes the importance of carefully

defining the physiological state of the animals used for an experiment when drawing appropriate conclusions and generating further hypotheses. Finally, the higher expression of *ANG* in the theca cells of the preovulatory follicle population post-LH observed in the animals from the 2nd cycle, suggests that appropriate vasculature during that period could be important for allowing progesterone to prime the oviduct and could partially explain the differences in embryo survival observed in these animals. Together, these observations confirm that complex regulatory mechanisms involving several growth factors are present in the pig preovulatory follicle. Correct orchestration of changes in the expression of these growth factors and receptors is necessary for the normal ovulatory process and steroidogenic activity of the follicle.

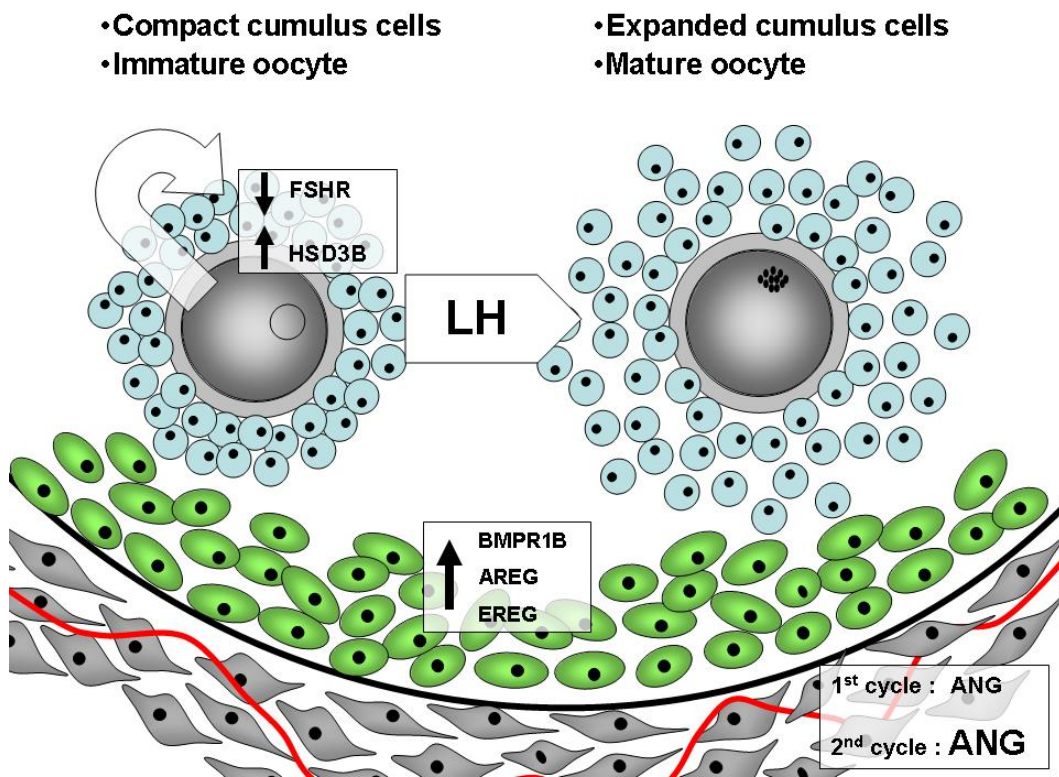


Figure 7.2 Schematic representation of the effect of the porcine preovulatory oocyte and several growth factors and receptors in large preovulatory follicles in the period immediately preceding and following the LH surge.

The observations and conclusions drawn from the series of experiments described in the current thesis also form the basis for suggesting future studies that would further improve our understanding of the role of specific growth factors during porcine follicle development. First, given the pattern of mRNA expression of many angiogenic factors, and their proposed involvement in the process of selection and in establishing differences in follicle quality, it would be particularly valuable to confirm the angiogenic activity present in the follicular fluid of the follicle at the different stages studied. Since the availability of porcine antibodies is relatively limited, establishing a culture system using the cells present in the thecal layer that would support the proliferation, migration and assembly of the endothelial cells present in that cell population into blood vessel-like structures would be valuable. A similar approach has recently been developed to study angiogenesis in the bovine corpus luteum (Robinson *et al.*, 2008, Woad *et al.*, 2009). Using follicular fluid from the different follicle categories to supplement the culture media, the ability of such fluid to stimulate angiogenesis could therefore be assayed. Such a culture system would also permit the use of recombinant angiogenic factors to evaluate the individual and combined abilities of those factors to modulate blood vessel formation.

The observation that the expression of *BMPRI1B*, *AREG* and *EREG* all increased in abundance in the period surrounding the preovulatory LH surge, suggest that they could somehow be involved in similar biological processes. Using the *in vitro* culture system defined in Chapter 6, it would be very informative to delineate the exact series of events triggered by the preovulatory LH surge leading to the up-regulation of those genes, but also the impact that those genes have on the subsequent processes of ovulation such as cumulus cell expansion and oocyte meiotic resumption. The use of RNAi would allow the knockdown of specific factors in the granulosa and/or cumulus cells to further evaluate the impact of that loss of function.

Finally, the observation that fully grown GV oocytes modulate their environment in a manner that reflects the needs of the follicle at each stage of

follicle growth is of great interest. In the experiment described in Chapter 6, attempts were made to quantify progesterone concentrations in the culture media following the 22h of culture. Unfortunately, the progesterone concentration was below the detection limit of the assay. Many factors could have affected the ability to quantify progesterone, including the limited number of cumulus cells cultured in a small volume of medium. Moreover, steroids are lipid-soluble and the use of mineral oil during culture could have absorbed and sequestered much of the progesterone produced. Finally, it is not clear whether the cumulus cells possess the same ability as the mural granulosa cells to produce cholesterol *de novo*. The absence of precursors for progesterone synthesis in our culture media could also explain the low production observed in this experiment. As a first step, it would be valuable to reproduce this culture system using a much greater number of cumulus cells, no mineral oil and the addition of cholesterol to the culture media. This would allow the quantification of progesterone concentrations and the validation that the up-regulation of *HSD3B* mRNA leads to higher progesterone production. The use of RNAi to knockdown BMP15 and GDF9 would then be useful to assess the ability of the oocyte to modulate the steroidogenic ability of the cumulus cells.

In conclusion, the results presented in this thesis provide convincing evidence that several growth factor families are expressed in ovarian follicular cells during *in vivo* follicle development in the pig. It also provides useful information regarding the temporal changes in mRNA abundance for these growth factors and receptors, allowing the temporal associations between their expression and the processes of recruitment and selection, and changes during the periovulatory period to be established. Finally, these studies also demonstrate that specific growth factors such as IGF1 and ANG are important mediators of follicle and oocyte quality. Future studies arising from the results presented in this thesis may be able to focus on the role of these factors on granulosa or theca cell functions, or on their involvement in improving oocyte competence in *in vivo* situations that have relevance to the swine industry.

REFERENCES

- Chen X, Zhou B, Yan J, Xu B, Tai P, Li J, Peng S, Zhang M & Xia G** 2008 Epidermal growth factor receptor activation by protein kinase C is necessary for FSH-induced meiotic resumption in porcine cumulus-oocyte complexes. *J Endocrinol* **197** 409-419.
- Clowes EJ, Aherne FX & Foxcroft GR** 1994 Effect of delayed breeding on the endocrinology and fecundity of sows. *J Anim Sci* **72** 283-291.
- Eppig JJ, Wigglesworth K & Pendola FL** 2002 The mammalian oocyte orchestrates the rate of ovarian follicular development. *Proc Natl Acad Sci U S A* **99** 2890-2894.
- Foxcroft GR, Vinsky MD, Paradis F, Tse WY, Town SC, Putman CT, Dyck MK & Dixon WT** 2007 Macroenvironment effects on oocytes and embryos in swine. *Theriogenology* **68** Suppl 1 S30-39.
- Gilchrist RB, Lane M & Thompson JG** 2008 Oocyte-secreted factors: regulators of cumulus cell function and oocyte quality. *Hum Reprod Update* **14** 159-177.
- Gueripel X, Brun V & Gougeon A** 2006 Oocyte bone morphogenetic protein 15, but not growth differentiation factor 9, is increased during gonadotropin-induced follicular development in the immature mouse and is associated with cumulus oophorus expansion. *Biology of Reproduction* **75** 836-843.
- Hanahan D** 1997 Signaling vascular morphogenesis and maintenance. *Science* **277** 48-50.
- Hunter MG & Paradis F** 2009 Intra-follicular regulatory mechanisms in the porcine ovary. *Control of Pig Reproduction VIII*.
- Juengel JL & McNatty KP** 2005 The role of proteins of the transforming growth factor-beta superfamily in the intraovarian regulation of follicular development. *Hum Reprod Update* **11** 143-160.
- Kawashima I, Okazaki T, Noma N, Nishibori M, Yamashita Y & Shimada M** 2008 Sequential exposure of porcine cumulus cells to FSH and/or LH is critical for appropriate expression of steroidogenic and ovulation-related genes that impact oocyte maturation *in vivo* and *in vitro*. *Reproduction* **136** 9-21.
- Matzuk MM, Burns KH, Viveiros MM & Eppig JJ** 2002 Intercellular communication in the mammalian ovary: oocytes carry the conversation. *Science* **296** 2178-2180.

- Mazerbourg S, Bondy CA, Zhou J & Monget P** 2003 The insulin-like growth factor system: a key determinant role in the growth and selection of ovarian follicles? a comparative species study. *Reprod Domest Anim* **38** 247-258.
- Pan H, O'Brien M J, Wigglesworth K, Eppig JJ & Schultz RM** 2005 Transcript profiling during mouse oocyte development and the effect of gonadotropin priming and development *in vitro*. *Dev Biol* **286** 493-506.
- Paradis F, Novak S, Murdoch G, Dyck MK, Dixon WT & Foxcroft GR** 2009 Temporal regulation of BMP2, BMP6, BMP15, GDF-9, BMPR1A, BMPR1B, BMPR2 and TGFBR1 mRNA expression in the oocyte, granulosa and theca cells of developing preovulatory follicles in the pig. *Reproduction* **138** 115-129.
- Park JY, Su YQ, Ariga M, Law E, Jin SL & Conti M** 2004 EGF-like growth factors as mediators of LH action in the ovulatory follicle. *Science* **303** 682-684.
- Robinson RS, Hammond AJ, Mann GE & Hunter MG** 2008 A novel physiological culture system that mimics luteal angiogenesis. *Reproduction* **135** 405-413.
- Shimizu T, Iijima K, Ogawa Y, Miyazaki H, Sasada H & Sato E** 2008 Gene injections of vascular endothelial growth factor and growth differentiation factor-9 stimulate ovarian follicular development in immature female rats. *Fertility and Sterility* **89** 1563-1570.
- Spicer LJ & Echtenkamp SE** 1995 The ovarian insulin and insulin-like growth factor system with an emphasis on domestic animals. *Domest Anim Endocrinol* **12** 223-245.
- Spicer LJ, Aad PY, Allen DT, Mazerbourg S, Payne AH & Hsueh AJ** 2008 Growth differentiation factor 9 (GDF9) stimulates proliferation and inhibits steroidogenesis by bovine theca cells: Influence of follicle size on responses to GDF9. *Biology of Reproduction* **78** 243-253.
- Su YQ, Wu X, O'Brien MJ, Pendola FL, Denegre JN, Matzuk MM & Eppig JJ** 2004 Synergistic roles of BMP15 and GDF9 in the development and function of the oocyte-cumulus cell complex in mice: genetic evidence for an oocyte-granulosa cell regulatory loop. *Dev Biol* **276** 64-73.
- Taft RA, Denegre JM, Pendola FL & Eppig JJ** 2002 Identification of genes encoding mouse oocyte secretory and transmembrane proteins by a signal sequence trap. *Biol Reprod* **67** 953-960.
- Woad K, Hammond A, Hunter M, Mann G & Robinson B** 2009 FGF2 is crucial for the development of bovine luteal endothelial networks *in vitro*. *Reproduction*.

Yamashita Y, Kawashima I, Yanai Y, Nishibori M, Richards JS & Shimada M 2007 Hormone-induced expression of tumor necrosis factor alpha-converting enzyme/A disintegrin and metalloprotease-17 impacts porcine cumulus cell oocyte complex expansion and meiotic maturation via ligand activation of the epidermal growth factor receptor. *Endocrinology* **148** 6164-6175.

Yan CN, Wang P, DeMayo J, DeMayo FJ, Elvin JA, Carino C, Prasad SV, Skinner SS, Dunbar BS, Dube JL, Celeste AJ & Matzuk MM 2001 Synergistic roles of bone morphogenetic protein 15 and growth differentiation factor 9 in ovarian function. *Molecular Endocrinology* **15** 854-866.

Yi SE, LaPolt PS, Yoon BS, Chen JYC, Lu JKH & Lyons KM 2001 The type IBMP receptor BmprIB is essential for female reproductive function. *Proceedings of the National Academy of Sciences of the United States of America* **98** 7994-7999.

Yoshino O, McMahon HE, Sharma S & Shimasaki S 2006 A unique preovulatory expression pattern plays a key role in the physiological functions of BMP-15 in the mouse. *PNAS* **103** 10678-10683.

Zak LJ, Xu X, Hardin RT & Foxcroft GR 1997a Impact of different patterns of feed intake during lactation in the primiparous sow on follicular development and oocyte maturation. *J Reprod Fertil* **110** 99-106.

APPENDIX I: Supplementary Table 3.3: Use of Affymetix GeneChip Porcine Genome Array in combination with gene ontology annotation to identify transcripts expressed in oocyte (Oo), granulosa (GC) and theca (TC) cells of porcine antral follicles that grouped under the gene ontology term “extracellular region” (GO:0005576).

Probe Set ID	Name	Gene Symbol	Public ID	Raw signal		
				Oo	GC	TC
Ssc.2165.2.S1_a_at	14-3-3 protein sigma	SFN	CN164785	88.9		
Ssc.4021.1.S1_at	1-acyl-sn-glycerol-3-phosphate acyltransferase alpha	AGPAT1	BG608754	75.9	173.95	183.6
Ssc.26726.1.S1_a_at	1-O-acylceramide synthase precursor	LYPLA3	BX677245	205.8	101.95	75.3
Ssc.3522.2.S1_at	2',3'-cyclic-nucleotide 3'-phosphodiesterase	CNP	CF366785	316.55	177.05	228.1
Ssc.6719.1.A1_at	60 kDa heat shock protein, mitochondrial precursor	HSPD1	CB469603	429.4	1531.8	1480.45
Ssc.19625.1.S1_at	62 kDa protein	TGFBR3	BF198193	262.95	532.4	557.2
Ssc.5713.1.S1_at	72 kDa type IV collagenase precursor	MMP2	NM_214192.1		94.3	565.65
Ssc.30817.1.A1_at	A disintegrin and metalloproteinase domain 9, precursor	ADAM9	CO950124	55.55	756.75	781.25
Ssc.8904.1.A1_at	a disintegrin-like and metalloprotease domain with thrombospondin type I motifs-like 3	ADAMTSL3	CF362847			68.65
Ssc.1282.1.A1_at	acid phosphatase 6, lysophosphatidic	ACP6	BQ602332	258.55	247.65	152.6
Ssc.30672.1.A1_at	Activity-dependent neuroprotector	ADNP	AJ654455	86.6	610.9	525.85
Ssc.1692.1.A1_at	ADAM 12 precursor	ADAM12	BF709272			136.45
Ssc.16051.1.A1_at	A disintegrin and metalloproteinase domain 9	ADAM9	AJ681165		118.95	89.35
Ssc.16051.1.S1_at	A disintegrin and metalloproteinase domain 9	ADAM9	AJ681165		101.5	
Ssc.29157.1.A1_at	A disintegrin and metalloproteinase domain 9	ADAM9	CO950227		88.1	98.35
Ssc.12365.1.A1_at	A disintegrin and metalloproteinase with thrombospondin motifs 1	ADAMTS1	CK463677		129.55	390.8
Ssc.16451.1.A1_at	A disintegrin and metalloproteinase with thrombospondin motifs 1	ADAMTS1	CN161145		232.4	823.65
Ssc.5754.1.A1_at	A disintegrin and metalloproteinase with thrombospondin motifs 12	ADAMTS12	BI404252	545.05	331.35	303.2
Ssc.1703.1.S1_at	A disintegrin and metalloproteinase with thrombospondin motifs 17	ADAMTS17	CN153134	481.6	710.5	525.35
Ssc.28905.1.A1_at	A disintegrin and metalloproteinase with thrombospondin motifs 18, precursor	ADAMTS18	CO954471		182.7	116.05

Ssc.28905.2.S1_at	A disintegrin and metalloproteinase with thrombospondin motifs 18, precursor	ADAMTS18	BP435964		83.05		
Ssc.1206.1.A1_at	A disintegrin and metalloproteinase with thrombospondin motifs 19, precursor	ADAMTS19	BM190132	383.1			
Ssc.17487.1.A1_at	A disintegrin and metalloproteinase with thrombospondin motifs 19, precursor	ADAMTS19	CD572548		110.35	302.9	
Ssc.18083.1.A1_at	A disintegrin and metalloproteinase with thrombospondin motifs 2, precursor	ADAMTS2	CF179745			73.4	
Ssc.18806.1.A1_at	A disintegrin and metalloproteinase with thrombospondin motifs 2, precursor	ADAMTS2	CF362353	74.6			
Ssc.24305.1.A1_at	A disintegrin and metalloproteinase with thrombospondin motifs 20, precursor	ADAMTS20	CK456871		101.15		
Ssc.30575.1.A1_at	A disintegrin and metalloproteinase with thrombospondin motifs 3, precursor	ADAMTS3	CO994151			466.95	
Ssc.18190.1.A1_at	A disintegrin and metalloproteinase with thrombospondin motifs 9, precursor	ADAMTS9	CF180747		130.1	469.45	
Ssc.16584.1.A1_at	adipocyte enhancer binding protein 1 precursor	AEBP1	CO947340			408.4	
Ssc.6323.1.S1_at	Adipophilin	ADFP	AY550037.1	769.95	103.85	136.55	
Ssc.26238.1.S1_at	ADM precursor	ADM	BX923240		72.7	77	
Ssc.314.1.S1_at	ADM precursor	ADM	NM_214107.1		149.15	186.45	
Ssc.3240.1.A1_at	Agrin precursor (Fragment)	AGRN	CF175761		667.8	588	
Ssc.3059.1.S1_at	Aldose reductase	AKR1B1	NM_001001539.1	502.05	199.7	244.4	
Ssc.7101.1.A1_at	Alpha-2-HS-glycoprotein precursor	AHSG	X56021.1	127.7			
Ssc.16603.1.A1_at	Alpha-2-macroglobulin precursor	A2M	BI181630			2475.85	
Ssc.26317.1.A1_at	Alpha-2-macroglobulin precursor	A2M	AY509877.1			227.45	
Ssc.26317.1.S1_at	Alpha-2-macroglobulin precursor	A2M	AY509877.1			168.15	
Ssc.9440.1.A1_at	Alpha-2-macroglobulin precursor	A2M	CN069729			81.2	
Ssc.2922.1.A1_a_at	Alpha-amylase 2B precursor	AMY2B	CN165301	299.75	132.3	90.25	
Ssc.2922.2.A1_at	Alpha-amylase 2B precursor	AMY2B	BQ598309	739.5	76.4	60	
Ssc.6009.1.S1_a_at	Alpha-amylase 2B precursor	AMY2B	NM_214195.1	155.95	1259.4	765.05	
Ssc.6009.1.S1_at	Alpha-amylase 2B precursor	AMY2B	NM_214195.1	210.65	1574.05	1152.45	
Ssc.8589.1.S1_at	Alpha-amylase 2B precursor	AMY2B	CN153848	455.6	124.25	69.75	
Ssc.8589.2.S1_a_at	Alpha-amylase 2B precursor	AMY2B	BF712854	437.05	123.55	71	
Ssc.23363.1.S1_at	Alpha-galactosidase A precursor	GLA	AJ659578	652.8	256.9	159.5	

Ssc.7423.1.S1_at	Alpha-galactosidase A precursor	GLA	CN154058	386.3	174.6	130.65
Ssc.13765.1.A1_at	Alpha-lactalbumin precursor	LALBA	NM_214360.1	283.75		
Ssc.7107.1.A1_at	Alpha-tectorin precursor	TECTA	CN154593		467.2	324.85
Ssc.4216.1.S1_at	Aminopeptidase B	RNPEP	CN156382	61.7	100.25	99.05
Ssc.14467.2.S1_a_at	Amphiregulin precursor	AREG	AY028311.1		684.65	
Ssc.14258.1.S1_at	Amyloid beta A4 protein precursor	APP	NM_214372.1	68.65	957.6	1096.75
Ssc.9950.1.A1_at	Amyloid beta A4 protein precursor	APP	CF792729	336.55	355.95	177.5
Ssc.3176.1.S1_at	Amyloid-like protein 1 precursor	APLP1	CK465083			64.95
Ssc.11079.1.A1_at	Angiogenin precursor	ANG	NM_213936.1		380.4	750
Ssc.4679.1.S1_at	Angiogenin precursor	ANG	CN157788		182.45	219.25
Ssc.16730.1.S1_at	Angiopoietin-1	ANGPT1	NM_213959.1	58.5	168.1	
Ssc.24374.1.S1_at	Angiopoietin-1	ANGPT1	CK452350		204.5	117.95
Ssc.6943.1.A1_at	Angiopoietin-1 precursor	ANGPT1	BF703917		86.3	
Ssc.240.1.S1_at	Angiopoietin-2 precursor	ANGPT2	NM_213808.1			229.45
Ssc.29929.1.S1_at	Angiopoietin-related protein 2 precursor	ANGPTL2	CO938780			329.15
Ssc.28458.1.A1_at	Angiopoietin-related protein 3 precursor	ANGPTL3	CN025175	140.95	119.5	98.55
Ssc.17345.1.S1_at	Angiopoietin-related protein 4 precursor	ANGPTL4	AY307772.1		63.6	
Ssc.8980.1.A1_at	Angiopoietin-related protein 4 precursor	ANGPTL4	BI183736		441.5	466.65
Ssc.15257.1.S1_a_at	angiotensin I converting enzyme 2 precursor	ACE2	CF362452	1043.2	568.55	537.6
Ssc.24528.1.S1_at	Angiotensin-converting enzyme, somatic isoform precursor	ACE	CK459351	659.4	315.45	321.2
Ssc.4804.1.S1_at	Angiotensinogen precursor	AGT	BI182680			115.4
Ssc.12241.1.A1_at	Annexin A2	ANXA2	CB471539	429.6	1720.25	1825.65
Ssc.2652.1.A1_at	Anthrax toxin receptor 2 precursor	ANTXR2	CN163375	163.9	559.25	788.1
Ssc.6080.1.S1_at	Antileukoproteinase 1 precursor	SLPI	NM_213870.1			144.3
Ssc.3436.1.A1_at	Apelin precursor	APLN	BE233435			415.65
Ssc.19257.1.S1_at	apolipoprotein A-I binding protein	APOA1BP	CN164748	141.75	165.6	207.3
Ssc.807.1.S1_at	Apolipoprotein A-I precursor	APOA1	NM_214398.1		703.45	474.5
Ssc.24987.3.A1_at	Apolipoprotein B-100 precursor	APOB	CF176070	85.15		
Ssc.8573.1.A1_at	Apolipoprotein D precursor	APOD	BX667312	120.35	416	1716.8
Ssc.1342.1.A1_at	Apolipoprotein E precursor	APOE	NM_214308.1			67.25
Ssc.1342.1.S1_at	Apolipoprotein E precursor	APOE	NM_214308.1	180		991.1

Ssc.23221.1.S1_at	Apolipoprotein F precursor	APOF	AY583018.1	69.95	62.05	
Ssc.170.1.S1_at	Arginase 1	ARG1	NM_214048.1			96.65
Ssc.20071.1.S1_at	ARMET protein precursor	ARMET	CO993738	1187.9	1678.65	1815.8
Ssc.2861.1.A1_at	ARMET protein precursor	ARMET	CN153468	218.15	261	387.4
Ssc.11033.1.S1_at	Arylsulfatase A precursor	ARSA	NM_213933.1		51.8	128.6
Ssc.1716.1.S1_at	Asporin precursor	ASPN	CN165456			114.45
Ssc.7686.1.S1_at	Attractin precursor	ATRN	BX917611	92.3	349.6	188.9
Ssc.837.1.A1_at	Bactericidal permeability-increasing protein precursor	BPI	BF708439			81.4
Ssc.22268.1.A1_at	Basement membrane-specific heparan sulfate proteoglycan core protein precursor	HSPG2	CF789779	350.45	659.4	650.45
Ssc.19531.1.A1_at	Beta-1,3-N-acetylglucosaminyltransferase lunatic fringe	LFNG	CF368484	140.2		159.85
Ssc.19861.1.S1_at	Beta-1,3-N-acetylglucosaminyltransferase manic fringe	MFNG	BX675375			60.4
Ssc.8617.1.A1_at	Beta-1-syntrophin	SNTB1	BF712945		120.55	353.45
Ssc.12348.1.S1_at	beta-2-microglobulin precursor	B2M	NM_213978.1		536.1	1790
Ssc.12348.2.S1_at	beta-2-microglobulin precursor	B2M	CO943625	63.65	266.4	962.5
Ssc.1730.1.A1_at	Beta-2-syntrophin	SNTB2	BF710246		96.65	154
Ssc.28449.1.A1_at	Beta-2-syntrophin	SNTB2	CN032498	1587.1		
Ssc.14392.1.A1_at	Beta-microseminoprotein precursor	MSMB	NM_213852.1		781	200.45
Ssc.5943.1.S1_at	Biglycan precursor	BGN	BF193177			592.15
Ssc.16679.1.S1_at	Bone morphogenetic protein 1 precursor	BMP1	BF079341		485.1	155.55
Ssc.25797.1.S1_at	Bone morphogenetic protein 1 precursor	BMP1	BI346244		345.25	158.7
SscAffx.24.1.S1_at	Bone morphogenetic protein 15 precursor	BMP15	NM_001005155.1	996.2		
Ssc.4190.1.S1_at	Bone morphogenetic protein 2 precursor	BMP2	CA779719	112.35		
Ssc.16690.1.S1_at	Bone morphogenetic protein 4 precursor	BMP4	CN159298	157.3		70.35
Ssc.1179.1.S1_at	Bone morphogenetic protein 5 precursor	BMP5	BX924864		226.65	206.5
Ssc.30159.1.A1_at	Bone morphogenetic protein 6 precursor	BMP6	CO987354		174.4	84.35
Ssc.21278.1.S1_at	Bone morphogenetic protein 8B precursor	BMP8A	CF796011	63.5		
Ssc.21895.1.S1_at	Bullous pemphigoid antigen 1, isoforms 6/9/10	DST	CO993970	190.15	843.1	436
Ssc.2426.1.S1_at	Bullous pemphigoid antigen 1, isoforms 6/9/10	DST	BQ599601		64.7	117.25
Ssc.27547.1.A1_at	Bullous pemphigoid antigen 1, isoforms 6/9/10	DST	CN162768	245.75	480.15	813.45
Ssc.29588.1.A1_at	Bullous pemphigoid antigen 1, isoforms 6/9/10	DST	CO941201		120.8	

Ssc.11162.1.S1_at	C4b-binding protein alpha chain precursor	C4BPA	NM_213942.1				209.15
Ssc.12939.1.S1_at	Cadherin-13 precursor	CDH13	CK465596	86.45			99.85
Ssc.6987.1.A1_at	Cadherin-13 precursor	CDH13	CK458044	210.95			
Ssc.17879.1.S1_at	Calcitonin gene-related peptide II precursor	CALCB	NM_213746.1	491.75			
Ssc.3106.1.S1_at	Calreticulin precursor	CALR	CK466345	98.85	435.5		214.7
Ssc.1622.1.S1_at	Calumenin precursor	CALU	CO938226	529	987.35		848.05
Ssc.6685.1.S1_at	Calumenin precursor	CALU	BP458282	132.45	273.15		204.55
Ssc.6685.2.A1_at	Calumenin precursor	CALU	CF359539	320.8	497		406.55
Ssc.5464.1.A1_at	Carboxypeptidase E precursor	CPE	CD571929	111.65	76.35		369.95
Ssc.25224.1.A1_at	Carboxypeptidase N catalytic chain precursor	CPN1	CK461033	102.7			
Ssc.14477.1.S1_at	cartilage intermediate layer protein	CILP	U83114.1	450.9			
Ssc.3508.1.A1_at	Cartilage-associated protein precursor	CRTAP	CF180240		245.8		490.9
Ssc.1181.1.S1_at	Cathepsin B precursor	CTSB	CK466199	1670.85	1557.35		1560.05
Ssc.28893.1.A1_at	Cathepsin D precursor	CTSD	CN165455		347.85		248.2
Ssc.17203.1.A1_at	Cathepsin S precursor	CTSS	CO989650	64			256.3
Ssc.17203.2.S1_at	Cathepsin S precursor	CTSS	CB480218	103.2			294.3
Ssc.17203.3.S1_at	Cathepsin S precursor	CTSS	BX673584				181.5
Ssc.13343.1.A1_at	CD109	CD109	BI404867		306.95		
Ssc.5053.1.S1_at	CD163 antigen isoform a	CD163	NM_213976.1				74.65
Ssc.16055.1.S1_at	CD59 glycoprotein precursor	CD59	NM_214170.1		69.1		61.25
Ssc.20559.1.A1_at	CD59 glycoprotein precursor	CD59	BQ604202	1113.25	1170.05		1206.7
Ssc.3348.1.S1_at	CD97 antigen precursor	CD97	NM_213925.1				127.8
Ssc.8308.1.A1_at	cell adhesion molecule with homology to L1CAM precursor	CHL1	BQ601282	289.4			
Ssc.18164.1.A1_at	Cholinesterase precursor	BCHE	CK452065				116.95
Ssc.7268.1.A1_at	Chondromodulin-I precursor	LECT1	BQ598411		217.25		69.95
Ssc.26080.1.A1_at	chordin-like 2	CHRDL2	BX915686	56.2	138.05		83.8
Ssc.11310.2.A1_at	Chordin-like protein 1 precursor	CHRDL1	CO992488		260.15		573.7
Ssc.13276.1.A1_at	Chordin-like protein 1 precursor	CHRDL1	BQ605152				58
Ssc.4653.1.S1_at	Chromogranin A precursor	CHGA	AW431372		83.75		
Ssc.31171.1.S1_at	chromosome X open reading frame 36	CXorf36	BG610311		146.65		120.9
Ssc.11992.1.A1_at	Clusterin precursor	CLU	NM_213971.1		91.75		204.2

Ssc.26345.2.S1_at	Coagulation factor XIII A chain precursor	F13A1	CB478193			82.2
Ssc.24450.1.S1_at	Coagulation factor XIII B chain precursor	F13B	CK457201	118.45		
Ssc.31044.1.S1_at	Coagulation factor XIII B chain precursor	F13B	CK463688		135.45	133.15
Ssc.13207.1.A1_at	Coatomer alpha subunit	COPA	CK459946	611.5	785.15	763.6
Ssc.13207.2.S1_at	Coatomer alpha subunit	COPA	BQ604787		82.95	76.25
Ssc.31124.1.S1_at	COL14A1 protein	COL14A1	CO946528	1047.25		1065.25
Ssc.6778.1.S1_at	COL14A1 protein	COL14A1	BE693212			223.85
Ssc.514.1.S1_at	Colipase precursor	CLPS	NM_214203.1	717.05		
Ssc.1091.1.S1_at	Collagen alpha 1(I) chain precursor	COL1A1	CN163303			2443.2
Ssc.1091.3.A1_at	Collagen alpha 1(I) chain precursor	COL1A1	BI184901			1966.4
Ssc.9778.1.S1_at	Collagen alpha 1(I) chain precursor	COL1A1	CK464602			140
Ssc.25009.1.A1_at	Collagen alpha 1(II) chain precursor	COL5A2	CK459968	276.05		80.35
Ssc.11302.1.S1_at	Collagen alpha 1(III) chain precursor	COL3A1	CF176410		63.55	2749.85
Ssc.11302.1.S2_at	Collagen alpha 1(III) chain precursor	COL3A1	CO951188			2041.55
Ssc.4345.1.S1_at	Collagen alpha 1(IV) chain precursor	COL4A1	BI183311		315.7	832.35
Ssc.4345.1.S2_at	Collagen alpha 1(IV) chain precursor	COL4A1	CO992417		1242.6	1969.35
Ssc.6435.1.S1_at	Collagen alpha 1(IV) chain precursor	COL4A1	CN154120			114.45
Ssc.18545.1.A1_at	Collagen alpha 1(V) chain precursor	COL5A1	BQ605049			56.35
Ssc.4993.1.A1_at	Collagen alpha 1(V) chain precursor	COL5A1	CO946277			699.1
Ssc.9002.1.A1_at	Collagen alpha 1(V) chain precursor	COL5A1	CO952384			1944.55
Ssc.5895.1.A2_at	Collagen alpha 1(VI) chain precursor	COL6A1	CN162503			432.05
Ssc.5895.2.A1_at	Collagen alpha 1(VI) chain precursor	COL6A1	CO949072			137.05
Ssc.14299.1.A1_at	Collagen alpha 1(VIII) chain precursor	COL8A1	BQ601752	311.65	76.1	
Ssc.30550.1.A1_at	Collagen alpha 1(XI) chain precursor	COL11A1	CO993779	206.05	91.05	239.55
Ssc.4083.1.S1_at	Collagen alpha 1(XI) chain precursor	COL11A1	BF711439	272	139.65	181.5
Ssc.6325.1.A1_at	Collagen alpha 1(XI) chain precursor	COL11A1	BQ601729	100.65	186.5	120.15
Ssc.6763.1.A1_at	Collagen alpha 1(XI) chain precursor	COL11A1	BQ597906		210.9	142.95
Ssc.1049.1.S1_at	Collagen alpha 1(XII) chain precursor	COL12A1	CK463783	103.25	85.7	1120.6
Ssc.23125.1.S1_at	Collagen alpha 1(XIX) chain precursor	COL19A1	BX674423	83.4		
Ssc.25168.1.S1_a_at	Collagen alpha 1(XVI) chain precursor	COL16A1	CK460853			1322.7
Ssc.19873.1.S1_a_at	Collagen alpha 1(XVII) chain	COL17A1	BE013813		239.35	268.4

Ssc.19873.1.S1_at	Collagen alpha 1(XVII) chain	COL17A1	BE013813		310.05	386
Ssc.26128.1.S1_at	Collagen alpha 1(XVII) chain	COL17A1	BX917834	57.35		
Ssc.4892.1.S1_at	Collagen alpha 1(XVIII) chain precursor	COL18A1	CN155194			392.85
Ssc.21023.1.S1_at	Collagen alpha 1(XXVI) chain precursor	EMID2	CF789072		447.75	513.5
Ssc.21011.1.S1_at	Collagen alpha 2(I) chain precursor	COL1A2	Z99081			2710.95
Ssc.24975.1.S1_at	Collagen alpha 2(I) chain precursor	COL1A2	CN161030			98.95
Ssc.19233.1.S1_at	Collagen alpha 2(IX) chain precursor	COL9A2	CK455548		213.15	106.5
Ssc.16475.1.S1_at	Collagen alpha 3(IV) chain precursor	COL4A3	CB287584		980.4	557.15
Ssc.27225.1.S1_at	Collagen alpha 3(IV) chain precursor	COL4A3	CN159467	267.3		
Ssc.6900.1.A1_at	Collagen alpha 3(IV) chain precursor	COL4A3	BF711595	743.25	250.7	246.35
Ssc.12617.1.S1_at	Collagen alpha 3(V) chain precursor	COL5A3	BX923015			90.45
Ssc.12068.1.A1_at	Collagen alpha 3(VI) chain precursor	COL6A3	BI182335			337.9
Ssc.16589.1.S1_at	Collagen alpha 3(VI) chain precursor	COL6A3	CO956872			1722.15
Ssc.23368.1.A1_at	Collagen alpha 5(IV) chain precursor	COL4A5	BQ599629		422.3	443.45
Ssc.24114.1.A1_at	Collagen alpha 5(IV) chain precursor	COL4A5	BX918013	214	127.65	92.45
Ssc.23234.1.S1_at	collagen, type XXIV, alpha 1	COL24A1	BX675219	731.35	114.95	139.1
Ssc.30042.1.A1_at	collagen, type XXIV, alpha 1	COL24A1	CO948768	138.35		
Ssc.8729.1.A1_at	collagen, type XXIV, alpha 1	COL24A1	CN156106	306.7	692.65	633.25
Ssc.9866.1.A1_at	collagen, type XXIV, alpha 1	COL24A1	BI399160	405.95		
Ssc.23816.1.S1_at	collagen, type XXVII, alpha 1	COL27A1	CF795977			156.75
Ssc.894.1.A1_at	collagen, type XXVII, alpha 1	COL27A1	BQ604410		173.65	205.05
Ssc.4688.2.A1_a_at	collectin sub-family member 11 isoform a	COLEC11	CN166582			118.2
Ssc.833.1.S1_at	Complement C1q subcomponent, A chain precursor	C1QA	AY349424.1			68.85
Ssc.11004.1.S1_at	Complement C1q subcomponent, B chain precursor	C1QB	CN162228			247.2
Ssc.12900.1.A1_at	Complement C1q tumor necrosis factor-related protein 2 precursor	C1QTNF2	BI404122			211.85
Ssc.27811.1.S1_at	Complement C1q tumor necrosis factor-related protein 6 precursor	C1QTNF6	BF078047			177.6
Ssc.4191.1.A1_at	Complement C1q tumor necrosis factor-related protein 7 precursor	C1QTNF7	BG733187	56.25		
Ssc.983.1.S1_at	Complement C1r subcomponent precursor	C1R	CO952050			808.8
Ssc.1177.1.S1_at	Complement C1s subcomponent precursor	C1S	AY349426.1			872
Ssc.23205.2.A1_at	Complement C3 precursor	C3	BF704375		338.2	202.95
Ssc.61.1.S1_at	Complement C3 precursor	C3	NM_214009.1			921.6

Ssc.17026.1.S1_at	Complement C4 precursor	C4A	CF366280		380.4	1054.4
Ssc.21108.1.S1_at	Complement C5 precursor	C5	NM_001001646.1			122.95
Ssc.870.1.S1_at	Complement component C7 precursor	C7	NM_214282.1			134.85
Ssc.5829.1.S1_at	Complement component C8 beta chain precursor	C8B	CK451184	76.95	394.05	302
Ssc.864.1.S1_at	Complement factor H precursor	CFH	NM_214281.1			86.1
Ssc.8562.2.S1_a_at	Connective tissue growth factor precursor	CTGF	U83916.1			66.5
Ssc.8562.3.A1_at	Connective tissue growth factor precursor	CTGF	BI181686	205.45	879.2	1461.05
Ssc.21823.1.S1_at	Cortistatin precursor	CORT	CK458744	1266	323.55	255.25
Ssc.13115.1.A1_at	Coxsackievirus and adenovirus receptor precursor	CXADR	BQ604345	90.65	69.2	90.65
Ssc.18938.1.A1_at	CPZ gene product	CPZ	CF366109			134.15
Ssc.5236.1.S1_at	Crumbs protein homolog 1 precursor	CRB1	BX926660	508.55	65.8	
Ssc.6773.1.A1_at	Crumbs protein homolog 1 precursor	CRB1	CO938744	141.45	250.55	168.05
Ssc.9720.1.A1_at	CYR61 protein precursor	CYR61	CF365800	61.55	248.2	398.8
Ssc.9029.1.S1_at	Cystatin C precursor	CST3	CF180804	145.35	358.55	944
Ssc.18546.1.S1_at	cysteine-rich motor neuron 1	CRIM1	CK458407	348.05	694.65	413.15
Ssc.4900.1.A1_at	cysteine-rich motor neuron 1	CRIM1	BQ600081	565.7	652.55	372.15
Ssc.4900.2.S1_at	cysteine-rich motor neuron 1	CRIM1	CK453765	317.4	481.35	240.95
Ssc.20245.1.S1_at	cystine knot-containing secreted protein	SOSTDC1	BX677279	507.7	653.55	694.35
Ssc.4051.1.S1_at	cystine knot-containing secreted protein	SOSTDC1	BI344266		126.5	123.2
Ssc.5204.1.S1_at	Cytidine deaminase	CDA	CK463412	219.95		
Ssc.10245.2.A1_a_at	Decorin precursor	DCN	BI182181			1540.05
Ssc.10045.1.A1_s_at	Deformed epidermal autoregulatory factor 1 homolog	DEAF1	BI399692		56.2	
Ssc.11945.1.A1_at	Delta-sarcoglycan	SGCD	CK465989	99.45		195.8
Ssc.23926.1.S1_at	Delta-sarcoglycan	SGCD	CK452876	136.9		
Ssc.24020.1.S1_at	Delta-sarcoglycan	SGCD	CK455702			70.65
Ssc.30925.1.A1_at	Dickkopf related protein-2 precursor	DKK2	CO956747		213.4	185.95
Ssc.8027.1.A1_at	Dickkopf related protein-3 precursor	DKK3	CO949346	855	1424.7	1650.3
Ssc.1802.1.S1_at	DnaJ (Hsp40) homolog, subfamily C, member 10	DNAJC10	CK461289	115.5	712.5	777.8
Ssc.4500.1.S1_at	Down syndrome cell adhesion molecule precursor	DSCAM	CK458080			71.25
Ssc.3466.1.S1_at	Dual specificity mitogen-activated protein kinase kinase 2	MAP2K2	BI183410	179.95	425.35	468.05
Ssc.24608.1.S1_at	Dystroglycan precursor	DAG1	CK461177		53.6	

Ssc.3402.1.S1_at	Dystroglycan precursor	DAG1	CN160310	350.5	984	661.05
Ssc.8762.1.A1_at	Dystroglycan precursor	DAG1	CK452309	169.65	335.95	185.95
Ssc.13877.1.A1_at	Dystrophin	DMD	CN154758	177.75	93.75	84.75
Ssc.21634.1.A1_at	Dystrophin	DMD	CF792512	145	213.05	275.3
Ssc.24205.1.S1_at	Dystrophin	DMD	BX922019		523.2	345.95
Ssc.24205.2.S1_at	Dystrophin	DMD	BP153510		285.95	125.05
Ssc.25324.1.S1_at	Dystrophin	DMD	CO946796	63.1		583
Ssc.3948.2.A1_at	Dystrophin	DMD	CK460322	63.7	172.9	124.4
Ssc.2560.1.S1_at	Ectodysplasin A	EDA	AW360214	170.7	1318.8	505.2
Ssc.4913.1.A1_at	Ectonucleotide pyrophosphatase/phosphodiesterase 1	ENPP1	AW430739	355	79.9	480.45
Ssc.5142.1.S1_at	Ectonucleotide pyrophosphatase/phosphodiesterase 2	ENPP2	BX919892		535.6	528.2
Ssc.21302.1.A1_at	ectonucleotide pyrophosphatase/phosphodiesterase 6	ENPP6	CF795369		117.85	127.2
Ssc.21302.2.S1_at	ectonucleotide pyrophosphatase/phosphodiesterase 6	ENPP6	BE232076		61.4	
Ssc.20515.1.S1_at	EGF-containing fibulin-like extracellular matrix protein 1 precursor	EFEMP1	BG382428			185.15
Ssc.16951.1.S1_at	EGF-containing fibulin-like extracellular matrix protein 2 precursor	EFEMP2	BG835316			100.1
Ssc.4267.1.A1_at	EGF-containing fibulin-like extracellular matrix protein 2 precursor	EFEMP2	CF175814			419.8
Ssc.4267.2.S1_at	EGF-containing fibulin-like extracellular matrix protein 2 precursor	EFEMP2	BE235141			68.05
Ssc.4267.3.S1_at	EGF-containing fibulin-like extracellular matrix protein 2 precursor	EFEMP2	BF198910			105.55
Ssc.15424.1.S1_at	EGF-like repeats and discoidin I-like domains protein 3 precursor	EDIL3	CA779516		97.3	72.1
Ssc.16570.1.S1_at	Elastin precursor	ELN	CN160866			304.9
Ssc.2078.1.S1_at	EMILIN 1 precursor	EMILIN1	CK464934			247.75
Ssc.3016.1.S1_at	EMILIN 2 precursor	EMILIN2	BF709303	173.65		
Ssc.3016.2.S1_at	EMILIN 2 precursor	EMILIN2	CB475063	325.85		70.45
Ssc.26505.1.A1_at	EMILIN 3 precursor	MMRN2	CN070255	58.4	93.7	217.9
Ssc.21143.1.A1_at	EMILIN 5	EMILIN3	CN161064		73.2	124.45
Ssc.120.1.S1_at	Endoglin precursor	ENG	NM_214031.1			281
Ssc.21663.1.A1_at	Endothelial lipase precursor	LIPG	BX915625			553.35
Ssc.13571.1.A1_at	Ephrin-A5 precursor	EFNA5	BQ602740		295.85	257.9
Ssc.7697.1.A1_at	Ephrin-A5 precursor	EFNA5	CK451279		60.85	
Ssc.55.1.S1_at	Epidermal growth factor receptor precursor	EGFR	NM_214007.1		214.75	150.7
Ssc.529.1.S1_at	Epididymal secretory protein E1 precursor	NPC2	CO950937	353.35	436.2	951.05

Ssc.3772.1.A1_at	Epsilon-sarcoglycan precursor	SGCE	BF713344	168.05	531.95	506.55
Ssc.6169.1.S1_at	Extracellular matrix protein 1 precursor	ECM1	BQ600899		117.35	412.45
Ssc.6169.2.S1_at	Extracellular matrix protein 1 precursor	ECM1	CB477333		58.65	245.8
Ssc.7294.1.A1_at	Extracellular matrix protein 2 precursor	ECM2	BQ598513		207	605.4
Ssc.19106.1.S1_at	Extracellular sulfatase Sulf-1 precursor	SULF1	BG834200			67.05
Ssc.1475.1.A1_at	Extracellular sulfatase Sulf-2 precursor	SULF2	BQ600408	1645.3	564.6	608.65
Ssc.18296.1.A1_a_at	Extracellular sulfatase Sulf-2 precursor	SULF2	BX671601	150.15	55.8	531.3
Ssc.18296.2.S1_a_at	Extracellular sulfatase Sulf-2 precursor	SULF2	BE233255			139.25
Ssc.22298.1.A1_at	Extracellular sulfatase Sulf-2 precursor	SULF2	CF790602	206.95	184.8	152.25
Ssc.17978.1.S1_at	Fc fragment of IgG binding protein	FCGBP	CN165219	124.4		
Ssc.7175.1.S1_at	Fetuin-B precursor	FETUB	CN154658	124.4		
Ssc.16045.1.S1_at	Fibrillin 1 precursor	FBN1	NM_001001771.1	63.05		245.25
Ssc.16045.2.A1_at	Fibrillin 1 precursor	FBN1	BF703108	576.3	386.2	2179.85
Ssc.27981.1.A1_at	Fibrillin 1 precursor	FBN1	CN032719	232.4		
Ssc.27671.1.S1_at	Fibrillin 2 precursor	FBN2	AW435636		70.2	103.55
Ssc.27703.1.S1_at	Fibrillin 2 precursor	FBN2	AW786568		779.35	764.55
Ssc.8792.1.A1_at	Fibrillin 2 precursor	FBN2	BF711878		141.7	491.3
Ssc.18891.1.A1_at	Fibrinogen alpha/alpha-E chain precursor	FGA	CF365298		60	128.9
Ssc.1882.1.S1_at	Fibroblast growth factor receptor 2 precursor	FGFR2	BX666107	208.15	85.25	122.7
Ssc.10836.1.S1_at	Fibroblast growth factor-12	FGF12	CO943884	165.4	397.25	498.2
Ssc.30632.1.S1_at	Fibroblast growth factor-12	FGF12	CO945349		99.45	108.25
Ssc.26269.1.S1_at	Fibroblast growth factor-18 precursor	FGF18	BX922015		500.85	96.75
Ssc.27685.1.S1_at	Fibroblast growth factor-23 precursor	FGF23	CO946698			158.35
Ssc.12579.1.A1_s_at	Fibroleukin precursor	FGL2	BI402879		141.45	423.2
Ssc.22050.1.S1_s_at	Fibroleukin precursor	FGL2	BP433439			76.6
SscAffx.9.1.S1_at	Fibroleukin precursor	FGL2	NM_001005152.1		119.1	339.75
Ssc.11858.1.S1_at	Fibromodulin precursor	FMOD	CN163410			1371.8
Ssc.16743.1.S1_at	Fibronectin precursor	FN1	CB468993		78.4	672.8
Ssc.6656.1.A1_at	fibronectin type III domain containing 1 (predicted)	FNDC1	CF366197	53.4		66.45
Ssc.20870.1.S1_at	Fibulin-1 precursor	FBLN1	CN158073		134	1088.9
Ssc.4479.1.S1_at	Fibulin-2 precursor	FBLN2	CN166884	67.25		99

Ssc.11038.1.A1_at	Fibulin-5 precursor	FBLN5	BI183108	397.95	234.3	883.6
Ssc.11779.1.S1_at	Folate receptor alpha precursor	FOLR1	BI180978			119.95
Ssc.14544.1.S1_at	Folate receptor beta precursor	FOLR2	U89949.1			275.45
Ssc.30951.1.A1_at	Follistatin precursor	FST	CO946381		512.95	
Ssc.3666.1.A1_at	Follistatin precursor	FST	CK459289	117.4	763.35	164.55
Ssc.4747.1.S1_at	Follistatin precursor	FST	NM_001003662.1	170.05	1834.65	369.05
Ssc.11743.1.S1_at	follistatin-like 4	FSTL4	BI184304	141		68.5
Ssc.13167.1.A1_at	follistatin-like 4	FSTL4	BQ604611	72.65		
Ssc.12255.1.A1_at	follistatin-like 5	FSTL5	BQ604014		210.85	206.85
Ssc.26915.1.S1_at	follistatin-like 5	FSTL5	CN163123	732.9	391.75	652.55
Ssc.3638.1.S1_at	follistatin-like 5	FSTL5	CK461915	166.6	211.15	195.7
Ssc.8170.1.A1_at	follistatin-like 5	FSTL5	AJ660082	60.4	236.85	331.05
Ssc.23242.1.A1_at	Follistatin-related protein 1 precursor	FSTL1	CF365374	159.7	1386.2	1875.1
Ssc.16849.1.S1_at	Follistatin-related protein 3 precursor	FSTL3	BI467833	545.9	377.55	409.4
Ssc.22534.1.S1_at	Fraser syndrome 1 isoform 1	FRAS1	CN167192			67.2
Ssc.8149.1.A1_at	Frizzled-related protein precursor	FRZB	CO948697	157.35		995.35
Ssc.27968.1.A1_at	Furin precursor	FURIN	AW785659	422.65	424.85	293.5
Ssc.5157.1.S1_at	FXYD domain-containing ion transport regulator 6 precursor	FXYD6	CK458461	1662.7	223.1	531.8
Ssc.2185.2.S1_at	galactosidase, beta 1-like	GLB1L	CF365844		124.85	154.2
Ssc.1320.1.A1_at	Galectin-1	LGALS1	AY604429.1		722.75	1956.6
Ssc.17815.1.S1_at	Galectin-3	LGALS3	BX676137	558.35	143.35	215.9
Ssc.1207.1.S1_at	Galectin-8	LGALS8	CK461812	469.95	56.4	103.05
Ssc.5228.1.S1_at	Galectin-8	LGALS8	BF080287	318.05		56.75
Ssc.10993.1.S1_a_at	Galectin-9	LGALS9	NM_213932.1			75.7
Ssc.15306.1.S1_at	Gamma-glutamyl hydrolase precursor	GGH	AJ747241	709.1	740.7	418.85
Ssc.15306.2.S1_at	Gamma-glutamyl hydrolase precursor	GGH	BP447685	138.4	113.6	
Ssc.15306.3.S1_at	Gamma-glutamyl hydrolase precursor	GGH	CB475847	418.55	439.65	225.85
Ssc.30758.1.S1_s_at	Gamma-interferon inducible lysosomal thiol reductase precursor	IFI30	CB479812		121.05	690.3
Ssc.809.1.S1_at	Gamma-interferon inducible lysosomal thiol reductase precursor	IFI30	CK456242		97.2	621.3
Ssc.21763.1.A1_at	Gamma-sarcoglycan	SGCG	CK456888	90.15		
Ssc.14246.1.S1_at	Gelsolin precursor, plasma	GSN	BX667508	122.3	146.1	1430.55

Ssc.12016.1.A1_at	Glia derived nexin precursor	SERPINE2	BI185243		287.4		
Ssc.16342.1.A1_at	Glia derived nexin precursor	SERPINE2	NM_214287.1	290.2	1968.25	1474.25	
Ssc.20464.1.S1_at	Glioma pathogenesis-related protein 1	GLIPR1	BI399129	1300.5		205.75	
Ssc.17225.1.S1_at	Glucagon precursor	GCG	NM_214324.1		353.05	111.3	
Ssc.2375.1.S1_at	Glucose-6-phosphate isomerase	GPI	NM_214330.1	363.25	1079.1	906.15	
Ssc.25136.2.A1_a_at	Glutamate carboxypeptidase-like protein 2 precursor	CNDP1	CK467341	68.75			
Ssc.11374.1.S1_at	Glutathione peroxidase 7 precursor	GPX7	CN159630		201.85	487.1	
Ssc.11374.2.A1_at	Glutathione peroxidase 7 precursor	GPX7	BI183697			58.55	
Ssc.1308.1.S1_at	Glypican-1 precursor	GPC1	CO956692		150.8	366.85	
Ssc.25791.1.S1_a_at	Glypican-3 precursor	GPC3	BX924305	684.55			
Ssc.29309.1.A1_at	Glypican-3 precursor	GPC3	CO953675	697.65			
Ssc.23886.1.A1_at	Glypican-4 precursor	GPC4	CN165537	601.1	774.8	251.6	
Ssc.25943.1.S1_at	Glypican-4 precursor	GPC4	BX925334	67.1			
Ssc.29046.1.S1_at	Glypican-4 precursor	GPC4	BI343513	371.75	693.05	285.6	
Ssc.29437.1.S1_at	Glypican-4 precursor	GPC4	CN157608	417.75	235.45	167.35	
Ssc.29487.1.A1_at	Glypican-4 precursor	GPC4	CO956423	274.55	318.85	103.95	
Ssc.20047.1.S1_at	Glypican-5 precursor	GPC5	CF176372		51.75	69.65	
Ssc.26750.1.A1_at	Glypican-5 precursor	GPC5	CN159021	56.05			
Ssc.27447.1.S1_at	Glypican-5 precursor	GPC5	CN160182		247.2	226.65	
Ssc.21229.1.A1_at	Glypican-6 precursor	GPC6	CK450097	113.15		121.2	
Ssc.22092.1.S1_at	Glypican-6 precursor	GPC6	CF365067		170.95	230.9	
Ssc.26966.1.A1_at	Glypican-6 precursor	GPC6	CN163875		82.4		
Ssc.2834.1.A1_at	Glypican-6 precursor	GPC6	BQ603378	383.4	205.05	265.85	
Ssc.14563.1.S1_at	Granulins precursor	GRN	BX916833		84.45	184.8	
Ssc.20986.2.S1_at	Granulins precursor	GRN	BG382626		342.15	314.4	
Ssc.21946.1.S1_at	Granulins precursor	GRN	BG834099	96.2	483	402.2	
Ssc.1762.1.S1_at	Group X secretory phospholipase A2 precursor	PLA2G10	AW416837	108.5	82.65	67.35	
Ssc.1762.2.A1_at	Group X secretory phospholipase A2 precursor	PLA2G10	BI400547	77.05			
Ssc.15437.1.S1_at	Group XIIA secretory phospholipase A2 precursor	PLA2G12A	CA779682	235.3	214.7	261.85	
Ssc.15583.1.S1_at	Growth hormone receptor precursor	GHR	CF175347	69.35	82.9		
Ssc.20042.1.S1_at	Growth/differentiation factor 9 precursor	GDF9	NM_001001909.1	1790.1	87.35	68.85	

Ssc.25172.1.S1_at	Growth-arrest-specific protein 6 precursor	GAS6	BI359656			63.75
Ssc.21595.1.S1_at	guanine nucleotide binding protein	GNAS	CN163983	139.9	201.1	142
Ssc.6675.1.S1_a_at	guanine nucleotide binding protein	GNAS	NM_214312.1	102.85	1277.85	1605.45
Ssc.18818.1.S1_at	Guanine nucleotide-binding protein-like 1	GNL1	BX918511		69.95	94.35
Ssc.7528.1.A1_at	hedgehog-interacting protein	HHIP	CF359222	191.4	613.1	558.75
Ssc.7528.2.S1_at	hedgehog-interacting protein	HHIP	AJ660552	87.25	133.6	78.7
Ssc.115.1.S1_s_at	Heme oxygenase 1	HMOX1	X60677.1		270.95	514.55
Ssc.27285.1.A1_at	heparan sulfate D-glucosaminyl 3-O-sulfotransferase 4	HS3ST4	CN152978		100.1	
Ssc.24835.1.S1_at	Heparin-binding growth factor 1 precursor	FGF1	CK465956	93.4	169.65	94.8
Ssc.24923.1.S1_at	Hepatocyte growth factor-like protein precursor	MST1	CK459058	65.15		
Ssc.11590.1.A1_at	Hepatoma-derived growth factor	HDGF	BI181666	92.4		
Ssc.21553.1.S1_at	Hepatoma-derived growth factor	HDGF	CN160438		182.7	160.75
Ssc.2803.1.S1_at	Histidine triad nucleotide-binding protein 2	HINT2	BI342739	231.7	800	798.45
Ssc.2667.1.S1_a_at	Histidine-rich glycoprotein precursor	HRG	CN166294	67.9		
Ssc.2667.2.S1_a_at	Histidine-rich glycoprotein precursor	HRG	BI359809	69.2		
Ssc.17029.1.A1_at	Histo-blood group ABO system transferase	ABO	CK456293	76.45	57.85	
Ssc.13780.4.S1_x_at	HLA class I histocompatibility antigen, Cw-7 alpha chain precursor	HLA-C	AF464011.1		228.4	1261.15
Ssc.16756.1.S1_at	HLA class I histocompatibility antigen, Cw-7 alpha chain precursor	HLA-C	CK450398		335	297.95
Ssc.18278.1.S1_at	hyaluronan binding protein 2	HABP2	CK459919	177		
Ssc.13778.1.S1_at	Ig alpha-1 chain C region	IGHM	NM_213828.1			196.5
Ssc.7706.1.A1_at	Ig alpha-1 chain C region	IGHM	BF711734		484.45	285.45
Ssc.16506.1.A1_at	Immunoglobulin J chain	IGJ	CB287867	127.8		
Ssc.1064.1.A1_at	immunoglobulin superfamily containing leucine-rich repeat	ISLR	BI182302			520.3
Ssc.5566.1.S1_at	Inhibin alpha chain precursor	INHA	NM_214189.1		1734.2	862.1
Ssc.19304.2.S1_at	Inhibin beta A chain precursor	INHBA	AJ746628	53.95	1458.2	412.8
Ssc.112.1.S1_at	Inhibin beta A chain precursor	INHBA	NM_214028.1	308.8	129.6	90.3
Ssc.29662.1.A1_at	Inhibin beta A chain precursor	INHBA	CO943658		1264.7	158.1
Ssc.16230.1.S1_at	Inhibin beta B chain precursor	INHBB	X03267.1		155.75	
Ssc.8909.1.A1_at	Inhibin beta B chain precursor	INHBB	BI400976	389.1	1279.35	794.45
Ssc.8909.2.S1_at	Inhibin beta B chain precursor	INHBB	AJ681476	83.5	1092.95	244.9
Ssc.20224.1.S1_at	Insulin-degrading enzyme	IDE	CN163293	675.1	295.65	322

Ssc.9109.1.A1_at	Insulin-degrading enzyme	IDE	CK451212	853.8	264.1	251
Ssc.47.1.S1_at	Insulin-like growth factor binding protein 2 precursor	IGFBP2	NM_214003.1		297.85	223.35
Ssc.15588.1.S2_at	Insulin-like growth factor binding protein 3 precursor	IGFBP3	AJ657291			116.65
Ssc.3298.1.A1_at	Insulin-like growth factor binding protein 5 precursor	IGFBP5	BI118964			359.85
Ssc.14062.1.S1_at	Insulin-like growth factor binding protein 6 precursor	IGFBP6	CN163405			108.05
Ssc.14062.2.S1_a_at	Insulin-like growth factor binding protein 6 precursor	IGFBP6	BX921939	66.8		102
Ssc.17186.2.S1_at	Insulin-like growth factor binding protein 7 precursor	IGFBP7	CF175359	843.05	1456.75	1870.15
Ssc.17186.2.S2_at	Insulin-like growth factor binding protein 7 precursor	IGFBP7	CO956421	146.55	998.05	1153.25
Ssc.17186.3.A1_at	Insulin-like growth factor binding protein 7 precursor	IGFBP7	BQ605041	284.3	655.2	849.15
Ssc.12578.1.A1_at	Insulin-like growth factor IA precursor	IGF1	BI402878		503.85	546
Ssc.16231.1.S1_a_at	Insulin-like growth factor IA precursor	IGF1	NM_214256.1		224.65	244.4
Ssc.16231.2.A1_a_at	Insulin-like growth factor IA precursor	IGF1	CN157588		248.5	300.25
Ssc.16231.3.S1_a_at	Insulin-like growth factor IA precursor	IGF1	AY632379.1		176.75	165.45
Ssc.31130.1.A1_at	Insulin-like growth factor IA precursor	IGF1	CN153555		497	378.9
Ssc.1280.1.S1_at	inter-alpha trypsin inhibitor heavy chain precursor 5 isoform 1	ITIH5	CK456827			200.8
Ssc.16981.2.S1_at	Inter-alpha-trypsin inhibitor heavy chain H3 precursor	ITIH3	BF077393			486.85
Ssc.4217.1.S1_at	Inter-alpha-trypsin inhibitor heavy chain H4 precursor	ITIH4	NM_001001537.1			74.9
Ssc.11187.1.S1_at	Intercellular adhesion molecule-1 precursor	ICAM1	AF156712.1			57.85
Ssc.8997.1.A1_at	Intercellular adhesion molecule-1 precursor	ICAM1	BF710790			133.35
Ssc.4815.1.A1_at	Interferon alpha-8 precursor	IFNA8	BQ604399		67.75	96.95
Ssc.4933.1.A1_at	Interferon-alpha/beta receptor beta chain precursor	IFNAR2	CF363094		173.9	231.7
Ssc.16250.1.S2_at	Interleukin-1 receptor antagonist protein precursor	IL1RN	BF441608		168.25	96.3
Ssc.71.1.S1_at	Interleukin-12 beta chain precursor	IL12B	U08317.1	446.95		
Ssc.25858.1.S1_at	Interleukin-17D precursor	IL17D	CN152994		81.2	126.15
Ssc.25858.2.A1_at	Interleukin-17D precursor	IL17D	CO939120	79.4	120.3	186.65
Ssc.20.1.S1_at	Interleukin-18 precursor	IL18	AY450287.1			265.7
Ssc.6256.1.A1_at	Interleukin-4 receptor alpha chain precursor	IL4R	BI186333		89.7	94.5
Ssc.25033.1.A1_at	Interleukin-6 receptor beta chain precursor	IL6ST	CK458940	904.35		
Ssc.8466.1.A1_at	Jagged 1 precursor	JAG1	BF704538	459.65	79.15	67
Ssc.9400.1.A1_at	Jagged 1 precursor	JAG1	CO943323	1339.55	667.85	620.5
Ssc.4091.1.S1_at	KIAA0892	KIAA0892	BX918046	145.7	119.1	91.95

Ssc.19197.2.A1_at	kin of IRRE like 3	KIRREL3	CF368148			108	
Ssc.14075.1.A1_at	Kininogen precursor	KNG1	CK459115	61.3			
Ssc.18557.1.A1_at	Kininogen precursor	KNG1	BX676446	338.1			
Ssc.24401.1.A1_at	Kininogen precursor	KNG1	CK457947	238			
Ssc.24401.1.A1_s_at	Kininogen precursor	KNG1	CK457947	312.8			
Ssc.1248.1.S1_at	Kunitz-type protease inhibitor 1 precursor	SPINT1	BG383179			80.65	
Ssc.9221.2.A1_a_at	Kunitz-type protease inhibitor 2 precursor	SPINT2	CK457448	187.75			
Ssc.16345.1.S1_at	Lactadherin precursor	SPAG10	CO940433			412.7	
Ssc.13769.1.S1_at	Lactotransferrin precursor	LTF	M81327.1	93.05			
Ssc.16888.1.S1_at	Ladinin 1	LAD1	BE033347	243.95			
Ssc.3122.1.S1_at	Laminin alpha-1 chain precursor	LAMA1	CK454137		695.8	411.65	
Ssc.10383.1.A1_at	Laminin alpha-2 chain precursor	LAMA2	BI400876		81.3	214.4	
Ssc.1138.1.A1_at	Laminin alpha-2 chain precursor	LAMA2	BF712024		69.9	121.6	
Ssc.11623.1.A1_at	Laminin alpha-2 chain precursor	LAMA2	CO994035		265.6	780.85	
Ssc.11815.1.A1_s_at	Laminin alpha-2 chain precursor	LAMA2	BI184933		170.4	443.5	
Ssc.12029.1.S1_at	Laminin alpha-2 chain precursor	LAMA2	BI185686		478.65	338.3	
Ssc.1959.1.S1_at	Laminin alpha-2 chain precursor	LAMA2	BF710621	226.3	856.2	866.65	
Ssc.27500.1.A1_at	Laminin alpha-2 chain precursor	LAMA2	CN163845		104.25	108.55	
Ssc.28001.1.A1_at	Laminin alpha-2 chain precursor	LAMA2	CN032769	60.9			
Ssc.29333.1.A1_at	Laminin alpha-2 chain precursor	LAMA2	CO953974		93.25		
Ssc.2444.2.A1_a_at	Laminin alpha-3 chain precursor	LAMA3	CN154909	444.25			
Ssc.24909.1.S1_at	Laminin alpha-4 chain precursor	LAMA4	CK460085			533.35	
Ssc.15823.1.S1_at	Laminin beta-1 chain precursor	LAMB1	CN155839	187.95		95.95	
Ssc.5299.1.S1_at	Laminin beta-1 chain precursor	LAMB1	CO992470	1445.4		1330.05	
Ssc.5067.1.S1_at	Laminin beta-2 chain precursor	LAMB2	CK461363		581.5	513.65	
Ssc.4332.1.A1_at	Laminin beta-3 chain precursor	LAMB3	BI403674	76.9	59.95	88.7	
Ssc.10398.1.S1_at	Laminin gamma-1 chain precursor	LAMC1	BI400942		99.05	176.4	
Ssc.1099.1.S1_at	Laminin gamma-1 chain precursor	LAMC1	CK465900	514.25	711	917.4	
Ssc.18721.1.A1_at	Laminin gamma-1 chain precursor	LAMC1	CK462389	99.45	212.3	362.25	
Ssc.18721.2.A1_s_at	Laminin gamma-1 chain precursor	LAMC1	CF362305		87.25	197.85	
Ssc.9784.1.S1_at	Laminin gamma-2 chain precursor	LAMC2	BI398896			89.05	

Ssc.7309.1.S1_at	LAP2 protein	ERBB2IP	BQ598594	155.15	146.5	163.85
Ssc.7633.1.A1_at	LAP2 protein	ERBB2IP	CF793344		380.7	417.9
Ssc.7633.2.A1_at	LAP2 protein	ERBB2IP	CN158956		379.55	315.2
Ssc.7633.3.S1_at	LAP2 protein	ERBB2IP	AW346725		481.3	402.15
Ssc.9165.1.A1_at	LAP2 protein	ERBB2IP	BF709744	138.05	152.05	141.3
Ssc.9051.1.A1_at	Latent transforming growth factor beta binding protein 3 precursor	LTBP3	CN163558	167.5	175.1	196.3
Ssc.1375.1.A1_at	Latent transforming growth factor beta binding protein, isoform 1L precursor	LTBP1	BQ599578		56.7	55.65
Ssc.8072.1.A1_at	Latent transforming growth factor beta binding protein, isoform 1L precursor	LTBP1	BF709385	366.2	449.6	543.1
Ssc.8072.2.A1_at	Latent transforming growth factor beta binding protein, isoform 1L precursor	LTBP1	CO950891	439.1	340.6	727.1
Ssc.19136.1.S1_at	Latent transforming growth factor-beta-binding protein 2 precursor	LTBP2	C94539			101.8
Ssc.13283.1.S1_at	Leptin receptor gene-related protein	LEPR	BI404777		81.9	
Ssc.816.1.S1_at	Leptin receptor gene-related protein	LEPR	CF790758	354.55	494.8	541.9
Ssc.3670.1.S1_a_at	leucine proline-enriched proteoglycan	LEPRE1	BI181715		316.65	352.55
Ssc.24159.1.S1_at	leucine rich repeat and sterile alpha motif containing 1	LRSAM1	CK456956	559.55		
Ssc.26289.1.S1_at	Leucine-rich repeat LGI family member 3 precursor	LGI3	BX915047		111.15	
Ssc.10602.1.A1_at	Leucine-rich repeat transmembrane protein FLRT3 precursor	FLRT3	BQ597359			61.9
Ssc.10060.1.A1_at	Leukemia inhibitory factor receptor precursor	LIFR	BI399724	345.4		
Ssc.16175.1.A1_at	Leukemia inhibitory factor receptor precursor	LIFR	U91518.1	83		
Ssc.16175.1.S1_at	Leukemia inhibitory factor receptor precursor	LIFR	BF078710	89.75		
Ssc.2874.1.S1_at	lipase, member H	LIPH	CK456826	218.6	493.85	384.35
Ssc.1147.1.A1_at	Lipoprotein lipase precursor	LPL	X91327		130.75	61.3
Ssc.1147.2.S1_at	Lipoprotein lipase precursor	LPL	BF712908		176.85	120.2
Ssc.16335.1.S2_at	Lipoprotein lipase precursor	LPL	X62984.1		108.55	
Ssc.167.2.S1_a_at	Low affinity immunoglobulin gamma Fc region receptor III-A precursor	FCGR3A	AF372455.1			186.7
Ssc.167.4.S1_at	Low affinity immunoglobulin gamma Fc region receptor III-A precursor	FCGR3A	CB483332			112.9
Ssc.1417.1.A1_at	Low-density lipoprotein receptor-related protein 8 precursor	LRP8	CO949101	61.25	2201.2	710.8
Ssc.31016.1.A1_at	Low-density lipoprotein receptor-related protein 8 precursor	LRP8	CO949604	110.55	2249.15	983.75
Ssc.1128.1.S1_at	Lumican precursor	LUM	BX668296			529.3
Ssc.25550.1.S1_at	Lymphocyte antigen 96 precursor	LY96	BX918583			275.35

Ssc.15277.1.S1_at	Lymphotoxin-beta	LTB	CA780895			51.55
Ssc.670.1.S1_at	Lysozyme C precursor	LYZ	NM_214392.1			75.35
Ssc.8560.1.A1_at	lysozyme-like 2	LYZL2	CF365481		67.65	
Ssc.10137.1.A1_at	Lysyl oxidase homolog 1 precursor	LOXL1	BI399930			514.75
Ssc.2598.1.S1_at	Lysyl oxidase homolog 2 precursor	LOXL2	CN160419	116.1		413.1
Ssc.12056.1.A1_at	Lysyl oxidase homolog 4 precursor	LOXL4	BI181507		181.65	94.8
Ssc.21665.1.A1_at	Macrophage colony stimulating factor-1 precursor	CSF1	CN163140		234.1	243.05
Ssc.6369.1.A1_at	Macrophage colony stimulating factor-1 precursor	CSF1	BI398860			59.7
Ssc.4871.1.S1_at	Macrophage inflammatory protein-2-alpha precursor	CXCL2	NM_001001861.1			131.1
Ssc.551.1.S1_at	Macrophage migration inhibitory factor	MIF	BX918657	124.1	653	575.7
Ssc.29636.1.A1_at	MAM domain containing protein 2 precursor	MAMDC2	CO943432			141.2
Ssc.26201.1.S1_at	Mammaglobin B precursor	SCGB2A1	BX920553		58.2	
Ssc.16096.2.S1_a_at	Mast/stem cell growth factor receptor precursor	KIT	BP141688		235.4	
Ssc.7756.1.A1_at	Matrilin-2 precursor	MATN2	CK460011		94.25	876.7
Ssc.373.1.S1_at	Matrix Gla-protein precursor	MGP	NM_214116.1			1676.9
Ssc.734.1.S1_at	Matrix metalloproteinase-14 precursor	MMP14	NM_214239.1			111.85
Ssc.29059.1.A1_at	Matrix metalloproteinase-28 precursor	MMP28	CN153291			149.85
Ssc.12240.1.S1_at	Meprin A beta-subunit precursor	MEP1B	CN162066	461.3		
Ssc.12735.1.A1_s_at	Meprin A beta-subunit precursor	MEP1B	BI403430	650.9		
Ssc.11784.1.S1_at	Metalloproteinase inhibitor 1 precursor	TIMP1	NM_213857.1	76.25	1622.1	2216.8
Ssc.1082.1.S1_at	Metalloproteinase inhibitor 2 precursor	TIMP2	BX672630		654.5	991.25
Ssc.11257.1.S1_at	Metalloproteinase inhibitor 2 precursor	TIMP2	CK461818	63.2	291.6	738.25
Ssc.1125.1.A1_at	Metalloproteinase inhibitor 3 precursor	TIMP3	BI182045		476.45	626.85
Ssc.1169.1.A1_s_at	Microfibril-associated glycoprotein 4 precursor	MFAP4	CF366047	129.6		738.65
Ssc.23279.1.S1_at	Microfibril-associated glycoprotein 4 precursor	MFAP4	BX666973			94.6
Ssc.4348.1.A1_at	Microfibrillar-associated protein 1	MFAP1	BQ599350	354.5	175	196.25
Ssc.4348.2.S1_at	Microfibrillar-associated protein 1	MFAP1	BP436657	71.3		
Ssc.2445.1.S1_at	Microfibrillar-associated protein 2 precursor	MFAP2	CN153355		94.1	102.85
Ssc.1086.1.A1_at	Microfibrillar-associated protein 5 precursor	MFAP5	BQ603941			66.05
Ssc.20489.1.S1_at	Midkine precursor	MDK	CN166538		83.3	141.6
Ssc.20489.1.S1_s_at	Midkine precursor	MDK	CN166538		144.8	280.8

Ssc.26180.1.S1_at	Mimecan precursor	OGN	BX916384			1127
Ssc.13675.1.A1_at	mucin 4 isoform d	MUC4	BQ601824	102.85		61.4
Ssc.18383.1.S1_at	Mucin 5B precursor	MUC5B	CF176103	63.1		
Ssc.14368.1.A1_at	Multimerin 1 precursor	MMRN1	BQ602025			659.4
Ssc.7366.1.A1_at	multiple coagulation factor deficiency 2	MCFD2	CO987038	415.55	710.25	667.3
Ssc.9246.1.S1_a_at	Multisynthetase complex auxiliary component p43	SCYE1	AJ658150	734.4	756.4	783.5
Ssc.9246.1.S1_at	Multisynthetase complex auxiliary component p43	SCYE1	AJ658150	808.65	834.6	791.25
Ssc.20816.1.S1_at	Neural cell adhesion molecule 1, 140 kDa isoform precursor	NCAM1	BP459811		66.75	172
Ssc.6092.1.A1_at	Neural cell adhesion molecule 1, 140 kDa isoform precursor	NCAM1	CN166399		271.3	362.95
Ssc.6092.2.S1_at	Neural cell adhesion molecule 1, 140 kDa isoform precursor	NCAM1	BG381949			67.4
Ssc.4398.1.S1_at	Neuregulin-1, sensory and motor neuron-derived factor isoform	NRG1	BG895153		262.5	92.05
Ssc.6156.1.A1_at	Neuroblastoma suppressor of tumorigenicity 1 precursor	NBL1	CO955588		443	485.75
Ssc.19565.2.A1_at	Neurokinin B precursor	TAC3	CF362726			132.55
Ssc.2083.1.A1_at	Neuromedin B-32 precursor	NMB	CN156167		66.1	
Ssc.22627.1.S1_at	Neuronal pentraxin II precursor	NPTX2	BX666127	156.75	285.6	
Ssc.6948.1.A1_at	Neuroserpin precursor	SERPINI1	BI404568	57.85		
Ssc.1916.1.A1_at	Neurotrophin-3 precursor	NTF3	CF368973			53.3
Ssc.1053.1.S1_at	Nidogen-2 precursor	NID2	CN156760	565.45	190.85	984.95
Ssc.8494.1.A1_at	Noelin 3 precursor	OLFM3	BF703131		413.9	545.45
Ssc.16434.1.A1_at	NOV protein homolog precursor	NOV	BI400122			106.05
Ssc.1697.1.S1_at	Nucleobindin 1 precursor	NUCB1	CN160639	99.65	390.15	497.6
Ssc.22512.1.S1_at	Nucleobindin 2 precursor	NUCB2	BQ597948	484.95	625.35	620.1
Ssc.26536.1.S1_at	odz, odd Oz/ten-m homolog 1	ODZ1	CN153146	58.45	233.5	283.55
Ssc.6491.1.S1_at	olfactomedin-like 1	OLFML1	CN162831	86.75		83.4
Ssc.17387.1.A1_at	olfactomedin-like 2A	OLFML2A	CO948677		127.9	264.65
Ssc.15592.1.S1_at	Olfactomedin-like protein 3 precursor	OLFML3	CN163348		407.85	1223.15
Ssc.16554.1.S1_at	Osteocalcin precursor	BGLAP	CB285782	119.15		62.6
Ssc.16554.2.S1_at	Osteocalcin precursor	BGLAP	BG382669	90.2	52.65	
Ssc.101.1.S1_at	Osteopontin precursor	SPP1	NM_214023.1			118.45
Ssc.13428.1.A1_at	otoancorin	OTOA	BI404659		65.85	
Ssc.15888.1.S1_at	oxidised low density lipoprotein (lectin-like) receptor 1	OLR1	NM_213805.1		86.6	

Ssc.29837.1.A1_at	oxidised low density lipoprotein (lectin-like) receptor 1	OLR1	CO937226		58.25		
Ssc.11457.1.A1_at	Palmitoyl-protein thioesterase 1 precursor	PPT1	BQ602829	529.8	707.5	698.95	
Ssc.11298.1.S1_at	Palmitoyl-protein thioesterase 2 precursor	PPT2	CN162740	327.25	237	122.25	
Ssc.2632.1.A1_at	pregnancy-associated plasma preproprotein-A2	PAPPA2	CO993389	343.35	211.55	212.75	
Ssc.10731.1.A1_at	Pregnancy-associated plasma protein-A	PAPPA	BQ597811		417.25	51	
Ssc.4707.1.A1_at	Pregnancy-associated plasma protein-A	PAPPA	BI118246	121.35			
Ssc.9991.1.S1_at	Parathyroid hormone-related protein precursor	PTH1H	NM_213916.1		361.7	343.5	
Ssc.8162.1.S1_at	Pentaxin-related protein PTX3 precursor	PTX3	CN153343		776.85	664	
Ssc.8162.2.S1_at	Pentaxin-related protein PTX3 precursor	PTX3	BP454691		159.95	83.55	
Ssc.6988.1.A1_at	Peptidyl-glycine alpha-amidating monooxygenase precursor	PAM	CK455877		611.3	492.8	
Ssc.8046.1.A1_at	peptidylprolyl isomerase A isoform 1; cyclophilin A	PPIA	NM_214353.1	1268.65	1549.2	1700.9	
Ssc.7266.1.A1_at	Periostin precursor	POSTN	CO955086			349.15	
Ssc.27727.1.S1_at	Phosphoglucomutase-like protein 5	PGM5	BG895597	215.4		581.05	
Ssc.28465.1.S1_at	Phosphoglucomutase-like protein 5	PGM5	CK464548	83.35		215.1	
Ssc.16207.1.S1_at	Phospholipase A2 precursor	PLA2G1B	M21055.1		103.1		
Ssc.3517.1.S1_at	Phospholipid transfer protein precursor	PLTP	NM_214283.1		53.6	128.9	
Ssc.10451.1.S1_at	Pigment epithelium-derived factor precursor	SERPINF1	BI181553			327.6	
Ssc.27005.1.A1_at	plasma carboxypeptidase B2 isoform a preproprotein	CPB2	CN165466	378.6			
Ssc.19694.1.S1_at	Plasma glutathione peroxidase precursor	GPX3	BX671405	112.75	760.65	515.95	
Ssc.957.1.S1_at	Plasma protease C1 inhibitor precursor	SERPING1	CN153484			1123.6	
Ssc.20156.1.S1_at	Plasma serine protease inhibitor precursor	SERPINA5	BI344159			58	
Ssc.9781.1.S1_at	Plasminogen activator inhibitor-1 precursor	SERPINE1	NM_213910.1		1370.85	717.55	
Ssc.10303.1.A1_at	platelet derived growth factor D isoform 1 precursor	PDGFD	BI400525		774.2	896.45	
Ssc.26136.1.S1_at	platelet derived growth factor D isoform 1 precursor	PDGFD	BX924762		65.4		
Ssc.8185.1.A1_at	platelet derived growth factor D isoform 1 precursor	PDGFD	CK457288		310.1	135.85	
Ssc.6050.1.A1_at	Platelet endothelial cell adhesion molecule precursor	PECAM1	CN157410	55		519.35	
Ssc.14558.1.S1_at	Platelet endothelial cell adhesion molecule precursor	PECAM1	NM_213907.1			89.4	
Ssc.19691.1.S1_at	Platelet-activating factor acetylhydrolase precursor	PLA2G7	BQ603958		862	542.8	
Ssc.25067.1.S1_at	platelet-derived growth factor C precursor	PDGFC	CO987060		286.2	572.65	
Ssc.4323.1.A1_at	platelet-derived growth factor C precursor	PDGFC	BI181064	98.5		59.35	
Ssc.1161.1.A1_at	platelet-derived growth factor receptor-like protein	PDGFRL	BI185596	140.85	79.85	293.55	

Ssc.6173.3.S1_a_at	Platelet-derived growth factor, A chain precursor	PDGFA	BX914490	70.4		
Ssc.12975.1.S1_at	Pleiotrophin precursor	PTN	D89546.1			1076.25
Ssc.6105.1.A1_at	Plexin B1 precursor	PLXNB1	BI402259		134.55	88.9
Ssc.6105.2.S1_at	Plexin B1 precursor	PLXNB1	AW416696		65.9	
Ssc.14134.1.S1_at	Polypeptide N-acetylgalactosaminyltransferase 1	GALNT1	CF362462	95.5	243.7	224.35
Ssc.7435.1.A1_at	Polypeptide N-acetylgalactosaminyltransferase 1	GALNT1	BQ600736	229.2	591.85	574.35
Ssc.7435.2.A1_at	Polypeptide N-acetylgalactosaminyltransferase 2	GALNT1	CO987549	108.7	497	422.25
Ssc.4417.1.A1_at	Polypeptide N-acetylgalactosaminyltransferase 2	GALNT2	BF703687	53.6	449.75	331.1
Ssc.26276.1.S1_at	Potential carboxypeptidase-like protein X2 precursor	CPXM2	BX918155			77.3
Ssc.984.1.S1_at	Proactivator polypeptide precursor	PSAP	CF368912	159.55	877.05	658.3
Ssc.8758.1.A1_at	procollagen C-endopeptidase enhancer 2	PCOLCE2	CF795440	1395.8	136.35	90.45
Ssc.1122.1.S1_at	Procollagen C-proteinase enhancer protein precursor	PCOLCE	CN164778			988.45
Ssc.11281.1.A1_at	Proenkephalin A precursor	PENK	BI181438		68.1	147.25
Ssc.87.1.S1_at	Pro-epidermal growth factor precursor	EGF	NM_214020.1	118.8		
Ssc.9392.1.S1_at	Pro-epidermal growth factor precursor	EGF	CF367607	83.25		
Ssc.9392.2.S1_at	Pro-epidermal growth factor precursor	EGF	BE013075		54.05	
Ssc.9392.3.A1_at	Pro-epidermal growth factor precursor	EGF	CF368947		84.45	
Ssc.24706.1.A1_at	Prolactin receptor precursor	PRLR	CK463265	101.15		
Ssc.18135.1.S1_at	Prolargin precursor	PRELP	BX919267			376.05
Ssc.10078.1.A1_at	Proprotein convertase subtilisin/kexin type 5 precursor	PCSK5	BI399804			92.75
Ssc.162.1.S1_at	Prorelaxin H1 precursor	RLN1	NM_213872.1			206.6
Ssc.16187.1.S1_at	Prostaglandin-H2 D-isomerase precursor	PTGDS	NM_214228.1		114.25	384.9
Ssc.1510.1.S1_at	Prostasin precursor	PRSS8	BI400373	125.95		
Ssc.11168.1.A1_at	Proteasome subunit beta type 10 precursor	CTRL	CF368750			126.05
Ssc.12867.1.A1_at	Protein C14orf93 precursor	C14orf93	BI403979	67.9	62.6	
Ssc.4092.1.S1_at	Protein C19orf10 precursor	C19orf10	CN153195	133.1	383.7	289.45
Ssc.3803.1.S1_at	Protein C20orf116 precursor	C20orf116	CN152878	66.45	87.2	123.35
Ssc.20598.1.A1_at	Protein disulfide-isomerase precursor	P4HB	CK458950	169.05	602.3	590.2
Ssc.26264.1.S1_at	Protein FAM20B precursor	FAM20B	CN153889	57.95	268.1	158.1
Ssc.1543.1.A1_at	Protein FAM3A precursor	FAM3A	CK465729	63.95	289.45	268.85
Ssc.12921.1.S1_at	Protein FAM3C precursor	FAM3C	BX674124	242.7	630.65	572.85

Ssc.9156.1.A1_at	Protein FAM3C precursor	FAM3C	BF709690		61	59.35
Ssc.30669.1.A1_at	Protein FAM3D precursor	FAM3D	CO941565	161.95		
Ssc.6507.1.S1_a_at	Protein kinase C-binding protein NELL1 precursor	NELL1	CN164846	96.25	306.2	381.45
Ssc.11561.1.A1_at	Protein kinase C-binding protein NELL2 precursor	NELL2	CN154539		107.1	101.4
Ssc.10386.1.S1_at	Protein-lysine 6-oxidase precursor	LOX	CK452593			126.6
Ssc.8224.1.S1_at	Protein-lysine 6-oxidase precursor	LOX	CN162555		90.25	335.6
Ssc.15302.1.S1_at	Prothrombin precursor	F2	CA781014	658.25		
Ssc.13555.2.S1_at	Protocadherin 15 precursor	PCDH15	CK466176		64.5	57.55
Ssc.26510.1.A1_at	Protocadherin 15 precursor	PCDH15	CK467111		57.75	55.1
Ssc.30063.1.A1_at	Protocadherin 15 precursor	PCDH15	CO951943		91.4	77.6
Ssc.9111.1.A1_at	Protocadherin 15 precursor	PCDH15	BF709472		126.3	150.95
Ssc.290.1.S1_at	P-selectin precursor	SELP	NM_214078.1			122.95
Ssc.29667.1.A1_at	Pulmonary surfactant-associated protein C precursor	SFTPC	CO942888		886.6	
Ssc.16430.1.S1_at	Putative mucin core protein 24 precursor	CD164	CO943642	676.1	824.1	902.5
Ssc.22306.1.A1_at	Putative mucin core protein 24 precursor	CD164	CF790711	437.1	372.45	454.25
Ssc.17391.1.S1_at	Ras-related protein Rab-35	RAB35	CK466064	191.6	261.4	216
Ssc.17391.2.S1_at	Ras-related protein Rab-35	RAB35	CD572075	422.2	137	111.6
Ssc.22616.1.S1_at	Ras-related protein Rab-35	RAB35	CN153752	164.6	104.15	122.35
Ssc.13715.1.S1_at	Red protein	IK	AJ656040	435.1	263.5	263.2
Ssc.24729.1.A1_s_at	Red protein	IK	CK463908	468.85	381.75	433.2
Ssc.8019.1.A1_at	Reelin precursor	RELN	BF702940			136.4
Ssc.10623.1.A1_at	Reticulon protein 3	RTN3	BI182397		182	181.15
Ssc.10623.2.S1_at	Reticulon protein 3	RTN3	BQ597425		102.65	75.45
Ssc.1080.1.A1_at	Reticulon protein 3	RTN3	BQ598799	132.3	394.65	190.95
Ssc.15604.1.S1_at	Reticulon protein 4	RTN3	CB478205	195	724.15	487.4
Ssc.27245.1.S1_at	Reticulon protein 5	RTN3	CN154172	73.4	157.95	96.95
Ssc.1494.1.S1_at	Retinoic acid receptor responder protein 2 precursor	RARRES2	BI182970			832.4
Ssc.3037.2.S1_at	Retinoid-inducible serine carboxypeptidase precursor	SCPEP1	CB472152	114.2	150.45	132.7
Ssc.3037.3.A1_at	Retinoid-inducible serine carboxypeptidase precursor	SCPEP1	BI185371	285.6	356.45	386.95
Ssc.2824.1.S1_at	Ribonuclease pancreatic precursor	RNASE1	BG894750		210.2	427.1
Ssc.3214.1.S1_at	Ribonuclease T2 precursor	RNASET2	CK457660		148.85	323.7

Ssc.3214.3.S1_at	Ribonuclease T2 precursor	RNASET2	CB482119		271.2	606.55
Ssc.25882.1.S1_at	Sarcospan	SSPN	BX924101		453.75	733.75
Ssc.2283.1.S1_at	secreted frizzled-related protein 1; secreted apoptosis-related protein 2	SFRP1	BI182321			1017.05
Ssc.3232.1.S1_at	secreted frizzled-related protein 2 precursor	SFRP2	BE234240			62.05
Ssc.13645.1.A1_at	Secretogranin II precursor	SCG2	BX676772		142.3	
Ssc.28522.1.S1_at	Selenoprotein N precursor	SEPN1	CN167189	509.65	1106.7	839.35
Ssc.8479.1.A1_at	Selenoprotein P precursor	SEPP1	CF175878	194.7	875.1	1072.7
Ssc.27381.1.A1_at	Semaphorin 3A precursor	SEMA3A	CN155288	85.3		
Ssc.22683.1.S1_at	Semaphorin 3D precursor	SEMA3D	BX667086	757.65	65.7	
Ssc.17824.1.A1_at	Semaphorin 3E precursor	SEMA3E	CN159688		230.25	819.6
Ssc.17824.2.A1_at	Semaphorin 3E precursor	SEMA3E	CF178651		284.6	772.25
Ssc.4538.1.S1_at	Serine protease 23 precursor	PRSS23	CK465820		355.7	676.45
Ssc.9035.1.A1_at	Serine protease 23 precursor	PRSS23	BQ602007		287.7	746.35
Ssc.18947.1.A1_at	Serine protease inhibitor Kazal-type 5 precursor	SPINK5	CF364907		55.35	
Ssc.19808.1.S1_at	Serine protease inhibitor Kazal-type 5 precursor	SPINK5	BX675314	157.1		
Ssc.10439.1.S1_at	Serum albumin precursor	ALB	BX921097	62.2		
Ssc.16708.1.A1_at	Serum paraoxonase/arylesterase 2	PON2	CO951896	86.8	842.15	791.3
Ssc.27233.1.S1_at	Sialic acid binding Ig-like lectin 10 precursor	SIGLEC10	CF366024		118.1	187.8
Ssc.18568.1.A1_at	signal peptide-CUB domain-EGF-related 1	SCUBE1	CN159125		184	151.05
Ssc.24342.2.A1_at	Slit homolog 2 protein precursor	SLIT2	CF360236			58
Ssc.7743.1.A1_at	Slit homolog 2 protein precursor	SLIT2	BF712064			879.7
Ssc.25081.1.S1_at	Slit homolog 3 protein precursor	SLIT3	CN160176			67.4
Ssc.29302.1.A1_at	Slit homolog 3 protein precursor	SLIT3	CO953488		56.95	77.1
Ssc.5753.1.S1_at	Slit homolog 3 protein precursor	SLIT3	BF440920	71.4		99.25
Ssc.9803.1.A1_at	Small inducible cytokine A15 precursor	CCL15	BI398959			114.45
Ssc.657.1.A1_at	Small inducible cytokine A2 precursor	CCL2	NM_214214.1			557.45
Ssc.18613.1.S1_at	Small inducible cytokine A21 precursor	CCL21	AY312067.1			790.05
Ssc.7568.1.A1_at	Small inducible cytokine A28 precursor	CCL28	BQ599287	90.25	329	186.2
Ssc.8790.1.A1_at	Small inducible cytokine A28 precursor	CCL28	BF711871		274.85	159.9
Ssc.4984.1.S1_at	Small inducible cytokine B14 precursor	CXCL14	BF192019			63.15
Ssc.6583.1.S1_at	Small inducible cytokine B16 precursor	CXCL16	NM_213811.1			99.4

Ssc.26146.1.S1_at	Small inducible cytokine B9 precursor	CXCL9	BX914993	74.9		
Ssc.1632.1.S1_at	Soggy-1 protein precursor	DKKL1	CK466538		299.75	141.4
Ssc.3005.1.S1_at	Sorbitol dehydrogenase	SORD	CN153768	102.95	164.25	241.1
Ssc.1458.3.A1_a_at	SPARC precursor	SPARC	BF193535	95	1903.1	3350.9
Ssc.1458.4.A1_at	SPARC precursor	SPARC	BI183973			215.4
Ssc.13419.1.A1_at	SPARC related modular calcium-binding protein 2 precursor	SMOC2	BI405215	90.5	91.2	73.55
Ssc.6531.1.A1_at	SPARC-like protein 1 precursor	SPARCL1	BQ604418			725.55
Ssc.17833.1.A1_at	SS18-like protein 1	SS18L1	CF180946		98.7	99.7
Ssc.15105.2.A1_at	Stanniocalcin 1 precursor	STC1	BI184757			98.7
Ssc.2464.1.S1_at	Stanniocalcin 1 precursor	STC1	BI400766		52.5	895.45
Ssc.26221.1.S1_at	Stromal cell-derived factor 1 precursor	CXCL12	AY312066.1			113.2
Ssc.7243.1.A1_at	Stromal cell-derived factor 1 precursor	CXCL12	CO945718			394.4
Ssc.1463.1.S1_at	Stromal cell-derived factor 2 precursor	SDF2	CO950580	867.8	353.6	257.15
Ssc.29376.1.A1_at	Stromelysin-1 precursor	MMP3	CO954578	106.75		
Ssc.12514.1.A1_at	Stromelysin-3 precursor	MMP11	BI402666		99.3	
Ssc.12390.1.S1_at	Superoxide dismutase	SOD1	CO992469	1346.45	1336.75	1014.15
Ssc.4899.1.S1_at	sushi-repeat-containing protein, X-linked 2	SRPX2	BF711239		63.05	178.7
Ssc.23793.1.S1_at	T-cell surface antigen CD2 precursor	CD2	NM_213776.1	75.1		
Ssc.5738.1.A1_at	Tenascin N precursor	TNN	BI182108	507.5		
Ssc.29245.1.A1_at	tenascin R	TNR	CO952773	175.25		
Ssc.19638.1.S1_at	tenascin XB isoform 2	TNXB	CF359969			187.25
Ssc.27043.1.A1_at	tenascin XB isoform 2	TNXB	CN165952	1111.8		
Ssc.2543.1.S1_at	Testican-2 precursor	SPOCK2	BI404130		60.05	95.75
Ssc.25051.1.S1_at	Testican-3 precursor	SPOCK3	CK459787		314.3	
Ssc.28317.1.S1_at	Testican-3 precursor	SPOCK3	CN032370	266		
Ssc.6472.1.S1_at	Testican-3 precursor	SPOCK3	BQ603115	150.65	1110.2	390.95
Ssc.20396.1.S1_at	Testis expressed sequence 264 precursor	TEX264	CN165918	137.7	131.45	142.5
Ssc.1176.1.A1_at	TGF-beta receptor type III precursor	TGFBR3	BM190033		600.7	948.55
Ssc.29416.1.A1_at	TGF-beta receptor type III precursor	TGFBR3	CO955080	107.95	170.25	117.85
Ssc.10406.1.A1_at	Thrombospondin 1 precursor	THBS1	BI400960			90.5
Ssc.924.1.A1_at	Thrombospondin 1 precursor	THBS1	CB470327			66.3

Ssc.924.2.A1_at	Thrombospondin 1 precursor	THBS1	BQ601960	108.45	475.7	1251.2
Ssc.924.3.A1_at	Thrombospondin 1 precursor	THBS1	BF710863			120.25
Ssc.992.1.S1_at	Thrombospondin 2 precursor	THBS2	BF191700			183.8
Ssc.11559.1.A1_at	Thrombospondin 3 precursor	THBS3	BI233986		77.25	
Ssc.11559.2.A1_at	Thrombospondin 3 precursor	THBS3	CF792724	153.6	333.95	250.3
Ssc.11559.3.S1_at	Thrombospondin 3 precursor	THBS3	BE012675	139.8	375.3	230.85
Ssc.1411.1.S1_at	Thrombospondin 4 precursor	THBS4	BM190304	763.5		
Ssc.5956.1.S1_at	Tissue factor pathway inhibitor 2 precursor	TFPI2	BI185509	178.4	507.95	570.05
Ssc.196.1.S1_at	Tissue-type plasminogen activator precursor	PLAT	NM_214054.1		206.25	274.4
Ssc.8750.1.A1_at	tolloid-like 1	TLL1	BQ603517	92.65	104.2	68.95
Ssc.31176.1.A1_at	Transcobalamin II precursor	TCN2	CO956727		317.95	412
Ssc.3753.1.S1_at	Transferrin receptor protein 1	TFRC	CK464458	96.5	518.25	343.25
Ssc.76.1.S1_a_at	Transforming growth factor beta 1 precursor	TGFB1	M23703.1			97.15
Ssc.10287.1.A1_at	Transforming growth factor beta 2 precursor	TGFB2	BI400474			57.85
Ssc.27593.1.S1_at	Transforming growth factor beta 3 precursor	TGFB3	NM_214198.1		87.4	183.2
Ssc.16671.1.S1_at	Transforming growth factor-beta induced protein IG-H3 precursor	TGFB1	CB478477	52.5	213.15	397.3
Ssc.16671.2.S1_at	Transforming growth factor-beta induced protein IG-H3 precursor	TGFB1	CB478757	114.35	407.9	716.85
Ssc.14343.1.S1_at	Translationally controlled tumor protein	TPT1	NM_214373.1	1268.45	2176.95	2562.9
Ssc.4587.1.S1_at	Transmembrane 6 superfamily member 2	HAPLN4	BI341201		65.45	135.25
Ssc.11284.1.A1_at	Transmembrane gamma-carboxyglutamic acid protein 1 precursor	PRRG1	BI181449	395.95	154.3	174.65
Ssc.1312.1.S1_at	transmembrane protein 25	TMEM25	BQ603339	202.35		
Ssc.25371.1.S1_at	Trypsin I precursor	PRSS2	BX920826	470.35		
Ssc.21592.1.S1_at	Trypsin III precursor	PRSS3	BX667010	64.6		
Ssc.23477.1.S1_at	Tuftelin-interacting protein 11	TFIP11	CN154403	540.45	109.35	116.85
Ssc.23477.2.S1_a_at	Tuftelin-interacting protein 11	TFIP11	CB468953	603.45	148.45	185.3
Ssc.4674.1.S1_at	Tumor necrosis factor receptor superfamily member 1A precursor	TNFRSF1A	NM_213969.1	65.45	156.45	303.1
Ssc.15242.1.S1_at	Tumor necrosis factor receptor superfamily member 1B precursor	TNFRSF1B	CK467716		332.1	303.05
Ssc.938.1.S1_at	twisted gastrulation	TWSG1	BE235010		249.95	149.85
Ssc.16687.1.S1_at	Tyrosyl-tRNA synthetase, cytoplasmic	YARS	CN158140	284.15	263.85	342
Ssc.10351.1.A1_at	Urokinase plasminogen activator surface receptor precursor	PLAUR	CF363340			70.6
Ssc.11194.1.S1_at	Urokinase-type plasminogen activator precursor	PLAU	NM_213945.1			80.15

Ssc.437.1.S1_a_at	Urotensin II precursor	UTS2	NM_214143.1	249.55		
Ssc.2004.1.A1_at	usherin isoform A	USH2A	BF712866	53.85	255.4	323.75
Ssc.15283.1.A1_at	usherin isoform A	USH2A	CO942595		424	938.55
Ssc.24741.1.A1_at	Utrophin	UTRN	CK464409	425.1	120.05	123.75
Ssc.24741.2.S1_at	Utrophin	UTRN	CK466495	85.85		
Ssc.30061.1.A1_at	Utrophin	UTRN	CO949382	105.95		
Ssc.31004.1.A1_at	Utrophin	UTRN	CK463123		332.05	452.55
Ssc.4696.1.S1_at	uveal autoantigen with coiled-coil domains and ankyrin repeats	UACA	AJ651598	147.75	78.7	230.25
Ssc.14522.1.S1_at	Vascular cell adhesion protein 1 precursor	VCAM1	NM_213891.1			527.2
Ssc.15740.1.S2_at	Vascular endothelial growth factor A precursor	VEGF	CF789391		324	116.85
Ssc.2095.1.S1_at	Vascular endothelial growth factor B precursor	VEGFB	CK453779	58.45	306.2	289.4
Ssc.12790.1.A1_at	Vascular endothelial growth factor C precursor	VEGFC	BI404162		269.75	338.95
Ssc.7152.1.A1_at	Vascular endothelial growth factor D precursor	FIGF	BX925296	406.6	588.7	534.5
Ssc.5604.1.S1_at	Vitamin K-dependent protein S precursor	PROS1	CN154806		514.25	678.7
Ssc.978.1.S1_at	Von Willebrand factor precursor	VWF	CO956260			530.6
Ssc.9108.1.S1_at	WAP four-disulfide core domain protein 1 precursor	WFDC1	CF363052	83.9		418.85
Ssc.9108.2.S1_at	WAP four-disulfide core domain protein 1 precursor	WFDC1	CF361753			123.35
Ssc.5799.1.S1_at	Wnt inhibitory factor 1 precursor	WIF1	BF709288	1323.7		
Ssc.27747.1.S1_at	Wnt-2b protein precursor	WNT2B	BE033059	1116.2		169.2
Ssc.4025.1.S1_at	Wnt-3 proto-oncogene protein precursor	WNT3	CK453392	210.05	146.35	172.35
Ssc.1391.1.S1_at	Wnt-4 protein precursor	WNT4	BF440788	437.75		
Ssc.24694.1.S1_at	Wnt-5a protein precursor	WNT5A	CN160579			127.3
Ssc.26099.1.S1_at	Wnt-9b protein precursor	WNT9B	CN159177	407.65	73.4	
Ssc.11300.1.S1_at	xylosyltransferase I	XYLT1	BI181590			235.25
Ssc.293.1.S1_at	Zona pellucida sperm-binding protein 2 precursor	ZP2	NM_213848.1	1749.35		
Ssc.14525.1.S1_at	Zona pellucida sperm-binding protein 3 precursor	ZP3	NM_213893.1	1886.5		
Ssc.156.1.A1_at	Zona pellucida sperm-binding protein 4 precursor	ZP4	NM_214045.1	2656.2		
Ssc.12764.1.A1_at		C6orf1	BI403538	264	91.1	112.05
Ssc.2163.1.A1_at		C19orf24	BI181082		269.4	218
Ssc.24411.3.S1_a_at		Q6P4A8	CK463788		55	
Ssc.27116.1.A1_at		C18orf54	CN166842		75.5	

Ssc.7331.1.S1_at	Q6P4A8	BX918407		270.2	443.3
Ssc.8051.1.A1_at	C10orf59	BF703463	168.3	68.7	118.4
Ssc.8099.1.S1_at	C10orf58	BM189931	556.05	291.75	799.3

APPENDIX II: Supplementary Table 3.4: Use of Affymetix GeneChip Porcine Genome Array in combination with gene ontology annotation to identify transcripts expressed in oocyte (Oo), granulosa (GC) and theca (TC) cells of porcine antral follicles that grouped under the gene ontology term “receptor activity” (GO:0004872).

Probe Set ID	Gene Name	Gene Symbol	GenBank	raw signal		
				Oo	GC	TC
Ssc.4021.1.S1_at	1-acyl-sn-glycerol-3-phosphate acyltransferase alpha	AGPAT1	BG608754	75.9	173.95	183.6
Ssc.11692.1.A1_at	27 kDa Golgi SNARE protein	GOSR2	BI185395	554.5	100.3	106.35
Ssc.11692.2.S1_at	27 kDa Golgi SNARE protein	GOSR2	BG608928	645.1	241.9	163.5
Ssc.28472.1.S1_at	27 kDa Golgi SNARE protein	GOSR2	BF199283	101.3	64.4	
Ssc.5045.1.S1_at	3-beta-hydroxysteroid-delta(8),delta(7)-isomerase	EBP	BI400297	323.1	579.65	477.5
Ssc.26752.1.S1_at	5-hydroxytryptamine (serotonin) receptor 3B precursor	HTR3B	CN159097		118.1	141.65
Ssc.15993.1.S1_at	5-hydroxytryptamine 1D receptor	HTR1D	AF117655.1	102.05		
Ssc.13380.1.A1_at	5-hydroxytryptamine 2A receptor	HTR2A	BI405026		82.15	
Ssc.12462.1.A1_at	5-hydroxytryptamine 2C receptor	HTR2C	BI402432		53.4	
Ssc.15372.1.A1_at	5-hydroxytryptamine 2C receptor	HTR2C	CO992279		155.6	328.4
Ssc.19625.1.S1_at	62 kDa protein	TGFBR3	BF198193	262.95	532.4	557.2
Ssc.9902.1.A1_at	Activin receptor type I precursor	ACVR1	BQ597961	576.95	207	309.35
Ssc.24084.1.A1_at	Activin receptor type IIB precursor	ACVR2B	CK455958	293	89.95	
Ssc.13269.1.S1_at	Adiponectin receptor protein 1	ADIPOR1	CN163488	792.4	415.2	312.25
Ssc.16499.1.S1_at	ADP-ribosyl cyclase 1	CD38	CN163664		53.95	65.6
Ssc.5050.1.S1_at	AH receptor-interacting protein	AIP	CF360125	59.4	105.45	98.75
Ssc.10055.1.A1_at	Alpha platelet-derived growth factor receptor precursor	PDGFRA	CN153907			686.15
Ssc.20942.1.S1_at	Alpha platelet-derived growth factor receptor precursor	PDGFRA	BX676407			90.05
Ssc.20942.2.A1_at	Alpha platelet-derived growth factor receptor precursor	PDGFRA	CF180268			109.65
Ssc.15722.1.S1_at	Alpha-2-macroglobulin receptor-associated protein precursor	LRPAP1	CN159213		360.6	355.9
Ssc.6344.1.S1_at	Amyloid beta A4 precursor protein-binding family B member 3	SRA1	CK464720	62.25	247.9	296.35
Ssc.4753.1.A1_at	Angiopoietin 1 receptor precursor	TEK	CK451939	265.3		87.15

Ssc.15257.1.S1_a_at	angiotensin I converting enzyme 2 precursor; angiotensin converting enzyme-like protein	ACE2	CF362452	1043.2	568.55	537.6
Ssc.4737.1.S1_at	angiotensin II receptor-associated protein; angiotensin II, type I receptor-associated protein	AGTRAP	CK457453	62.75	82.5	91.1
Ssc.20172.1.A1_at	Anthrax toxin receptor 1 precursor	ANTXR1	BX676733		493.5	708.55
Ssc.2652.1.A1_at	Anthrax toxin receptor 2 precursor	ANTXR2	CN163375	163.9	559.25	788.1
Ssc.22109.1.A1_at	Anti-Muellerian hormone type II receptor precursor	AMHR2	AU298695		354.65	122.75
Ssc.25227.1.S1_at	Aryl hydrocarbon receptor nuclear translocator-like protein 1	ARNTL	CK462218	108.95	57.15	65.35
Ssc.9019.1.A1_at	Atrial natriuretic peptide clearance receptor precursor	NPR3	BF709118		166.95	
Ssc.1844.1.S1_at	Atrial natriuretic peptide receptor B precursor	NPR2	BG382992	61.6	485.75	355.6
Ssc.7686.1.S1_at	Attractin precursor	ATRN	BX917611	92.3	349.6	188.9
Ssc.3777.1.A1_at	Autocrine motility factor receptor, isoform 2	AMFR	CK460969	754.7	679.95	361.4
Ssc.24095.2.A1_at	Basic fibroblast growth factor receptor 1 precursor	FGFR1	CK456158		124.9	230.55
Ssc.8429.1.S1_at	B-cell receptor-associated protein 29	BCAP29	CK457455	366.05	281.85	305.05
Ssc.1178.1.S1_at	B-cell receptor-associated protein 31	BCAP31	CB473380	436.4	630.95	684.4
Ssc.9595.1.S1_at	Beta platelet-derived growth factor receptor precursor	PDGFRB	BF710995			257
Ssc.29683.1.A1_at	Bile acid receptor	NR1H4	CO944149	59.95		
Ssc.903.1.A1_at	Bone morphogenetic protein receptor type IA precursor	BMPR1A	CN160858	153.1	114.45	118
Ssc.66.1.S2_at	Bone morphogenetic protein receptor type IB precursor	BMPR1B	AF432128.1	303.9	847.65	75
Ssc.28116.1.A1_at	Brain-specific angiogenesis inhibitor 3 precursor	BAI3	CN031514	139.55	94.55	76.95
Ssc.6170.1.S1_at	Brain-specific angiogenesis inhibitor 3 precursor	BAI3	BI401250	353.4	272.95	278.85
Ssc.2181.2.A1_a_at	Brain-type organic cation transporter	SLC22A17	CN159919		840.7	754.55
Ssc.7279.1.A1_at	bromodomain containing 8 isoform 1	BRD8	BF709308	156.25	560.7	433.7
Ssc.12445.1.A1_at	Cadherin EGF LAG seven-pass G-type receptor 1 precursor	CELSR1	BI402342	305.1		
Ssc.3705.1.A1_at	Cadherin EGF LAG seven-pass G-type receptor 1 precursor	CELSR1	CK454602	944.25	167.35	314.85
Ssc.5930.1.S1_at	Cadherin EGF LAG seven-pass G-type receptor 2 precursor	CELSR2	CK457068	120.55	53.95	
Ssc.14275.1.A1_at	Calcitonin receptor precursor	CALCR	BQ601658	62.9		
Ssc.2563.1.S1_at	Cation-dependent mannose-6-phosphate receptor precursor	M6PR	CK456554	308.6	174.1	132.85
Ssc.422.1.S1_at	Cation-independent mannose-6-phosphate receptor precursor	IGF2R	BQ601689	241.15	297.6	197.25
Ssc.18359.1.S1_at	C-C chemokine receptor type 1	CCR1	NM_001001621.1	74.8		
Ssc.26328.1.S1_at	C-C chemokine receptor type 5	CCR5	NM_001001618.1			61.9

Ssc.15271.1.A1_at	C-C chemokine receptor type 6	CCR6	CN031624	693.25	102.7	
Ssc.5053.1.S1_at	CD163 antigen isoform a	CD163	NM_213976.1			74.65
Ssc.15556.1.S1_at	CD44 antigen precursor	CD44	BP462317		76.85	
Ssc.21213.1.S1_at	CD44 antigen precursor	CD44	BG733308	88.35	153.55	96.75
Ssc.25070.1.A1_at	CD44 antigen precursor	CD44	CK461396		101.35	
Ssc.930.1.A1_at	CD44 antigen precursor	CD44	X91729	94.8	123	100.45
Ssc.3348.1.S1_at	CD97 antigen precursor	CD97	NM_213925.1			127.8
Ssc.5772.1.A1_at	class I cytokine receptor	IL27RA	BI181334	124.65	451.15	333.35
Ssc.19544.1.A1_at	collectin sub-family member 12 isoform I	COLEC12	CK449800			144.35
Ssc.4654.1.S1_at	Contactin associated protein 1 precursor	CNTNAP1	BQ601434			63.4
Ssc.17872.1.A1_at	COUP transcription factor 1	NR2F1	CF175649			68.75
Ssc.3282.1.S1_at	COUP transcription factor 1	NR2F1	BE235240			295.8
Ssc.3282.2.A1_at	COUP transcription factor 1	NR2F1	BX915371			160.2
Ssc.1205.1.S1_at	COUP transcription factor 2	NR2F2	BF712930		105.9	317.4
Ssc.19579.1.A1_at	COUP transcription factor 2	NR2F2	CF368927		139.1	373.7
Ssc.19579.3.S1_at	COUP transcription factor 2	NR2F2	CF177263			86.2
Ssc.8676.1.S1_at	COUP transcription factor 2	NR2F2	CK453857		62.9	243.15
Ssc.13115.1.A1_at	Coxsackievirus and adenovirus receptor precursor	CXADR	BQ604345	90.65	69.2	90.65
Ssc.2033.1.S1_at	cryptochrome 1	CRY1	AW480140	181.15	86.45	144.7
Ssc.4549.1.A1_at	Cullin homolog 5	CUL5	BQ597564	57.25	132.8	134.4
Ssc.7176.1.A1_at	C-X-C chemokine receptor type 4	CXCR4	NM_213773.1	385.2	384	945.1
Ssc.18546.1.S1_at	cysteine-rich motor neuron 1; cysteine-rich repeat-containing protein S52 precursor	CRIM1	CK458407	348.05	694.65	413.15
Ssc.4900.1.A1_at	cysteine-rich motor neuron 1; cysteine-rich repeat-containing protein S52 precursor	CRIM1	BQ600081	565.7	652.55	372.15
Ssc.4900.2.S1_at	cysteine-rich motor neuron 1; cysteine-rich repeat-containing protein S52 precursor	CRIM1	CK453765	317.4	481.35	240.95
Ssc.16114.1.S1_at	Dihydropyridine-sensitive L-type, calcium channel alpha-2/delta subunits precursor	CACNA2D1	NM_214183.1		113.65	97.8
Ssc.5541.1.S1_at	Dihydropyridine-sensitive L-type, calcium channel alpha-2/delta subunits precursor	CACNA2D1	BQ601095		61.5	
Ssc.16799.1.A1_at	Discoidin domain receptor 2 precursor	DDR2	CK464641	96.8	240.05	220.7

Ssc.16951.1.S1_at	EGF-containing fibulin-like extracellular matrix protein 2 precursor	EFEMP2	BG835316				100.1
Ssc.4267.1.A1_at	EGF-containing fibulin-like extracellular matrix protein 2 precursor	EFEMP2	CF175814				419.8
Ssc.4267.2.S1_at	EGF-containing fibulin-like extracellular matrix protein 2 precursor	EFEMP2	BE235141				68.05
Ssc.4267.3.S1_at	EGF-containing fibulin-like extracellular matrix protein 2 precursor	EFEMP2	BF198910				105.55
Ssc.120.1.S1_at	Endoglin precursor	ENG	NM_214031.1				281
Ssc.26308.1.S1_at	Endothelial protein C receptor precursor	PROCR	BX922318				59.75
Ssc.27603.1.S1_at	Endothelin B receptor precursor	EDNRB	CB478930	73.5	125.6		
Ssc.3295.1.S1_at	Endothelin B receptor precursor	EDNRB	BM658700	155.75	1011.95		370.75
Ssc.3295.2.A1_at	Endothelin B receptor precursor	EDNRB	BQ603701	67	666.85		155.4
Ssc.298.1.S1_at	Enteropeptidase precursor	PRSS7	NM_001001259.1	480			
Ssc.7872.1.A1_at	Enteropeptidase precursor	PRSS7	CF792126	226.55	477.8		287.85
Ssc.21909.1.S1_at	Ephrin type-A receptor 4 precursor	EPHA4	BX666832		70.05		129.45
Ssc.27504.1.S1_at	Ephrin-B3 precursor	EFNB3	CN164991		89.45		75.95
Ssc.20009.1.S1_at	Epidermal growth factor receptor kinase substrate EPS8	EPS8	CN157951		319.15		234.75
Ssc.55.1.S1_at	Epidermal growth factor receptor precursor	EGFR	NM_214007.1		214.75		150.7
Ssc.3179.1.S1_at	Epithelial discoidin domain receptor 1 precursor	DDR1	CK457958	427.35	595.55		295.55
Ssc.16606.1.S1_at	ER lumen protein retaining receptor 1	KDELRL1	BI184979	128.2	489.2		428.25
Ssc.997.1.S1_at	ER lumen protein retaining receptor 2	KDELRL2	CN152884	793.5	1021.8		1226.2
Ssc.997.2.S1_at	ER lumen protein retaining receptor 2	KDELRL2	CF363588	905.1	1316.05		1307.35
Ssc.997.3.A1_at	ER lumen protein retaining receptor 2	KDELRL2	CO989093	762.8	1097.7		1177.65
Ssc.21548.2.A1_at	ER lumen protein retaining receptor 3	KDELRL3	CO990012		74.65		137.9
Ssc.16991.1.A1_at	Estradiol 17-beta-dehydrogenase 8	HSD17B8	CN166885	84.7	444.2		388.95
Ssc.12290.1.A1_at	Estrogen receptor	ESR1	CO949474		516.8		564
Ssc.30162.1.A1_at	Estrogen receptor	ESR1	CO987406		144.65		
Ssc.13026.1.S1_at	Estrogen receptor	ESR1	CO948427		187.85		137.15
Ssc.13333.1.A1_at	estrogen-related receptor gamma isoform 2	ESRRG	BI404678		61.6		
Ssc.22407.1.A1_at	estrogen-related receptor gamma isoform 2	ESRRG	CN159240		66.95		
Ssc.28547.1.S1_at	estrogen-related receptor gamma isoform 2	ESRRG	BG835577	461.75			
Ssc.2144.1.S1_at	Exportin 7	XPO7	BF712291	164.3	109.9		76.85
Ssc.7490.1.A1_at	Exportin 7	XPO7	BQ598954	810.35	641.6		779.55
Ssc.1882.1.S1_at	Fibroblast growth factor receptor 2 precursor	FGFR2	BX666107	208.15	85.25		122.7

Ssc.5018.1.S1_at	FK506-binding protein 1A	FKBP1A	CN158159	468.35	622.9	862.25
Ssc.7555.1.S1_at	FK506-binding protein 3	FKBP3	CO989038	135.55	472.2	608.7
Ssc.7581.1.A1_at	FL cytokine receptor precursor	FLT3	BQ599341	79.35	143.9	84.1
Ssc.11779.1.S1_at	Folate receptor alpha precursor	FOLR1	BI180978			119.95
Ssc.14544.1.S1_at	Folate receptor beta precursor	FOLR2	U89949.1			275.45
Ssc.14498.1.S1_at	Follicle stimulating hormone receptor precursor	FSHR	NM_214386.1		87.65	
Ssc.3590.1.A1_at	Frizzled 1 precursor	FZD1	CN166109		68.7	165.85
Ssc.28993.1.S1_s_at	Frizzled 1 precursor	FZD1	AJ682600			79.05
Ssc.20193.1.S1_at	Frizzled 3 precursor	FZD3	BX676757	115.95		
Ssc.1093.2.A1_at	Frizzled 4 precursor	FZD4	AJ747681	72.95	144.1	144.65
Ssc.25230.1.S1_at	Frizzled 4 precursor	FZD4	CN163765	110.65	224.5	259.3
Ssc.29483.1.A1_at	Frizzled 5 precursor	FZD5	CF179887	71.25	462.05	
Ssc.1107.1.A1_at	Frizzled 6 precursor	FZD6	CO951114		106.75	
Ssc.1107.2.A1_at	Frizzled 6 precursor	FZD6	BQ604682		152.15	
Ssc.13659.1.A1_at	Frizzled 6 precursor	FZD6	BQ603070		52.05	
Ssc.25065.1.S1_at	Frizzled 6 precursor	FZD6	CK461072	481.6	108.65	71.2
Ssc.9253.1.A1_at	Frizzled 7 precursor	FZD7	BI399766	83.6		613.45
Ssc.9938.1.A1_at	G protein-coupled receptor 120	GPR120	BI402064	206.3		
Ssc.29196.1.A1_at	G protein-coupled receptor 133	GPR133	CO951711			480.7
Ssc.9799.1.A1_at	G protein-coupled receptor 133	GPR133	BI398952			79.9
Ssc.27266.1.S1_at	G protein-coupled receptor 143	GPR143	CK453252			53.65
Ssc.28878.1.S1_at	G protein-coupled receptor 153	GPR153	BF190382			79.15
Ssc.5003.1.S1_at	G protein-coupled receptor 158	GPR158	BQ604419	88.5	121.25	80.2
Ssc.5105.2.S1_a_at	G protein-coupled receptor family C group 5 member B precursor	GPRC5B	BX671422		409.35	108.15
Ssc.30072.1.A1_at	G protein-coupled receptor kinase 5	GRK5	CO949532		215.45	122.4
Ssc.22287.1.S1_at	Gamma-aminobutyric-acid receptor alpha-3 subunit precursor	GABRA3	CF789935			122.4
Ssc.8348.1.A1_at	Gamma-aminobutyric-acid receptor alpha-4 subunit precursor	GABRA4	CF179895	62.4	216.2	
Ssc.11508.1.A1_at	Gamma-aminobutyric-acid receptor alpha-5 subunit precursor	GABRA5	CO955587		379.45	372.3
Ssc.29362.1.A1_at	Gamma-aminobutyric-acid receptor beta-1 subunit precursor	GABRB1	CO954368	1775		
Ssc.13330.1.A1_at	Gamma-aminobutyric-acid receptor gamma-2 subunit precursor	GABRG2	CA779811	552.35		
Ssc.29433.1.A1_at	GDNF family receptor alpha 1 precursor	GFRA1	CO955346	481		

Ssc.4886.1.S1_at	GNDF family receptor alpha 1 precursor	GFRA1	CK465894	239.35	177	126.2
Ssc.11085.1.S1_at	Glucagon-like peptide 2 receptor precursor	GLP2R	CF180635	104.1	78.75	105.6
Ssc.19028.1.A1_at	Glutamate [NMDA] receptor subunit epsilon 2 precursor	GRIN2B	CF368114	732.3	306.95	283.5
Ssc.19028.2.S1_at	Glutamate [NMDA] receptor subunit epsilon 2 precursor	GRIN2B	CF366699	425.8	131.05	
Ssc.25475.1.S1_at	Glutamate receptor 3 precursor	GRIA3	BX917243			72.95
Ssc.8500.1.A1_at	Glutamate receptor 4 precursor	GRIA4	BF704185			93.9
Ssc.25159.1.A1_at	Glutamate receptor delta-1 subunit precursor	GRID1	CN165962	443.15	244.05	367.55
Ssc.29679.1.A1_at	Glutamate receptor delta-1 subunit precursor	GRID1	CO943770			60.8
Ssc.4506.1.A1_at	Glutamate receptor delta-1 subunit precursor	GRID1	BQ602668	106.35	119.7	
Ssc.27144.1.A1_at	Glutamate receptor, ionotropic kainate 1 precursor	GRIK1	CN167165	213.5		
Ssc.19883.1.S1_at	Glutamate receptor, ionotropic kainate 2 precursor	GRIK2	AW347236			373.6
Ssc.27289.1.S1_at	Glutamate receptor, ionotropic kainate 2 precursor	GRIK2	CN153418		131.3	
Ssc.4849.1.A1_at	Glutamate receptor, ionotropic kainate 2 precursor	GRIK2	CF177468	423.45	519.95	456.6
Ssc.27589.1.S1_at	Glutamate receptor, ionotropic kainate 5 precursor	GRIK5	CN166445		109.65	
Ssc.14374.1.A1_at	Glycine receptor alpha-2 chain precursor	GLRA2	BQ602053		181.35	117.85
Ssc.8413.1.A1_at	Glycine receptor alpha-3 chain precursor	GLRA3	CK455173		232.35	250.3
Ssc.21857.1.S1_at	Growth factor receptor-bound protein 10	GRB10	CF795733			96.8
Ssc.15583.1.S1_at	Growth hormone receptor precursor	GHR	CF175347	69.35	82.9	
Ssc.135.1.S1_a_at	Growth hormone-releasing hormone receptor precursor	GHRHR	NM_214035.1	90.9		
Ssc.8549.1.A1_at	Guanylate cyclase soluble, alpha-3 chain	GUCY1A3	BF704147		117.4	61.75
Ssc.19532.1.S1_at	Guanylate cyclase soluble, beta-1 chain	GUCY1B3	CF365595		77.3	67.3
Ssc.29926.1.A1_at	hepatitis A virus cellular receptor 1	HAVCR1	CO938614		70.25	75.35
Ssc.508.1.S1_at	High affinity immunoglobulin epsilon receptor gamma-subunit precursor	FCER1G	AF148221.1			83.35
Ssc.24944.1.S1_a_at	High affinity immunoglobulin gamma Fc receptor I precursor	FCGR1A	BI359768	130.8		
Ssc.16947.1.A1_at	Histamine H4 receptor	HRH4	BI404251	459.2	189.35	182.95
Ssc.16947.2.S1_at	Histamine H4 receptor	HRH4	BI341482	445	210.55	247.6
Ssc.13780.1.S1_x_at	HLA class I histocompatibility antigen, A-3 alpha chain precursor	HLA-A	AF464016.1		385.9	909.05
Ssc.13780.10.A1_at	HLA class I histocompatibility antigen, A-3 alpha chain precursor	HLA-A	AY135590.1			63.95
Ssc.13780.2.S1_x_at	HLA class I histocompatibility antigen, A-3 alpha chain precursor	HLA-A	AF464049.2		181.55	1089.4
Ssc.13780.3.S1_at	HLA class I histocompatibility antigen, A-3 alpha chain precursor	HLA-A	AF464006.1	119.55		265.3
Ssc.13780.7.S1_at	HLA class I histocompatibility antigen, A-3 alpha chain precursor	HLA-A	AY463542.1		129.9	247

Ssc.13780.9.S1_a_at	HLA class I histocompatibility antigen, A-3 alpha chain precursor	HLA-A	AY463537.1		140.8	768.25
Ssc.13780.10.S1_x_at	HLA class I histocompatibility antigen, A-3 alpha chain precursor	HLA-A	AY135590.1		176.55	614.25
Ssc.23510.1.A1_s_at	HLA class I histocompatibility antigen, alpha chain G precursor	HLA-G	CF365277		185.65	339.95
Ssc.13780.12.S1_a_at	HLA class I histocompatibility antigen, B-7 alpha chain precursor	HLA-B	CO948288		160.7	1641.15
Ssc.13780.12.S1_x_at	HLA class I histocompatibility antigen, B-7 alpha chain precursor	HLA-B	CO948288		62.9	946.55
Ssc.13780.5.S1_x_at	HLA class I histocompatibility antigen, B-7 alpha chain precursor	HLA-B	AY247775.1		188.1	1029.65
Ssc.13780.6.S1_a_at	HLA class I histocompatibility antigen, B-7 alpha chain precursor	HLA-B	AF464013.1		624.9	1183.75
Ssc.13780.6.S1_x_at	HLA class I histocompatibility antigen, B-7 alpha chain precursor	HLA-B	AF464013.1		335.55	933.9
Ssc.18554.1.A1_s_at	HLA class I histocompatibility antigen, B-7 alpha chain precursor	HLA-B	AB105380.1			173.55
Ssc.13780.4.S1_x_at	HLA class I histocompatibility antigen, Cw-7 alpha chain precursor	HLA-C	AF464011.1		228.4	1261.15
Ssc.16756.1.S1_at	HLA class I histocompatibility antigen, Cw-7 alpha chain precursor	HLA-C	CK450398		335	297.95
Ssc.13777.1.S1_at	HLA class II histocompatibility antigen, DM alpha chain precursor	HLA-DMA	AB032169.1			57.45
Ssc.11102.1.S1_at	HLA class II histocompatibility antigen, DQ(5) alpha chain precursor	HLA-DQA1	AY285927.1			235.2
Ssc.222.1.S1_at	HLA class II histocompatibility antigen, DR alpha chain precursor	HLA-DRA	AY285933.1			209.85
Ssc.11063.1.S1_at	HLA class II histocompatibility antigen, DX beta chain precursor	HLA-DQB2	AY459300.1			219.8
Ssc.26770.1.S1_at	Hyaluronan mediated motility receptor	HMMR	CN159851	1147.25	214.9	139.55
Ssc.6149.1.S1_at	Hyaluronidase 2 precursor	HYAL2	NM_214440.1			55.35
Ssc.6117.1.S1_at	IgG receptor FcRn large subunit p51 precursor	FCGRT	NM_214197.1		210.9	393.35
Ssc.5605.1.A1_at	Inositol 1,4,5-trisphosphate receptor type 1	ITPR1	AJ661915	649.65	161.2	734.15
Ssc.12677.1.S1_at	Inositol 1,4,5-trisphosphate receptor type 3	ITPR3	CN153289	151.4		
Ssc.8679.1.A1_at	Insulin receptor precursor	INSR	BF703401		320.2	354
Ssc.19009.1.S1_at	Insulin-like growth factor I receptor precursor	IGF1R	BE031010		58.3	
Ssc.18457.1.S1_at	Integral membrane protein DGCR2/IDD precursor	DGCR2	CK461408	277	825.7	595.75
Ssc.16218.1.A1_at	Integrin alpha-2 precursor	ITGA2	Z12137.1	177.9		
Ssc.16218.1.S1_at	Integrin alpha-2 precursor	ITGA2	Z12137.1	212.3		
Ssc.17512.1.S1_at	Integrin alpha-2 precursor	ITGA2	BE032615	203.9	322.5	198.75
Ssc.26342.1.A1_at	Integrin alpha-2 precursor	ITGA2	CN031694	371		
Ssc.26342.1.S1_at	Integrin alpha-2 precursor	ITGA2	AY553922.1	334.2		
Ssc.16663.1.S1_at	Integrin alpha-5 precursor	ITGA5	CN162878		142.1	407.95
Ssc.11399.2.A1_at	Integrin alpha-6 precursor	ITGA6	B1182344	127.25	84.95	
Ssc.25207.1.A1_at	Integrin alpha-6 precursor	ITGA6	CK460874	1029.2	1040.5	461.25

Ssc.6258.1.A1_a_at	Integrin alpha-6 precursor	ITGA6	CK463022	139.65	163.35	69.95
Ssc.2786.1.S1_at	Integrin alpha-7 precursor	ITGA7	BI341137			131.35
Ssc.1377.1.A1_at	Integrin alpha-8 precursor	ITGA8	CO994999			361.05
Ssc.1377.2.S1_at	Integrin alpha-8 precursor	ITGA8	BI343023			185.25
Ssc.1377.3.S1_at	Integrin alpha-8 precursor	ITGA8	BP157471			189.15
Ssc.29185.1.A1_at	Integrin alpha-8 precursor	ITGA8	CO951446			199.8
Ssc.27437.1.S1_at	Integrin alpha-9 precursor	ITGA9	CN159365	181.65		61.05
Ssc.7306.1.A1_at	Integrin alpha-9 precursor	ITGA9	BQ598586			421.6
Ssc.8347.1.A1_at	Integrin alpha-E precursor	ITGAE	CK465810	490.8	163.75	138.9
Ssc.25199.1.S1_at	Integrin alpha-M precursor	ITGAM	CK459825	74.85	493.25	482.25
Ssc.15932.1.S1_at	Integrin alpha-V precursor	ITGAV	BF078387	57.35	255.1	190.25
Ssc.6737.1.S1_at	Integrin alpha-V precursor	ITGAV	AJ682028		551.55	508.2
Ssc.6737.2.A1_at	Integrin alpha-V precursor	ITGAV	CF365450		320.85	203.05
Ssc.9451.1.S1_at	Integrin alpha-V precursor	ITGAV	CN163082		237.65	152.2
Ssc.4621.1.S1_at	Integrin beta-1 precursor	ITGB1	NM_213968.1	211.45	1059.55	894.5
Ssc.44.1.S1_at	Integrin beta-3 precursor	ITGB3	NM_214002.1			90.9
Ssc.26290.1.S1_at	Integrin beta-5 precursor	ITGB5	CF176275	369.6	98.5	186.4
Ssc.26277.1.S1_at	Integrin beta-7 precursor	ITGB7	BX914942	112	83.95	53.6
Ssc.11187.1.S1_at	Intercellular adhesion molecule-1 precursor	ICAM1	AF156712.1			57.85
Ssc.8997.1.A1_at	Intercellular adhesion molecule-1 precursor	ICAM1	BF710790			133.35
Ssc.11381.1.S1_at	Interferon-alpha/beta receptor alpha chain precursor	IFNAR1	NM_213772.1		73.7	81.85
Ssc.4933.1.A1_at	Interferon-alpha/beta receptor beta chain precursor	IFNAR2	CF363094		173.9	231.7
Ssc.9565.1.S1_at	Interferon-gamma receptor alpha chain precursor	IFNGR1	BF710880	83.8	299.35	555.5
Ssc.3068.1.S1_at	interleukin 11 receptor, alpha isoform 1 precursor; interleukin-11 receptor alpha chain	IL11RA	CK466326		123.25	204.9
Ssc.19416.1.A1_at	Interleukin 21 receptor precursor	IL21R	CF359990		231.75	132.3
Ssc.11406.1.A1_a_at	Interleukin-1 receptor, type I precursor	IL1R1	CK451986	53.15	94.15	204.25
Ssc.25357.1.S1_at	Interleukin-1 receptor, type II precursor	IL1R2	BX915459		505.6	102.15
Ssc.19609.1.S1_at	Interleukin-1 receptor-associated kinase 1	IRAK1	BF190763		137.3	139.3
Ssc.71.1.S1_at	Interleukin-12 beta chain precursor	IL12B	U08317.1	446.95		
Ssc.17245.1.S1_at	Interleukin-13 receptor alpha-1 chain precursor	IL13RA1	NM_214341.1	105.05	53.55	76.9

Ssc.4145.1.S1_at	Interleukin-13 receptor alpha-1 chain precursor	IL13RA1	CF795078	609.75	315.05	487
Ssc.6256.1.A1_at	Interleukin-4 receptor alpha chain precursor	IL4R	BI186333		89.7	94.5
Ssc.25033.1.A1_at	Interleukin-6 receptor beta chain precursor	IL6ST	CK458940	904.35		
Ssc.17506.1.S1_at	killer cell lectin-like receptor subfamily G, member 1	KLRG1	CD572669	201.8		
Ssc.2980.1.S1_at	Kinectin	KTN1	CK456976	591.15	441	458.1
Ssc.26316.1.S1_at	Kinectin	KTN1	BX922553	318.25	237.5	190.05
Ssc.19071.2.A1_at	Krueppel-related zinc finger protein 3	TAS1R1	CF368834	82.2		
Ssc.22874.1.S1_at	Lamin B receptor	LBR	CN158395	177.65	123.65	162.95
Ssc.10493.1.A1_at	LanC-like protein 1	LANCL1	BF702283	130.95	164.1	130.25
Ssc.4873.1.S1_at	LanC-like protein 1	LANCL1	CN156998	442.75	282.05	299.95
Ssc.2337.1.S1_at	LAR protein precursor	PTPRF	CN158060		209	
Ssc.1375.1.A1_at	Latent transforming growth factor beta binding protein, isoform 1L precursor	LTBP1	BQ599578		56.7	55.65
Ssc.8072.1.A1_at	Latent transforming growth factor beta binding protein, isoform 1L precursor	LTBP1	BF709385	366.2	449.6	543.1
Ssc.8072.2.A1_at	Latent transforming growth factor beta binding protein, isoform 1L precursor	LTBP1	CO950891	439.1	340.6	727.1
Ssc.15595.1.S1_at	Latrophilin 2 precursor	LPHN2	AJ656216	901.8	377.35	504.15
Ssc.21512.1.A1_at	Latrophilin 2 precursor	LPHN2	CN165828		66.85	
Ssc.25029.1.A1_at	Latrophilin 2 precursor	LPHN2	CK458705		221.2	317.55
Ssc.25029.2.S1_at	Latrophilin 2 precursor	LPHN2	CB482802		193	280.1
Ssc.22633.1.A1_at	Latrophilin 3 precursor	LPHN3	BX666169		104.5	
Ssc.2297.1.A1_at	Latrophilin 3 precursor	LPHN3	BI400087		91.85	108.75
Ssc.27382.1.S1_at	Latrophilin 3 precursor	LPHN3	CN160920	83.95	65.9	
Ssc.27473.1.S1_at	Latrophilin 3 precursor	LPHN3	CN162786	194	173.85	125.6
Ssc.13283.1.S1_at	Leptin receptor gene-related protein	LEPR	BI404777		81.9	
Ssc.816.1.S1_at	Leptin receptor gene-related protein	LEPR	CF790758	354.55	494.8	541.9
Ssc.10060.1.A1_at	Leukemia inhibitory factor receptor precursor	LIFR	BI399724	345.4		
Ssc.16175.1.A1_at	Leukemia inhibitory factor receptor precursor	LIFR	U91518.1	83		
Ssc.16175.1.S1_at	Leukemia inhibitory factor receptor precursor	LIFR	BF078710	89.75		
Ssc.17562.1.S1_at	leukocyte receptor cluster	LENG4	BE014935	275	589.95	446.65
Ssc.12000.1.A1_at	leukocyte receptor cluster (LRC) member 8	LENG8	BI184606	357	1477.7	1299.95

Ssc.21653.1.S1_at	leukocyte receptor cluster (LRC) member 8	LENG8	CN158780	70.85	521.35	441.35
Ssc.21653.2.S1_a_at	leukocyte receptor cluster (LRC) member 8	LENG8	CF364889		108.35	61.85
Ssc.2634.1.S1_at	Leukotriene B4 receptor 2	LTB4R2	CK457748	349.05	67.05	86.35
Ssc.899.1.A1_at	Ligatin	LGTN	CO955631	152.8	108.65	150.1
Ssc.19598.1.S1_at	Liprin-alpha 4	PPFIA4	AW354080		56.75	
Ssc.15671.1.S1_at	Long transient receptor potential channel 3	TRPM3	BI346959			244.55
Ssc.8868.1.S1_at	Low affinity immunoglobulin gamma Fc region receptor II-b precursor	FCGR2B	BX926353			64.55
Ssc.167.2.S1_a_at	Low affinity immunoglobulin gamma Fc region receptor III-A precursor	FCGR3A	AF372455.1			186.7
Ssc.167.4.S1_at	Low affinity immunoglobulin gamma Fc region receptor III-A precursor	FCGR3A	CB483332			112.9
Ssc.21926.1.S1_at	Low-density lipoprotein receptor precursor	LDLR	BX667248	269.7	1309.75	916.25
Ssc.17905.1.A1_at	Low-density lipoprotein receptor-related protein 1 precursor	LRP1	CF176034	169.65	133.95	151.05
Ssc.3219.1.S1_at	Low-density lipoprotein receptor-related protein 1 precursor	LRP1	BF713436	56	113.95	295.9
Ssc.6785.1.S1_at	Low-density lipoprotein receptor-related protein 1 precursor	LRP1	BM190319	165.3	208.35	472.25
Ssc.2466.1.S1_at	Low-density lipoprotein receptor-related protein 10 precursor	LRP10	CN159522		359.5	337.25
Ssc.14282.1.A1_at	Low-density lipoprotein receptor-related protein 11 precursor	LRP11	BQ601688		354.3	458.4
Ssc.11641.1.A1_at	Low-density lipoprotein receptor-related protein 1B precursor	LRP1B	BQ603468		295.45	249.15
Ssc.11641.2.A1_at	Low-density lipoprotein receptor-related protein 1B precursor	LRP1B	BI182805		218.35	179.5
Ssc.13690.1.A1_at	Low-density lipoprotein receptor-related protein 1B precursor	LRP1B	BQ603189	196.3	70.8	110.6
Ssc.4274.1.S1_at	Low-density lipoprotein receptor-related protein 1B precursor	LRP1B	CN153359		429	940.05
Ssc.6108.1.A1_at	Low-density lipoprotein receptor-related protein 1B precursor	LRP1B	CF175498		60.45	
Ssc.8009.1.A1_at	Low-density lipoprotein receptor-related protein 1B precursor	LRP1B	CO951669	1070.75	1323.15	1167.9
Ssc.26207.1.S1_at	Low-density lipoprotein receptor-related protein 5 precursor	LRP5	CF362973	97.65	56.65	
Ssc.4693.1.S1_at	Low-density lipoprotein receptor-related protein 6 precursor	LRP6	CK451153	79.5	137.6	77.3
Ssc.4693.3.S1_at	Low-density lipoprotein receptor-related protein 6 precursor	LRP6	AJ683395		58.45	
Ssc.1417.1.A1_at	Low-density lipoprotein receptor-related protein 8 precursor	LRP8	CO949101	61.25	2201.2	710.8
Ssc.31016.1.A1_at	Low-density lipoprotein receptor-related protein 8 precursor	LRP8	CO949604	110.55	2249.15	983.75
Ssc.11449.1.A1_at	Lutropin-choriogonadotropic hormone receptor precursor	LHCGR	BI182640		78.85	
Ssc.16311.1.A1_a_at	Lutropin-choriogonadotropic hormone receptor precursor	LHCGR	NM_214449.1		1012.55	625.4
Ssc.16311.4.S1_a_at	Lutropin-choriogonadotropic hormone receptor precursor	LHCGR	M29528.1		733.9	420.95
Ssc.25550.1.S1_at	Lymphocyte antigen 96 precursor	LY96	BX918583			275.35
Ssc.23484.1.A1_a_at	Lysosome membrane protein II	SCARB2	CN163797	243.75	1297.85	1436

Ssc.23484.2.S1_at	Lysosome membrane protein II	SCARB2	BI185142	203.95	1444.75	1610.8
Ssc.810.1.S1_at	Lysosome membrane protein II	SCARB2	AY550058.1	235.45	875.65	1118.65
Ssc.810.1.S2_at	Lysosome membrane protein II	SCARB2	BP460116		208.35	137.85
Ssc.2598.1.S1_at	Lysyl oxidase homolog 2 precursor	LOXL2	CN160419	116.1		413.1
Ssc.12056.1.A1_at	Lysyl oxidase homolog 4 precursor	LOXL4	BI181507		181.65	94.8
Ssc.9229.1.S1_at	Macrophage mannose receptor precursor	MRC1	AY368183.1			285.45
Ssc.13430.1.A1_at	Macrophage scavenger receptor types I and II	MSR1	BI404701		183.45	212.9
Ssc.3088.1.S1_at	mannose receptor, C type 2; endocytic receptor	MRC2	CN166193		120.15	76.55
Ssc.16096.2.S1_a_at	Mast/stem cell growth factor receptor precursor	KIT	BP141688		235.4	
Ssc.9819.1.S1_at	Membrane associated progesterone receptor component 1	PGRMC1	NM_213911.1	98.3	1164.6	964.9
Ssc.8663.1.A1_at	Membrane associated progesterone receptor component 2	PGRMC2	BF703355	112.45	484.1	382.55
Ssc.3154.1.S1_at	Metabotropic glutamate receptor 5 precursor	GRM5	BQ603354	226.1	584.15	590.8
Ssc.25253.2.A1_at	Metabotropic glutamate receptor 7 precursor	GRM7	CF180830			85.15
Ssc.29298.1.A1_at	Metabotropic glutamate receptor 8 precursor	GRM8	CO953427	365.8	70.35	
Ssc.7503.1.A1_at	Metabotropic glutamate receptor 8 precursor	GRM8	BQ598997		111.4	115.65
Ssc.13855.1.S1_at	Mineralocorticoid receptor	NR3C2	Z98817	81.45		
Ssc.17877.1.A1_at	Mineralocorticoid receptor	NR3C2	CF175685	231.75		
Ssc.1868.1.S1_at	Mineralocorticoid receptor	NR3C2	AW429744	112.4		
Ssc.7547.1.S1_at	Mitochondrial import receptor subunit TOM22 homolog	TOMM22	BM190302	1000.45	1156.05	1112.25
Ssc.9858.1.A1_at	Muscarinic acetylcholine receptor M2	CHRM2	BI399146		102.5	304.7
Ssc.7788.1.A1_at	Muscle, skeletal receptor tyrosine protein kinase precursor	MUSK	BQ599454	61.9	83.25	61.1
Ssc.6463.1.A1_at	Myeloid differentiation primary response protein MyD88	MYD88	CO955543		178.85	354.2
Ssc.6463.2.S1_at	Myeloid differentiation primary response protein MyD88	MYD88	CB481896		146.05	312.1
Ssc.17433.1.S1_at	Neogenin precursor	NEO1	CK466136		157.2	189.35
Ssc.21326.1.S1_at	Neogenin precursor	NEO1	CA780972	56.45	61.05	73.9
Ssc.4048.1.A1_at	Neogenin precursor	NEO1	BG609692	592.7	561.85	707.7
Ssc.29672.1.A1_at	Neurexin 1-beta precursor	NRXN1	CO943197	142.85	110.7	282
Ssc.28128.1.A1_at	Neurexin 3-alpha precursor	NRXN3	CN031229	140.95	57.5	
Ssc.30499.1.A1_at	Neurexin 3-alpha precursor	NRXN3	CO992754		113.9	97.55
Ssc.19892.1.A1_at	Neurogenic locus notch homolog protein 2 precursor	NOTCH2	CB477659	60.85	456.45	493.95
Ssc.3778.1.S1_at	Neurogenic locus notch homolog protein 3 precursor	NOTCH3	BF199278		54.9	345.15

Ssc.16517.1.S1_at	Neuromedin-B receptor	NMBR	CB287724	142.15	192.8	155.3
Ssc.16348.1.S1_at	Neuropeptide Y receptor type 1	NPY1R	NM_214288.1		353.85	266.6
Ssc.19095.1.A1_at	neuropilin- and tolloid-like protein 2 precursor	NETO2	CF367951	79.15		
Ssc.8271.1.S1_at	neuropilin- and tolloid-like protein 2 precursor	NETO2	BF712594	407.55	138.1	87.55
Ssc.21862.1.A1_at	Neuropilin-2 precursor	NRP2	BG608506			109.15
Ssc.24899.1.S1_at	Neuropilin-2 precursor	NRP2	CK466196			145.75
Ssc.30598.1.A1_at	Neuropilin-2 precursor	NRP2	CO994833			95.95
Ssc.2264.1.S1_at	Neutral amino acid transporter B(0)	SLC1A5	CA780403	975.6	74	293.4
Ssc.1533.1.S1_at	Niemann-Pick C1 protein precursor	NPC1	NM_214322.1	941.15	616.05	593.7
Ssc.2696.1.S1_at	nischarin	NISCH	BX667229	247.9	377.35	359.05
Ssc.27154.1.S1_at	NT-3 growth factor receptor precursor	NTRK3	CN159468	103.1	279.05	218.05
Ssc.14500.1.S1_at	Nuclear receptor 0B1	NR0B1	NM_214387.1	822.45		
Ssc.13813.1.A1_at	Nuclear receptor coactivator 4	NCOA4	CO951684	1353.45	1447.9	688.65
Ssc.12924.1.A1_at	Nuclear receptor coactivator 5	NCOA5	BI404199	61.3	183.4	101.8
Ssc.14338.1.A1_at	Nuclear receptor ROR-alpha	RORA	BQ601893		58.4	
Ssc.7521.1.A1_at	Nuclear receptor ROR-beta	RORB	CF179283		673.05	697.6
Ssc.9081.1.S1_at	Nuclear receptor ROR-gamma	RORC	CN159150	226.45	354.6	546.8
Ssc.10888.1.S1_at	nucleoporin like 2	NUPL2	CN160683	295.25	61.35	
Ssc.8247.1.A1_at	Opioid binding protein/cell adhesion molecule precursor	OPCML	BF702490	483	772.75	711.15
Ssc.27928.1.S1_at	Opioid growth factor receptor	OGFR	BE014447		71.6	100.3
Ssc.16410.1.A1_at	opioid receptor, sigma 1 isoform 1	OPRS1	CK452041	69.7	95.1	117.85
Ssc.10401.1.A1_at	Orexin receptor type 2	HCRTR2	BI181454	366.2	281.7	306.7
Ssc.25690.1.S1_at	Orexin receptor type 2	HCRTR2	BX920842	151.55		
Ssc.13870.1.A1_at	Orphan nuclear receptor NR1D2	NR1D2	Z98836		204.7	226.95
Ssc.761.1.S1_at	Orphan nuclear receptor NR4A3	NR4A3	NM_214247.1		156.1	149.4
Ssc.19587.1.A1_at	Orphan nuclear receptor NR5A2	NR5A2	CN025797		1005.5	122.5
Ssc.20890.1.S1_at	Orphan nuclear receptor NR5A2	NR5A2	BX665622		1318.5	153.5
Ssc.29043.1.S1_at	Orphan nuclear receptor NR5A2	NR5A2	CK457175		946.5	66.6
Ssc.29043.2.A1_at	Orphan nuclear receptor NR5A2	NR5A2	CO949442		147.4	
Ssc.29813.1.A1_at	Orphan nuclear receptor NR5A2	NR5A2	CO946056		1547.4	302.6
Ssc.486.1.S1_at	Orphan nuclear receptor NR5A2	NR5A2	AJ236939.1		87.75	

Ssc.21863.1.S1_at	Orphan nuclear receptor NR6A1	NR6A1	CN154652	403.45		
Ssc.10207.1.A1_at	Orphan nuclear receptor TR2	NR2C1	CF365646	435	140.3	108.55
Ssc.16533.1.S1_at	Orphan nuclear receptor TR2	NR2C1	CF795376	184.05	85.3	60.75
Ssc.4068.1.S1_at	Orphan nuclear receptor TR2	NR2C1	CN165855	117.65	406.95	311.75
Ssc.26670.1.S1_at	Orphan nuclear receptor TR4	NR2C2	CN154484	525.3		
Ssc.15888.1.S1_at	oxidised low density lipoprotein	OLR1	NM_213805.1		86.6	
Ssc.29837.1.A1_at	oxidised low density lipoprotein (lectin-like) receptor 1	OLR1	CO937226		58.25	
Ssc.16354.1.S1_at	Oxysterols receptor LXR-alpha	NR1H3	BX674225	59	120.65	178.9
Ssc.21608.1.S1_at	Oxysterols receptor LXR-beta	NR1H2	CO994854	132.95		63
Ssc.108.1.S1_at	Oxytocin receptor	OXTR	X71796.1	677.15		
Ssc.18377.1.S1_at	P2X purinoceptor 4	P2RX4	CF176491		142.3	80.8
Ssc.18377.2.S1_at	P2X purinoceptor 4	P2RX4	AW482770		204.8	164.9
Ssc.24134.1.S1_at	P2X purinoceptor 7	P2RX7	CK456772		113	121.95
Ssc.16823.1.S1_at	P2Y purinoceptor 12	P2RY12	BG835209	99.25	407.55	353.65
Ssc.907.1.A1_at	P2Y purinoceptor 5	P2RY5	CO946728		113.2	299.05
Ssc.11298.1.S1_at	Palmitoyl-protein thioesterase 2 precursor	PPT2	CN162740	327.25	237	122.25
Ssc.14485.1.S1_at	Parathyroid hormone/parathyroid hormone-related peptide receptor precursor	PTH1R	NM_214382.1			80.5
Ssc.5243.1.A1_at	Patched protein homolog 1	PTCH	BI404769	69.15	178.55	484.95
Ssc.5936.1.A1_a_at	Peripheral-type benzodiazepine receptor	BZRP	NM_213753.1			116.95
Ssc.9348.1.S1_at	Peroxisome proliferator activated receptor alpha	PPARA	BF713592		69.7	
Ssc.3251.1.A1_at	Peroxisome proliferator activated receptor delta	PPARD	BI404339	87.5		
Ssc.14475.3.S1_a_at	Peroxisome proliferator activated receptor gamma	PPARG	AB097926.1	496.45	330.5	63.55
Ssc.1161.1.A1_at	platelet-derived growth factor receptor-like protein	PDGFRL	BI185596	140.85	79.85	293.55
Ssc.12817.1.S1_at	plexin A2	PLXNA2	BX670344			72.15
Ssc.28314.1.S1_at	plexin A2	PLXNA2	CN029638		113.8	67.85
Ssc.6105.1.A1_at	Plexin B1 precursor	PLXNB1	BI402259		134.55	88.9
Ssc.6105.2.S1_at	Plexin B1 precursor	PLXNB1	AW416696		65.9	
Ssc.4084.1.S1_at	Plexin B2 precursor	PLXNB2	BQ605077		196.7	149.8
Ssc.3879.1.S1_at	plexin C1	PLXNC1	AJ747527		204.45	125.75
Ssc.1551.1.S1_at	Plexin D1 precursor	PLXND1	AW485849	74.8		277.85

Ssc.23169.1.S1_at	Poliovirus receptor related protein 2 precursor	PVRL2	BX674778		72.7	
Ssc.3019.1.S1_at	Poliovirus receptor related protein 2 precursor	PVRL2	BG732549		439.85	272.7
Ssc.5967.1.A1_at	Polycomb complex protein RING1	RING1	BQ598538		198	226.45
Ssc.10673.1.A1_at	Polycystic kidney and hepatic disease 1 precursor	PKHD1	BI404740			69.45
Ssc.13101.1.A1_at	Polycystic kidney and hepatic disease 1 precursor	PKHD1	BQ604271		79.8	
Ssc.13557.1.A1_at	Polycystic kidney and hepatic disease 1 precursor	PKHD1	CF175409		208.5	139.3
Ssc.8497.1.A1_at	Polycystic kidney and hepatic disease 1 precursor	PKHD1	BF703870	94.35	179.55	242.45
Ssc.12032.1.S1_at	PREDICTED: plexin A4	PLXNA4	BI185725		74	71.9
Ssc.1702.1.S1_at	Probable G protein-coupled receptor 125 precursor	GPR125	AW482947	930.65	1199.8	292.5
Ssc.1702.2.S1_at	Probable G protein-coupled receptor 125 precursor	GPR125	CF361419	74.9	184.75	
Ssc.29771.1.A1_at	Probable G protein-coupled receptor 126 precursor	GPR126	CO953067		120.2	206.65
Ssc.30261.1.A1_at	Probable G protein-coupled receptor 126 precursor	GPR126	CO989315		73.7	
Ssc.2354.1.S1_at	Probable G protein-coupled receptor 160	GPR160	AW785890		973.4	
Ssc.5191.1.S1_at	Probable G protein-coupled receptor GPR4	GPR4	BQ598553	169.85		
Ssc.15997.1.S1_at	Progesterone receptor	PGR	S49016.1		281.55	100.6
Ssc.23944.1.A1_at	progesterin and adipoQ receptor family member III	PAQR3	CK452180	68.15	245.1	113.3
Ssc.28652.1.A1_at	progesterin and adipoQ receptor family member III	PAQR3	BI185897	343.15	108.7	94.25
Ssc.24706.1.A1_at	Prolactin receptor precursor	PRLR	CK463265	101.15		
Ssc.20438.1.S1_at	Prostaglandin F2-alpha receptor	PTGFR	CK465614		628.1	588.95
Ssc.11246.1.A1_at	Protein kinase C, alpha type	PRKCA	BI181165		62.6	
Ssc.12144.1.S1_at	Protein kinase C, alpha type	PRKCA	CK461505		245.35	104.45
Ssc.13637.1.A1_at	Protein kinase C, alpha type	PRKCA	BQ602979		189.2	225.15
Ssc.24226.1.A1_at	Protein kinase C, alpha type	PRKCA	CK452273	107.4		
Ssc.8482.1.A1_at	Protein kinase C, epsilon type	PRKCE	BF703085	123.4	68.65	87.25
Ssc.2011.1.A1_at	Protein kinase C, eta type	PRKCH	CN163635	679.45		100.85
Ssc.7253.1.A1_at	Protein kinase C, iota type	PRKCI	BQ598362	191.8	705.6	700.75
Ssc.20678.1.S1_at	Protein kinase C-like 1	PKN1	CK457129	106.8	271.1	328.3
Ssc.19164.1.A1_at	Protein kinase C-like 2	PKN2	CF362245		138	69.75
Ssc.9980.1.S1_at	Protein kinase C-like 2	PKN2	CO938025	124.45	520.55	285.6
Ssc.9034.1.A1_at	Proteinase activated receptor 1 precursor	F2R	BF709183		98.9	132.65
Ssc.11421.1.S1_at	Proteinase activated receptor 2 precursor	F2RL1	CK465831	118.35	61.1	

Ssc.11421.2.A1_at	Proteinase activated receptor 2 precursor	F2RL1	BF442949	163.3	92.85	
Ssc.10015.1.A1_at	Protein-tyrosine phosphatase delta precursor	PTPRD	CK465404	55.8	451.65	342.85
Ssc.19270.1.S1_at	Protein-tyrosine phosphatase delta precursor	PTPRD	BX670734		74.95	
Ssc.6106.1.S1_at	Protein-tyrosine phosphatase delta precursor	PTPRD	BI341817		193.9	105.05
Ssc.12448.1.S1_at	Protein-tyrosine phosphatase eta precursor	PTPRJ	BF442168	104.4	115.95	
Ssc.17301.1.A1_at	Protein-tyrosine phosphatase eta precursor	PTPRJ	CN160256	154.25	423.8	456.5
Ssc.29458.1.A1_at	Protein-tyrosine phosphatase gamma precursor	PTPRG	CO956431	204.25	90.65	93.6
Ssc.7658.1.A1_at	Protein-tyrosine phosphatase gamma precursor	PTPRG	BF704471		61.45	76.15
Ssc.26731.1.S1_at	Protein-tyrosine phosphatase, non-receptor type 18	PTPN18	CN157178		257	217.1
Ssc.27140.1.A1_at	Protein-tyrosine phosphatase, non-receptor type 2	PTPN2	CN167133	88.95		
Ssc.28535.1.S1_at	Protein-tyrosine phosphatase, non-receptor type 2	PTPN2	AJ651827	372.65	274.85	286.15
Ssc.22209.1.A1_at	Protein-tyrosine phosphatase, non-receptor type 22	PTPN22	CF789487		166.25	153.85
Ssc.5321.1.A1_at	Protein-tyrosine phosphatase, non-receptor type 22	PTPN22	CN155376		136.15	91.35
Ssc.13541.1.A1_at	protocadherin 21 precursor; MT-protocadherin	PCDH21	BQ602649		73.95	66.55
Ssc.29374.1.A1_at	protocadherin 21 precursor; MT-protocadherin	PCDH21	CO954544	59.05	106.95	112.35
Ssc.11200.1.S1_a_at	Proto-oncogene tyrosine-protein kinase ABL1	ABL1	BF703531	624.8	254.45	420.5
Ssc.30155.1.A1_at	Proto-oncogene tyrosine-protein kinase ABL1	ABL1	CO987295		83.15	
Ssc.23284.1.S1_at	Putative G protein-coupled receptor GPR39	GPR39	BX671257		131.85	93.2
Ssc.6102.1.S1_at	Putative G protein-coupled receptor GPR39	GPR39	BI341726	586.6		
Ssc.1941.1.A1_at	Ral guanine nucleotide dissociation stimulator-like 2	RGL2	CK457895		213.8	243.95
Ssc.15730.1.S1_at	Receptor activity-modifying protein 2 precursor	RAMP2	NM_214082.1			338.8
Ssc.5000.1.A1_at	Receptor protein-tyrosine kinase erbB-2 precursor	ERBB2	BI185975		321.75	346.45
Ssc.16444.1.S1_at	Receptor-type protein-tyrosine phosphatase kappa precursor	PTPRK	BQ602525	55.75	825.05	577.2
Ssc.9499.1.S1_at	Receptor-type protein-tyrosine phosphatase kappa precursor	PTPRK	BF710702		127.9	94.85
Ssc.21264.1.A1_at	Receptor-type protein-tyrosine phosphatase mu precursor	PTPRM	AW437058			230.35
Ssc.27106.1.A1_at	Receptor-type protein-tyrosine phosphatase mu precursor	PTPRM	CN166740			70
Ssc.2991.1.S1_at	Receptor-type protein-tyrosine phosphatase mu precursor	PTPRM	BI338583	93.4		
Ssc.31029.1.A1_at	Receptor-type protein-tyrosine phosphatase mu precursor	PTPRM	CF175718		501.8	456.15
Ssc.23033.1.S1_at	Receptor-type protein-tyrosine phosphatase N2 precursor	PTPRN2	BX673501	479.9		
Ssc.30359.1.A1_at	Receptor-type protein-tyrosine phosphatase N2 precursor	PTPRN2	CO990734	72.1		
Ssc.29687.1.A1_at	Receptor-type protein-tyrosine phosphatase O precursor	PTPRO	CO944324	207.8	97.4	126.3

Ssc.21194.1.S1_at	Receptor-type protein-tyrosine phosphatase R precursor	PTPRR	CK451828	60.4		69.5
Ssc.18521.1.A1_at	Receptor-type protein-tyrosine phosphatase R precursor	PTPRR	CF180907	195.25	228.25	79.15
Ssc.5069.1.S1_at	Receptor-type protein-tyrosine phosphatase S precursor	PTPRS	BP434926		699.4	955.1
Ssc.28111.1.A1_at	Receptor-type protein-tyrosine phosphatase T precursor	PTPRT	CN031709	312.15		
Ssc.6396.1.S1_at	Receptor-type protein-tyrosine phosphatase U precursor	PTPRU	BQ603843	85.1		
Ssc.15830.1.A1_at	Retinoic acid receptor beta	RARB	U82259.1	108.1		
Ssc.15830.1.S1_at	Retinoic acid receptor beta	RARB	U82259.1	122.4		
Ssc.8381.1.A1_at	Retinoic acid receptor beta	RARB	BI183435		62	78.45
Ssc.1598.1.S1_at	Retinoic acid receptor RXR-beta	RXRB	CN165522		68.6	57.2
Ssc.19608.1.S1_at	Retinoic acid receptor RXR-gamma	RXRG	CF181317	152.35		
Ssc.3899.1.S1_at	Ribosome-binding protein 1	RRBP1	CK465626	246.7	740.75	1558.7
Ssc.18398.1.S1_at	ring finger protein 139	RNF139	CK467421	693.9		
Ssc.12138.1.A1_at	Roundabout homolog 1 precursor	ROBO1	BI401101			112.75
Ssc.16713.1.S1_at	Roundabout homolog 1 precursor	ROBO1	BI360009		69.75	65.3
Ssc.23329.1.S1_at	Roundabout homolog 1 precursor	ROBO1	AW415941	324.65		
Ssc.23764.1.S1_at	Roundabout homolog 1 precursor	ROBO1	BG895329	86.9	267.4	187.5
Ssc.30907.1.S1_at	Roundabout homolog 2 precursor	ROBO2	CN161952		401.55	338.2
Ssc.13834.1.S1_at	Ryanodine receptor 2	RYR2	CN153597		83.8	
Ssc.14352.1.S1_at	Ryanodine receptor 2	RYR2	AJ656944		399.65	259.75
Ssc.25615.1.A1_at	Ryanodine receptor 2	RYR2	BX921068			234.9
Ssc.1921.1.A1_at	Ryanodine receptor 2	RYR2	BI399922	97.8	175.65	132.2
Ssc.1921.2.A1_at	Ryanodine receptor 2	RYR2	BX665303	162.05	332.3	231.6
Ssc.16179.2.A1_at	Ryanodine receptor 3	RYR3	U15975.1		54.5	
Ssc.11791.1.S1_at	Scavenger receptor class B member 1	SCARB1	NM_213967.1		678.55	511.3
Ssc.20832.1.S1_at	Secretin receptor precursor	SCTR	BX676279		54.2	
Ssc.27381.1.A1_at	Semaphorin 3A precursor	SEMA3A	CN155288	85.3		
Ssc.22683.1.S1_at	Semaphorin 3D precursor	SEMA3D	BX667086	757.65	65.7	
Ssc.17824.1.A1_at	Semaphorin 3E precursor	SEMA3E	CN159688		230.25	819.6
Ssc.17824.2.A1_at	Semaphorin 3E precursor	SEMA3E	CF178651		284.6	772.25
Ssc.27746.1.S1_at	Semaphorin 4B precursor	SEMA4B	BE033068	85.1	59.45	
Ssc.18375.1.A1_at	Semaphorin 4D precursor	SEMA4D	CK457225	284.05	112.2	

Ssc.26548.1.S1_at	Semaphorin 4G precursor	SEMA4G	BF191800		69.75		
Ssc.24144.1.S1_at	Serine/threonine-protein kinase receptor R2 precursor	ACVR1B	CK456702	740.5	156.65	86.3	
Ssc.10763.1.A1_at	Seven transmembrane helix receptor	Q8NGA3	CN154075			65.1	
Ssc.8461.1.S1_a_at	Seven transmembrane helix receptor	Q8NH35	BP160400	107.75	340.95	168.1	
Ssc.22027.1.S1_at	Signal recognition particle receptor beta subunit	SRPRB	BG383548		380.25	307	
Ssc.22027.2.A1_at	Signal recognition particle receptor beta subunit	SRPRB	BI342115		333.85	337.7	
Ssc.6583.1.S1_at	Small inducible cytokine B16 precursor	CXCL16	NM_213811.1			99.4	
Ssc.3117.1.S1_at	Smoothed homolog precursor	SMO	BF193404		113.45	127.35	
Ssc.1527.1.A1_at	solute carrier family 20	SLC20A1	BX922597	1171.75	433.9	407.45	
Ssc.1527.2.A1_at	solute carrier family 20	SLC20A1	BF712006	740.4	265.1	345.95	
Ssc.25077.1.S1_at	solute carrier family 20, member 2	SLC20A2	CK461293	101.35	230.95	249.5	
Ssc.12492.1.A1_at	Sortilin precursor	SORT1	CN167016	181.35	242.35		
Ssc.12492.2.S1_at	Sortilin precursor	SORT1	BI402572	486.4	465	100.1	
Ssc.12492.3.S1_at	Sortilin precursor	SORT1	BP461669	289.45	233.5		
Ssc.21796.1.S1_at	Sortilin-related receptor precursor	SORL1	CK457083	749.1	847.9	678.35	
Ssc.27528.1.S1_at	sterile alpha and TIR motif containing 1	SARM1	BG609563		115.65	125.35	
Ssc.30909.1.A1_at	Steroidogenic factor 1	NR5A1	CO942601		203.55	317.05	
Ssc.23793.1.S1_at	T-cell surface antigen CD2 precursor	CD2	NM_213776.1	75.1			
Ssc.13463.1.S1_at	T-cell-specific surface glycoprotein CD28 precursor	CD28	BQ599790	158	272	181.35	
Ssc.13463.2.S1_at	T-cell-specific surface glycoprotein CD28 precursor	CD28	BX668283	222.7	309.5	148.05	
Ssc.23499.1.A1_at	T-cell-specific surface glycoprotein CD28 precursor	CD28	AY435219.1	161.1			
Ssc.23499.1.S1_at	T-cell-specific surface glycoprotein CD28 precursor	CD28	AY435219.1	136			
Ssc.5330.1.A1_at	TGF-beta receptor type II precursor	TGFBR2	CK464325			703.35	
Ssc.1176.1.A1_at	TGF-beta receptor type III precursor	TGFBR3	BM190033		600.7	948.55	
Ssc.29416.1.A1_at	TGF-beta receptor type III precursor	TGFBR3	CO955080	107.95	170.25	117.85	
Ssc.20987.1.S1_at	Thrombopoietin receptor precursor	MPL	BX676455	165.6	241.8	134.25	
Ssc.5569.1.S1_at	Thyroid hormone receptor alpha	THRA	BF190468	84.05		128.35	
Ssc.21187.2.A1_at	Thyroid hormone receptor-associated protein complex 150 kDa component	THRAP3	BE233204	396.8	697.1	723.85	
Ssc.21187.3.S1_at	Thyroid hormone receptor-associated protein complex 150 kDa component	THRAP3	BX922067		117.9	84.65	

Ssc.25404.1.S1_at	Thyroid hormone receptor-associated protein complex 150 kDa component	THRAP3	BX916208		98.45	91.05
Ssc.17224.1.S1_at	Toll-like receptor 8 precursor	TLR8	NM_214187.1	60.1		
Ssc.2201.1.A1_at	toll-like receptor adaptor molecule 2	TICAM2	BI403244		79.5	58.95
Ssc.2201.2.S1_at	toll-like receptor adaptor molecule 2	TICAM2	BX670675	101.05	159.2	114.65
Ssc.2201.3.S1_at	toll-like receptor adaptor molecule 2	TICAM2	CF795050	164.7	240	259.35
Ssc.8378.1.A1_at	toll-like receptor adaptor molecule 2	TICAM2	CK449324	217.05	370.65	240.35
Ssc.3753.1.S1_at	Transferrin receptor protein 1	TFRC	CK464458	96.5	518.25	343.25
Ssc.2145.1.S1_at	Transferrin receptor protein 2	TFR2	AW480117	150.05		
Ssc.26692.1.A1_at	transient receptor potential cation channel, subfamily M, member 1	TRPM1	CN157023	114.65	219.3	168.55
Ssc.28940.1.A1_at	transient receptor potential cation channel, subfamily M, member 6; hypomagnesemia, secondary hypocalcemia	TRPM6	AJ658538	287.15		
Ssc.13271.1.S1_at	Translocation associated membrane protein 1	TRAM1	AJ747649	281.35	348.8	380.3
Ssc.16859.1.A1_at	Translocation associated membrane protein 1	TRAM1	CN154634	405.3	818.05	950.5
Ssc.27228.1.S1_at	Translocation protein SEC63 homolog	SEC63	BE013457	155.1	397.05	319.8
Ssc.27228.2.S1_at	Translocation protein SEC63 homolog	SEC63	CF178111		68.7	
Ssc.6708.1.A1_at	Translocation protein SEC63 homolog	SEC63	CK450354	152.6	371.25	315.9
Ssc.4478.1.A1_at	Transportin 3	TNPO3	CA780383	242.15	271.55	163.75
Ssc.6497.1.A1_at	Transportin 3	TNPO3	CO991878	344	281.85	289.2
Ssc.6027.1.S1_at	triggering receptor expressed on myeloid cells-like 2	TREML2	BI339141		665	
Ssc.4674.1.S1_at	Tumor necrosis factor receptor superfamily member 1A precursor	TNFRSF1A	NM_213969.1	65.45	156.45	303.1
Ssc.15242.1.S1_at	Tumor necrosis factor receptor superfamily member 1B precursor	TNFRSF1B	CK467716		332.1	303.05
Ssc.1509.1.S1_at	Tumor necrosis factor receptor superfamily member 21 precursor	TNFRSF21	CF175812			110.15
Ssc.27574.1.S1_at	Tumor necrosis factor receptor superfamily member 3 precursor	LTBR	CN166612		284	324.75
Ssc.2084.1.S1_at	Tumor necrosis factor receptor superfamily member EDAR precursor	EDAR	CN026018	542.45	160.65	159.55
Ssc.1864.1.A1_a_at	Tumor necrosis factor receptor superfamily member Fn14 precursor	TNFRSF12A	BF710490		219.65	324.7
Ssc.1864.1.A1_at	Tumor necrosis factor receptor superfamily member Fn14 precursor	TNFRSF12A	BF710490		146.5	181.9
Ssc.2627.2.S1_at	Tumor-associated calcium signal transducer 2 precursor	TACSTD2	BE012532	569.1		
Ssc.19059.1.A1_at	Type-1 angiotensin II receptor	AGTR1	CF368623			129.35
Ssc.10263.1.A1_at	Type-2 angiotensin II receptor	AGTR2	BI400382	205.75	794.95	788.4
Ssc.1630.1.S1_at	Tyrosine-protein kinase receptor TYRO3 precursor	TYRO3	CK454217	113.5	171.05	305.6

Ssc.29644.1.A1_at	Tyrosine-protein kinase receptor UFO precursor	AXL	CO943665	222.5		
Ssc.6566.1.A1_at	Tyrosine-protein kinase receptor UFO precursor	AXL	BI399410		389.8	322.85
Ssc.2961.1.S1_at	Tyrosine-protein kinase RYK precursor	RYK	BX924023		448.8	136.4
Ssc.7194.1.S1_at	Tyrosine-protein kinase RYK precursor	RYK	CF181242	90.05	456.4	213.9
Ssc.29681.1.A1_at	Tyrosine-protein kinase transmembrane receptor ROR1 precursor	ROR1	CO944080			155.05
Ssc.9860.1.A1_at	Tyrosine-protein kinase transmembrane receptor ROR1 precursor	ROR1	BI399154			55.55
Ssc.9797.1.S1_at	Unc-13 homolog B	UNC13B	CK456294	373.7	86.85	
Ssc.10672.1.A1_at	unc5C	UNC5C	BQ597611		98.85	
Ssc.29615.1.A1_at	unc5C; homolog of C. elegans transmembrane receptor Unc5; unc5	UNC5C	CO942332	172.95	91.75	72.75
Ssc.5140.1.S1_at	unc5C; homolog of C. elegans transmembrane receptor Unc5; unc5	UNC5C	BF075617	109.85	85.95	73.55
Ssc.10351.1.A1_at	Urokinase plasminogen activator surface receptor precursor	PLAUR	CF363340			70.6
Ssc.7690.1.A1_at	Vacuolar ATP synthase membrane sector associated protein M8-9	ATP6AP2	CB474497	875.75	509.75	484.4
Ssc.25045.1.S1_at	Vascular endothelial growth factor receptor 2 precursor	KDR	BI360137			257.55
Ssc.7860.1.A1_at	Vasoactive intestinal polypeptide receptor 2 precursor	VIPR2	BI398837	122.25	253.9	389.65
Ssc.8564.1.A1_at	Very low-density lipoprotein receptor precursor	VLDLR	CF365775	491.75	551.1	636.1
Ssc.27427.1.S1_a_at	VPS10 domain-containing receptor SorCS1 precursor	SORCS1	CN154840	203.15		
Ssc.7417.1.A1_at	VPS10 domain-containing receptor SorCS1 precursor	SORCS1	BQ598617	55.85		
Ssc.12349.1.A1_at	VPS10 domain-containing receptor SorCS2 precursor	SORCS2	BI401885		55.4	55.15
Ssc.17608.1.S1_at	VPS10 domain-containing receptor SorCS2 precursor	SORCS2	AW430747			111
Ssc.29177.1.A1_at	VPS10 domain-containing receptor SorCS3 precursor	SORCS3	CO951310			108.8
Ssc.9754.1.A1_at	VPS10 domain-containing receptor SorCS3 precursor	SORCS3	BI398809	215.05	71.6	66.2
Ssc.13519.1.A1_at	xenotropic and polytropic retrovirus receptor	XPR1	CO993512	81	67.45	
Ssc.13519.2.A1_at	xenotropic and polytropic retrovirus receptor	XPR1	BQ602572	265.65	242.8	123
Ssc.14324.1.A1_at	xenotropic and polytropic retrovirus receptor	XPR1	CF180021	108.85		
Ssc.18626.1.A1_at	X-linked interleukin-1 receptor accessory protein-like 1 precursor	IL1RAPL1	CF359788			96.6
Ssc.30854.1.S1_at	Zinc finger protein 219	ZNF219	BF443290		512.6	442.15
Ssc.293.1.S1_at	Zona pellucida sperm-binding protein 2 precursor	ZP2	NM_213848.1	1749.35		
Ssc.14525.1.S1_at	Zona pellucida sperm-binding protein 3 precursor	ZP3	NM_213893.1	1886.5		
Ssc.156.1.A1_at	Zona pellucida sperm-binding protein 4 precursor	ZP4	NM_214045.1	2656.2		